

Agrociencia

eISSN: 2521-9766

VOLUME 60, NUMBER 3 | April 01 - May 15, 2026 | MEXICO



AGRICULTURA
SECRETARÍA DE AGRICULTURA

EDITORIAL TEAM

EDITOR IN CHIEF, AGROCIENCIA

Fernando Carlos Gómez-Merino

DEPUTY EDITOR, AGROCIENCIA

Libia Iris Trejo-Téllez

INTERNATIONAL

EDITORIAL COUNCIL

Roger Austin (UK)

José Sarukhán Kermez (Mexico)

Barry C. Arnold (USA)

INTERNAL EDITORIAL ADVISORY COMMITTEE

Jorge Alvarado López

Jorge D. Etchevers Barra

Víctor A. González Hernández

Said Infante Gil

Leopoldo E. Mendoza Onofre

José A. Villaseñor Alva

DESIGN AND COMPOSITION

L. Brenda Espejel Lagunas

TRANSLATORS

Inés Enríquez

Joel Castillo González

Nicolas Crossa

METADATA HARVESTER

Moisés Quintana Arévalo

PLATFORM SUPPORT

L. Brenda Espejel Lagunas

Ana Luisa Mejía Sandoval

Valeria Abigail Martínez Sias

COPYRIGHT AND RELATED RIGHTS, Volume 60, Number 3, April 01 - May 15, 2026, Agrociencia is an open access scientific publication edited by the Colegio de Postgraduados, which is located at Carretera Mexico-Texcoco km 36.5, Montecillo, Texcoco, State of Mexico, Mexico. C. P. 56264. Phone: +52 5959284427. www.colpos.mx. Editor in chief: Dr. Fernando Carlos Gómez Merino. Reservations of Rights to Exclusive Use 04-2021031913431800-203. eISSN: 2521-9766, granted by the National Copyright Institute. Last modification date, May 15, 2026.

The opinions expressed by the authors do not necessarily reflect the position of the editor of the publication.

All correspondence (subscription information, sales, advertising, author contributions, etc.) should be addressed to:

Central Office:

AGROCIENCIA

Guerrero No. 9, Esquina con Avenida Hidalgo,

San Luis Huexotla, Texcoco 56220,

State of Mexico. MEXICO

Tel.: +52-595 92 84427

<https://agrociencia-colpos.org/index.php/agrociencia>

DISCLAIMER: Trade marks or any commercial representations cited on scientific articles, essays or notes do not imply nor should be inferred as Agrociencia endorsement. No criticism, disclosure or rejection should be assumed either. Likewise, statements or recommendations expressed by authors are solely their responsibility and may not totally agree with those of the Editor.

Cover: Coffee cherry

Designed by Freepik



AGRICULTURA

SECRETARÍA DE AGRICULTURA Y DESARROLLO RURAL

ANIMAL SCIENCE

**TECHNICAL AND ECONOMIC ANALYSIS OF WHITE SHRIMP
(*Penaeus vannamei*) CULTURE IN THREE DIFFERENT
SYSTEMS BASED ON STOCKING DENSITY**

302

Sergio Gustavo **Castillo-Vargasmachuca**, Delia **Rodríguez-Olague**,
Raúl **Claro-de los Santos**, Enrique **Valenzuela-Wood**, Eulalio **Arámbul-Muñoz**

**CHALLENGES IN THE SUSTAINABILITY OF GOAT PRODUCTION
SYSTEMS IN ZACATECAS, MEXICO**

318

Ma. Enriqueta **Luna-Coronel**, Alberto **Muro-Reyes**, Einar **Vargas-Bello-Pérez**,
Alejandro **Espinoza-Canales**, Daniel **García-Cervantes**,
Héctor **Gutiérrez-Bañuelos**

BIOTECHNOLOGY

**ARBUSCULAR MYCORRHIZAL FUNGI AND INDOLE-3-BUTYRIC
ACID ON ROOTING AND GROWTH OF *Stevia rebaudiana*
Bertoni STEM CUTTINGS**

339

Evangelina Esmeralda **Quiñones-Aguilar**, Marcela **Ríos-Sandoval**,
Sergio David **Valerio-Landa**, Luis Guillermo **Hernández-Montiel**,
Gabriel **Rincón-Enríquez**

FOOD SCIENCE

**COMPARATIVE ANALYSIS OF SENSORY PROFILES OF TEMPEH
PREPARED WITH AMARANTH vs. SOY USING
Rhizopus oligosporus AS INOCULUM**

355

Jessica Michel **Cruz-González**, Ricardo **Hernández-Martínez**,
Fernando Carlos **Gómez-Merino**, Adrián **Argumedo-Macías**,
Mirna **López-Espíndola**, Estela **Chicuellar-Trujillo**,
José Andrés **Herrera-Corredor**

NATURAL RENEWABLE RESOURCES

PRESSURE-STATE-RESPONSE MODEL FOR THE DIAGNOSIS OF ENVIRONMENTAL IMPACTS ON A PROTECTED FOREST ECOSYSTEM

372

Dafne Fernanda Juárez-Zavala, Elizabeth Hernández-Acosta

PLANT PROTECTION

YOLOV8-POWERED COMPUTER VISION FOR COFFEE CHERRY RIPENESS, DEFECT, AND MORPHOLOGICAL ASSESSMENT

389

Kavitha Subramani, Senduru Srinivasulu,
Saravanan Raju, Surendran Rajendran

GEOGRAPHIC INFORMATION SYSTEMS AS KEY TOOLS IN THE PHYTOSANITARY MANAGEMENT OF MEZCAL AGAVE (*Agave angustifolia* Haw) IN THE STATE OF MEXICO, MEXICO

412

Atenas Tapia-Rodríguez, José Francisco Ramírez-Dávila,
Agustín David Acosta-Guadarrama, Alfredo Ruiz-Orta

SOCIOECONOMICS

INFLUENCE OF HEALTH ON THE WORK PERFORMANCE OF RASPBERRY PICKERS: A PILOT STUDY

424

Alejandra García-Becerra, María Guadalupe Sánchez-Cervantes,
Nancy María Aguilar-Hernández, Silvia Rosario Villa-Ramos,
José Abel Chocoteco-Campos

CONSUMER PREFERENCES AND WILLINGNESS TO PAY FOR TRADITIONAL TORTILLA USING CONTINGENT VALUATION

439

Judith de la Cruz-Marcial, Miguel A. Martínez-Damian, Enrique Melo-Guerrero,
Juan Hernández-Ortiz, Gustavo Ramírez-Valverde

ORGANIC SHADE-GROWN COFFEE: A PRODUCTION SYSTEM WITH A
LOW CARBON FOOTPRINT AND HIGH SUSTAINABILITY POTENTIAL

Adán **Villa-Herrera**, Martín Alejandro **Bolaños-González**,
José Manuel **Salvador-Castillo**, Luz María **Ramírez-Armas**

TECHNICAL AND ECONOMIC ANALYSIS OF WHITE SHRIMP (*Penaeus vannamei*) CULTURE IN THREE DIFFERENT SYSTEMS BASED ON STOCKING DENSITY

Sergio Gustavo Castillo-Vargasmachuca¹, Delia Rodríguez-Olague¹, Raúl Claro-de los Santos¹, Enrique Valenzuela-Wood², Eulalio Arámbul-Muñoz^{2*}

¹Universidad Autónoma de Nayarit. Programa de Doctorado en Ciencias Biológico-Agropecuarias. Carretera Tepic-Compostela km 9, Xalisco, Nayarit, Mexico. C. P. 63780.

²Universidad Autónoma de Baja California. Instituto de Investigaciones Oceanológicas. Carretera Transpeninsular 3917, Ensenada, Baja California, Mexico. C. P. 22860.

* Author for correspondence: eulalio.arambul@uabc.edu.mx

ABSTRACT

Given the increasing global demand for aquaculture products and the necessity to enhance production systems, it is important to produce comparative evidence to inform decision-making in aquaculture investments. This is particularly relevant in contexts such as Nayarit, Mexico, where aquaculture is a key activity for local economic development. This study evaluated the technical and economic variables of three white shrimp (*Penaeus vannamei*) production systems in the San Blas region of Nayarit. The hypothesis was that the hyper-intensive (HI) system would have a higher benefit-cost ratio and better yields per unit area due to its high level of technology and stocking density, compared to the semi-intensive (SI) and intensive (I) systems. Using principal component analysis with VARIMAX rotation, 14 key variables were identified that reflected significant differences in production intensity, with yields ranging from 1124 kg ha⁻¹ (SI) to 36 409 kg ha⁻¹ (HI) per cycle. Results showed that the HI system had the highest total costs (USD 54 419.28 year⁻¹) but also the highest net income (USD 14 857.36 year⁻¹) due to its high stocking density and technification. However, the SI system stood out with the best benefit-cost ratio (B:C) (1.51) and an internal rate of return (IRR) of 30 %, surpassing HI (1.21 B:C, 11.56 % IRR) and I (1.66 B:C, 7.53 % IRR). Despite requiring a higher break-even point (588.89 kg cycle⁻¹), HI demonstrated greater efficiency in resource utilization per kilogram of shrimp produced, reducing the environmental impact. Although hyperintensive systems require higher initial investments, their profitability improves over time due to cost amortization and higher yields per unit area.

Keywords: shrimp farming, cost-benefit ratio, break-even point.

INTRODUCTION

Aquaculture is experiencing rapid growth in a highly versatile and uncertain environment due to climate change and the globalization of trade. This growth is driven by demand, improvements in technologies available to fish farmers, diversification

Citation: Castillo-Vargasmachuca SG, Rodríguez-Olague D, Claro-de los Santos R, Valenzuela-Wood E, Arámbul-Muñoz E. 2025. Technical and economic analysis of white shrimp (*Penaeus vannamei*) culture in three different systems based on stocking density.

Agrociencia 60(3): 302-317.
<https://doi.org/10.47163/agrociencia.v60i3.3377>

Editor in Chief:
 Dr. Fernando C. Gómez Merino

Received: October 13, 2025.

Approved: April 10, 2026.

Published in *Agrociencia*:
 April 17, 2026.

This work is licensed under a Creative Commons Attribution-Non-Commercial 4.0 International license.



of farmed species, intensification of production, and the expansion of aquaculture farms (Ottinger *et al.*, 2016). The success of an aquaculture business depends not only on production techniques but also on cost control and cash flow analysis. Efficient production management and administration are key factors in increasing productivity and reducing costs. Simulating decision scenarios and training staff working on shrimp farms are crucial strategies for improving operational economic performance (Dávila-López *et al.*, 2020), while also analyzing cash flow using specialized tools that facilitate the visualization of prospective economic returns (Buarque, 1984).

Companies that provide a product or service rely on cost analysis to assess the profitability of their operations and recoup investments. Additionally, it helps identify the profit, which represents the excess of revenue over expenses incurred during operations or upon the liquidation of a company. The general criterion for defining the relevant costs and benefits of a project involves considering those that will occur if the project is undertaken and those that will not occur if it is not (Dávila-López *et al.*, 2020).

The growing global demand for seafood has made aquaculture a continuously expanding activity (Hamilton *et al.*, 2018). The largest single market for seafood imports is the European Union, whose purchases amounted to EUR 20.6 billion in 2014 and EUR 22.2 billion in 2016. Of these values, 56.1 % came from developing countries (Zhang and Tveterås, 2019). However, environmental constraints continue to hinder productivity, and therefore, development models adopted must not only increase the efficiency of companies but also mitigate environmental impacts (Drabo, 2017). Furthermore, farming intensification driven by high market demand has increased the associated risk of disease. Although researchers tend to agree that shrimp farming is highly risky and considered a gamble by many (Flaherty *et al.*, 2009), it remains a widely adopted production system, raising questions about how aquaculturists perceive and manage these risks.

Models for predicting risks in aquaculture, specifically shrimp farming, are complex, given the industry's diverse operational practices and cultural strategies (Little *et al.*, 2016), making it difficult to design a model that encompasses all aspects. In this context, risk categories have been identified and classified into two main groups: external (market, reputational, regulatory, technological, and production-related) and internal (financial, strategic, and operational) (Llorente and Luna, 2013). Ecological risk is related to environmental degradation resulting from aquaculture activities, such as the introduction of genetically modified or exotic species (Tidbury *et al.*, 2016), as well as the effects of new production systems.

Risk research in aquaculture has primarily focused on assessing ecological risks (Tidbury *et al.*, 2016) or economic approaches that analyze production at the farm level (Araneda *et al.*, 2011; Piamsomboon *et al.*, 2015). Some studies have evaluated fish farmers' perceptions of risks related to climate or disease (Chitmanat *et al.*, 2016; Kabir *et al.*, 2017), while others have adopted more analytical approaches using bioeconomic models, which allowed them to identify, through sensitivity analyses, the most

appropriate ways to improve farming and determine risk levels associated with shrimp diseases (Estrada-Pérez *et al.*, 2020). Luna *et al.* (2023) classify risks into four main categories: market, production, technological, and regulatory risks. Furthermore, Posadas and Hanson (2006) pointed out that many proposals continue to be evaluated using a deterministic approach, in which all biological, technological, and economic inputs are considered stable and without variance. Finally, other research has focused on the study of production and operational risks, as well as market risks (Asche, 2008; Llorente and Luna, 2013; Gobillon *et al.*, 2016; Khan *et al.*, 2018).

Based on previous studies highlighting the productive efficiency of hyper-intensive aquaculture systems (Chatvijitkul *et al.*, 2017; Junge *et al.*, 2017), this study hypothesized that the hyper-intensive (HI) system not only offers a better benefit-cost ratio but also higher yields per unit area and per kilogram produced compared to semi-intensive (SI) and intensive (I) systems in commercial production taking place in the municipality of San Blas, Nayarit, Mexico. Therefore, the objective of this study was to comparatively evaluate technical variables (production, survival) and economic variables (benefit-cost ratio, internal rate of return (IRR), and break-even point) using principal component and profitability analyses to identify the most sustainable and viable system in productive and financial terms.

MATERIALS AND METHODS

The analysis of the technical and economic variables of three commercial farms dedicated to the production of white shrimp (*Penaeus vannamei*), cultivated under three cultivation systems, was carried out in the municipality of San Blas, in Nayarit, Mexico. The study variables were the cultured hectares (ha), annual cycles, stocking density (org m^{-2} and/or org m^{-3}), survival (%), final size (g), production ($\text{kg ha}^{-1} \text{ cycle}^{-1}$), selling price in 2023 (USD), equipment and services used (motor, pump, pump filters, water intake, ponds, aerators, greenhouse, pipe, post-larvae, drugs, electricity, labor, feed, diesel, pond preparation, molasses, harvest, probiotic, silica sand), fixed costs (USD year^{-1}), variable costs (USD year^{-1}), total costs (USD year^{-1}), net income (USD year^{-1}), break-even point (BEP, kg cycle^{-1} ; USD cycle^{-1}), benefit-cost (B:C), and internal rate of return (IRR).

Technical variables

Semi-intensive system (SI)

Production data from the shrimp farm "Oro Azul" were analyzed. The farm has a surface area of 13 000 m^2 of water, where 15.4 organisms per square meter (org m^{-2}) are regularly stocked, with an average survival rate of 73 %. Four cycles are carried out during the year. This farm produces 5800 kg year^{-1} , with an average shrimp size of 10 g, which are sold locally at an average price of USD 4 per kg^{-1} .

Intensive system (I)

Production data from the “Natanael López” farm was analyzed. This farm has a water surface area of 20 000 m², where 28 org m⁻² are regularly stocked, with an average survival rate of 69 %. Three cycles are carried out per year. At this facility, 20 336 kg of fish are obtained per year, with an average size of 13 g, which are sold locally at an average price of USD 4.36 per kg⁻¹.

Hyper-intensive (HI) system

Production data from a shrimp farm belonging to the Coastal Bioengineering Laboratory of the Autonomous University of Nayarit was analyzed. This farm has a water surface area of 315 m², where 500 org m⁻³ are regularly stocked in circular geomembrane ponds, with an average survival rate of 78.3 % over four cycles per year. These facilities yield 4587.59 kg year⁻¹ with an average size of 9.3 g, which are sold locally at an average price of USD 5.89 kg⁻¹.

The information was obtained through direct interviews with farm owners and production managers. The collected data were verified against the daily logbooks kept by the farms for monitoring purposes.

Economic variables

Total cost

The costs considered for culture over one year (C_t) were considered according to Horngren *et al.* (2012):

$$C_t = C_f - C_v$$

where C_t is the total annual cost, C_f are the annual fixed costs, and C_v are the annual variable costs. The net income (nr) was determined as a function of time:

$$nr_t = i_t - c_t$$

where the total income (i_t) is the product of the total shrimp biomass (kg) multiplied by its market price.

Break-even point

The break-even point (BEP) was calculated according to Shawon *et al.* (2018):

$$BEP = \frac{C_f}{I_s - C_v}$$

where C_f are the fixed costs, I_s is the income per kilogram of shrimp (USD), and C_v are the variable costs needed to produce one kilogram of shrimp.

Cost-benefit ratio

To calculate the benefit-cost ratio ($B:C$), the total revenue (I_T) was evaluated in relation to the total costs (C_t).

$$B:C = \frac{I_T}{C_t}$$

Internal rate of return

For the calculation of the internal rate of return (IRR), a five-year period was estimated. The present value (PV/VP) was calculated using a cash flow for the same period of time, considering the net present value (NPV/VPN).

Profitability analysis

To determine how profitable the culture systems are over time, a direct profitability analysis was carried out with projections to 1, 5, and 10 years, based on technical-economic factors as well as financial profitability (Hornngren *et al.*, 2012) with the following formula:

$$\text{Profitability (\%)} = (\text{Net income} / \text{Total costs}) * 100$$

Principal component analysis

A total of 35 technical and economic variables were evaluated using principal component analysis. The variables were normalized and subsequently analyzed and rotated using VARIMAX with Kaiser normalization, using an orthogonal rotation procedure to improve their interpretability (Milstein *et al.*, 2005), with the SPSS v26 software (IBM SPSS Statistics, Armonk, NY, USA).

RESULTS AND DISCUSSION

There is a marked trend toward intensifying global shrimp production systems to reduce confinement space, avoid overexploitation of land, and decrease the impact of wastewater discharges on systems adjacent to farming units. However, production intensification presents several limitations, such as the need for trained personnel, operating equipment, cultivation techniques, market knowledge, initial capital, risk of disease, and facilities, among other factors. It also offers advantages such as smaller cultivation areas, better control of the physicochemical variables of water quality, use of *in situ* analysis equipment, higher yields per hectare, better product quality, and consistent production cycles throughout the year. However, much of the literature on sustainability lacks a systematic, data-driven approach that would allow for the identification of the most sustainable production systems or species (Engle and D'Abramo, 2016).

Technical variables

To determine the costs of the cultivation systems and to infer which offers the highest yields, the costs associated with the technical and economic variables were tallied (Table 1) and compared (Table 2). Although the HI system uses higher stocking densities compared to the other systems, the final production per hectare was also higher. System I incurred the highest costs, particularly in labor, post-larvae, and feed. This disparity is attributed to the fact that intensive systems operate over relatively large cultivation areas while primarily adjusting the stocking density, which consequently raises the expenses for these variables (Ahsan, 2011). This pattern aligns with the limitations typically associated with intensified systems (Le and Cheong, 2010). Survival rates were higher in system HI. However, system I recorded the smallest final size, surpassing system HI in this aspect. These results suggest that, in addition to being associated with the level of confinement of the organisms, whether due to lack of space or competition for food, other factors influence this variable, such as the genetic line of the postlarvae, weather conditions, and the overall management practices of the farm.

Table 1. Technical variables of the three culture systems evaluated in the municipality of San Blas, in Nayarit, Mexico.

Variable	Amount		
	Semi-intensive (SI)	Intensive (I)	Hyperintensive (HI)
Hectares	1.3	2.0	0.0315
Annual cycles	4	3	4
Stocking density (m ⁻² , m ⁻³)	15.4	28.0	500
Survival (%)	73.0	69.0	78.3
Final weight (g)	10.0	13.0	9.3
Production (kg ha ⁻¹ cycle ⁻¹)	1124.33	2511.60	36 409.20
Sale price (USD)	4.00	4.36	5.90
Pump (parts)	1	1	0
Pump filters (parts)	1	1	2
Water inlet (parts)	0	0	1
Tanks (parts)	1	4	9
Aerators (parts)	0	5	1
Greenhouse (parts)	0	0	1
Polyvinyl chloride (PVC) accessories	0	0	Several
Postlarvae (organisms)	800 800	1 680 000	630 000
Drugs (part)	0	0	2
Electricity (kW h ⁻¹)	0	81 176.47	30 545
Labor force (employees)	2.00	3.00	2.00
Food (kg)	5903.13	18 648.64	2810.84
Diesel (L)	4700	5800	0
Pond preparations	4	4	1
Molasses (L)	106	213	248
Harvest (people employed)	4	1	0
Probiotic (L)	0	20	15
Silica sand (kg)	0	0	300

Table 2. Cost of the technical variables in the three culture systems evaluated in the municipality of San Blas, in Nayarit, Mexico.

Variable	Cost (USD)*		
	Semi-intensive (SI)	Intensive (I)	Hyperintensive (HI)
Production (kg ha ⁻¹ cycle ⁻¹)	4496.80	7534.80	145 636.80
Sale price	4.00	4.36	5.90
Engines	2051.28	2051.28	422.82
Pumps	4102.56	4102.56	0
Pump filters	82.05	82.05	3610.56
Water inlets	1025.64	1025.64	1897.44
Tanks	8717.95	13 333.33	12 406.15
Aerators	0	2769.23	1205.13
Greenhouse	0	0	24 079.79
Polyvinyl chloride (PVC) accessories	0	0	519.85
Postlarvae	3285.33	6892.31	2584.62
Drugs	0	0	511.38
Electricity	0	3538.46	1331.49
Labor force	2461.54	3461.54	2531.08
Food	5600.41	17 692.31	2666.67
Diesel	2461.54	6923.08	0
Pond preparations	615.38	707.69	0
Molasses	30.77	61.54	71.79
Harvest	1554.62	517.95	0
Probiotic	0	461.54	215.38
Silica sand	0	0	12.21

*Costs are expressed in USD, based on an exchange rate of 19.8 MXN/USD for the year 2023.

Economic variables

In terms of costs (Table 3), System I had the highest expenses for labor, postlarvae, and feed, in addition to harvesting costs due to poor pond design that hindered gravity harvesting. Although system HI incurred the highest fixed and total costs, it also generated the highest net income. This distinction is due to the direct relationship between stocking density and economic returns (Chatvijitkul *et al.*, 2017). However, this same system required a higher break-even point (BEP) (588.89 kg cycle⁻¹), which implies that it needs approximately 50 % of its usual production to avoid losses, in contrast to the 5.64 and 18.92 % observed in systems I and SI, respectively (Figure 1). The IRR results show that system I achieved 30.18 %, surpassing system HI by 18 % and system SI by 22 %. This indicates that for every USD invested, an annual return of 30 % is expected, reflecting that system I generates greater value per unit of investment. Although system HI presents a lower return percentage, it compensates with higher absolute income but requires a longer time to recover the initial investment.

Table 3. Economic variables of the three culture systems evaluated in the municipality of San Blas, in Nayarit, Mexico.

Variable	Production system		
	Semi-intensive (SI)	Intensive (I)	Hyperintensive (HI)
Fixed costs (USD year ⁻¹)	15 979.49	23 364.10	44 422.87
Variable costs (USD year ⁻¹)	16 009.59	40 256.41	7688.72
Total costs (USD)	16 522.41	41 037.59	54 419.28
Net income (USD year ⁻¹)	7914.54	26 212.77	14 857.36
BEP (kg cycle ⁻¹)	365.89	282.14	588.89
BEP (USD cycle ⁻¹)	1463.57	1229.86	3472.94
Cost-benefit analysis (B:C)	1.51	1.66	1.21
IRR (%)	7.53	30.18	11.56

BEP: break-even point; IRR: internal rate of return.

These results are consistent with previous studies (Junge *et al.*, 2017), which indicate that initial investments increase operating costs during the first cycles; however, these costs tend to decrease over time, favoring long-term economic sustainability (Rego *et al.*, 2017). Barros *et al.* (2018) reported that the largest investment (43.18 %) is concentrated in the acquisition of the cultivation system equipment, while only 11.9 % corresponds directly to shrimp farming. The present study confirmed this pattern, identifying even higher percentage values. Furthermore, Rego *et al.* (2017) indicate that, in biofloc systems, expenses can be 10 times higher compared to conventional systems due to the use of more extensive equipment to maintain adequate oxygen levels. According to Junge *et al.* (2017), the highest costs occur in systems with artificial bottoms, as they require more technology and skilled labor, which increases production costs.

The HI system recorded the highest total costs in this study, primarily because of the initial investment. Most of these costs were concentrated in greenhouse construction, geomembrane installation, pumps, blowers, piping, acquisition of reagents for measuring the water's physicochemical variables, labor, periodic pumping, molasses application for nitrogen regulation, and constant aeration, which resulted in higher electricity consumption. In contrast, the costs for the other systems were primarily related to the ponds. However, these initial costs gradually amortize over time, thereby reducing operating costs in future cycles and allowing for a gradual increase in net income.

Despite the high initial costs, the HI system generates higher revenues due to its greater production and selling price, with potential for improved profitability as the investment is amortized. These results are consistent with Chatvijitkul *et al.* (2017) regarding the positive relationship between stocking density and economic yields (Table 4).

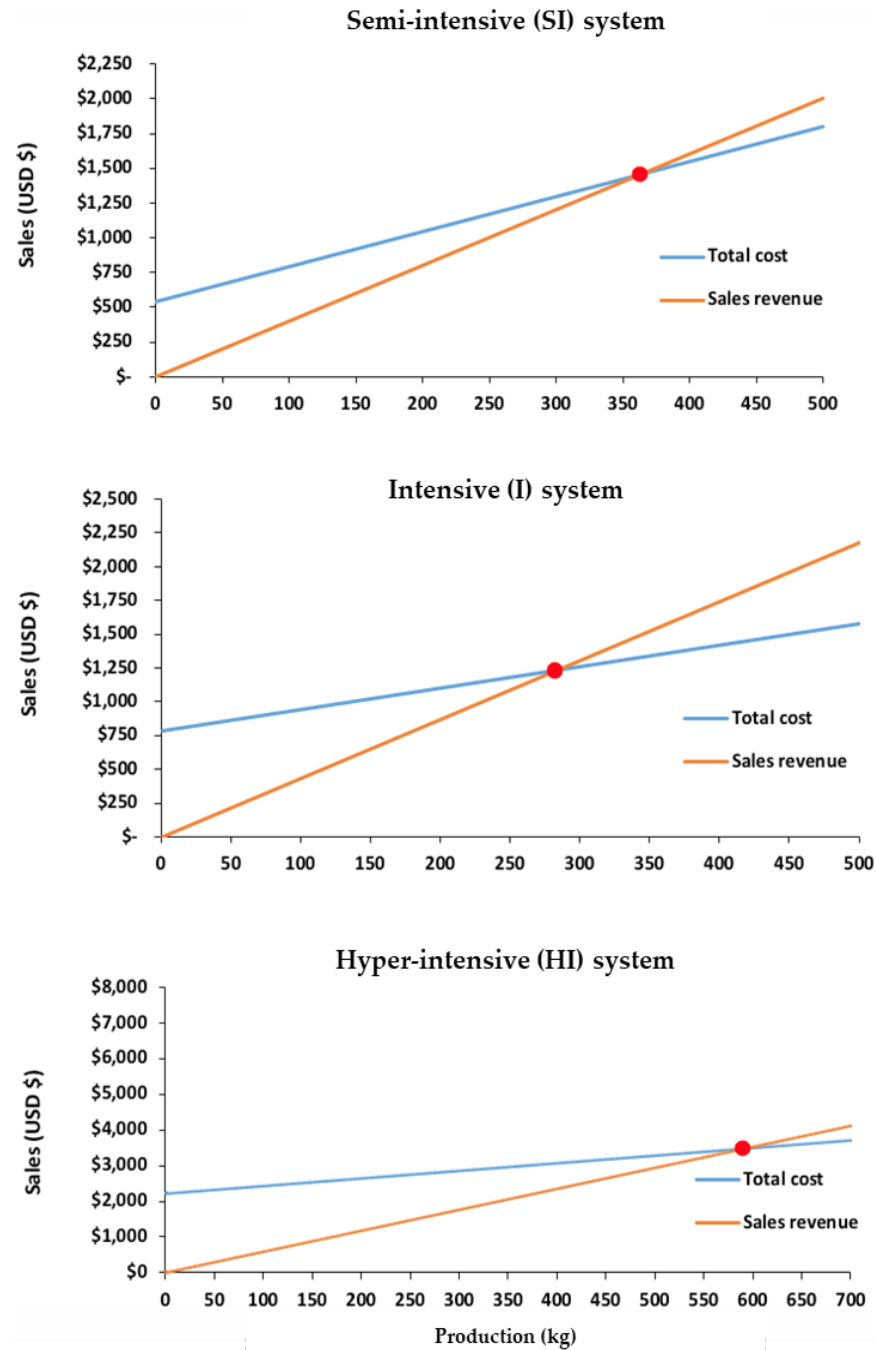


Figure 1. Break-even points resulting from the analysis of total costs (green line) in relation to net income (orange line) per crop cycle in the three production systems evaluated.

Table 4. Time horizon of profitability (%) by system at different years of operation (1, 5, and 10 years).

System	1 year	5 years	10 years
Semi-intensive (SI)	47.9 %	~50 %*	~52 %*
Intensive (I)	63.9 %	~65 %*	~68 %*
Hyperintensive (HI)	27.3 %	40–45 % (after amortization)	50–55 % (optimum)

*Projections based on the reduction of fixed costs through amortization and operational efficiency.

Principal component analysis

The component matrix showed that the highest costs were concentrated in initial expenses, not in post-larvae or feed, which contrasts with the findings of Ponce-Palafox *et al.* (2011). However, revenues increased with higher stocking densities and levels of technology (Chatvijitkul *et al.*, 2017), contrary to the findings of Boyd *et al.* (2016) and Engle *et al.* (2017). Furthermore, the principal component analysis clearly identified two orthogonal linear combinations derived from the 35 original variables (Table 5, Figure 2), which explained 62.25 % of the total variation.

Table 5. Rotated factor matrix derived from principal component analysis applied to 35 variables in the three evaluated farming systems (semi-intensive, intensive, and hyperintensive).

Variable	Component	
	1	2
Hectares	-0.869	0.495
Cycles	0.356	-0.934**
Planting density (m ²)	0.991**	-0.136
Survival (%)	0.824	-0.567
Weight(g)	-0.517	0.856
Production (kg ha ⁻¹ cycle ⁻¹)	0.992**	-0.124
Production (kg ha ⁻¹ year ⁻¹)	0.990**	-0.140
Sale price (USD)	0.999**	0.020
Fixed costs (USD)	0.995**	0.093
Variable costs (USD)	-0.575	0.818
Total costs (USD)	0.862	0.508
Net income (USD)	0.021	0.999**
BEP (kg cycle ⁻¹)	0.910**	-0.414
BEP (\$ cycle ⁻¹)	0.968	-0.251
Benefit-cost (B:C)	-0.881	0.473
IRR	-0.196	0.980**
Engines	-0.987**	0.159
Pumps	-0.987**	0.159

Table 5. Continued.

Variable	Component	
	1	2
Filters	0.987**	-0.159
Water inlets	0.987**	-0.159
Tanks	0.472	0.881
Aerators	0.084	0.996**
Greenhouse	0.987**	-0.159
Pipelines	0.987**	-0.159
Postlarvae	-0.494	0.870
Drugs	0.987**	-0.159
Electricity	0.017	0.999**
Labor	-0.297	0.955**
Food	-0.522	0.853
Diesel	-0.661	0.750
Pond preparation	-0.961**	0.276
Molasses	0.799	0.601
Harvest	-0.850	-0.527
Probiotics	0.121	0.992**
Silica sand	0.987**	-0.159

BEP: break-even point; IRR: internal rate of return. **Significant parameter ($p < 0.05$).

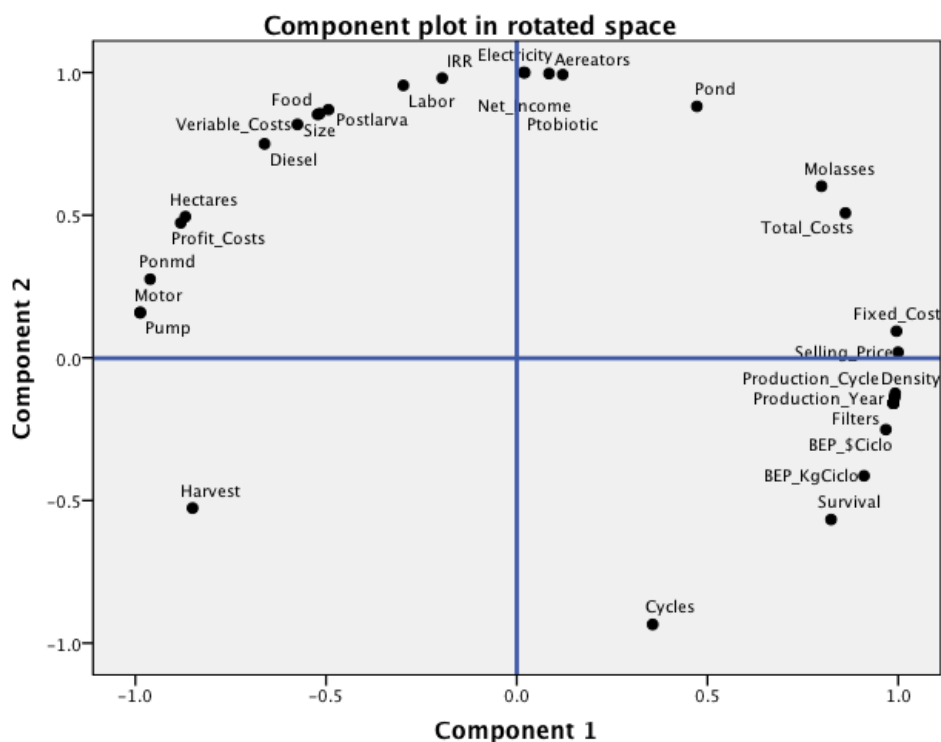


Figure 2. Principal component graph comparing the technical and economic aspects of shrimp farming production in the municipality of San Blas, Nayarit, Mexico.

In the first component, 16 main variables were identified (loads with absolute values ≥ 0.9): three with a negative sign (two related to fixed costs: engine and pump) and 13 with a positive sign. Among the latter, five are related to net income (production $\text{kg ha}^{-1} \text{ cycle}^{-1}$, production $\text{kg ha}^{-1} \text{ year}^{-1}$, selling price, BEP kg cycle^{-1} , and BEP USD cycle^{-1}), four correspond to total costs (fixed costs, water inlets, greenhouse, and piping), and three are associated with variable costs (filters, drugs, and silica sand). All these variables represent essential expenses for the operation of the system, which increase as stocking densities rise and the cultivated area is expanded.

The second component showed seven main variables (loads with absolute values ≥ 0.9). Five were positive, two of which are related to net income based on annual production, while three correspond to variable costs directly associated with increased stocking density (aerators, electricity, and probiotics), whose demand increases to meet the organism's requirements as density rises. One variable had a negative sign (culture cycles). These patterns support the idea that more technologically advanced systems require higher initial expenses but generate better returns per unit area (Hernández-Llamas *et al.*, 2013; Estrada-Pérez *et al.*, 2015).

Hierarchical cluster analysis (Figure 3) revealed two distinct groups: one comprised of systems SI and I, characterized by similar techniques and costs, and another

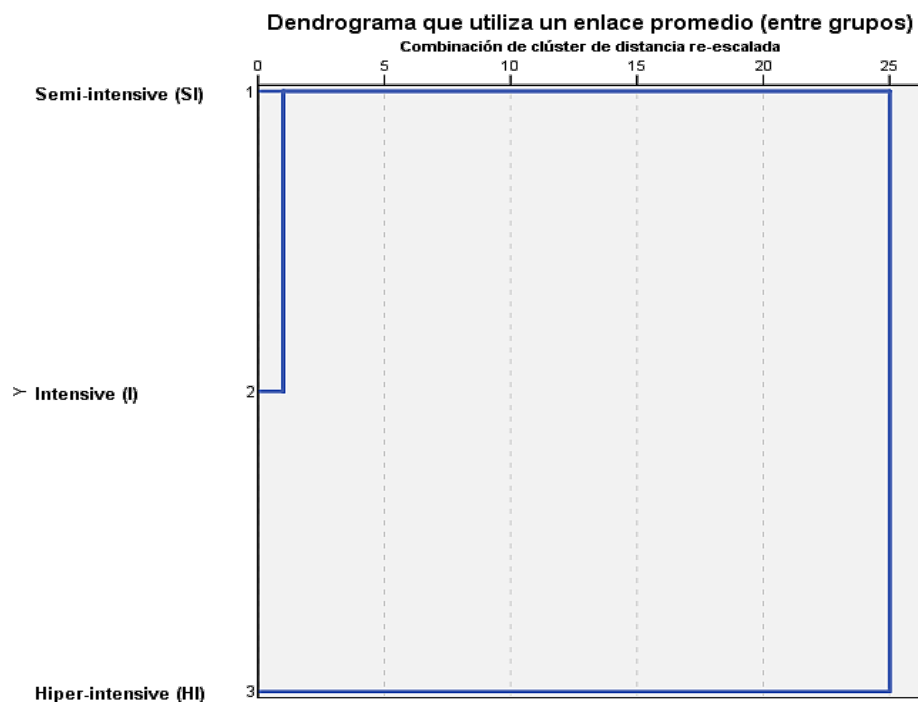


Figure 3. Dendrogram of farming system groups (semi-intensive, intensive, hyperintensive), comparing the technical and economic aspects of shrimp production in the municipality of San Blas Nayarit, Mexico.

corresponding to system HI, which exhibited significant disparities in total costs and final production. These differences reflect the potential of hyperintensive systems to maximize production in a smaller area, albeit at a considerably higher initial cost. It is worth noting that the potential of hyperintensive shrimp farming is remarkable, as it can generate equal or greater yields ($\text{kg ha}^{-1} \text{ cycle}^{-1}$) in a smaller area, and not necessarily at a higher operating cost.

CONCLUSIONS

The results of the technical and economic analyses showed improvements as stocking density increased, reflected in higher yields. These increases allowed fixed costs to be spread over time through amortization, maintaining favorable economic results, since the burden of initial expenses ceases to have an impact as the operation progresses. Within the range of yields and systems evaluated, the more intensive system proved to be more economical in the long term. The analysis showed that higher-intensity systems use fewer resources per unit of shrimp produced. It is recommended to continue evaluating groups of farming systems based on sets of management practices identified through multivariate analysis, rather than relying solely on a single variable such as stocking density.

ACKNOWLEDGEMENTS

We thank the production units “Oro azul”, owned by Mr. Felipe Ramos; Natanael López, owned by Mr. Natanael López; and the Coastal Bioengineering Laboratory of the Autonomous University of Nayarit.

REFERENCES

- Ahsan DA. 2011. Farmers’ motivations, risk perceptions and risk management strategies in a developing economy: Bangladesh experience. *Journal of Risk Research* 14 (3): 325–349. <https://doi.org/10.1080/13669877.2010.541558>
- Araneda M, Hernández JM, Gasca E. 2011. Optimal harvesting time of farmed aquatic populations with nonlinear size-heterogeneous growth. *Natural Resource Modeling* 24 (4): 477–513. <https://doi.org/10.1111/j.1939-7445.2011.00099.x>
- Asche F. 2008. Farming the sea. *Marine Resource Economics* 23 (4): 527–547. <https://doi.org/10.1086/mre.23.4.42629678>
- Barros LC, Almeida FH, Henriques MB, Seiffert WQ. 2018. Economic evaluation of the commercial production between Brazilian samphire and whiteleg shrimp in an aquaponics system. *Aquaculture International* 26 (5): 1187–1206. <https://doi.org/10.1007/s10499-018-0277-8>
- Boyd CE, McNevin AA, Racine P, Tinh HQ, Minh HN, Viriyatum R, Paungkaew D, Engle C. 2016. Resource use of shrimp *Litopenaeus vannamei* and *Penaeus monodon* production in Thailand and Vietnam. *Journal of the World Aquaculture Society* 48 (2): 201–226. <https://doi.org/10.1111/jwas.12394>

- Buarque C. 1984. *Avaliação econômica de projetos: uma apresentação didática*. Elsevier Campus: Rio de Janeiro, Brasil.
- Chatvijitkul S, Boyd CE, Davis DA, McNevin AA. 2017. Embodied resources in shrimp and fish feeds. *Journal of the World Aquaculture Society* 48 (1): 7–19. <https://doi.org/10.1111/jwas.12360>
- Chitmanat C, Lebel P, Whangchai N, Promya J, Lebel L. 2016. Tilapia diseases and management in river-based cage aquaculture in northern Thailand. *Journal of Applied Aquaculture* 28 (1): 9–16. <https://doi.org/10.1080/10454438.2015.1104950>
- Dávila-López KM, Carvajal-Romero HR, Vite-Cevallos HA. 2020. Análisis de rentabilidad económica del camarón (*Litopenaeus vannamei*) en el sitio Balao Chico, provincia del Guayas. *Polo del Conocimiento* 5 (1): 450–476.
- Drabo A. 2017. Climate change mitigation and agricultural development models: Primary commodity exports or local consumption production. *Ecological Economics* 137: 110–125. <https://doi.org/10.1016/j.ecolecon.2017.03.014>
- Engle CR, D'Abramo L. 2016. Showcasing research focusing on sustainability of aquaculture enterprises and global food security. *Journal of the World Aquaculture Society* 47 (3): 311–313. <https://doi.org/10.1111/jwas.12296>
- Engle CR, McNevin A, Racine P, Boyd CE, Paungkaew D, Viriyatum R, Minh HN. 2017. Economics of sustainable intensification of aquaculture: Evidence from shrimp farms in Vietnam and Thailand. *Journal of the World Aquaculture Society* 48 (2): 227–239. <https://doi.org/10.1111/jwas.12423>
- Estrada-Pérez M, Ruiz-Velazco JM, Hernández-Llamas A, Zavala-Leal I. 2015. A bio-economic approach to analyze the role of alternative seeding-harvesting schedules, water quality, stocking density and duration of cultivation in semi-intensive production of shrimp in Mexico. *Latin American Journal of Aquatic Research* 43 (3): 466–472. <https://doi.org/10.3856/vol43-issue3-fulltext-8>
- Estrada-Pérez N, Ruiz-Velazco JM, Hernández-Llamas A. 2020. Economic risk scenarios for semi-intensive production of *Litopenaeus (Penaeus) vannamei* shrimp affected by acute hepatopancreatic necrosis disease. *Aquaculture Reports* 18: 100442. <https://doi.org/10.1016/j.aqrep.2020.100442>
- Flaherty M, Samal KC, Pradhan D, Ray S. 2009. *Coastal aquaculture in India: Poverty, environment and rural livelihood*. Concept Publishing Company: New Delhi, India. 296 p.
- Gobillon L, Wolff FC, Guillotreau P. 2016. The effect of buyers and sellers on fish market prices. The effect of buyers and sellers on fish market prices. *European Review of Agricultural Economics* 44 (1): 149–176. <https://doi.org/10.1093/erae/jbw006>
- Hamilton K, Chen A, de-Graft E, Gitter A, Kozak S, Niquice C, Gurian P. 2018. *Salmonella* risks due to consumption of aquaculture-produced shrimp. *Microbial Risk Analysis* 9: 22–32. <https://doi.org/10.1016/j.mran.2018.04.001>
- Hernández-Llamas A, Ruiz-Velazco JM, Gómez-Muñoz VM. 2013. Economic risk associated with white spot disease and stochastic variability in economic, zootechnical and water quality parameters for intensive production of *Litopenaeus vannamei*. *Reviews in Aquaculture* 5 (2): 121–131. <https://doi.org/10.1111/raq.12008>
- Horngren CT, Datar SM, Rajan MV. 2012. *Cost accounting: A managerial emphasis* (14th edition). Prentice Hall: Hoboken, NJ, USA. 730 p.
- Junge R, König B, Villarroel M, Komives T, Jijakli MH. 2017. Strategic points in aquaponics. *Water* 9 (3): 182. <https://doi.org/10.3390/w9030182>

- Kabir MJ, Cramb R, Alauddin M, Roth C, Crimp S. 2017. Farmers' perceptions of and responses to environmental change in southwest coastal Bangladesh. *Asia Pacific Viewpoint* 58 (3): 362–378. <https://doi.org/10.1111/apv.12165>
- Khan A, Guttormsen A, Roll KH. 2018. Production risk of pangas (*Pangasius hypophthalmus*) fish farming. *Aquaculture Economics and Management* 22 (2): 192–208. <https://doi.org/10.1080/13657305.2017.1284941>
- Le TC, Cheong F. 2010. Perceptions of risk and risk management in Vietnamese catfish farming: an empirical study. *Aquaculture Economics and Management* 14 (4): 288–314. <https://doi.org/10.1080/13657305.2010.526019>
- Little DC, Newton RW, Beveridge MCM. 2016. Aquaculture: A rapidly growing and significant source of sustainable food? Status, transitions and potential. *Proceedings of the Nutrition Society* 75 (3): 274–286. <https://doi.org/10.1017/S0029665116000665>
- Llorente I, Luna L. 2013. The competitive advantages arising from different environmental conditions in seabream, *Sparus aurata*, production in the Mediterranean Sea. *Journal of the World Aquaculture Society* 44 (5): 611–627. <https://doi.org/10.1111/jwas.12069>
- Luna M, Llorente I, Luna L. 2023. A conceptual framework for risk management in aquaculture. *Marine Policy* 147: 105377. <https://doi.org/10.1016/j.marpol.2022.105377>
- Milstein A, Islam MS, Wahab MA, Kamal AHM, Dewan S. 2005. Characterization of water quality in shrimp ponds of different sizes and with different management regimes using multivariate statistical analysis. *Aquaculture International* 13 (6): 501–518. <https://doi.org/10.1007/s10499-005-9001-6>
- Ottinger M, Clauss K, Kuenzer C. 2016. Aquaculture: Relevance, distribution, impacts and spatial assessments – A review. *Ocean and Coastal Management* 119: 244–266. <https://doi.org/10.1016/j.ocecoaman.2015.10.015>
- Piamsomboon P, Inchaosri C, Wongtavatchai J. 2015. White spot disease risk factors associated with shrimp farming practices and geographical location in Chanthaburi province, Thailand. *Diseases of Aquatic Organisms* 117 (2): 145–153. <https://doi.org/10.3354/dao02929>
- Ponce-Palafox JT, Ruiz-Luna A, Castillo-Vargasmachuca S, García-Ulloa M, Arredondo-Figueroa JL. 2011. Technical, economics and environmental analysis of semi-intensive shrimp (*Litopenaeus vannamei*) farming in Sonora, Sinaloa and Nayarit states, at the east coast of the Gulf of California, México. *Ocean and Coastal Management* 54 (7): 507–513. <https://doi.org/10.1016/j.ocecoaman.2011.03.008>
- Posadas BC, Hanson TR. 2006. Economics of integrating nursery systems into indoor biosecure recirculating saltwater shrimp grow-out systems. In *Shrimp Culture: Economics, Market, and Trade*. Wiley: Hoboken, NJ, USA, pp: 279–289. <https://doi.org/10.1002/9780470277850.ch18>
- Rego MAS, Sabbag OJ, Soares R, Peixoto S. 2017. Financial viability of inserting the biofloc technology in a marine shrimp *Litopenaeus vannamei* farm: A case study in the state of Pernambuco, Brazil. *Aquaculture International* 25 (1): 473–483. <https://doi.org/10.1007/s10499-016-0044-7>
- Shawon NAA, Prodhan MMH, Khan MA, Mitra S. 2018. Financial profitability of small scale shrimp farming in a coastal area of Bangladesh. *Journal of the Bangladesh Agricultural University* 16 (1): 104–110. <https://doi.org/10.3329/jbau.v16i1.36490>
- Tidbury HJ, Taylor NGH, Copp GH, Garnacho E, Stebbing PD. 2016. Predicting and mapping the risk of introduction of marine non-indigenous species into Great Britain and Ireland. *Biological Invasions* 18 (11): 3277–3292. <https://doi.org/10.1007/s10530-016-1219-x>

Zhang D, Tveterås R. 2019. A fish out of water? Survival of seafood products from developing countries in the EU market. *Marine Policy* 103: 50–58. <https://doi.org/10.1016/j.marpol.2019.02.030>

Agrociencia

CHALLENGES IN THE SUSTAINABILITY OF GOAT PRODUCTION SYSTEMS IN ZACATECAS, MEXICO

Ma. Enriqueta Luna-Coronel¹, Alberto Muro-Reyes¹, Einar Vargas-Bello-Pérez², Alejandro Espinoza-Canales¹, Daniel García-Cervantes¹, Héctor Gutiérrez-Bañuelos^{1*}

¹Universidad Autónoma de Zacatecas. Unidad Académica de Medicina Veterinaria y Zootecnia. Carretera Panamericana km 31.5, El Cordovel, Enrique Estrada, Zacatecas, Mexico. C. P. 98500.

²Universidad Autónoma de Chihuahua, Facultad de Zootecnia y Ecología. Periférico R. Aldama km 1, Chihuahua, Mexico. C. P. 31031.

* Author for correspondence: hgutierrez@uaz.edu.mx

ABSTRACT

Goat (*Capra hircus* Linnaeus, 1758) production is a key livelihood activity in Zacatecas, Mexico, but it faces increasing environmental, social, and economic pressures typical of dryland systems. This study offers an integrative narrative review with a systematic search and transparent selection criteria to synthesize evidence on the sustainability of goat production systems in Zacatecas. Peer-reviewed literature and technical documents were analyzed alongside official contextual indicators. The synthesis shows a decline in the caprine sector over recent census periods, with a producer profile marked by demographic vulnerability. Across the evidence, sustainability challenges stem from interconnected pathways where drought and rainfall variability decrease forage and water availability, worsen seasonal feed shortages, and boost reliance on purchased inputs, raising costs and increasing land degradation risks. These environmental pressures interact with herd management issues such as feeding, preventive health, parasite control, and reproduction, while limited access to coordinated services, infrastructure, and stable markets hampers value capture and reinvestment. Significant evidence gaps remain for Zacatecas-specific, outcome-based assessments (profitability during drought, rangeland condition metrics, health burdens, and value-chain performance), indicating the need for ongoing monitoring. Key leverage points include drought preparedness and feed planning, improving water access, preventive herd health, strengthening producer organizations and extension services, and developing feasible value-added options for dairy and meat products.

Keywords: drylands, drought resilience, rural livelihoods, value chain, feed planning.

INTRODUCTION

Goat production is a key part of smallholder livelihoods in Mexico's drylands, where herds contribute to household income and food supply through meat and milk. Nationally, goat farming mainly takes place in arid and semi-arid regions and is mostly extensive; more than 70 % of goats are raised in extensive systems, with fewer in intensive and semi-intensive systems (Tajonar *et al.*, 2022). These systems are

Citation: Luna-Coronel ME, Muro-Reyes A, Vargas-Bello-Pérez E, Espinoza-Canales A, García-Cervantes D, Gutiérrez-Bañuelos H. 2026. Challenges in the sustainability of goat production systems in Zacatecas, Mexico. *Agrociencia* 60(3): 318-338. <https://doi.org/10.47163/agrociencia.v60i3.3447>

Editor in Chief:
Dr. Fernando C. Gómez Merino

Received: March 14, 2025.

Approved: March 24, 2026.

Published in Agrociencia:
April 22, 2026.

This work is licensed under a Creative Commons Attribution-Non-Commercial 4.0 International license.



usually multi-functional and rooted in local food traditions, providing kids with meat and various dairy products. Goat milk is known as a nutrient-rich food containing proteins, vitamins, and minerals, and goat meat is often described as a lean red meat with a favorable protein-to-fat ratio (Al-Kaisy *et al.*, 2023; Gawat *et al.*, 2023).

In Zacatecas, goat production operates under environmental constraints and structural limitations that affect both productivity and resilience. The National Institute of Statistics and Geography (INEGI) Agricultural Census 2022 tabulations report 5946 goat-keeping production units in the state, and census comparisons indicate a substantial contraction of the activity since 2007 (INEGI, 2023). This contraction is relevant for sustainability because it is consistent with mounting pressures on dryland livelihoods, including climate-related forage and water constraints, rising costs and market uncertainty, and barriers to upgrading and value addition in smallholder value chains.

Sustainability, broadly defined, means meeting current needs without harming the ability of future generations to meet their own needs by integrating environmental health, economic sustainability, and social fairness (WCED, 1987). Applying this concept to goat production involves examining how climate and resource limits affect household income, animal health, and value-chain performance. This is especially crucial in semiarid areas where rangeland conditions and management are key factors affecting feed availability and environmental outcomes. Studies across the San Luis Potosi-Zacatecas high plateau describe ongoing rangeland decline, emphasizing the need to align livestock practices with ecosystem capacity (Aguirre-Rivera *et al.*, 2023). In these environments, goats can serve as both a flexible resource and a system at risk, depending on forage availability, grazing practices, and access to services and markets (Tajonar *et al.*, 2022).

Goat production systems in Mexico show significant diversity, ranging from extensive to semi-intensive and intensive approaches, each with unique trade-offs in productivity, input needs, welfare, and environmental impact (Chávez-Espinoza *et al.*, 2022; Tajonar *et al.*, 2022). Mixed crop-livestock systems are also common in drylands, where crops and livestock interact through residue use, nutrient cycling, and risk management, which can boost system resilience when managed properly (Schiere *et al.*, 2006). However, in Zacatecas, the evidence remains scattered across environmental, socio-demographic, technical, and market aspects, limiting a full understanding of sustainability challenges and opportunities.

Therefore, this review synthesizes current knowledge on the sustainability of goat production systems in Zacatecas, Mexico, by combining environmental, social, and economic aspects. Key challenges and opportunities for sustainable development were identified, along with suggested research priorities and interventions aimed at enhancing resilience, productivity, and livelihoods within the state's goat production systems sector.

MATERIALS AND METHODS

This work is an integrative narrative review with a systematized search and transparent selection criteria, designed to synthesize evidence on the sustainability of goat production systems in Zacatecas, Mexico. The integrative review approach was chosen because it allows the inclusion and synthesis of diverse evidence (peer-reviewed studies, technical reports, and institutional documents) while maintaining methodological rigor through clear procedures for identification, screening, and data extraction (Whittemore and Knafl, 2005).

Information sources

Two complementary evidence streams were used: (1) Official statistical sources for regional context and trend indicators relevant to sustainability: the National Institute of Statistics and Geography (INEGI) (Agricultural Census); the Agri-food and Fisheries Information Service (SIAP)/Ministry of Agriculture and Rural Development (SADER) (livestock and agricultural statistics); and the National Council for the Evaluation of Social Development Policy (CONEVAL) (state poverty and social deprivation context for Zacatecas); and (2) scientific and technical literature (peer-reviewed articles, technical reports) addressing goat production systems, dryland livestock sustainability, value chains, rangeland/feed-water constraints, animal health challenges, and socio-economic/organizational factors relevant to Zacatecas or similar semi-arid regions.

Search strategy

Searches were carried out in both English and Spanish using combinations of keywords and Boolean operators. Examples of search strings included: (“goat” OR “caprine” OR “caprinos”) AND (“Zacatecas”) AND (“sustainability” OR “resilience” OR “value chain” OR “drought”). Also, (“sistemas de producción caprina” OR “caprinocultura”) AND (“Zacatecas”) AND (“sustentabilidad” OR “sequía” OR “cadena de valor” OR “manejo”).

Additionally, reference lists of relevant documents were screened to identify further sources (snowballing). Given the limited number of publications specifically addressing the “sustainability” of goat systems in Zacatecas, evidence from comparable semi-arid goat systems was included only when mechanisms and constraints were clearly transferable and relevance was explicitly stated. Searches were conducted in Google Scholar, PubMed, Scopus, and Latindex covering 2000–January 2026.

Eligibility criteria and screening

Documents were eligible if they (i) focused on goat production systems or closely related small-ruminant systems relevant to semi-arid regions; (ii) provided evidence related to at least one sustainability dimension (environmental, economic, or social/cultural), including cross-cutting components such as animal health and the value chain; and (iii) offered verifiable information (data, methods, or clearly documented

technical/policy evidence). Documents were excluded if they were unrelated to small ruminants, lacked methodological clarity, or contained claims without traceable sources.

Search outputs and selection transparency (PRISMA-lite)

The identification and selection process was reported following PRISMA 2020 as a reporting framework (not as a claim of a full systematic review of interventions) (Page *et al.*, 2021). The search yielded approximately 250 records; after removing duplicates, about 155 records remained for screening of titles and abstracts; roughly 62 full texts were assessed for eligibility; and around 44 documents were included in the qualitative synthesis. The main reasons for exclusion at the full-text stage were irrelevance to goat systems/semi-arid contexts, insufficient methodological detail, or lack of verifiable sources. Records were managed in Zotero, which was used to remove duplicates and support systematic screening and tagging.

Data extraction and analytical framework

Data were collected into a standardized evidence matrix that captured (i) document type, (ii) geographic scope (Zacatecas vs. comparable semi-arid contexts), (iii) production system type (extensive, semi-intensive, intensive, and mixed crop-livestock when applicable), (iv) drivers and constraints (climate variability/drought, feed and water resources, rangeland condition, animal health, labor/demography, organization and services, and markets and value chain), (v) reported outcomes and indicators (productivity proxies, costs and income proxies, vulnerability, adoption, and coordination), and (vi) evidence direction (constraint vs. opportunity). Synthesis was performed through thematic integration by (1) sustainability dimension, (2) system type, and (3) mechanism and outcome pathways to identify trade-offs, synergies, and evidence gaps (Whittemore and Knafl, 2005).

Use of official datasets in the synthesis

Official sources (INEGI, SIAP/SADER, and CONEVAL) were used to contextualize and interpret findings from the literature (such as production structure, socio-demographic vulnerability, and socio-economic constraints). These statistics were not considered “results of the review” but rather as contextual evidence supporting the interpretation of sustainability bottlenecks and leverage points in Zacatecas.

Limitation: scarcity of state-specific sustainability literature

A key limitation was the small number of publications specifically focused on the sustainability of goat production systems in Zacatecas. This was addressed by (a) incorporating robust official datasets for context and (b) selectively using evidence from comparable semi-arid systems to explain mechanisms, while explicitly identifying state-specific knowledge gaps as priorities for future research.

REGIONAL CONTEXT: GEOGRAPHY, CLIMATE, AND CENSUS-BASED GOAT SECTOR PROFILE

This section offers the regional baseline essential for understanding sustainability challenges in Zacatecas' goat production systems. The state's geographic and climatic limitations that impact forage and water availability are briefly outlined. Following this, a census-based profile of the goat sector is provided, including inventory and production units, to establish a consistent territorial framework for discussing the environmental, social, and economic pressures faced by the industry (INEGI, 2013).

Geographic and climate constraints

Zacatecas is located in north-central Mexico on the Mexican Plateau, where predominantly dry and semi-dry conditions constrain agricultural and livestock production. Official state profiles report an average annual temperature around 17 °C and an average annual precipitation of approximately 510 mm, with rainfall occurring mainly in the warm season (June–September), which creates strong seasonality in water and forage resources and heightens drought risk. These climatic constraints interact with the state's land cover and rangeland base: nearly half of Zacatecas is covered by natural vegetation, with xerophytic shrubland and grassland as major components, reinforcing the dependence of extensive livestock systems on variable rangeland productivity under dryland conditions (INEGI, 2013).

Goat sector size and structure (census-based)

INEGI census indicators show a marked long-term contraction of the caprine sector in Zacatecas (Table 1). Between 1991 and 2022, the census-based goat inventory declined by ~55 %, while the number of goat-keeping production units decreased by ~38 % between 2007 and 2022, indicating a substantial reduction in both the animal base and the production-unit base over time (INEGI, 2009, 2013, 2023). This concurrent decline provides a consistent baseline for interpreting sustainability pressures discussed in subsequent sections, particularly under dryland conditions where climate variability,

Table 1. Census-based caprine sector indicators in Zacatecas, Mexico (INEGI, 1991, 2009, 2023).

Census year	Goat inventory (head)	Goat production units
1991	431 668	Not available
2007	237 534	9659
2022	194 870 (total)	5946

Note: Goat inventory corresponds to INEGI Agricultural Census figures by entity. For 2022, INEGI reports caprine inventory separately for production units and households; the total inventory shown here is the sum of both (189 076 in production units + 5794 in households). Goat production units are reported for 2007 and 2022; a directly comparable production-unit count was not available in the 1991 census compilation used in this review.

resource constraints, and market limitations can jointly affect the viability of goat production systems.

Goat production is also spatially concentrated within the state. Based on the Individual Livestock Identification System (SIINIGA) municipal registry data for 2024, the highest registered inventories are located in Pinos, General Francisco R. Murguía, Sombrerete, Mazapil, and Río Grande, which together account for 53 % of the state's registered goat inventory (SIINIGA, 2024) (Figure 1). To emphasize the main production clusters, only municipalities reporting more than 10 000 head in the SIINIGA 2024 registry were considered.

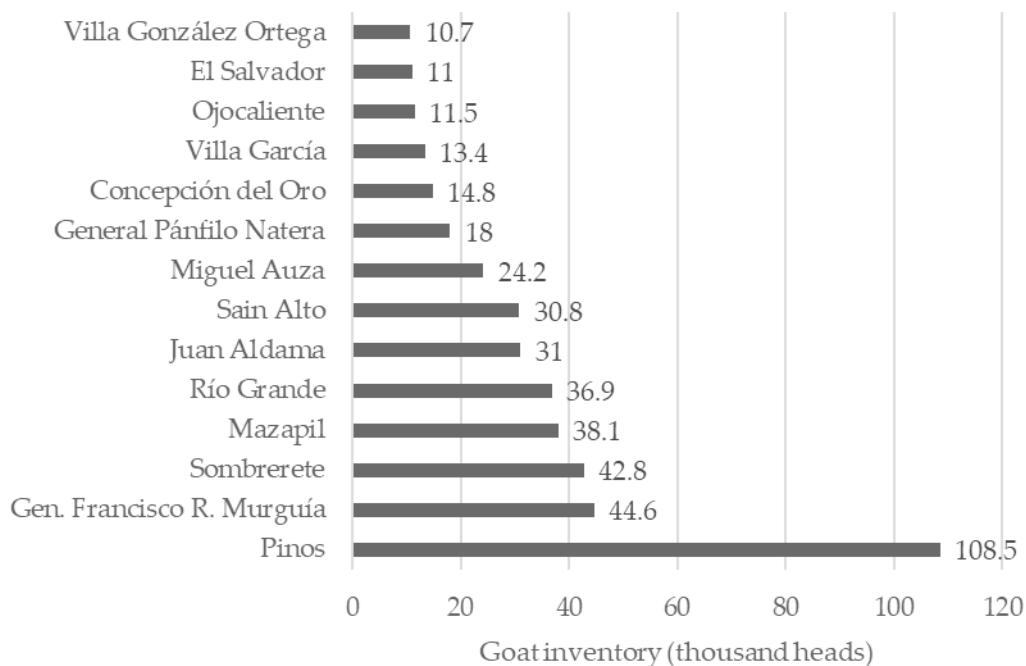


Figure 1. Municipal distribution of goat inventory in Zacatecas (SIINIGA, 2024): municipalities with >10 000 registered heads.

Socioeconomic context of main goat municipalities

Goat production in Zacatecas is closely linked to rural well-being because it is concentrated in municipalities where poverty and social deprivation persist. This concentration overlaps with municipalities where poverty remains high to moderate; for example, CONEVAL classifies Pinos in the highest municipal poverty bracket, while most of the other high-inventory municipalities fall within moderate poverty categories (CONEVAL, 2020). This socioeconomic environment acts as a cross-cutting

constraint on sustainability by limiting producers' ability to invest in feed and water buffering, preventive health, and collective commercialization, thereby amplifying the effects of drought and market volatility described in the following diagnostic sections (CONEVAL, 2020).

SUSTAINABILITY DIAGNOSIS OF GOAT SYSTEMS IN ZACATECAS

This section synthesizes the main sustainability constraints affecting goat production systems in Zacatecas by integrating (i) official territorial and sectoral evidence (e.g., climate and land-cover context) with (ii) mechanistic insights from the scientific literature on dryland livestock systems. The diagnosis is organized around how environmental pressures translate into forage and water constraints, which then propagate into higher production costs, land degradation risks, and reduced resilience for smallholder goat systems.

Environmental constraints and resource base

Environmental constraints serve as the main sustainability bottleneck for goat production systems in Zacatecas because herd performance and household profitability heavily rely on the availability of forage and water in a highly variable dryland environment. Recurrent droughts and significant interannual climate fluctuations shape rangeland productivity, influence the length and severity of seasonal feed shortages, and increase dependence on purchased or conserved feeds, thus directly linking environmental stress to production costs and economic vulnerability. These pressures also interact with grazing management and land condition, as reduced vegetation cover during dry periods can heighten erosion risk and hasten the degradation of the resource base that supports extensive goat systems over the long term.

Zacatecas's mostly dry and semi-dry climate creates a structural limit on goat production because rainfall mainly occurs in the summer and varies greatly between years, leading to recurrent periods of feed and water shortages. Under these conditions, drought and climate variability directly reduce the availability of rangeland forage and crop residues, increasing reliance on purchased feed and water strategies, which in turn raises costs and increases vulnerability for smallholders (Thornton *et al.*, 2015). Additionally, long dry spells can worsen soil exposure and erosion risk by reducing plant cover, which diminishes the long-term ability of grazing lands to supply stable forage.

The resource base in Zacatecas supports this reliance on climate-sensitive grazing lands: official land-cover data show that a significant part of the state is covered by natural vegetation, mainly xerophytic shrubland and grassland, which are inherently affected by rainfall pulses and drought conditions. Consistent with the municipal concentration of registered herds in semi-arid areas (Figure 2), the effects of rainfall variability are expected to be particularly relevant for the main goat-producing clusters.

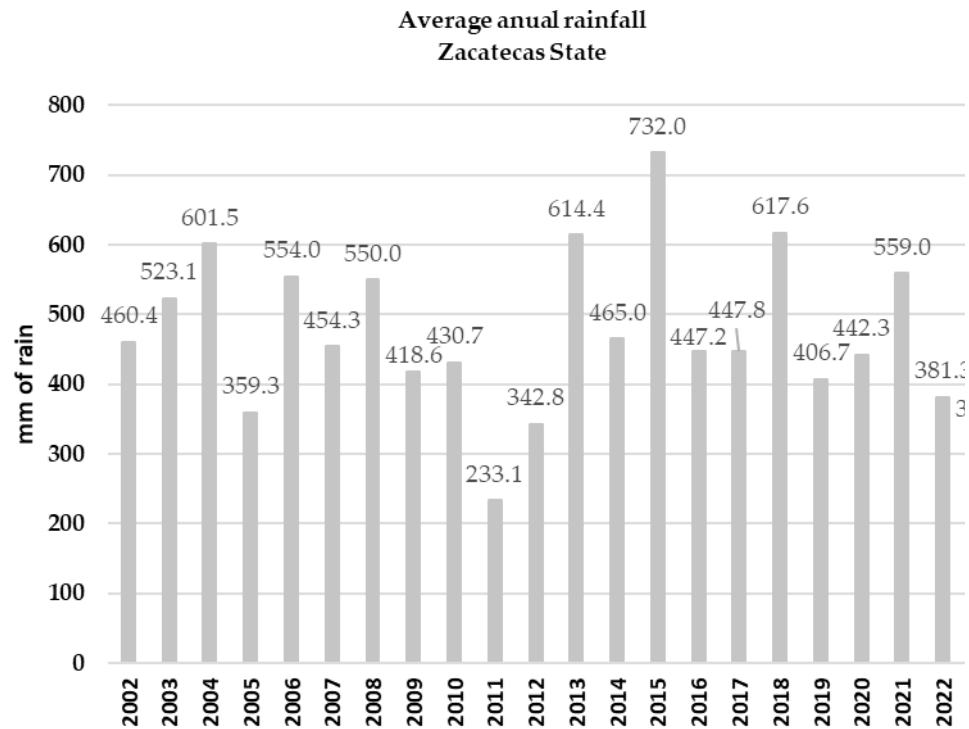


Figure 2. Average annual rainfall (2002–2023) in Zacatecas State, Mexico (Medina *et al.*, 2023).

Seasonal forage scarcity is a direct pathway through which rainfall variability affects goat productivity and household profitability in Zacatecas. During dry periods, reduced pasture growth and limited availability of crop residues create feed gaps that often lead producers to increase supplementation, often through purchased feeds, which raises production costs and can erode already narrow margins in smallholder systems (Herrero *et al.*, 2009; Thornton *et al.*, 2015). Nutritional stress during these periods commonly translates into lower growth rates, reduced reproductive performance, and higher susceptibility to disease, thereby amplifying both biological and economic vulnerability (Herrero *et al.*, 2009).

Because feed shortages recur seasonally and intensify in drought years, they make outputs and income more variable and highlight the importance of feed planning, forage conservation, and low-cost supplementation strategies as key resilience measures (Dida, 2021; Thornton *et al.*, 2015). This drought-driven instability of forage supply is consistent with evidence synthesized for Mexican drylands, where recurrent drought can cascade into lower forage reliability and household vulnerability in grassland-based livestock systems (Luna-Coronel *et al.*, 2026).

Water scarcity acts as a coupled constraint in Zacatecas' goat systems because it directly affects animal performance and indirectly limits forage and crop productivity.

Limited access to drinking water during drought can reduce intake and compromise thermoregulation and lactation, with negative consequences for milk and meat outputs (Doreau *et al.*, 2012). At the same time, water shortages constrain rangeland growth and crop production, thereby reducing the availability of both grazing biomass and crop residues that partially buffer seasonal feed gaps in mixed systems (Akinmoladun *et al.*, 2019). For smallholders, these biophysical constraints translate into higher costs through water hauling and/or investments in basic water infrastructure, reinforcing the link between drought, resource scarcity, and economic vulnerability (Pretty, 2008). Mixed crop-livestock strategies can buffer drought-driven feed deficits in Zacatecas by linking crop production to goat feeding through the use of residues and by-products. In the state, the cropping pattern is dominated by beans and maize, which together account for most of the cultivated area and therefore generate substantial amounts of crop residues that can be mobilized as seasonal feed resources (SIAP, 2024). When managed appropriately, this integration can improve resource-use efficiency and reduce dependence on purchased feeds by recycling biomass and nutrients within the farm system (Schiere *et al.*, 2006; Herrero *et al.*, 2013). However, the benefits depend on balancing residue use, grazing pressure, and soil cover: excessive removal of residues or high stocking rates under drought conditions can exacerbate soil degradation and compromise the long-term productivity of the resource base (Lemaire *et al.*, 2014). Evidence from mixed farming systems evaluated in Zacatecas indicates that, even when environmental practices perform relatively well, the main weaknesses tend to concentrate in the technical-productive and climate-resilience dimensions, reinforcing the need to link resource management with practical decision tools for drought adaptation (Luna-Coronel *et al.*, 2025).

Soil condition is a cross-cutting constraint in Zacatecas' dryland goat systems because it regulates both forage production on rangelands and the productivity of crops that generate residues used as seasonal feed. Under drought, reduced vegetative cover and concentrated grazing around water points and settlement areas can accelerate erosion and compaction, lowering infiltration and soil water storage and further destabilizing forage supply (Lal, 2001; Teague and Barnes, 2017). In mixed crop-livestock settings, a key trade-off emerges between using crop residues as livestock feed and retaining sufficient ground cover to protect soil and conserve moisture; excessive residue removal can weaken soil protection and compromise future yields, increasing reliance on purchased feeds over time (Lal, 2001). Therefore, soil-water conservation and grazing management that maintains ground cover are central leverage points for sustaining the feed base and reducing vulnerability to rainfall variability in Zacatecas. These environmental constraints strongly interact with grazing management and soil conditions. In dryland rangelands, insufficient recovery periods or stocking rates that exceed carrying capacity can accelerate vegetation loss and diminish ecosystem function, creating a negative feedback loop between drought, forage scarcity, and land degradation. Evidence reviews on grazing systems highlight that adaptive grazing management, especially strategies that emphasize recovery time and flexibility during

variable rainfall, can enhance socio-ecological resilience and help maintain grazing land function over time (Teague and Barnes, 2017).

In parallel, soil physical condition and organic matter are vital for drought buffering: soils with improved structure and higher organic matter typically hold more plant-available water and support more stable plant growth amid rainfall variability, which is critical to maintaining forage production in semi-arid areas (Lal, 2001). Overall, the interplay of seasonal and variable rainfall, rangeland-based feed resources, and the susceptibility to degradation underscores the importance of drought preparedness, grazing management, and soil-water conservation as key environmental strategies for the sustainability of goat systems in Zacatecas. In this context, drought resilience can be interpreted through resistance, recovery, and persistence mechanisms that link vegetation traits and grazing management to system stability under recurrent drought (Luna-Coronel *et al.*, 2026).

Production and management constraints (feed-health-reproduction)

In Zacatecas, the performance and resilience of goat systems are heavily influenced by management constraints that follow from the environmental factors described earlier. During dry seasons and recurrent drought, feed planning becomes a key bottleneck: reduced rangeland biomass and lower forage quality during dry months increase nutritional stress. This stress can hinder growth and milk production, diminish reproductive success, and increase susceptibility to disease (Joy *et al.*, 2020). In this context, supplementation strategies, such as using crop residues, conserved forages, or balanced feeds, can help buffer seasonal feed shortages and also raise cash costs and reliance on input markets, creating trade-offs between immediate productivity and long-term economic sustainability, especially for smallholders with limited liquidity. A practical interpretation of this seasonal constraint is the predictable dry-season protein/energy gap in C4 grasslands typical of many Mexican drylands, which can be buffered by integrating forage shrubs and/or targeted supplementation (Luna-Coronel *et al.*, 2026).

Preventive animal health and parasite management are essential pillars for sustainability. Grazing goats are frequently exposed to gastrointestinal nematodes and other endemic health issues; evidence highlights that parasitism is a major obstacle to performance and that repeated anthelmintic use can lead to resistance, making integrated control and targeted treatments increasingly vital (Hoste *et al.*, 2002, 2005; Reyes-Guerrero *et al.*, 2021). In this context, access to veterinary services, vaccination, deworming routines, and producer knowledge are critical for maintaining herd health, kid survival, and overall efficiency. INEGI's 2007 Agricultural Census explicitly captures management indicators for goat production, such as balanced feed, vaccination, and deworming, offering an official framework to describe these practices and their presence or absence at the production-unit level (INEGI, 2009).

Reproductive management and kid survival are particularly vulnerable to nutritional and health constraints in semi-arid systems. Periods of feed scarcity can decrease

body condition and hinder conception and lactation, while disease and parasitism can further impair reproductive success and juvenile survival, reinforcing cycles of low productivity and limited capacity for reinvestment (Hoste *et al.*, 2005; Joy *et al.*, 2020). Therefore, strengthening management strategies that combine (i) seasonal feed planning (including strategic supplementation), (ii) preventive health protocols and integrated parasite control, and (iii) basic reproductive management and record-keeping, is a key leverage point for boosting productivity and resilience without increasing pressure on the natural resource base.

Finally, these management improvements rely on service delivery and learning pathways. The CA2007 questionnaire structure also records whether production units received technical assistance and related support, allowing analysis of management constraints within broader “services and adoption” bottlenecks (INEGI, 2009). This is especially important in drylands, where timely advisory support, such as drought early actions, ration formulation, and herd health calendars, can decrease losses and enhance decision-making under climate condition variability.

Economic and value-chain constraints

Economic viability is a central sustainability bottleneck for goat systems in Zacatecas because dryland conditions translate biophysical stress into higher and more variable costs, while market and service constraints limit producers’ ability to capture value. Feed supplementation during recurrent dry seasons is a dominant cost driver in smallholder herds, and it can quickly erode margins when forage availability declines and producers must purchase concentrates or roughage (Herrero *et al.*, 2009; Dida, 2021). Limited access to credit and investment further constrains adaptation, reducing the capacity of producers to improve water infrastructure, housing, herd health management, and feeding strategies that would stabilize productivity under climatic variability (Negrete, 2014).

Value-chain limitations also restrict income opportunities. In smallholder settings, weak aggregation, cold chain, processing capacity, and transport infrastructure reduce market access and limit value addition in dairy and meat products, reinforcing dependence on local sales and intermediated marketing channels (Hemme and Otte, 2010). Value-chain analyses in Mexican dryland goat dairy systems similarly highlight the central role of intermediaries and the potential of coordinated upgrading (e.g., collective action, quality control, and targeted infrastructure) to improve profitability and market outcomes for producers (Gómez-Ruiz *et al.*, 2012).

Social, labor, and demographic constraints

Social and demographic conditions in Zacatecas create structural constraints that can limit the continuity, adaptive capacity, and innovation uptake of goat production systems. Official results from the INEGI Agricultural Census 2022 show an aging producer profile in the state: most producers are older than 45 years, including a substantial share aged 65 years or older, which can reduce labor availability, weaken

generational succession, and constrain the adoption of new practices without strong extension support (INEGI, 2023). In addition, census-based profiles report basic educational constraints (with primary schooling predominating), which can further slow the diffusion of innovations and the implementation of more complex management responses to drought and market risk (INEGI, 2023).

The lack of generational succession is a major social constraint for the long-term viability of goat production systems in Zacatecas. Rural outmigration can reduce the availability of young labor and weaken intergenerational knowledge transfer, leaving herds increasingly dependent on older producers and limiting the capacity to adopt improved practices and technologies. INEGI demographic statistics indicate population outflows from Zacatecas during 2015–2020, reflecting broader livelihood pressures that can undermine continuity in agricultural activities (INEGI, 2024). In goat systems, this demographic shift can translate into lower management intensity and slower innovation uptake, increasing vulnerability to climatic shocks and market volatility. Strengthening entry pathways for youth (training, access to productive assets, and profitability-oriented upgrading) is therefore a priority to sustain the sector over the medium term.

Gender dynamics are relevant for sustainability in Zacatecas' goat systems because women often contribute to smallholder livestock activities, yet they are underrepresented in formal decision-making roles within production units. Agricultural Census 2022 profiles for Zacatecas indicate that women constitute a minority among producers/responsible persons, which can limit access to training, veterinary services, and finance and reduce participation in upgrading and value addition (INEGI, 2023). At the same time, rural evidence consistently describes women's key roles in milking, artisanal dairy processing, and local marketing, activities that directly support household income and food security (FAO, 2011; Garay-Rodríguez *et al.*, 2022). Strengthening gender-responsive extension and improving access to services and resources are therefore relevant not only for equity, but also for expanding adoption capacity and improving the economic viability of smallholder goat systems (FAO, 2011; Unay-Gailhard and Bojnec, 2021).

Local knowledge about herd management, grazing patterns, and seasonal cycles remains an important asset for goat production in semi-arid regions. In drylands, pastoral mobility (including seasonal movements of herds) can function as an adaptive strategy to track spatial and temporal variability in forage and water availability, helping reduce localized grazing pressure and buffer climatic uncertainty (Dong, 2016; Manzano and Casas, 2010). In Zacatecas, local reports suggest that these practices are becoming harder to sustain as herding labor declines and shepherds age, which can reduce flexibility in grazing management and increase the risk of concentrating animals near settlements and water points (Hatfield and Davies, 2006). Preserving and adapting traditional knowledge, combined with practical innovations such as grazing planning, water-point management, and community-based coordination, may therefore contribute to resilience under recurrent drought in the state's goat systems (Dong, 2016).

Governance and services (organization/extension)

Governance conditions, particularly producer organization, access to extension, and service delivery, are key determinants of sustainability in Zacatecas' goat systems because they shape producers' capacity to manage risk, adopt improved practices, and coordinate along the value chain. The INEGI Agricultural Census 2007 includes items that capture whether production units are organized and what types of support or services are obtained through organizations (e.g., technical assistance, input purchasing, financing, commercialization, and training), indicating that these enabling conditions are measurable and policy-relevant components of production systems (INEGI, 2009). Evidence from small-scale livestock value chains indicates that, when organization and extension are limited, smallholders tend to face higher transaction costs, fragmented marketing channels, and weaker access to reliable information, technologies, and services, factors that can constrain upgrading, investment, and resilience (FAO, 2012). Participatory training approaches such as Farmer Field Schools have been implemented in Zacatecas and provide a relevant platform to strengthen technical and organizational capacities, which are often identified as limiting factors for sustainable performance in mixed systems (Luna-Coronel *et al.*, 2025).

In dryland contexts, extension is especially important because management decisions must be adaptive to rainfall variability and drought. Timely advisory services, such as seasonal feed planning, forage conservation, herd health calendars, and grazing management guidance, can support decision-making under uncertainty and reduce avoidable losses. However, limited coverage of technical assistance and uneven access to veterinary and organizational support are frequently reported constraints in small-ruminant systems, restricting the adoption of preventive health practices, improved feeding strategies, and value addition. Consequently, strengthening governance and services through (i) scalable producer organization, (ii) bundled extension and animal-health support, and (iii) coordinated market access strategies emerge as a cross-cutting leverage point to improve the sustainability of goat production systems in Zacatecas (FAO, 2012; INEGI, 2009).

INTEGRATED SYNTHESIS: TRADE-OFFS, SYNERGIES, AND EVIDENCE GAPS

Across the evidence synthesized in this review, sustainability in Zacatecas' goat systems emerges as the outcome of interacting trade-offs and synergies among the environmental resource base, household livelihoods, and value-chain conditions. A central trade-off is that drought-driven feed and water scarcity often leads producers to adopt short-term coping strategies (greater reliance on purchased feed, reduced grazing mobility, herd downsizing), which can stabilize production temporarily but increase cash costs and financial vulnerability in smallholder contexts (FAO, 2012; Thornton *et al.*, 2015). At the same time, responses aimed at raising productivity, such as supplementation, preventive health protocols, and improved reproductive

management, can improve outputs but may increase dependence on external inputs if not supported by coordinated services and reliable market access (INEGI, 2009; FAO, 2012).

These patterns suggest that sustainability is shaped not by a single constraint but by how constraints cascade through the system, from climate variability to feed and water shortages to costs, market participation, and reinvestment capacity (Table 2). Recent cross-sectional assessments in Zacatecas provide useful snapshots of sustainability levels, but they also underscore the need for longitudinal evaluation to track how technical assistance and training translate into sustained improvements over time (Luna-Coronel *et al.*, 2025).

Table 2. Integrated sustainability diagnosis matrix for goat production systems in Zacatecas: constraints, mechanisms, evidence and leverage points.

Sustainability dimension	Key constraint (Zacatecas)	Mechanism (what it affects)	Evidence in Zacatecas (official/context)	Sustainability implication	Leverage point (priority)
Environmental	Rainfall variability and recurrent drought	Reduced forage growth and water availability; increased reliance on supplementation	INEGI territorial/climate context; state rainfall records (e.g., SMN/CONAGUA) (Medina <i>et al.</i> , 2023)	Higher costs and lower productivity; increased pressure on grazing lands	Drought preparedness: forage conservation, strategic supplementation, and water harvesting and storage
Environmental	Risk of rangeland degradation and overgrazing	Loss of vegetation cover, increased erosion risk, reduced carrying capacity	INEGI land cover (xerophytic shrubland and grassland) and rangeland condition evidence (Aguirre-Rivera <i>et al.</i> , 2023)	Long-term decline of the feed resource base	Adaptive grazing management: recovery periods, mobility where feasible, and restoration practices
Production and health	Seasonal feed deficits	Lower body condition, reduced reproductive performance, higher disease susceptibility	Census/literature anchors on production and feeding in drylands; evidence on seasonal protein/energy gaps (Luna-Coronel <i>et al.</i> , 2026)	Lower kid survival and reduced output	Seasonal feed planning and low-cost supplementation aligned with dry-season constraints
Production and health	Limited preventive herd health services	Higher parasite and disease burden, reduced efficiency, higher mortality risk	Evidence on gastrointestinal nematodes and anthelmintic resistance in goats (Hoste <i>et al.</i> , 2002, 2005; Reyes-Guerrero <i>et al.</i> , 2021)	Productivity losses and animal welfare risks	Veterinary extension and preventive health packages (health calendars, integrated parasite control, targeted treatments)

Table 2. Continued.

Sustainability dimension	Key constraint (Zacatecas)	Mechanism (what it affects)	Evidence in Zacatecas (official/context)	Sustainability implication	Leverage point (priority)
Economic and value chain	Price volatility and limited bargaining power	Income instability and reduced investment capacity	SIAP production/value time series (context indicators)	Low profitability and potential exit from activity	Collective marketing, improved market information, and feasible local value addition
Economic and value chain	Weak infrastructure for collection, processing, and transport	Quality losses and restricted market access	Evidence from Mexican dryland dairy value chains (Gómez-Ruiz <i>et al.</i> , 2012), institutional and technical reports	Limited value capture	Scalable infrastructure through producer groups and local institutional support
Social and demographic	Aging producers and weak generational succession	Labor constraints and slower innovation uptake	CA2022 producer age structure; migration context (INEGI, 2023, 2024b)	Continuity risk for production systems	Youth inclusion via training, entry pathways, and improved profitability conditions
Social and gender	Underrepresentation of women in formal decision-making roles	Reduced access to decision-making, training, and finance; lower participation in upgrading	CA2022 producer profile (women as a minority among producers and responsible persons) and contextual literature (FAO, 2011)	Missed opportunities for productivity and household welfare gains	Gender-responsive extension, training, and improved access to services and finance
Governance and services	Low organization and limited service coordination	Higher transaction costs and reduced adoption of improved practices	Census instruments and value-chain evidence indicating the role of organization or extension (INEGI, 2009; FAO, 2012); local FFS experience (Luna-Coronel <i>et al.</i> , 2025)	Fragmented value chain and low innovation uptake	Strengthening producer groups and bundling extension, animal health, and market services

Note: “Evidence in Zacatecas” refers to official sources used as contextual anchors (INEGI, 2007, 2023; CONEVAL, 2020; Medina *et al.*, 2023; SIAP, 2023) and is complemented by peer-reviewed literature for mechanistic interpretation.

Important synergies are also evident. Grazing management and rangeland restoration can support both environmental and economic sustainability by stabilizing forage supply and reducing land degradation risk under variable rainfall; evidence syntheses on adaptive grazing emphasize the role of recovery time and flexibility in maintaining grazing land function (Teague *et al.*, 2017). Complementary synergies arise when soil-

water conservation improves infiltration and plant-available water, buffering drought impacts and supporting more stable forage production in semi-arid settings (Lal, 2001).

At the production level, integrated packages that combine seasonal feed planning with preventive animal health and parasite control can improve kid survival and reproductive outcomes, enhancing efficiency without necessarily increasing pressure on the natural resource base, provided that access to services, inputs, and knowledge is reliable (Hoste *et al.*, 2005). Finally, governance and market synergies occur when producer organization enables collective purchasing and marketing, reduces transaction costs, and facilitates value addition, improving price realization and strengthening incentives for adopting better management practices (FAO, 2012).

The review also identifies clear evidence gaps that limit a comprehensive sustainability assessment in Zacatecas. First, while census and official statistics provide robust structural baselines (inventories, production units, demographic context), state-specific studies that quantify sustainability outcomes (e.g., profitability, productivity under drought, animal health burdens, rangeland condition metrics, and adoption impacts) remain scarce, requiring cautious inference from comparable semi-arid systems. Second, there is limited peer-reviewed evidence on value-chain performance and governance in Zacatecas specifically (e.g., margins, market power, quality standards, transaction costs, and the effectiveness of collective action). Third, few studies integrate environment-health-economics in a single analytical framework, which constrains the identification of optimal intervention bundles and the assessment of trade-offs (e.g., supplementation costs vs. productivity gains; grazing intensity vs. rangeland recovery). These gaps reinforce the need for targeted research linking official datasets with field-based measurements and system-level indicators, and for evaluation of integrated strategies that combine drought preparedness, animal health, and market upgrading. These findings inform the priorities outlined in the Conclusions section.

STRATEGIC PRIORITIES FOR ACTION AND RESEARCH

Priorities for action (short-term to medium-term)

Based on the integrated diagnosis, five priorities emerge as the most actionable leverage points for improving sustainability in Zacatecas' goat systems:

Drought preparedness and feed planning. Priority actions include strengthening seasonal feed budgets, forage conservation (hay/silage where feasible), and strategic supplementation aligned with rainfall seasonality to reduce crisis-driven losses and stabilize outputs (Thornton *et al.*, 2015). These priorities, including drought preparedness, grazing timing, and forage diversification (native grasses and shrubs), are consistent with evidence syntheses for Mexican drylands that translate resilience into operational rules and monitoring needs (Luna-Coronel *et al.*, 2026).

Water access and low-cost infrastructure. Priority options include water harvesting, storage, and context-appropriate distribution solutions for smallholders and grazing settings to reduce time and cost burdens associated with water scarcity (Pretty, 2008; Doreau *et al.*, 2012).

Preventive herd health and parasite management. Scaling basic health calendars (vaccination and targeted parasite control) and improving access to veterinary support are priority measures to reduce avoidable productivity losses and welfare risks (Hoste *et al.*, 2005).

Producer organization and bundled services. Strengthening local producer groups can facilitate collective purchasing, coordinated extension/veterinary services, and collective marketing, reducing transaction costs and improving adoption capacity (FAO, 2012).

Value addition and market access. Feasible upgrading pathways, including aggregation, basic quality control, simple processing, and cold-chain solutions where relevant, can improve price realization and reduce income variability, particularly for dairy products and kids for meat markets (FAO, 2012).

Priorities for research and monitoring

To address the evidence gaps identified, future work should prioritize: (i) state-specific quantification of productivity, profitability, and drought-related risk across system types; (ii) integrated assessments linking rangeland condition, feed–water strategies, animal health burdens, and economic outcomes; (iii) value-chain studies in Zacatecas documenting margins, governance, and performance of organizational models; and (iv) evaluation of bundled interventions (drought preparedness + health + market upgrading) using transparent designs and measurable indicators to identify scalable pathways for sustainability.

CONCLUSION

Goat production in Zacatecas remains a relevant livelihood activity in Mexico's drylands; however, comparisons across agricultural census rounds indicate a structural contraction of the sector over time, alongside a producer base characterized by demographic vulnerability. Within this context, sustainability constraints arise from the interaction of (i) recurrent drought and rainfall variability that limit forage and water availability, (ii) management bottlenecks in feeding, herd health, and reproduction that reduce productivity and resilience, and (iii) value-chain limitations, including weak coordination, limited infrastructure, and price volatility, that restrict producers' ability to capture value and reinvest. These constraints are compounded by gaps in service coverage and organizational capacity, which can limit adoption of

preventive health practices, drought preparedness measures, and feasible upgrading options.

Overall, the review indicates that sustainability in Zacatecas' goat production systems is not constrained by a single limiting factor but by the cumulative and interacting effects of environmental variability, technical inefficiencies, and institutional and market limitations. Addressing these challenges therefore requires integrated strategies that simultaneously protect the natural resource base, improve herd-level productivity, and strengthen value-chain participation, rather than isolated interventions targeting individual constraints.

REFERENCES

- Aguirre-Rivera JR, Negrete-Sánchez LO, Castro-Rivera R. 2023. Traditional and updated evaluation of the rangeland site and condition in the semiarid scrub of the high plateau. *Agrociencia* 57 (3): 589–621. <https://doi.org/10.47163/agrociencia.v57i3.2620>
- Akinmoladun OF, Muchenje V, Fon FN, Mpendulo CT. 2019. Small ruminants: Farmers' hope in a world threatened by water scarcity. *Animals* 9 (7): 456. <https://doi.org/10.3390/ani9070456>
- Al-Kaisy QH, Al-Saadi JS, Al-Rikabi AKJ, Altemimi AB, Hesarinejad MA, Abedelmaksoud TG. 2023. Exploring the health benefits and functional properties of goat milk proteins. *Food Science and Nutrition* 11 (10): 5641–5656. <https://doi.org/10.1002/fsn3.3531>
- Chávez-Espinoza M, Cantú-Silva I, González-Rodríguez H, Montañez-Valdez OD. 2022. Sistemas de producción de pequeños rumiantes en México y su efecto en la sostenibilidad productiva. *Revista MVZ Córdoba* 27 (1): e2246.
- CONEVAL (Consejo Nacional de Evaluación de la Política de Desarrollo Social). 2020. Medición de pobreza municipal 2020. Ciudad de México, México. https://www.coneval.org.mx/Medicion/Documents/Pobreza_municipal/2020/Presentacion_Pobreza_Municipal_2020.pdf (Retrieved: October 2024).
- Dida MF. 2021. Strategies for goat feeding and management during drought. In Kukovics S. (ed.), *Goat Science - Environment, Health and Economy*. IntechOpen. <https://doi.org/10.5772/intechopen.101161>
- Dong S. 2016. Overview: Pastoralism in the world. In Dong S, Kassam KA, Tourrand J, Boone R. (eds.), *Building Resilience of Human-Natural Systems of Pastoralism in the Developing World*. Springer: Cham, Switzerland. https://doi.org/10.1007/978-3-319-30732-9_1
- Doreau M, Corson MS, Wiedemann SG. 2012. Water use by livestock: A global perspective for a regional issue? *Animal Frontiers* 2 (2): 9–16. <https://doi.org/10.2527/af.2012-0036>
- FAO (Food and Agriculture Organization of the United Nations). 2011. *The state of food and agriculture 2010-2011: Women in Agriculture - Closing the Gender Gap for Development*. Rome, Italy. <https://www.fao.org/4/i2050e/i2050e00.htm> (Retrieved: October 2024).
- FAO (Food and Agriculture Organization of the United Nations). 2012. *Smallholder integration in changing food markets*. Rome, Italy. 45 p.
- Garay-Rodríguez S, Torres-Maldonado JE, Murcia-Venegas DL, Torres-Rodríguez GA. 2022. Caracterización y tipificación socioeconómica del trabajo de la mujer rural del municipio de Vistahermosa-Meta. *Aglala* 13 (2): 84–99.
- Gawat M, Boland M, Singh J, Kaur L. 2023. Goat meat: Production and quality attributes. *Foods* 12 (16): 3130. <https://doi.org/10.3390/foods12163130>

- Gómez-Ruiz WJ, Pinos-Rodríguez JM, Aguirre-Rivera JR, García-López JC. 2012. Analysis of a goat milk cheese industry in a desert rangeland of Mexico. *Pastoralism: Research, Policy and Practice* 2 (1). <https://doi.org/10.1186/2041-7136-2-5>
- Hatfield R, Davies J. 2006. Global review of the economics of pastoralism. World Initiative for Sustainable Pastoralism. Nairobi, Kenya. 44 p.
- Hemme T, Otte J. 2010. Status and prospects for smallholder milk production. A global perspective. Food and Agriculture Organization of the United Nations: Rome, Italy. 181 p.
- Herrero M, Havlík P, Valin H, Notenbaert A, Rufino MC, Thornton PK, Obersteiner M. 2013. Biomass use, production, feed efficiencies, and greenhouse gas emissions from global livestock systems. *Proceedings of the National Academy of Sciences* 110 (52): 20888–20893. <https://doi.org/10.1073/pnas.1308149110>
- Herrero M, Thornton PK, Gerber P, Reid RS. 2009. Livestock, livelihoods and the environment: Understanding the trade-offs. *Current Opinion in Environmental Sustainability* 1 (2): 111–120. <https://doi.org/10.1016/j.cosust.2009.10.003>
- Hoste H, Chartier C, Le Frileux Y. 2002. Control of gastrointestinal parasitism with nematodes in dairy goats by treating the host category at risk. *Veterinary Research* 33 (5): 531–545. <https://doi.org/10.1051/vetres:2002037>
- Hoste H, Torres-Acosta JF, Paolini V, Aguilar-Caballero A, Etter E, Lefrileux Y, Chartier C, Broqua C. 2005. Interactions between nutrition and gastrointestinal infections with parasitic nematodes in goats. *Small Ruminant Research* 60 (1–2): 141–151. <https://doi.org/10.1016/j.smallrumres.2005.06.008>
- INEGI (Instituto Nacional de Estadística y Geografía). 1991. Censo agrícola, ganadero y forestal (CAGF) 1991. Ciudad de México, México. <https://www.inegi.org.mx/programas/cagf/1991/> (Retrieved: October 2024).
- INEGI (Instituto Nacional de Estadística y Geografía). 2009. Censo agrícola, ganadero y forestal (CAGF) 2007. Ciudad de México, México. <https://www.inegi.org.mx/programas/cagf/2007/> (Retrieved: October 2024).
- INEGI (Instituto Nacional de Estadística y Geografía). 2013. Conociendo Zacatecas. Aguascalientes, México. 32 p.
- INEGI (Instituto Nacional de Estadística y Geografía). 2023. Censo agropecuario 2022. Ciudad de México, México. <https://www.inegi.org.mx/programas/ca/2022/> (Retrieved: October 2024).
- INEGI (Instituto Nacional de Estadística y Geografía). 2024. Movimientos migratorios en Zacatecas. Ciudad de México, México. https://cuentame.inegi.org.mx/monografias/informacion/zac/poblacion/m_migratorios.aspx?tema=me&e=32 (Retrieved: November 2024).
- Joy A, Dunshea FR, Leury BJ, Clarke IJ, DiGiacomo K, Chauhan SS. 2020. Resilience of small ruminants to climate change and increased environmental temperature: A review. *Animals* 10 (5): 867. <https://doi.org/10.3390/ani10050867>
- Lal R. 2001. Soil degradation by erosion. *Land Degradation and Development* 12 (6): 519–539. <https://doi.org/10.1002/ldr.472>
- Lemaire G, Franzluebbers A, de Faccio Carvalho PC, Dedieu B. 2014. Integrated crop-livestock systems: Strategies to achieve synergy between agricultural production and environmental quality. *Agriculture, Ecosystems and Environment* 190: 4–8. <https://doi.org/10.1016/j.agee.2013.08.009>

- Luna-Coronel ME, Cortés-Vega CM, Dorado-González GE, García-Cervantes D, Muñoz-Sálas LC, Gutiérrez-Bañuelos H. 2025. Sustainability assessment of mixed farming systems among farmer field school participants in Zacatecas, Mexico. *Agro Productividad*. <https://doi.org/10.32854/79gh1y36>
- Luna-Coronel ME, Gutiérrez-Bañuelos H, García-Cervantes D, Espinoza-Canales A, Muñoz-Sálas LC, Gutiérrez-Piña F J. 2026. Drought-resilience in Mexican drylands: integrative C4 grasses and forage shrubs. *Grasses* 5 (1): 2. <https://doi.org/10.3390/grasses5010002>
- Manzano P, Casas R. 2010. Past, present and future of trashumancia in Spain: Nomadism in a developed country. *Pastoralism* 1 (1): 72–90. <https://doi.org/10.6084/m9.figshare.12253130>
- Medina GG, Casas FJI, Rodríguez MVM, Ramírez CNYZ. 2023. Estadísticas climatológicas horarias del estado de Zacatecas (Periodo 2002-2022). Instituto Nacional de Investigaciones Forestales, Agrícolas y Pecuarias, Centro de Investigación Regional Norte Centro, Campo Experimental Zacatecas. Calera, México. 246 p.
- Negrete JC. 2014. Rural poverty and agricultural mechanization policies in Mexico. *Journal of Agriculture and Environmental Sciences* 3 (1): 45–66.
- Page MJ, McKenzie JE, Bossuyt PM, Boutron I, Hoffmann TC, Mulrow CD, Shamseer L, Tetzlaff JM, Akl EA, Brennan SE, *et al.* (2021). The PRISMA 2020 statement: An updated guideline for reporting systematic reviews. *BMJ* n71. <https://doi.org/10.1136/bmj.n71>
- Pretty J. 2008. Agricultural sustainability: Concepts, principles and evidence. *Philosophical Transactions of the Royal Society B: Biological Sciences* 363 (1491): 447–465. <https://doi.org/10.1098/rstb.2007.2163>
- Reyes-Guerrero DE, Olmedo-Juárez A, Mendoza-de Gives P. 2021. Control and prevention of nematodiasis in small ruminants: Background, challenges and outlook in Mexico. *Revista Mexicana de Ciencias Pecuarias* 12: 186–204. <https://doi.org/10.22319/rmcp.v12s3.5840>
- Schiere H, Louis Baumhardt R, van Keulen H, Whitbread AM, Bruinsma AS, Goodchild, T, Hartwell B. 2006. Mixed crop-livestock systems in semiarid regions. *Dryland Agriculture* 23: 227–291. <https://doi.org/10.2134/agronmonogr23.2ed.c8>
- SIAP (Servicio de Información Agroalimentaria y Pesquera). 2024. Anuario estadístico de la producción agrícola. Gobierno de México. Servicio de Información Agroalimentaria y Pesquera. Ciudad de México, México. <https://nube.siap.gob.mx/cierreagricola/> (Retrieved: October 2024).
- SIINIGA (Sistema Nacional de Identificación Individual de Ganado). 2024. Registro municipal de existencias caprinas. Información Zacatecas. Ciudad de México, México.
- Tajonar K, López Díaz CA, Sánchez Ibarra LE, Chay-Canul AJ, González-Ronquillo M, Vargas-Bello-Pérez E. 2022. A brief update on the challenges and prospects for goat production in Mexico. *Animals* 12: 837. <https://doi.org/10.3390/ani12070837>
- Teague R, Barnes M. 2017. Grazing management that regenerates ecosystem function and grazingland livelihoods. *African Journal of Range and Forage Science* 34 (2): 77–86. <https://doi.org/10.2989/10220119.2017.1334706>
- Thornton PK, Boone RB, Ramírez Villegas J. 2015. Climate change impacts on livestock. Working Paper 120. CGIAR Research Program on Climate Change, Agriculture and Food Security. Copenhagen, Denmark. 19 p.
- Unay-Gailhard I, Bojnec S. 2021. Gender and the environmental concerns of young farmers: Do young women farmers make a difference on family farms? *Journal of Rural Studies* 88: 71–82. <https://doi.org/10.1016/j.jrurstud.2021.09.027>

- WCED (World Commission on Environment and Development). 1987. *Our Common Future*. Oxford University Press, Oxford, UK. 300 p.
- Whittemore R, Knafk K. 2005. The integrative review: Updated methodology. *Journal of Advanced Nursing* 52 (5): 546–553. <https://doi.org/10.1111/j.1365-2648.2005.03621.x>

Agrociencia

ARBUSCULAR MYCORRHIZAL FUNGI AND INDOLE-3-BUTYRIC ACID ON ROOTING AND GROWTH OF *Stevia rebaudiana* Bertoni STEM CUTTINGS

Evangelina Esmeralda Quiñones-Aguilar¹, Marcela Ríos-Sandoval¹, Sergio David Valerio-Landa¹, Luis Guillermo Hernández-Montiel², Gabriel Rincón-Enríquez^{1*}

¹Centro de Investigación y Asistencia en Tecnología y Diseño del Estado de Jalisco, A.C. Laboratorio de Fitopatología, Biotecnología Vegetal. Camino Arenero 1227, El Bajío del Arenal, Zapopan, Jalisco, Mexico. C. P. 45019.

²Centro de Investigaciones Biológicas del Noroeste. Avenida Instituto Politécnico Nacional 195, Colonia Playa Palo de Santa Rita Sur, La Paz, Baja California Sur, Mexico. C. P. 23019.

* Author for correspondence: grincon@ciatej.mx

ABSTRACT

Stevia is an herb used as a raw material to manufacture a low-calorie natural sweetener. Stevia plants are generally propagated by stem cuttings. Nonetheless, this method is not sufficient to meet global demand. The aim of this study was to determine the effect of applying an arbuscular mycorrhizal fungus (AMF) consortium and indole-3-butyric acid (IBA), in both powder and solution, on the greenhouse propagation of stevia stem cuttings. Applying AMF and IBA promoted greater growth across the different parameters assessed in stevia stem cuttings, increasing mycorrhizal colonization, particularly arbuscule content in roots. Therefore, the use of AMF and IBA should allow the production of stevia stem cuttings with greater vigor in a shorter period of time, reducing crop production costs by optimizing the dosage and methods of plant hormone application.

Keywords: mycorrhizal colonization, vegetative propagation, plant hormone.

INTRODUCTION

Stevia (*Stevia rebaudiana* Bertoni) is a perennial herb that belongs to the family Asteraceae and has gained global interest as a natural low-calorie sweetener (Kumar *et al.*, 2019; Dydych-Siemnińska *et al.*, 2020; Muñoz-Labrador *et al.*, 2023). Stevia leaves are a source of diterpene glucosides (mainly steviosides and rebaudiosides), compounds that are 300 times sweeter than saccharose (Adari *et al.*, 2016; Ameer *et al.*, 2017; de Andrade *et al.*, 2024). Additionally, steviosides exhibit several health-promoting properties, such as blood pressure-lowering effects in individuals with hypertension, increased insulin levels in blood, and the elimination of reactive oxygen species, among others (Ciriminna *et al.*, 2019; Shahu *et al.*, 2023; Munir *et al.*, 2024).

Currently, stevia extracts have been approved for use in food and beverages in most countries worldwide, including Japan, Singapore, Switzerland, the United States, the

Citation: Quiñones-Aguilar EE, Ríos-Sandoval M, Valerio-Landa SD, Hernández-Montiel LG, Rincón-Enríquez G. 2026. Arbuscular mycorrhizal fungi and indole-3-butyric acid on rooting and growth of *Stevia rebaudiana* Bertoni stem cuttings. *Agrociencia* 60(3): 339-354. <https://doi.org/10.47163/agrociencia.v60i3.3392>

Editor in Chief:

Dr. Fernando C. Gómez Merino

Received: September 27, 2025.

Approved: April 14, 2026.

Published in *Agrociencia*:

April 27, 2026.

This work is licensed under a Creative Commons Attribution-Non-Commercial 4.0 International license.



United Kingdom, Russia, China, India, Canada, and Brazil (Ashwell, 2015; Siddique *et al.*, 2016; Tey *et al.*, 2016; Farhat *et al.*, 2019). Worldwide demand has increased the cultivation area of this crop. However, low germination and seed viability have necessitated the use of vegetative propagation strategies, such as stem cutting cultivation (applying indole-3-butyric acid, IBA). Nevertheless, this propagation method is not sufficient to meet the seedling demand required by the global market for stevia commercial production, in addition to the fact that IBA must be applied constantly to plants (Sharma *et al.*, 2015; Galo, 2019). Moreover, these hormones have been reported as weak growth promoters in stevia (Kassahun and Mekonnen, 2011). An alternative to improve the propagation of plant cuttings is the use of beneficial microorganisms, which improve root and shoot growth (Bezerra *et al.*, 2019; Vicente-Hernández *et al.*, 2018). Arbuscular mycorrhizal fungi (AMF) are microorganisms from the phylum Glomeromycota and are obligate symbionts of nearly 90 % of terrestrial plant species (Ganugi *et al.*, 2019; Ferreira *et al.*, 2021; Szentpéteri *et al.*, 2023). The symbiosis, denominated mycorrhizal, involves the transfer of nutrients from the fungus to the plant (mainly phosphorus and nitrogen) and carbon sources from the plant to the fungus (mainly sugars and lipids) (Luginbuehl *et al.*, 2017).

The inoculation of different AMF species promotes plant growth and provides protection against abiotic and biotic stress (Trinidad-Cruz *et al.*, 2017a; Chen *et al.*, 2018; Wahab *et al.*, 2023; Bhupenanchandra *et al.*, 2024). The interaction of mycorrhizae with hormones such as auxins has been previously reported, suggesting a positive correlation between auxin content and the level of mycorrhizal colonization (Chen *et al.*, 2023; Abd-Alla *et al.*, 2024).

In *S. rebaudiana*, AMF application has increased yield and improved the nutritional, physiological, and quality attributes of the harvested crop. In particular, an increase in stevioside and rebaudioside content due to inoculation with AMF has been reported (Hoseini *et al.*, 2016; Tavarini *et al.*, 2018). Nonetheless, no information exists on the effect of AMF during the initial rooting and propagation stages in stevia plants. Therefore, the objective of this research was to quantify the effect of AMF inoculation and IBA application on the propagation of stevia stem cuttings in a greenhouse, hypothesizing that AMF and its interaction with IBA positively affect cutting quality.

MATERIALS AND METHODS

Arbuscular mycorrhizal fungi inoculum

The study was performed in the Plant Biotechnology greenhouse at the Research and Assistance Center in Technology and Design of the State of Jalisco, A.C. (CIATEJ), located at 20°42' N, 103° 28' W, and an altitude of 1675 m. *Funneliformis mosseae*, *Rhizophagus intraradices*, and two mycorrhizal consortia, "Las Campesinas" (consisting of *Acaulospora* spp., *Claroideoglossum* sp., *Entrophospora* sp., *Funneliformis* sp., *Glomus* spp., and *Septoglossum* sp.) and "Cerro del Metate" (*Acaulospora* spp., *Glomus* spp., *Septoglossum* sp., and *Dentiscutata* sp.) (Trinidad-Cruz *et al.*, 2017b), were used in

the inoculation experiment. These belonged to the microorganism collection of the Phytopathology Laboratory at CIATEJ.

Indole-3-butyric acid treatments and seedbeds

Three concentrations of indole-3-butyric acid (IBA: 0, 0.075, and 0.15 %) in two application forms (powder and liquid solution) were prepared. Radix 1500 (Intercontinental Import Export, Celaya, Mexico), formulated as an impregnated powder containing 0.15 % indole-3-butyric acid, was used as the IBA source for the powder treatments, and reagent-grade IBA at ≥ 98.0 % (Sigma-Aldrich, St. Louis, MO, USA) was used to prepare the liquid treatments.

For powder application, IBA powder was added to perlite powder (Agrolita ground, 0.01–0.001 mm in diameter, ACCIMIN, Mexico City, Mexico) until it reached each of the evaluated concentrations. For liquid solution application, IBA was diluted in sterile distilled water at 0, 0.075, and 0.15 %. For stevia stem cutting rooting, a seeder with sterile substrate (120 °C, 1.05 kg cm⁻², 6 h), composed of a mixture of perlite, peat moss, and coconut fiber in a volume ratio of 2:6:2, was used.

Treatment applications, mycorrhizal fungi inoculation, and growing conditions

Stevia stem cuttings of 10 cm in height, with two leaves at the main apex, were used. The stems were provided by Agrostevia SAPI de C.V. (Tepic, Mexico). IBA powder impregnation was performed 1 cm from the base of each cutting before transplant, whereas treatments with IBA solution were carried out by immersing the cuttings for 1 h.

AMF inoculation was performed using 20 g of inoculum (equivalent to 40 spores) deposited on the substrate during transplant. The seeders were maintained in the greenhouse at a relative humidity of 80–90 % using a fogger system with tap water and a photoperiod of 16 h of light for 45 d. At this point, the experiment ended, and all measurements of the response variables were taken.

Microbiological response and plant growth

Root staining was performed using the method of Phillips and Hayman (1970) 45 d after the experiment was established, and mycorrhizal activity in the roots was evaluated as the percentage of total, hyphal, vesicular, and arbuscular colonization (McGonigle *et al.*, 1990) using an optical microscope (Velab VE-BC3 Plus, Mexico City, Mexico). The plant growth variables of height (cm), root length (cm), stem diameter (mm), number of leaves, and number of lateral roots (NLR) were measured, and root and shoot dry weight (g) were determined after oven-drying the plant tissue at 65 °C for 120 h.

Experimental design and statistical methods

A completely randomized experiment was performed with a bifactorial treatment arrangement: (1) AMF factor with five levels: (a) *Funneliformis mosseae*; (b) *Rhizophagus intraradices*; (c) “Las Campesinas” consortium; (d) “Cerro del Metate” consortium; and

(e) without AMF; and (2) IBA factor with six levels: (a) IBA mixed with perlite powder at 0, (b) 0.075, and (c) 0.15%; and (d) IBA dissolved in water (solution) at 0, (e) 0.075, and (f) 0.15%. The combination of bifactorial levels resulted in a total of 30 treatments. Four replicates were performed per treatment.

Data for microbiological and plant growth variables were analyzed using bifactorial and unifactorial analysis of variance (ANOVA) after assessing the assumptions of normality (Shapiro-Wilk test) and homogeneity of variances (Bartlett test). When significant differences were found, a comparison of means (Tukey's test) was performed; both analyses were conducted at a significance level of 5% ($p \leq 0.05$) using the statistical program Statgraphics Centurion XVII (StatPoint, 2005).

RESULTS AND DISCUSSION

Microbiological response

Differences in mycorrhizal colonization were quantified in stevia stem cuttings treated with AMF and IBA (Table 1). The highest total AMF colonization was observed in cuttings inoculated with *Rhizophagus intraradices*; however, this value was not statistically significant compared to the other AMF treatments and the treatment with a 0.15% IBA solution.

The highest value of arbuscular content was observed in cuttings colonized by *Funnelformis mosseae*, "Las Campesinas," and "Cerro del Metate" consortia; vesicle content was highest in cuttings inoculated with "Cerro del Metate," and hyphal content in cuttings inoculated with *R. intraradices* (Figure 1). No differences were observed in mycorrhizal colonization (%) for the AMF \times IBA interaction. Stem cuttings treated with 0.15% IBA solution showed an increase in total, arbuscular, and hyphal colonization, whereas vesicular colonization increased with 0.075% IBA solution.

Differences in total arbuscular colonization were observed in the analysis of the effect of IBA application on stevia roots with each AMF (Figure 2). Both variables for *F. mosseae* increased with the application of 0.15% IBA solution, whereas for *R. intraradices*, only total colonization increased with the application of IBA at 0.075 and 0.15% in solution and 0.075% in powder form. No differences were observed in the remaining treatments.

Table 1. Effect of arbuscular mycorrhizal fungi (AMF) and indole-3-butyric acid (IBA) on mycorrhizal colonization of stevia stem cuttings, 45 d after the experiment was established.

Factor	Total	Mycorrhizal colonization (%)		
		Arbuscular	Vesicular	Hyphal
		AMF		
“Cerro del Metate”	17.3 ± 3.6 a*	1.8 ± 0.6 ab	4.5 ± 1.5 a	11.0 ± 1.9 bc
“Las Campesinas”	19.8 ± 3.2 a	2.8 ± 0.7 a	3.0 ± 0.7 ab	13.9 ± 2.3 ab
<i>Funneliformis mosseae</i>	20.5 ± 3.3 a	3.0 ± 1.1 a	0.8 ± 0.3 b	16.7 ± 2.4 ab
<i>Rhizophagus intraradices</i>	21.2 ± 3.6 a	0.2 ± 0.1 b	0.3 ± 0.3 b	20.7 ± 3.5 a
Non-AMF	3.0 ± 1.0 b	0.0 ± 0.0 b	0.0 ± 0.0 b	3.0 ± 1.0 c
		IBA		
IBA powder 0 %	9.4 ± 3.1 b	1.0 ± 0.4 ab	1.7 ± 1.0 a	6.7 ± 2.1 c
IBA powder 0.075 %	11.8 ± 3.0 b	1.1 ± 0.4 ab	1.1 ± 0.5 a	9.7 ± 2.6 bc
IBA powder 0.15 %	15.0 ± 2.9 b	0.7 ± 0.3 b	1.3 ± 0.7 a	13.0 ± 2.6 abc
IBA solution 0 %	13.3 ± 3.0 b	2.0 ± 0.9 ab	1.2 ± 0.5 a	10.2 ± 2.0 bc
IBA solution 0.075 %	20.5 ± 3.9 ab	1.1 ± 0.4 ab	2.7 ± 1.2 a	16.7 ± 3.4 ab
IBA solution 0.15 %	28.1 ± 4.5 a	3.6 ± 1.4 a	2.5 ± 1.4 a	22.0 ± 3.3 a
		Interaction AMF × IBA		
F-distribution	1.10	1.57	0.77	1.60
p-value	0.3652	0.0795	0.7412	0.0698

*The values are the means ± standard error (SE) of four replicates. The same letter indicates no significant differences between treatments according to Tukey’s test ($p \leq 0.05$).

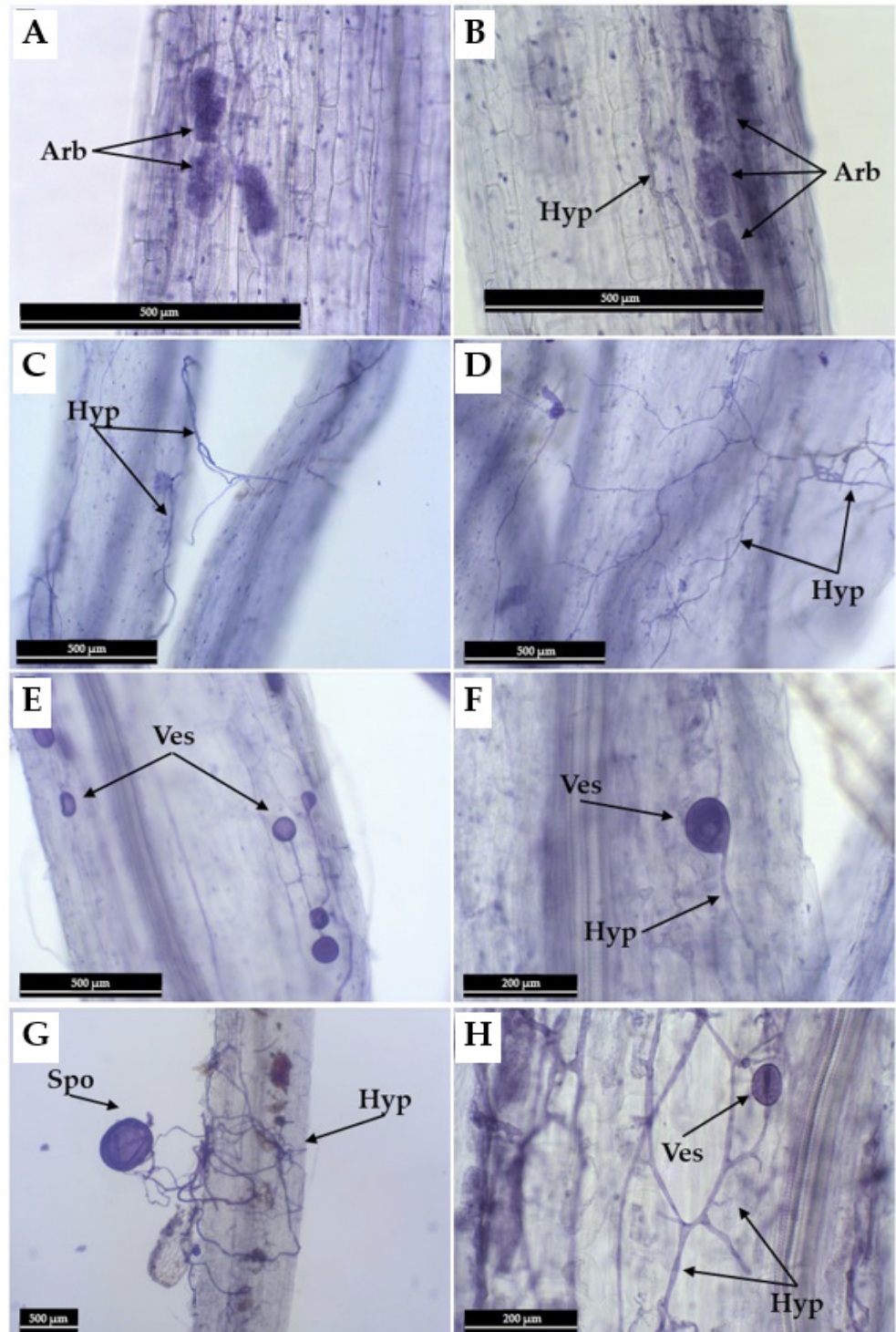


Figure 1. Arbuscular mycorrhizal fungi (AMF) structures in *Stevia rebaudiana* Bertoni roots. *Funneliformis mosseae* (A, B); *Rhizophagus intraradices* (C, D); "Cerro del Metate" (E, F); "Las Campesinas" (G, H). Arb: arbuscule; Hyp: hypha; Ves: vesicle; Spo: spore.

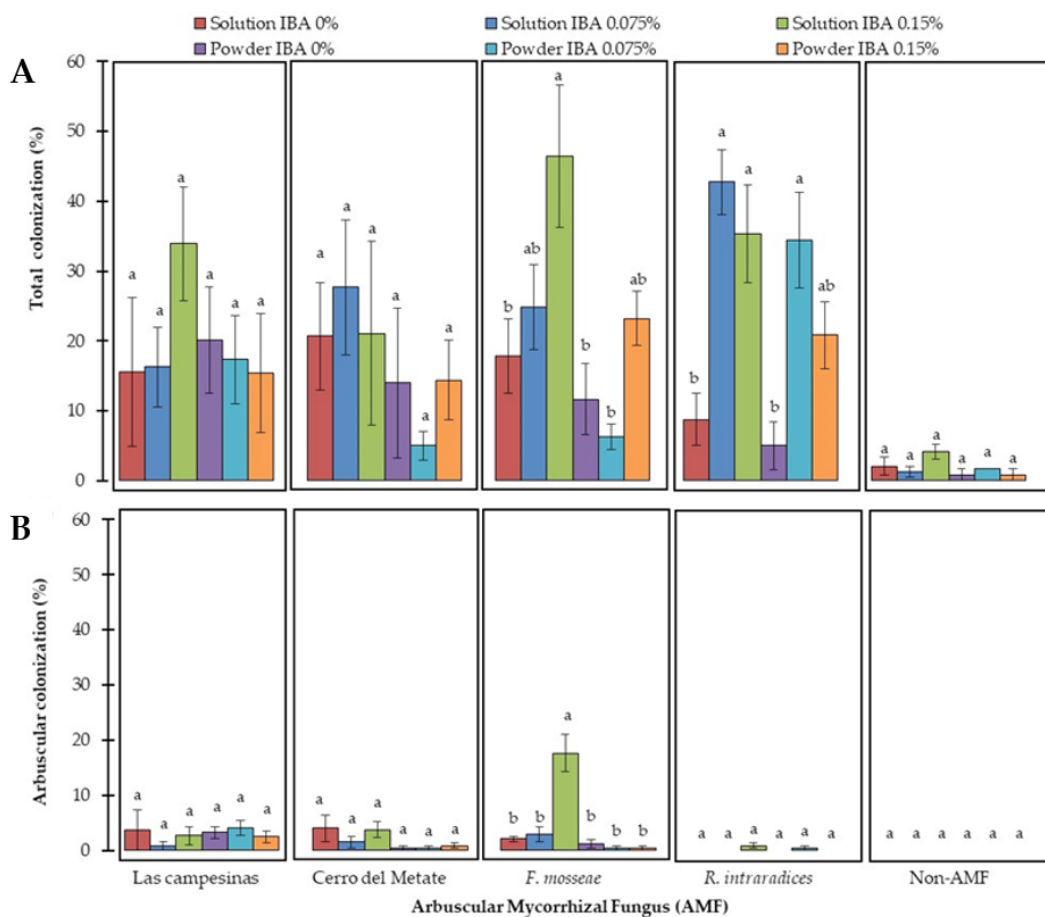


Figure 2. Effect of indole-3-butyric acid (IBA) on mycorrhizal colonization of stevia stem cuttings, 45 d after the experiment was established. A: total colonization; B: arbuscular colonization. The results are shown as means (n = 4) and the bars above the columns indicate the standard error (SE). The same letter indicates no significant differences between treatments according to Tukey’s test ($p \leq 0.05$).

Plant growth response

Differences were observed in stevia stem cutting growth variables with AMF and IBA (Table 2). For root dry weight, the highest values were observed in stevia stem cuttings without AMF; for root length, greater values were observed in the “Cerro del Metate” consortium, *F. mosseae*, and *R. intraradices*, as well as in cuttings treated with the recommended IBA dose (0.15 %). In the other morphological variables, no differences were observed in the response of stevia stem cuttings to AMF inoculation. In the analysis of the AMF effect and that of each IBA application on stevia stem cuttings, differences in root length and leaf dry weight were observed (Figures 3 and 4). The highest root length values were observed in cuttings treated with IBA 0.075 %

Table 2. Effect of arbuscular mycorrhizal fungi (AMF) and indole-3-butyric acid (IBA) on the morphological parameters of stevia stem cuttings, 45 d after the experiment was established.

Factor	Height (cm)	Root length (cm)	Stem diameter (mm)	Number		Dry weight (g)	
				Leaves	Lateral roots	Shoot	Root
AMF							
“Cerro del Metate”	12.8 ± 0.3 a*	7.3 ± 0.1 a	2.1 ± 0.1 a	11.2 ± 0.4 a	20.7 ± 1.0 a	0.22 ± 0.01 a	0.08 ± 0.00ab
“Las Campesinas”	11.7 ± 0.2 a	6.4 ± 0.2 b	2.0 ± 0.0 a	10.8 ± 0.4 a	19.0 ± 1.2 a	0.20 ± 0.01 a	0.06 ± 0.00 b
<i>Funneliformis mosseae</i>	12.2 ± 0.3 a	7.1 ± 0.2 a	2.0 ± 0.0 a	10.7 ± 0.3 a	17.9 ± 1.1 a	0.21 ± 0.01 a	0.06 ± 0.00 b
<i>Rhizophagus intraradices</i>	12.1 ± 0.4 a	7.1 ± 0.1 a	2.0 ± 0.0 a	11.8 ± 0.4 a	17.9 ± 1.2 a	0.21 ± 0.01 a	0.08 ± 0.01 ab
non-AMF	12.4 ± 0.3 a	7.2 ± 0.2 a	2.1 ± 0.0 a	11.9 ± 0.5 a	17.9 ± 1.2 a	0.23 ± 0.01 a	0.09 ± 0.01 a
IBA							
IBA powder 0 %	11.0 ± 0.3 b	6.6 ± 0.1 b	2.0 ± 0.0 a	10.5 ± 0.5 a	14.7 ± 1.1 b	0.18 ± 0.01 b	0.06 ± 0.00 b
IBA powder 0.075 %	12.5 ± 0.4 a	7.1 ± 0.2 ab	2.1 ± 0.1 a	11.8 ± 0.5 a	22.9 ± 1.0 a	0.23 ± 0.01 a	0.09 ± 0.01 a
IBA powder 0.15 %	13.0 ± 0.3 a	7.6 ± 0.1 a	2.0 ± 0.0 a	11.1 ± 0.4 a	18.9 ± 1.3 ab	0.21 ± 0.01 ab	0.07 ± 0.01 b
IBA solution 0 %	12.0 ± 0.4 ab	6.8 ± 0.2 b	2.1 ± 0.1 a	11.3 ± 0.5 a	18.5 ± 1.1 ab	0.22 ± 0.01 ab	0.07 ± 0.01 ab
IBA solution 0.075 %	12.5 ± 0.3 a	7.0 ± 0.2 ab	2.1 ± 0.0 a	11.6 ± 0.5 a	17.8 ± 1.3 b	0.22 ± 0.01 ab	0.07 ± 0.01 b
IBA solution 0.15 %	12.4 ± 0.3 ab	6.9 ± 0.2 b	2.1 ± 0.0 a	11.4 ± 0.5 a	19.0 ± 1.3 ab	0.23 ± 0.01 a	0.07 ± 0.01 ab
Interaction AMF × IBA							
F-distribution	1.42	3.45	1.24	1.11	0.74	0.75	1.98
p-value	0.1362	0.0000	0.2451	0.3566	0.7759	0.7593	0.0159

*The values are the means ± standard error (SE) of four replicates. The same letter indicates no significant differences between treatments according to Tukey’s test ($p \leq 0.05$).

+ *F. mosseae* (powder and solution) and IBA 0.15 % + *F. mosseae* (powder and solution). No differences in root length were observed in cuttings treated with IBA powder at 0 and 0.15 %, and IBA solution at 0 % + AMF. In shoot dry weight, differences were observed only with the application of IBA solution 0.15 % + AMF. The interactions found between AMF and IBA were observed in root variables (length and dry weight) (Table 2 and Figure 3). In particular, the “Las Campesinas” consortium and *F. mosseae* were influenced by the IBA application form and concentration, with a significantly higher effect for both root variables in stevia stem cuttings treated with *F. mosseae* + IBA solution 0.15 % (Figures 3 and 4).

The traditional propagation method in *S. rebaudiana* is the cultivation of cuttings using IBA as a root promoter (Rakibuzzaman *et al.*, 2018; Pigatto *et al.*, 2018; Galo, 2019; Muslihatin *et al.*, 2023; Neisiani *et al.*, 2024); however, the use of beneficial microorganisms, such as AMF, may represent an alternative in vegetative propagation (Abdel-Rahman *et al.*, 2019; Tchiehoua *et al.*, 2019; Dewir *et al.*, 2023; Taghizadeh *et al.*, 2023).

In this study, AMF did not promote plant growth in stevia stem cuttings; however, mycorrhizal symbiosis was successfully established, as evidenced by the presence of mycelium, arbuscules, and vesicles. These structures actively participate in the

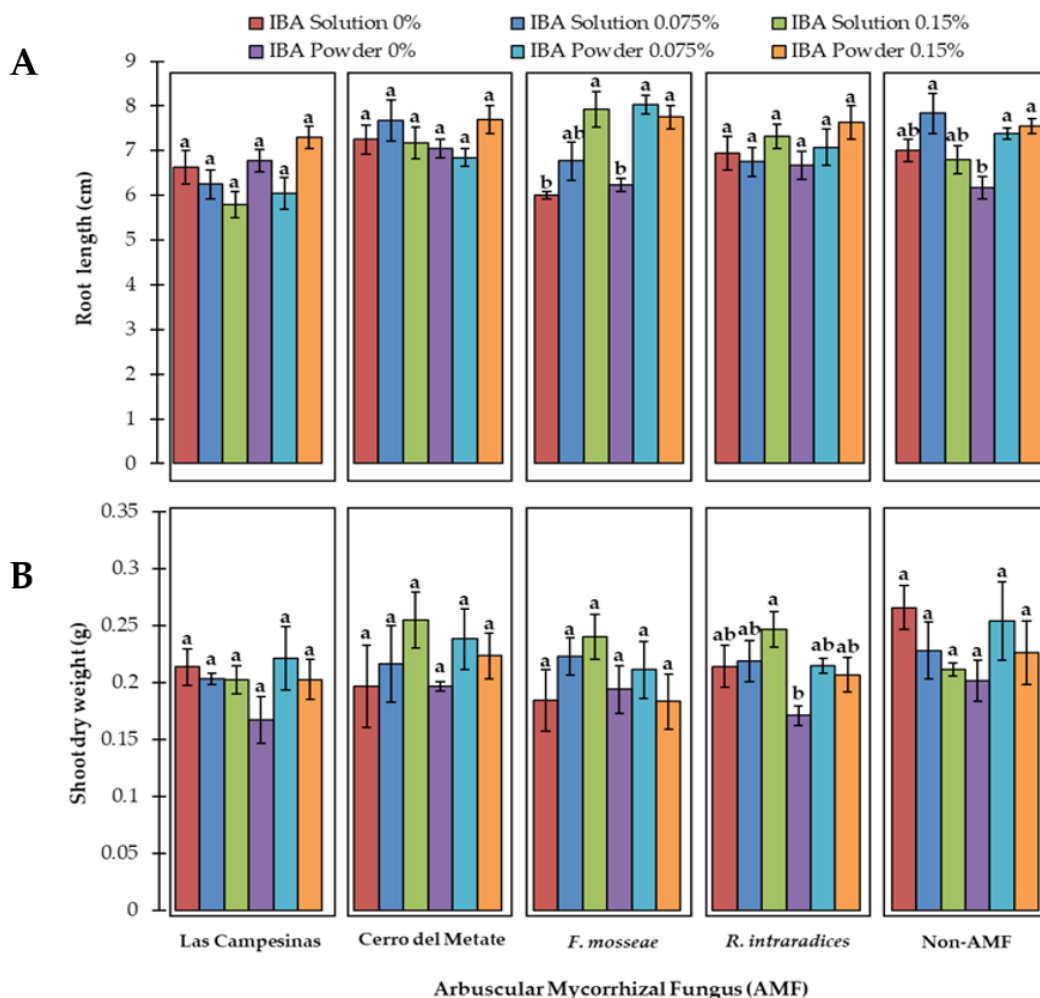


Figure 3. Effect of arbuscular mycorrhizal fungi (AMF) and indole-3-butyric acid (IBA) on growth of stevia stem cuttings, 45 d after the experiment was established. A. root length; B: shoot dry weight. The results are shown as means ($n = 4$) and the bars above the columns indicate the standard error (SE). The same letter indicates no significant differences between treatments according to Tukey's test ($p \leq 0.05$).

storage, exchange, and transport of soil nutrients to the host (Fernandes *et al.*, 2019; Chenchouni *et al.*, 2020; Tchichoua *et al.*, 2019). It is necessary to evaluate plant growth over a longer period to observe the effects of AMF on stevia plants. Moreover, since the substrate used was nutrient-poor, the stevia cuttings grew mainly at the expense of their accumulated reserves, making the benefits related to nutrient uptake by AMF barely detectable, which could explain why no marked differences in growth were observed among AMF treatments. On the other hand, the presence of hyphae in the non-mycorrhizal treatment is attributed to microorganisms that colonize after

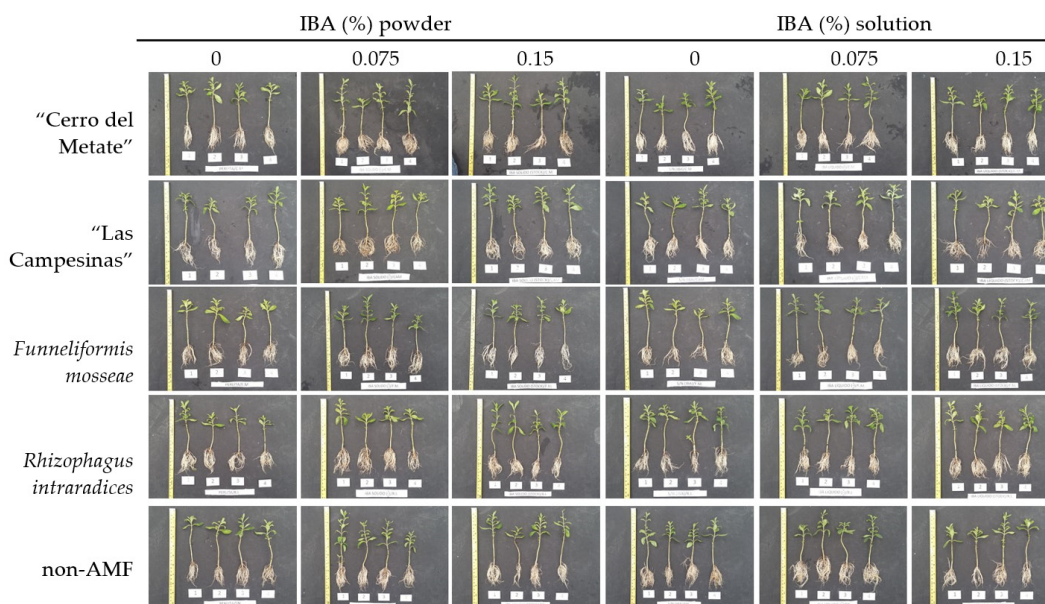


Figure 4. General appearance of stevia plant inoculated with arbuscular mycorrhizal fungi (AMF), 45 d after the experiment was established, across indole-3-butyric acid (IBA) treatments (powder and solution). The yellow bar indicates a scale of 30 cm.

the experiment is established, through spores carried by the wind; however, their presence is very low, and they correspond to non-mycorrhizal fungi, as no arbuscules or vesicles were observed.

The colonization of AMF in stevia plants has been previously reported (Bonfante and Genre, 2010; Tedone *et al.*, 2020); however, the results of this study show for the first time that different AMF species and consortia can colonize stevia stem cuttings during the rooting stage under greenhouse conditions. In particular, the presence of arbuscules in plant roots indicates functional symbiotic activity between AMF and the host, as nutrient exchange occurs in this fungal structure between the endophyte and the plant (Bao *et al.*, 2019; Thirkell *et al.*, 2020). Furthermore, the presence of mycelium and vesicles in roots indicates a differential response of stevia to colonization by the different AMF species inoculated. These results agree with those reported by Quiñones-Aguilar *et al.* (2016), where the same plant species may exhibit differential growth responses depending on colonization levels by different AMF consortia and species. According to Chen *et al.* (2018), the plant response to AMF inoculation may result from functional specificity between endophytes and the host, which could explain the differences in endophyte proliferation levels observed among the AMF consortia and species inoculated.

Moreover, stevia stem cuttings grew when inoculated with AMF, but root length and dry weight values were lower compared to those without AMF inoculation. Li *et al.*

(2015) reported that plants modify their root architecture during symbiotic association with AMF as a strategy to improve water and nutrient absorption; that is, plants reduce the energy expenditure required for root production and instead take advantage of the external AMF mycelium to absorb water and soil nutrients (Wang *et al.*, 2011). Additionally, plants have been reported to reduce growth parameters (mainly fresh and dry biomass) because mycorrhizal symbiosis requires a high carbon (C) allocation to maintain the association between endophyte and root (Tavarini *et al.*, 2018).

In relation to plant hormones such as auxins (IBA), these are defined as promoters of plant growth and development, intervening in plant responses to both biotic and abiotic factors and promoting lateral root development (Sukumar *et al.*, 2012; El-Banna *et al.*, 2024; Song *et al.*, 2024). Several studies have indicated that auxins act as signaling molecules in regulating interactions between AMF and the host, mainly in root architecture, modulation processes, endophyte spore germination, and arbuscule formation (Etemadi *et al.*, 2014; Chen *et al.*, 2017).

In this study, the application of IBA in solution increased mycorrhizal colonization in stevia stem cuttings compared to IBA in powder, which showed no effect on colonization levels. IBA powder can be denatured as a phytohormone by several factors, particularly chemical or biological oxidation by microorganisms, whereas IBA in solution does not present these potentially negative effects, as reported in studies on rooting of peach cuttings (*Prunus persica* (L.) Batsch) (Lesmes-Vesga *et al.*, 2021). On the other hand, in nasturtium plants (*Tropaeolum majus* L.) inoculated with *R. intraradices*, IBA levels (free and total) are significantly increased compared to plants without AMF (Jentschel *et al.*, 2007). In this context, it is hypothesized that when IBA powder is denatured, the available amount that promotes mycorrhizal colonization is reduced, which could explain the low colonization levels observed in stevia cuttings in this study.

Moreover, the IBA application dose played an important role in plant rooting response (Faisal *et al.*, 2018; Fan *et al.*, 2020), with reports indicating that low concentrations of this hormone improve root length and number in plants (Hoseini *et al.*, 2016). Similarly, better mycorrhizal colonization is expected at low IBA doses (Chen *et al.*, 2022), possibly because excess auxins affect root architecture as well as the hormonal balance required for proper plant function. Thus, the use of low IBA doses combined with AMF in stevia stem cuttings may represent an effective strategy for obtaining vigorous plants while reducing crop production costs by optimizing plant hormone dosage and application method.

CONCLUSIONS

This study showed the capability of arbuscular mycorrhizal fungus (AMF) to colonize stevia stem cutting during their rooting stage. Furthermore, the application of indole-3-butyric (IBA) influenced on endophyte colonization levels in the host root. Particularly, stimulating cutting by low IBA dose could be important to improve AMF-

Root interaction, mycorrhizal colonization, and obtaining plants with greater vigor. Although no significant differences were observed in the growth of cuttings inoculated with AMF compared to those not inoculated, colonization was successfully established. Therefore, longer term studies evaluating response parameters are needed to determine these differences. Furthermore, studies are needed to determine the influence of IBA application on the establishment of symbiosis between the plant and the endophyte. Integrating knowledge of the effects of applying different AMF species and consortia is crucial for the development and application of sustainable agricultural production of stevia.

ACKNOWLEDGEMENTS

We thank Diana Fischer for translation/editorial services.

REFERENCES

- Abd-Alla MH, Nafady NA, Hassan AA, Bashandy SR. 2024. Isolation and characterization of non-rhizobial bacteria and arbuscular mycorrhizal fungi from legumes. *BMC Microbiology* 24 (1): 454. <https://doi.org/10.1186/s12866-024-03591-z>
- Abdel-Rahman SSA, Ibrahim OHM, Mousa GT, Soliman HB. 2019. Combined effects of auxin application and beneficial microorganisms on rooting and growth of *Ficus benjamina* L. air-layers. *Assiut Journal of Agricultural Sciences* 50 (2): 120–139. <https://doi.org/10.21608/ajas.2019.43504>
- Adari BR, Alavala S, George SA, Meshram HM, Tiwari AK, Sarma AV. 2016. Synthesis of rebaudioside-A by enzymatic transglycosylation of stevioside present in the leaves of *Stevia rebaudiana* Bertoni. *Food Chemistry* 200: 154–158. <https://doi.org/10.1016/j.foodchem.2016.01.033>
- Ameer K, Bae SW, Jo Y, Lee HG, Ameer A, Kwon JH. 2017. Optimization of microwave-assisted extraction of total extract, stevioside and rebaudioside-A from *Stevia rebaudiana* (Bertoni) leaves, using response surface methodology (RSM) and artificial neural network (ANN) modelling. *Food Chemistry* 229: 198–207. <https://doi.org/10.1016/j.foodchem.2017.01.121>
- Ashwell M. 2015. Stevia, nature's zero-calorie sustainable sweetener: A new player in the fight against obesity. *Nutrition Today* 50 (3): 129–134. <https://doi.org/10.1097/NT.0000000000000094>
- Bao X, Wang Y, Olsson PA. 2019. Arbuscular mycorrhiza under water-Carbon-phosphorus exchange between rice and arbuscular mycorrhizal fungi under different flooding regimes. *Soil Biology and Biochemistry* 129 (9): 169–177. <https://doi.org/10.1016/j.soilbio.2018.11.020>
- Bezerra GA, Gabriel AVMD, Mariano EDA, Cardoso JC. 2019. *In vitro* culture and greenhouse acclimatization of *Oncidium varicosum* (Orchidaceae) with microorganisms isolated from its roots. *Ornamental Horticulture* 25 (4): 407–416. <https://doi.org/10.1590/2447-536X.v25i4.2046>
- Bhupenchandra I, Chongtham SK, Devi AG, Dutta P, Sahoo MR, Mohanty S, Kumar S, Choudhary AK, Devi EL, Sinyorita S, *et al.* 2024. Unlocking the potential of arbuscular mycorrhizal fungi: Exploring role in plant growth promotion, nutrient uptake mechanisms, biotic stress alleviation, and sustaining agricultural production systems. *Journal of Plant Growth Regulation* 44 (12): 6802–6840. <https://doi.org/10.1007/s00344-024-11467-9>

- Bonfante P, Genre A. 2010. Mechanisms underlying beneficial plant-fungus interactions in mycorrhizal symbiosis. *Nature Communications* 1 (1): 48. <https://doi.org/10.1038/ncomms1046>
- Chen M, Arato M, Borghi L, Nouri E, Reinhardt D. 2018. Beneficial services of arbuscular mycorrhizal fungi – From ecology to application. *Frontiers Plant Science* 9: 1270. <https://doi.org/10.3389/fpls.2018.01270>
- Chen W, Li J, Zhu H, Xu P, Chen J, Yao Q. 2017. The differential and interactive effects of arbuscular mycorrhizal fungus and phosphorus on the lateral root formation in *Poncirus trifoliata* (L.). *Scientia Horticulturae* 217: 258–265. <https://doi.org/10.1016/j.scienta.2017.02.008>
- Chen W, Shan W, Niu T, Ye T, Sun Q, Zhang J. 2023. Insight into regulation of adventitious root formation by arbuscular mycorrhizal fungus and exogenous auxin in tea plant (*Camellia sinensis* L.) cuttings. *Frontiers in Plant Science* 14: 1258410. <https://doi.org/10.3389/fpls.2023.1258410>
- Chen X, Chen J, Liao D, Ye H, Li C, Luo Z, Yan A, Zhao Q, Xie K, Li Y, *et al.* 2022. Auxin-mediated regulation of arbuscular mycorrhizal symbiosis: A role of SIG3.4 in tomato. *Plant, Cell and Environment* 45 (3): 955–968. <https://doi.org/10.1111/pce.14210>
- Chenchouni H, Mekahlia MN, Beddiar A. 2020. Effect of inoculation with native and commercial arbuscular mycorrhizal fungi on growth and mycorrhizal colonization of olive (*Olea europaea* L.). *Scientia Horticulturae* 261 (3): 108969. <https://doi.org/10.1016/j.scienta.2019.108969>
- Ciriminna R, Meneguzzo F, Pecoraino M, Pagliaro M. 2019. A bioeconomy perspective for natural sweetener stevia. *Biofuels, Bioproducts and Biorefining* 13 (3): 445–452. <https://doi.org/10.1002/bbb.1968>
- de Andrade MVS, Lucho SR, de Castro RD, Ribeiro PR. 2024. Alternative for natural sweeteners: Improving the use of stevia as a source of steviol glycosides. *Industrial Crops and Products* 208: 117801. <https://doi.org/10.1016/j.indcrop.2023.117801>
- Dewir YH, Habib MM, Alaizari AA, Malik JA, Al-Ali AM, Al-Qarawi AA, Alwahibi MS. 2023. Promising application of automated liquid culture system and arbuscular mycorrhizal fungi for large-scale micropropagation of red dragon fruit. *Plants* 12 (5): 1037. <https://doi.org/10.3390/plants12051037>
- Dyduch-Siemińska M, Najda A, Gawroński J, Balant S, Świca K, Żaba A. 2020. *Stevia rebaudiana* Bertoni, a source of high-potency natural sweetener-biochemical and genetic characterization. *Molecules* 25 (4): 767. <https://doi.org/10.3390/molecules25040767>
- El-Banna MF, Kasem MM, Hegazy AA, Helaly AA, Mosa A, El-Banna HY. 2024. Bee honey improved the performance of indole-3-butyric acid on promoting adventitious roots formation of *Cupressus macrocarpa* L. var. Goldcrest: Morpho-biochemical and histoanatomical investigation. *Industrial Crops and Products* 209: 117971. <https://doi.org/10.1016/j.indcrop.2023.117971>
- Etemadi M, Gutjahr C, Couzigou JM, Zouine M, Laouressergues D, Timmers A, Audran C, Bouzayen M, Bécard G, Combiér JP. 2014. Auxin perception is required for arbuscule development in arbuscular mycorrhizal symbiosis. *Plant Physiology* 166 (1): 281–292. <https://doi.org/10.1104/pp.114.246595>
- Faisal M, Ahmad N, Anis M, Alatar AA, Qahtan AA. 2018. Auxin-cytokinin synergism in vitro for producing genetically stable plants of *Ruta graveolens* using shoot tip meristems. *Saudi Journal of Biological Sciences* 25 (2): 273–277. <https://doi.org/10.1016/j.sjbs.2017.09.009>
- Fan Y, Yu X, Guo H, Wei J, Guo H, Zhang L, Zeng F. 2020. Dynamic transcriptome analysis reveals uncharacterized complex regulatory pathway underlying dose IBA-induced

- embryogenic redifferentiation in cotton. *International Journal of Molecular Sciences* 21 (2): 426. <https://doi.org/10.3390/ijms21020426>
- Farhat G, Berset V, Moore L. 2019. Effects of stevia extract on postprandial glucose response, satiety and energy intake: A three-arm crossover trial. *Nutrients* 11 (12): 3036. <https://doi.org/10.3390/nu11123036>
- Fernandes MDS, de Moraes MB, Mesquita-Oliveira FF, Ulisses C, de Medeiros JF, de Albuquerque CC. 2019. Arbuscular mycorrhizal fungi and auxin associated with microelements in the development of cuttings of *Varronia leucocephala*. *Revista Brasileira de Engenharia Agrícola e Ambiental* 23 (3): 167–174. <https://doi.org/10.1590/1807-1929/agriambi.v23n3p167-174>
- Ferreira DA, da Silva TF, Pylro VS, Salles JF, Andreote FD, Dini-Andreote F. 2021. Soil microbial diversity affects the plant-root colonization by arbuscular mycorrhizal fungi. *Microbial Ecology* 82 (1): 100–103. <https://doi.org/10.1007/s00248-020-01502-z>
- Galo EV. 2019. *In situ* clonal propagation of stevia (*Stevia rebaudiana* Bertoni) using hormones. *American Journal of Plant Sciences* 10 (10): 1789–1796. <https://doi.org/10.4236/ajps.2019.1010126>
- Ganugi P, Masoni A, Pietramellara G, Benedettelli S. 2019. A review of studies from the last twenty years on plant arbuscular mycorrhizal fungi associations and their uses for wheat crops. *Agronomy* 9 (12): 840. <https://doi.org/10.3390/agronomy9120840>
- Hoseini RZ, Goltapeh EM, Kalatejari S. 2016. Effect of bio-fertilizer on growth, development and nutrient content (leaf and soil) of *Stevia rebaudiana* Bertoni. *Journal of Crop Protection* 5 (4): 691–704.
- Jentschel K, Thiel D, Rehn F, Ludwig-Muller J. 2007. Arbuscular mycorrhiza enhances auxin levels and alters auxin biosynthesis in *Tropaeolum majus* during early stages of colonization. *Physiologia Plantarum* 129 (2): 320–333. <https://doi.org/10.1111/j.1399-3054.2006.00812.x>
- Kassahun BM, Mekonnen SA. 2011. Effect of cutting position and rooting hormone on propagation ability of stevia (*Stevia rebaudiana* Bertoni). *African Journal of Plant Science and Biotechnology* 6 (1): 5–8.
- Kumar A, Goswami A, Sagar A, Kumar P, Singh R. 2019. Effect of plant growth regulator on *in-vitro* callus induction and shoot proliferation of a natural sweetening crop, *Stevia rebaudiana* (Bertoni). *Progressive Agriculture* 19 (1): 118–122. <https://doi.org/10.5958/0976-4615.2019.00015.2>
- Lesmes-Vesga RA, Chaparro JX, Sarkhosh A, Ritenour MA, Cano LM, Rossi L. 2021. Effect of propagation systems and indole-3-butyric acid potassium salt (K-IBA) concentrations on the propagation of peach rootstocks by stem cuttings. *Plants* 10 (6): 1151. <https://doi.org/10.3390/plants10061151>
- Li X, Zeng R, Liao H. 2015. Improving crop nutrient efficiency through root architecture modifications. *Journal of Integrative Plant Biology* 58 (3): 193–202. <https://doi.org/10.1111/jipb.12434>
- Luginbuehl LH, Menard GN, Kurup S, Erp HV, Radhakrishnan GV, Breakspear A, Oldroyd GE, Eastmond PJ. 2017. Fatty acids in arbuscular mycorrhizal fungi are synthesized by the host plant. *Science* 356 (6343): 1175–1178. <https://doi.org/10.1126/science.aan0081>
- McGonigle TP, Miller MH, Evans DG, Fairchild GL, Swan JA. 1990. A new method which gives an objective measure of colonization of roots by vesicular-arbuscular mycorrhizal fungi. *New Phytologist* 115 (3): 495–501. <https://doi.org/10.1111/j.1469-8137.1990.tb00476.x>
- Munir S, Hameed S, Hussain N, Khurshid H, Hafeez M, Khan LA. 2024. Unveiling *Stevia rebaudiana*: Origins, composition, and health implications. *Food Science and Applied Microbiology Reports* 3 (1): 1–18. <https://doi.org/10.61363/8zyy5b06>

- Muñoz-Labrador A, Hernández-Hernández O, Moreno FJ. 2023. A review of the state of sweeteners science: The natural versus artificial non-caloric sweeteners debate. *Stevia rebaudiana* and *Siraitia grosvenorii* into the spotlight. *Critical Reviews in Biotechnology* 44 (6): 1080–1102. <https://doi.org/10.1080/07388551.2023.2254929>
- Muslihatin W, Febriawan Z, Nasution AMT, Patrialoka SN, Pratama IPEW, Aisyah PY, Jadid N, Fatmawati S, Antika TR, Shovitri M. 2023. Morphological and physiological characteristics of *Stevia rebaudiana* Bertoni stem cuttings under 3-indoleacetic acid (IAA) treatment. *Agriculture* 69 (4): 186–193. <https://doi.org/10.2478/agri-2023-0016>
- Neisiani AA, Saidi A, Tohidfar M. 2024. Investigation of the concentration and composition of various phytohormones in the efficiency of micropropagation of *Stevia rebaudiana* Bertoni. *Plant Productions*. <https://doi.org/10.22055/ppd.2024.47365.2187>
- Phillips JM, Hayman DS. 1970. Improved procedure for clearing roots and staining parasitic and vesicular-arbuscular mycorrhizal fungi for rapid assessment of infection. *Transactions of the British Mycological Society* 55 (1): 158–161. [https://doi.org/10.1016/s0007-1536\(70\)80110-3](https://doi.org/10.1016/s0007-1536(70)80110-3)
- Pigatto GB, Gomes EN, Tomasi JC, Ferriani AP, Deschamps C. 2018. Effects of indolebutyric acid, stem cutting positions and substrates on the vegetative propagation of *Stevia rebaudiana* Bertoni. *Revista Colombiana de Ciencias Hortícolas* 12 (1): 202–211. <https://doi.org/10.17584/rch.2018v12i1.6631>
- Quiñones-Aguilar EE, Montoya-Martínez AC, Rincón-Enriquez G, Lobit P, López-Pérez L. 2016. Effectiveness of native arbuscular mycorrhizal consortia on the growth of *Agave inaequidens*. *Journal of Soil Science and Plant Nutrition* 16 (4): 1052–1064. <https://doi.org/10.4067/s0718-95162016005000077>
- Rakibuzzaman M, Shimasaki K, Uddin AJ. 2018. Influence of cutting position and rooting hormones on rooting of stevia (*Stevia rebaudiana*) stem cutting. *International Journal of Business, Social and Scientific Research* 6 (4): 122–125.
- Shahu R, Kumar D, Ali A, Tungare K, Al-Anazi KM, Farah MA, Jobby R, Jha P. 2023. Unlocking the therapeutic potential of *Stevia rebaudiana* Bertoni: A natural antiglycating agent and non-toxic support for HDF cell health. *Molecules* 28 (19): 6797. <https://doi.org/10.3390/molecules28196797>
- Sharma S, Walia S, Singh B, Kumar R. 2015. Comprehensive review on agro technologies of low-calorie natural sweetener stevia (*Stevia rebaudiana* Bertoni): A boon to diabetic patients. *Journal of the Science of Food and Agriculture* 96 (6): 1867–1879. <https://doi.org/10.1002/jsfa.7500>
- Siddique AB, Rahman SM, Hossain MA. 2016. Chemical composition of essential oil by different extraction methods and fatty acid analysis of the leaves of *Stevia rebaudiana* Bertoni. *Arabian Journal of Chemistry* 9: S1185–S1189. <https://doi.org/10.1016/j.arabjc.2012.01.004>
- Song X, Huang R, Liu H, Zhang J, Chang Y, Pei D. 2024. Transcriptome profiling of indole-3-butyric acid-induced adventitious root formation in softwood cuttings of walnut. *Horticultural Plant Journal* 10 (6): 1336–1348. <https://doi.org/10.1016/j.hpj.2023.04.013>
- StatPoint. 2005. Inc. StatGraphics Centurion XV version 15.02.06. Warrenton, VA, USA.
- Sukumar P, Legué V, Vayssières A, Martin F, Tuskan GA, Kalluri UC. 2012. Involvement of auxin pathways in modulating root architecture during beneficial plant-microorganism interactions. *Plant, Cell and Environment* 36 (5): 909–919. <https://doi.org/10.1111/pce.12036>
- Szentpéteri L, Irmes K, Kristó I, Rácz A, Vályi-Nagy M, Tar M. 2023. The effect of arbuscular mycorrhiza on the yield of different winter wheat varieties at four nutrient levels. *Review on Agriculture and Rural Development* 12 (1–2): 88–94. <https://doi.org/10.14232/rard.2023.1-2.88-94>

- Taghizadeh M, Azimi Senejani Z, Solgi M. 2023. Improvement of *Zamioculcas zamiifolia* vegetative propagation by mycorrhizal biofertilizer and biochar application. *Agricultural Engineering* 46 (2): 195–214. <https://doi.org/10.22055/agen.2023.44719.1681>
- Tavarini S, Passera B, Martini A, Avio L, Sbrana C, Giovannetti M, Angelini LG. 2018. Plant growth, steviol glycosides and nutrient uptake as affected by arbuscular mycorrhizal fungi and phosphorous fertilization in *Stevia rebaudina* Bert. *Industrial Crops and Products* 111: 899–907. <https://doi.org/10.1016/j.indcrop.2017.10.055>
- Tchiechoua YH, Kinyua J, Ngumi VW, Odee DW. 2019. Effect of indigenous and introduced arbuscular mycorrhizal fungi on growth and phytochemical content of vegetatively propagated *Prunus africana* (Hook. f.) Kalkman provenances. *Plants* 9 (1): 37. <https://doi.org/10.3390/plants9010037>
- Tedone L, Ruta C, de Cillis F, De Mastro G. 2020. Effects of *Septoglomus viscosum* inoculation on biomass yield and steviol glycoside concentration of some *Stevia rebaudiana* chemotypes. *Scientia Horticulturae* 262: 109026. <https://doi.org/10.1016/j.scienta.2019.109026>
- Tey SL, Salleh NB, Henry J, Forde CG. 2016. Effects of aspartame-, monk fruit-, stevia- and sucrose-sweetened beverages on postprandial glucose, insulin and energy intake. *International Journal of Obesity* 41 (3): 450–457. <https://doi.org/10.1038/ijo.2016.225>
- Thirkell TJ, Pastok D, Field KJ. 2020. Carbon for nutrient exchange between arbuscular mycorrhizal fungi and wheat varies according to cultivar and changes in atmospheric carbon dioxide concentration. *Global Change Biology* 26 (3): 1725–1738. <https://doi.org/10.1111/gcb.14851>
- Trinidad-Cruz JR, Quiñones-Aguilar EE, Hernández-Cuevas LV, López-Pérez L, Rincón-Enríquez G. 2017b. Hongos micorrícicos arbusculares asociados a la rizósfera de *Agave cupreata* en regiones mezcaleras del Estado de Michoacán, México. *Scientia Fungorum* 45: 13–25. <https://doi.org/10.33885/sf.2017.0.1164>
- Trinidad-Cruz JR, Quiñones-Aguilar EE, Rincón-Enríquez G, López-Pérez L, Hernández-Cuevas LV. 2017a. Mycorrhization of *Agave cupreata*: Biocontrol of *Fusarium oxysporum* and plant growth promotion. *Revista Mexicana de Fitopatología* 35 (2): 151–169. <https://doi.org/10.18781/r.mex.fit.1607-5>
- Vicente-Hernández A, Salgado-Garciglia R, Valencia-Cantero E, Ramírez-Ordorica A, Hernández-García A, García-Juárez P, Macías-Rodríguez L. 2018. *Bacillus methylotrophicus* M4-96 stimulates the growth of strawberry (*Fragaria × ananassa* ‘Aromas’) plants *in vitro* and slows *Botrytis cinerea* infection by two different methods of interaction. *Journal Plant Growth Regulation* 38 (3): 765–777. <https://doi.org/10.1007/s00344-018-9888-6>
- Wahab A, Muhammad M, Munir A, Abdi G, Zaman W, Ayaz A, Khizar C, Reddy SPP. 2023. Role of arbuscular mycorrhizal fungi in regulating growth, enhancing productivity, and potentially influencing ecosystems under abiotic and biotic stresses. *Plants* 12 (17): 3102. <https://doi.org/10.3390/plants12173102>
- Wang X, Pan Q, Chen F, Yan X, Liao H. 2011. Effects of co-inoculation with arbuscular mycorrhizal fungi and rhizobia on soybean growth as related to root architecture and availability of N and P. *Mycorrhiza* 21 (3): 173–181. <https://doi.org/10.1007/s00572-010-0319-1>

COMPARATIVE ANALYSIS OF SENSORY PROFILES OF TEMPEH PREPARED WITH AMARANTH vs. SOY USING *Rhizopus oligosporus* AS INOCULUM

Jessica Michel Cruz-González¹, Ricardo Hernández-Martínez¹,
Fernando Carlos Gómez-Merino¹, Adrián Argumedo-Macías², Mirna López-Espíndola¹,
Estela Chicuellar-Trujillo³, José Andrés Herrera-Corredor^{1*}

¹Colegio de Postgraduados Campus Córdoba. Carretera Federal Córdoba-Veracruz km 348, Manuel León, Amatlán de los Reyes, Veracruz, Mexico. C. P. 94953.

²Colegio de Postgraduados Campus Puebla. Boulevard Forjadores de Puebla, Santiago Momoxpan, San Pedro Cholula, Puebla, Mexico. C. P. 72760.

³Universidad Tecnológica del Centro de Veracruz. Carretera Federal Cuitláhuac-La Tinaja, Dos Caminos, Cuitláhuac, Veracruz, Mexico. C. P. 94910.

* Author for correspondence: jandreshc@colpos.mx

ABSTRACT

The study aimed to develop a *Rhizopus oligosporus* starter culture for using it in the preparation of amaranth-based and soy-based tempeh and to compare their resulting sensory profiles using the Rate-All-That-Apply (RATA) technique. In this study, the *Rhizopus oligosporus* inoculum for tempeh preparation was produced by Solid State Fermentation in rice. During inoculum production, the effects of initial pH (4.5, 5.0, 5.5, 6.0, and 6.5) and initial temperature (25, 30, 35, and 40 °C) were determined. Products generated during fungal metabolism were analyzed: organic acid content by titration, lactic acid production by spectroscopy, and the final pH of the medium. Once the appropriate conditions for inoculum production were determined, a comparative analysis of the sensory profiles of amaranth-based and soy-based tempeh was performed using the Rate That Apply (RATA) technique. The results showed that the highest lactic acid production was obtained when the initial pH of the medium was adjusted to pH 5.5 (1.75 g L⁻¹) and at 40 °C (1.85 g L⁻¹). Likewise, the highest organic acid production was observed at an initial pH of 5.0 (0.066 g L⁻¹), pH 6.0 (0.105 g L⁻¹), and at 35 °C (0.69 g L⁻¹). Different sensory profiles were observed. The soy-based tempeh differed from the amaranth-based tempeh in its fishy odor and flavor. Therefore, the lactic acid content, organic acids, and final pH of the medium are influenced by the initial pH and temperature of the medium. The sensory profile of tempeh is influenced by the raw materials used in its preparation.

Keywords: fermentation, inoculum, amaranth, tempeh, sensory profile.

Citation: Cruz-González JM, Hernández-Martínez R, Gómez-Merino FC, Argumedo-Macías A, López-Espíndola M, Chicuellar-Trujillo E, Herrera-Corredor JA. 2026. Comparative analysis of sensory profiles of tempeh prepared with amaranth vs. soy using *Rhizopus oligosporus* as inoculum. *Agrociencia* 60(3): 355-371. <https://doi.org/10.47163/agrociencia.v60i3.3733>

Editor in Chief:
Dr. Fernando C. Gómez Merino

Received: December 20, 2025.

Approved: May 07, 2026.

Published in Agrociencia:
May 12, 2026.

This work is licensed under a Creative Commons Attribution-Non-Commercial 4.0 International license.



INTRODUCTION

The plant-based protein market is experiencing constant growth, driven by an increasing consumer demand for more sustainable, healthy, and innovative options (Das *et al.*, 2021). According to Mintel's global database, the plant-based protein market is projected to reach \$160 billion USD by 2030 (Mintel, 2025). Amaranth has emerged as a promising alternative within the plant-based protein market due to its high-quality protein content. This grain is recognized for its complete profile of essential amino acids, as well as its mineral and fiber content (Das *et al.*, 2021). Studying the diversification of amaranth uses is a strategy to leverage the nutritional benefits of this grain. Currently, various strategies are being explored to promote the diversification of amaranth-based products with the aim of integrating it into the human diet (FAO, 2024). A new alternative for diversifying amaranth-based products is incorporating this grain into tempeh preparation. Amaranth's nutritional properties can significantly enhance the product, including calcium, iron, potassium, vitamins B1, B2, B3, and B6, 14–20 % fiber, 7–9 % fat and 14–18 % protein (Mătieș *et al.*, 2024).

In 2023, the global tempeh market was valued at \$5.17 billion USD, and sustained growth of 5.8 % annually is projected through 2030 (Grand View Research, 2023). This traditional Indonesian food is traditionally prepared from soybeans fermented with fungi of the genus *Rhizopus* and is consumed as an accessible and inexpensive source of high-quality protein (Do Prado *et al.*, 2021). Tempeh has been recognized with multiple health benefits, such as glycemic control, antioxidant effects, antidiabetic effects, blood glucose reduction and cholesterol reduction (Do Prado *et al.*, 2021; Prativi *et al.*, 2023). The tempeh production process is considered an economical and sustainable technology that allows to produce protein-rich foods using various legumes or grains (Ahnán-Winarno *et al.*, 2021).

Currently, it has been shown that the use of *Rhizopus oligosporus* in fermented products improves their sensory properties compared to other species of the same genus, such as *Rhizopus oryzae* and *Rhizopus delemar* (Wikandari *et al.*, 2021). Therefore, commercial inoculants for tempeh production typically contain *Rhizopus oligosporus* spores mixed with rice flour, rice bran, or wheat bran (Codex Alimentarius, 2013). The interaction between the grain and the fungus results in the characteristics of tempeh, which are usually analyzed through sensory evaluation. In their study, Tan *et al.* (2024), used a 9-point hedonic scale, evaluated the liking and acceptability of soy tempeh, demonstrated that appearance, flavor, aroma, and texture impact consumer acceptability. Mahdi *et al.* (2023), using the Rate-All-That-Apply (RATA) technique, they identified the main attributes of tempeh, such as white color, mushroom odor, bean odor, umami flavor, and bitter flavor.

Tempeh production requires the availability of *Rhizopus oligosporus* inoculum. During fermentation for inoculum production, byproducts such as organic acids and CO₂ are generated. Studying fungal metabolic byproducts allows for the identification of suitable inoculum production conditions. Tempeh prepared from amaranth may have a different sensory profile than that prepared from soy, given the differences in

their chemical composition. The present study aimed to develop a *Rhizopus oligosporus* starter culture for using it in the preparation of amaranth-based and soy-based tempeh and to compare their resulting sensory profiles using the Rate-All-That-Apply (RATA) technique.

MATERIALS AND METHODS

Material

Medium-grain rice, Cies® brand (PROMEXA, Veracruz, Mexico), purchased at a local supermarket in downtown Córdoba, Veracruz was used as substrate for inoculum development. Amaranth grain was of the species *Amaranthus cruentus* cultivated in San Mateo Coatepec, Puebla, Mexico, during 2022. Soybeans were purchased at the local supermarket in Córdoba, Veracruz, Mexico.

Microorganism

The fungal strains of *Rhizopus oligosporus* were obtained according to the method proposed by Kim *et al.* (2013): 200 g of rice were soaked for 24 h. After reaching 80 % moisture, grains were incubated for 7 days at 30 °C. The fermented substrate was dried at 40 °C in an incubator (model 21-250ER, Quincy Lab, USA) for 24 h and pulverized in a cyclonic mill (model 310-014, UDY, Rome Court, USA). For the cultivation stage, the powder was spread onto PDA plates and incubated for 4 days at 25 °C. Finally, the cultures were subcultured in 250 mL Pyrex® flasks containing 50 mL of PDA and incubated for 5 days at 25 °C to obtain a pure culture.

For the strain preservation the fungal cultures were inoculated into Pyrex® test tubes containing 8 mL of Potato Dextrose Agar (PDA) medium and incubated for 48 h at 30 °C. The strain was harvested by adding 5 mL of 0.1 % Tween 20 sterile solution to the fungal cultures, then the mixture was vortexed (UNICO, L-VM1000, USA). A 0.5 mL aliquot of this suspension was transferred to Pyrex® flasks containing 50 mL of PDA medium and incubated for 6 days at 25 °C (Wikandari, 2021). Spores were harvested using a 0.1 % Tween 20 sterile solution and transferred to 250 mL Pyrex® glass flasks containing 20 mL of previously sterilized 10 % Svelty® nonfat dry milk. The mixture was stirred on a magnetic stirrer (model PC-353 Stirrer, Corning, USA). The suspension was transferred to 50 mL Falcon® tubes and homogenized using a vortex mixer. The fungi suspensions were frozen at -70 °C in a deep freezer and then freeze-dried. The stock cultures were preserved in 2 mL cryovials at -20 °C until use.

Inoculum

From the stock culture preserved in Svelty® skim milk, the inoculum for solid-state fermentation was produced at 30 °C for 4 days in 250 mL Pyrex® flasks containing 50 mL of PDA medium. Spores were harvested using 0.1 % Tween 20 and stored in 50 mL Corning® centrifuge tubes until used as inoculum for solid-state fermentation.

Substrate

Rice was pre-conditioned for use as a substrate during solid-state fermentation to produce inoculum for tempeh preparation. It was washed and soaked (1:1 rice:water ratio) for 1 h, then cooked for 3 min in boiling water and centrifuged using a manual food centrifuge.

Solid-State Fermentation

Solid-state fermentation (SSF) was carried out using rice as support/substrate in trays. The SSF conditions were adjusted at 1.5 cm bed height, 60 % moisture, and 1 % v/w inoculum (1×10^6 spores mL⁻¹ concentration). Samples of the fermented substrate were taken and stored at -20 °C until needed for the determination of lactic acid, organic acids, and final pH. To produce the inoculum intended for tempeh preparation, the fermented substrate was freeze-dried for three days. Two grams of inoculum were packaged in vacuum-sealed bags and stored at -20 °C until needed for tempeh production.

Determination of lactic acid, organic acids, and final pH analysis

Samples of rice fermented with *Rhizopus oligosporus* were ground in a mortar and suspended in distilled water at a 1:10 ratio (rice: water). The mixture was stirred and centrifuged at 1784 x g for 15 min. The supernatant was decanted and used for the quantification of lactic acid, organic acids, and final pH analysis.

Lactic Acid

The lactic acid content was analyzed using the spectrophotometric method (Borrshchevskaya, 2016). To analyze the lactic acid content in the fermented substrate, 50 µL of the supernatant sample was added to 2 mL of ferric chloride (FeCl₃) solution. The lactic acid concentration was calculated using the lactic acid standard curve with a detection range of 0.078–10.0 g L⁻¹. The analysis was performed in triplicate.

Organic acids

The determination of organic acids was performed according to the methodology proposed by Paul *et al.* (2010). The analysis was performed in triplicate.

Final pH

The pH determination was carried out according to AOAC 943.02/90. 10 mL of the supernatant sample were used, and the reading was taken with a potentiometer (model HI98103, Hanna Instruments®, México). The analysis was performed in triplicate.

Respiratory Analysis

The growth of *Rhizopus oligosporus* was monitored in two phases to identify when the exponential phase occurred. In the first phase, CO₂ levels were monitored for 35 h without adjusting the pH or temperature of the medium. In the second phase,

monitoring was performed under appropriate pH and temperature conditions that allowed for a higher production of lactic acid and organic acids as determined in the first phase.

To measure CO₂ release an SCD40 CO₂ sensor, an I2C digital interface with a digital output signal, and an integrated temperature and humidity sensor were used. The sensor allowed monitoring of CO₂ release over time, avoiding costly procedures. The sensor was integrated with an Arduino UNO board and a data logger base (TZZ, China). Temperature, relative humidity, and CO₂ levels were recorded every 20 min. The data was stored on a 64 GB MicroDrive® SD card.

Effect of pH on the production of lactic acid, organic acids, and final pH

The effect of pH on the production organic acids was evaluated by adjusting the substrate to values of 4.5, 5.0, 5.5, 6.0, and 6.5.

Effect of temperature on the production of lactic acid, organic acids, and final pH

Solid-state fermentation with rice was carried out at temperatures of 25, 30, 35, and 40 °C to evaluate its effect on the production of organic acids, and final pH of the substrate.

Tempeh Production

For tempeh preparation, the inoculum used was produced by solid-state fermentation of rice with *Rhizopus oligosporus*. The substrates were pre-conditioned for use in tempeh preparation.

Soybeans preconditioning

The soybeans were soaked for 24 h. The hulls were removed and the beans were cooked for 40 min and then cooled to room temperature. The thickness of their hulls is between 70-230 μm, being a thick layer, the soaking and cooking process facilitates its removal (Lemes & Catão, 2024). The hull is usually removed to facilitate the penetration of *Rhizopus oligosporus* and to allow it to obtain the necessary nutrients for its growth.

Amaranth

Amaranth grains were soaked for 24 h. They were then cooked for 5 min without removing the hull and allowed to cool to room temperature. The amaranth hull was not removed because the amaranth grain is very small, the thickness of its hull is between 3.7–50 μm. Unlike soybeans, the amaranth hull is thinner and is attached to the endosperm, which prevents its detachment during soaking or cooking (Ninfali *et al.*, 2020).

Preparation of Soy and Amaranth Tempeh

For tempeh preparation, 400 g of conditioned amaranth and 400 g of conditioned soybeans batches were used, inoculated with 2 g of *Rhizopus oligosporus* inoculum and

incubated for 12 h at 30 °C. Finally, the amaranth-based tempeh and the soy-based tempeh (Figure 1) were stored at -20 °C until used for sensory evaluation.

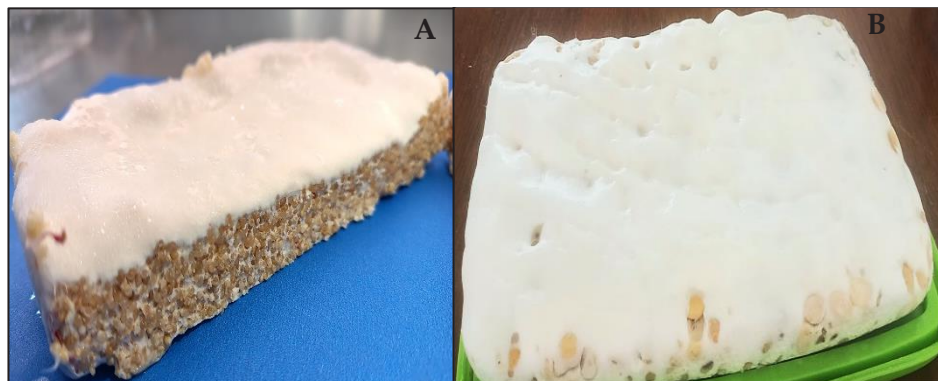


Figure 1. Tempeh prepared with amaranth and soy. A: amaranth tempeh; B: soy tempeh.

Protein Determination

The protein content was determined for soybeans and for raw, unconditioned soybeans. It was also determined for amaranth-based tempeh and soy-based tempeh. The analysis was performed on a dry basis using the Kjeldahl method according to AOAC 955.04. The tests were performed in triplicate.

Sensory testing

Sample Preparation

Sample size used for sensory testing were 2.5 x 2.5 x 2 cm tempeh cubes for soy (15 g) and amaranth (12 g). Cubes were baked for 50 min at 160 °C. Subsequently, each cube was placed in 60 mL souffle disposable containers and kept at room temperature prior to consumer testing.

Obtaining Attributes

For soy tempeh, 12 attributes were obtained for sight, 20 for smell, 18 for taste, and 10 for touch. For amaranth tempeh, 20 attributes were obtained for sight, 13 for smell, 12 for taste, and 9 for touch. To reduce the number of attributes, a refinement process was carried out to eliminate synonyms or words irrelevant to the product.

To select the most representative attributes of soy and amaranth tempeh, the CATA method was used. Participants were presented with a Google® Forms questionnaire containing the list of attributes and instructed to select all those that applied to the product. The selection of representative attributes for amaranth and soy tempeh

was based on attribute frequencies. A binomial test was performed to determine the attributes with frequencies significantly different from 0 (H_0 : frequency = 0; H_a : frequency \neq 0). The attributes that were significant ($p < 0.05$) were selected, included in the attribute list and used to perform the following evaluation of amaranth-based and soy-based tempeh.

Rate-All-That-Apply (RATA)

The Rate-All-That-Apply (RATA) technique was used to obtain the sensory profiles of soy-based and amaranth-based tempeh. The evaluation was carried out at the Technological University of Central Veracruz. 75 consumers participated, including students and academics from the municipalities of Amatlán de los Reyes, Atoyac, Carrillo Puerto, Córdoba, Coscomatepec, Cosolapa, Cuichapa, Yanga, Cuitláhuac, Fortín, Omealca, Orizaba, Paso del Macho, Potrero, Tezonapa, and Tierra Blanca.

Questionnaire Design

The first section of the questionnaire included questions related to demographic information. The second and third sections contained the space for the sample code and the list of attributes, which included: five for the sense of sight, eight for the sense of smell, eight for the sense of taste, and four for the sense of touch. A scale of 1 to 7 was used to collect the intensity values for the perceived attributes.

Statistical analysis

Statistical analysis of inoculum collection data.

Two Completely Randomized Designs (CRDs) were performed for: 1) initial medium pH with five levels (4.5, 5.0, 5.5, 6, and 6.5) and 2) temperature with four levels (25, 30, 35, and 40 °C). Each treatment was evaluated in three replicates. The response variables evaluated in both (initial medium pH and temperature) were lactic acid, organic acids, and final medium pH. Data was analyzed using one-way ANOVA. Mean comparisons were performed using Tukey's test to observe significant differences ($p < 0.05$) in lactic acid production, organic acids, and final pH.

Analysis for RATA test data

Two treatments were evaluated: amaranth-based tempeh and soy-based tempeh. Two approaches were used for data analysis: 1) as binomial data and 2) as rating data. For the first approach, the results were transformed into a binomial scale. All non-zero results were converted to 1. A 0 indicated absence and a 1 indicated presence of the attribute. Subsequently, the results were analyzed using the chi-square (χ^2) test to determine if there was an association between the raw material and the perceived attributes of soy-based tempeh versus amaranth-based tempeh. For the second approach, a t-test was performed to compare the intensity of the attributes between the sensory profiles of amaranth and soy (Meyners *et al.*, 2016).

The significance level for the study was $\alpha = 0.05$. The data were processed using R version 4.5.0 ucrt with RStudio version 2025.05.0 Build 496.

RESULTS AND DISCUSSION

Respirometry without defined pH and temperature parameters

The CO₂ profile recorded during solid-state fermentation reflected the *Rhizopus oligosporus* growth under uncontrolled conditions (Figure 2).

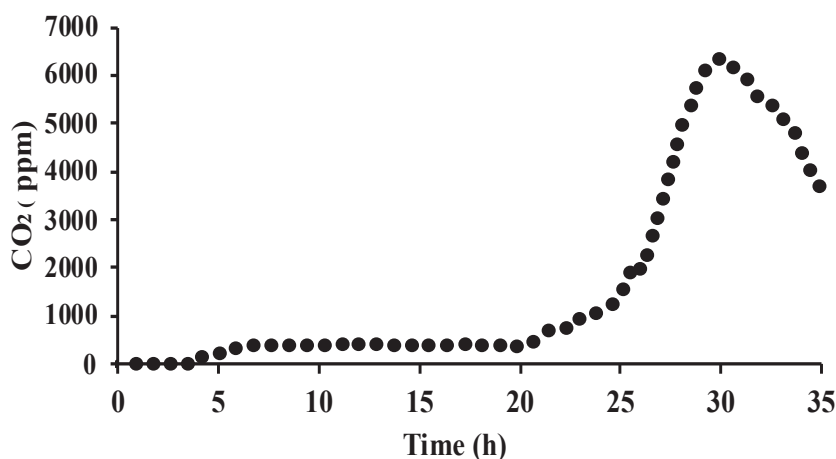


Figure 2. CO₂ profile without defined pH and initial temperature parameters. The CO₂ profile represents the metabolic activity of *Rhizopus oligosporus* over 35 h.

The peak of exponential fungal growth occurred at 30 h, indicating that solid-state fermentation should be stopped. After this time, CO₂ release began to decrease, indicating a slowdown in fungal metabolism. The decrease in CO₂ may indicate nutrient depletion, where the fungus was limited in resources to continue its growth (Sandoval *et al.*, 2024). Therefore, solid-state fermentations to produce inoculum for tempeh preparation were maintained for 30 h. Based on this, some of the physiological products generated during fungal metabolism, such as CO₂ and organic acids, were analyzed.

Effect of adjusting the initial pH of the medium on the production of organic acids

The data obtained (Table 1) indicated that the initial pH of the medium had a significant effect ($p < 0.05$) on organic acids content, and the decrease in pH at the end of solid-state fermentation with rice.

The lowest lactic acid production values at the end of fermentation occurred at pH 5 (1.34 g L⁻¹) and pH 6 (1.32 g L⁻¹), whereas the highest values were reached at pH 5.5 (1.75 g L⁻¹) and pH 6.5 (1.51 g L⁻¹). Therefore, adjusting the pH at the start of fermentation increased lactic acid production. Lactic acid content began to increase from pH 4.5 and gradually increased up to pH 5.5.

Table 1. Effect of initial pH on organic acid production and final pH of the medium at the end of solid-state fermentation.[†]

Initial pH	Lactic acid (g L ⁻¹)	Organic acids (g L ⁻¹)	Final pH
4.5	1.40 ± 0.145 b	0.126 ± 0.041 c	4.53 ± 0.208 ab
5.0	1.34 ± 0.076 b	0.066 ± 0.014 c	5.16 ± 0.252 a
5.5	1.75 ± 0.020 a	0.675 ± 0.024 a	3.76 ± 0.551 b
6.0	1.32 ± 0.065 b	0.105 ± 0.027 c	4.46 ± 0.416 ab
6.5	1.51 ± 0.158 ab	0.375 ± 0.019 b	4.50 ± 0.265 ab
P-value	0.00366	<0.0001	0.0122

[†]Means ± standard deviation with different letters in each column indicate significant differences between treatments (Tukey, $p \leq 0.05$); n= 3.

At the end of fermentation, the highest organic acid content was observed at pH 5.5 (0.675 g L⁻¹) and pH 6.0 (0.105 g L⁻¹). The pH values 4.5 and 5 remained constant throughout fermentation, whereas pH values 5.5, 6, and 6.5 showed a decrease over the process. This pH reduction suggests higher acidification of the medium associated with increased production of organic acids. These results indicate that *Rhizopus oligosporus* grows adequately using a pH of 5.5, which is ideal for obtaining higher organic acids production.

Effect of temperature adjustment on the production of lactic acid, organic acids, and final pH of the medium

As expected, the results obtained indicated that temperature had a significant effect ($p < 0.05$) on organic acids content, and the decrease in medium pH during fermentation with *Rhizopus oligosporus* (Table 2).

The highest lactic acid production occurred at 35 and 40 °C, with yields of 1.69 and 1.85 g L⁻¹, respectively. A correlation was observed where higher temperatures resulted in

Table 2. Effect of temperature on organic acid production and final pH of the medium at the end of solid-state fermentation.[†]

Temperature (°C)	Lactic Acid (g L ⁻¹)	Organic acids (g L ⁻¹)	Final pH
25	1.57 ± 0.036 c	0.05 ± 0.005 d	4.5 ± 0.05 a
30	1.69 ± 0.031 b	0.57 ± 0.036 c	4.2 ± 0.0 b
35	1.75 ± 0.050 b	0.96 ± 0.027 a	4.2 ± 0.0 b
40	1.85 ± 0.021 a	0.69 ± 0.014 b	4.6 ± 0.05 a
P-value	<0.0001	<0.0001	<0.0001

[†]Means ± standard deviation with different letters in each column indicate statistical differences between treatments (Tukey, $p \leq 0.05$); n= 3.

higher lactic acid production. The highest organic acid production occurred at 35 °C, with a yield of 0.966 g L⁻¹. However, production decreased above 40 °C. Although the initial pH for all four incubation temperatures was 5.5, a lower pH was recorded at 30 °C and 35 °C. These results demonstrate that *Rhizopus oligosporus* is a microorganism tolerant to high temperatures and capable of producing lactic acid at 40 °C.

The production of organic acids is affected by pH and temperature. The results indicated that higher production rates of lactic acid and organic acids are obtained at a pH of 5.5 and a temperature of 40 °C. These conditions are considered suitable for producing the inoculum intended for tempeh preparation. The growth curve of *Rhizopus oligosporus* was also plotted under these conditions.

Respirometry with selected pH and temperature conditions

The growth curve of *Rhizopus Oligosporus* presents a change over 30 h with an initial pH of 5.5 and a temperature of 40 °C (Figure 3). *Rhizopus oligosporus* behaved differently under adequate pH and temperature conditions, exhibiting higher CO₂ rates in a shorter time.

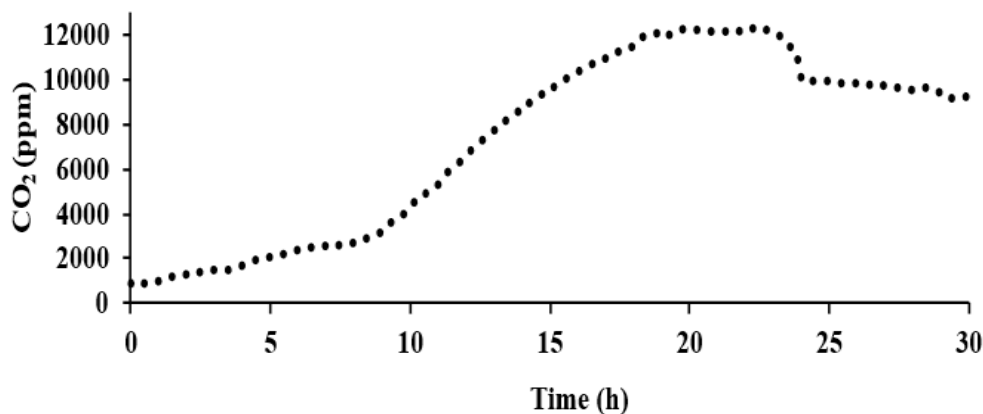


Figure 3. CO₂ profile under controlled conditions of pH 5.5 and temperature 40 °C. The CO₂ profile represents the metabolic activity of over 30 h.

It showed that the exponential phase began at 8 h. The peak of exponential fungal growth, with the highest CO₂ release, decreased from 30 to 19 h. After 24 h, fungal growth slowed with low CO₂ rates. This may be due to the finite amount of available nutrients in fungi, so after reaching maximum activity, growth continues, but at a slower rate (Sandoval *et al.*, 2024). According to the results, using appropriate pH and temperature conditions allows for a reduction in fermentation time. By adjusting the substrate to a pH of 5.5 and using a temperature of 40 °C, the exponential phase of

Rhizopus oligosporus occurs at 19 h and a higher production of lactic acid and organic acids is obtained.

Protein Content

Soybeans and soy-based tempeh had higher protein content than amaranth and amaranth-based tempeh ($p < 0.05$). Soybeans had 31.18 % and soy-based tempeh had 39.53 %. Amaranth grain was 18.93 %, while tempeh had 18.41 %. These protein content results are within the range reported in various studies. Amaranth has been reported to have between 14 % and 19 % protein (Baraniak & Kania-Dobrowolska, 2022), and soy tempeh between 25 % and 45 % (Toor *et al.*, 2022).

Amaranth did not show a significant change in protein content after fermentation. However, soy-based tempeh showed an 8.4 % increase compared to its initial protein content. This increase in protein content after fermentation with *Rhizopus oligosporus* has already been described in studies (Ferreira *et al.*, 2011; Bavia *et al.*, 2012). In our study, this increase in protein is attributed to the dehulling of the soybeans. Dehulling caused a change in the proportions of its components. This change in the proportions of soybean components has already been observed by other authors (Raji *et al.*, 2008; Bavia *et al.*, 2012). The soybean hull is composed mainly of fiber and constitutes a non-protein fraction. By reducing this fraction, a higher concentration of the remaining components, such as an increase in protein content, is expected (Kohli & Singha, 2024). Soybeans are primarily composed of protein (20-45 %), carbohydrates (36.37-65.71 %), lipids (5-21 %), and fiber (5-9 %) (Raji *et al.*, 2008; W; Kohli & Singha, 2024). Despite being an important source of nutrients, soybeans have limited digestibility in their whole form, making it important to remove the hull during processing (Kohli & Singha, 2024).

Sensory testing

The evaluation of intensity in sensory attributes included students, academics, employees, and merchants primarily from the municipalities of Córdoba (21 %), Cuitláhuac (13 %), Amatlán de los Reyes (12 %), Fortín (10 %), Atoyac (8 %), and Yanga (8 %). Sixty percent were female and 40 % were male. 85 % were between 18 and 24 years old, 7 % between 25 and 34, 5 % between 35 and 44, and 3 % between 45 and 54. 95 % reported never having consumed tempeh, while 3 % reported having consumed it.

Comparison of Sensory Profiles Using Data Transformed to a Binomial Scale

The results of the Chi-square test revealed significant associations with the type of grain (Table 3).

For amaranth-based tempeh, consumers more frequently reported the presence of the attribute of compactness ($p = 0.049$) perceived through sight and the attribute of roughness ($p < 0.0001$) perceived through touch. For soy tempeh, consumers most frequently indicated the presence of the attribute "fishy smell" ($p < 0.0001$) through the

Table 3. Significant attributes that depend on the grain used to prepare tempeh.[†]

Attribute	P-value
Compact	0.049
Fishy smell	<0.0001
Fishy flavor	0.0246
Moist	0.025
Soft	0.0044
Rough	<0.0001

[†] $p \leq 0.05$ indicates significant associations between the sensory attribute and the raw material used to prepare tempeh.

sense of smell, the attribute “fishy flavor” ($p = 0.0246$) through the sense of taste, and the attributes “moist” ($p = 0.025$) and “soft” ($p = 0.0044$) through touch. This suggests that the presence of each attribute is related to the type of grain used to prepare the tempeh.

Comparison of sensory profiles using RATA ratings

The intensities of the attributes perceived through sight, smell, taste, and touch showed significant differences between the two samples (Table 4). The attributes compactness ($P < 0.0001$), fishy odor ($P < 0.0001$), soy odor ($P = 0.0017$), amaranth odor ($P < 0.0001$), baked odor ($P = 0.0039$), fishy flavor ($P = 0.0035$), amaranth flavor ($P < 0.0001$), moistness ($P = 0.0011$), softness ($P < 0.0001$), and roughness ($P < 0.0001$) were perceived at different intensities in the two tempeh samples.

The characteristics of tempeh are usually the result of the enzymatic activity of the fungus, which biotransforms the components of amaranth and soybean grains to ensure its survival during growth (Jeleń *et al.*, 2013). The white color and the presence of mycelium are related to the growth of *Rhizopus oligosporus* on the substrate and the network of hyphae that allows it to penetrate, bind, and compact the grains. Hyphal penetration depends on the grain’s cell walls, as these act as a physical barrier. However, the fungus secretes enzymes such as cellulase and hemicellulose that degrade the grain’s cell wall, binding them together to form a compact cake (Wikandari *et al.*, 2021; Tan *et al.*, 2024). During fermentation, the raw material interacts with *Rhizopus oligosporus* and produces volatile compounds and amino acids that affect the sensory characteristics of tempeh (Gunawan-Puteri *et al.*, 2015). Compounds such as 1-octene-3-ol and 3-octanone impart mushroom-like odors, while 3-(methylthio) propanal contributes to boiled potato-like aromas (Jeleń *et al.*, 2013). The amino acids alanine, glycine, serine, and threonine are responsible for the sweet taste (Gunawan-Puteri *et al.*, 2015). Another characteristic of various types of tempeh is their meaty and bready flavor. The meaty flavor or notes are associated with umami. This flavor is

Table 4. Intensities of attributes perceived through the senses for amaranth-based tempeh and for soy-based tempeh.[†]

	Attribute	Amaranth	Soy	p-value
Sense of sight	Compact	4.88	2.76	<0.0001
	Spongy	2.64	2.37	0.4605
	White	2.85	2.24	0.0648
	Granular	4.61	4.24	0.3375
	Smell of baking	3.07	3.4	0.4332
	Meat	1.51	1.92	0.2055
Sense of smell	Fishy smell	1.21	4.03	<0.0001
	Soy smell	1.53	2.64	0.0017
	Cereal smell	3.35	2.52	0.0445
	Potato smell	1.56	1.41	0.6422
	Amaranth smell	3.8	0.67	<0.0001
	Smell of baking	3.31	2.2	0.0039
Sense of taste	Fungi	2.21	2.89	0.108
	Fish	1.2	2.24	0.0035
	Fungi	1.93	2.36	0.2717
	Meat	1.19	1.51	0.3155
	Peanut	2.12	2.87	0.0515
	Smoked	2.57	2.23	0.369
	Sweet	1.13	0.83	0.2339
	Bread	1.76	1.8	0.9098
	Amaranth	4.16	0.65	<0.0001
Sense of touch	Moist	1.96	3.19	0.0011
	Soft	2.2	3.87	<0.0001
	Spongy	2.49	2.93	0.2505
	Rough	4.05	2.08	<0.0001

[†] $p \leq 0.05$ indicates significant differences in attributes between treatments. Scores represent the average intensities of attributes perceived in amaranth-based and soy-based tempeh on a scale of 1 to 7, based on 75 consumers.

produced during fermentation with the generation of amino acids grouped as sodium monoglutamate (Gunawan-Puteri *et al.*, 2015).

Sensory Profile of Amaranth and Soy based tempeh

Amaranth-based and soy-based tempeh have different sensory profiles, and these differences are related to the grain used in their preparation (Figure 4).

In amaranth tempeh, the attributes of compactness ($P < 0.0001$), amaranth flavor ($P < 0.0001$), and rough texture ($P < 0.0001$) were perceived more intensely. The higher intensity of the perceived compactness and roughness is related to the size of the grain. Amaranth grains are very small. When the fungal hyphae penetrate and bind

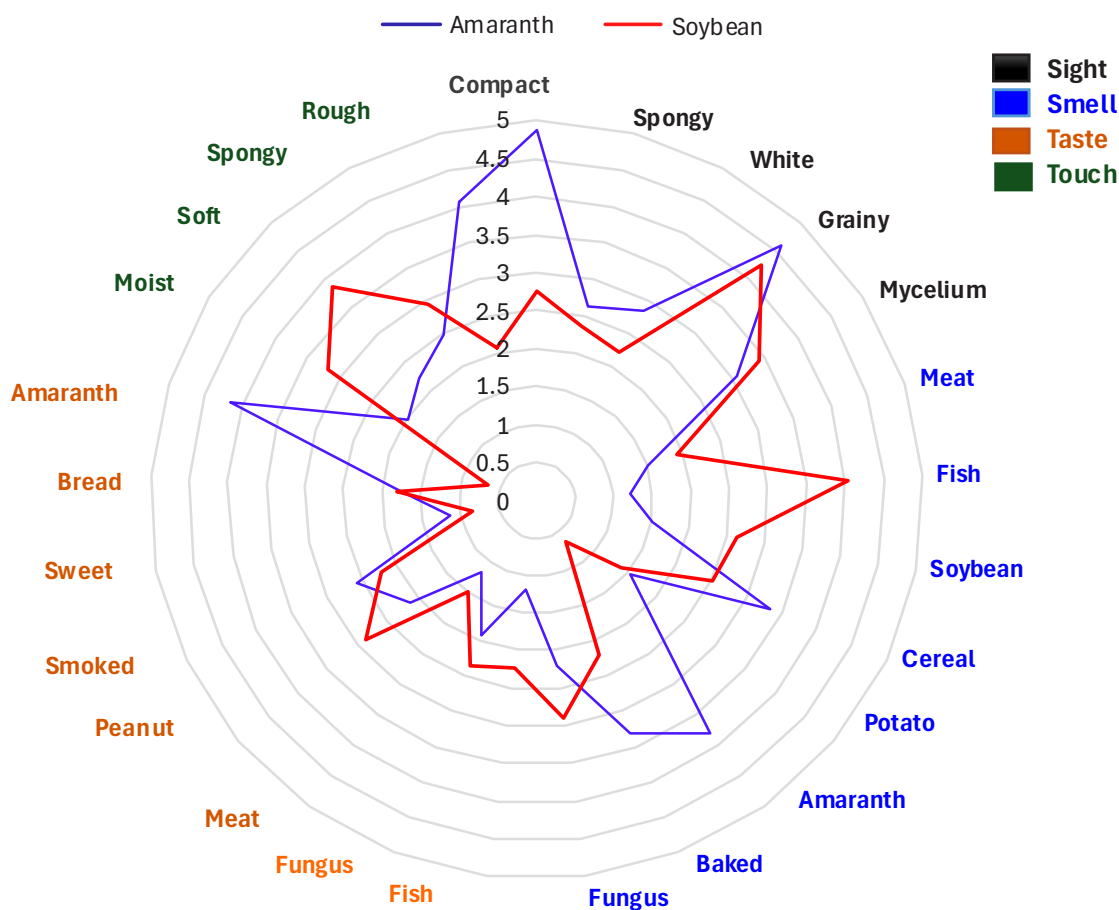


Figure 4. Sensory map for amaranth-based tempeh and soy-based tempeh. The sensory map represents the average intensity of the attributes perceived through the senses for both treatments, based on the 75 consumers who participated in the evaluation.

the grains together, a more compact tempeh with a rough surface is produced. Soy-based tempeh had a different sensory profile than amaranth-based tempeh, with the fishy odor ($P < 0.0001$), soy odor ($P = 0.0017$), fishy flavor ($P = 0.0035$), moistness ($P = 0.0011$), and softness ($P < 0.0001$) being perceived more intensely. The perception of soft and moist tempeh is associated to the grain's conditioning process, as the soaking and cooking process softens the grain and causes it to absorb more moisture. A predominant characteristic perceived in the soy tempeh was its fishy flavor and odor. These sensory characteristics are related to the composition of soybeans.

Soybeans have a significant lipid fraction (Jeleń *et al.*, 2013). Isoenzyme lipoxygenase is present in soybean. These enzymes are responsible for catalyzing the oxidation of fatty acids. Soybeans are an important source of fatty acids. They contain between 53 % and 54 % linoleic acid and 8 % α -linolenic acid. These polyunsaturated fatty acids are typically unstable and sensitive to oxidation. The interaction of lipoxygenase with fatty acids often results in strong or unpleasant odors and flavors in food (Chedea *et al.*, 2013). The degradation of fatty acids through lipoxygenase produces hydroperoxides, these are transformed into volatile compounds such as alcohols (1-octen-3-ol), amines (trimethylamine), sulfur compounds (dimethyl sulfide), aldehydes (heptanal) and ketones (1-octen-3-one) that are responsible for providing the fishy smell and flavor of soy-based tempeh (Chedea *et al.*, 2013).

CONCLUSIONS

The initial pH of the medium and the temperature are factors that affect the content of lactic acid, organic acids, the final pH, and CO₂ release. These factors influence the fungus' metabolism, allowing for higher concentrations of organic acids and CO₂ under appropriate pH and temperature conditions. The optimal conditions for inoculum production were established at pH 5.5 and a temperature of 40 °C. The peak of the fungus's exponential phase was reduced from 30 to 19 h. Soy tempeh and amaranth tempeh have different sensory profiles according to consumer perception. Amaranth tempeh exhibits characteristics related to the grain, such as the aroma and flavor of amaranth, whereas soy tempeh is predominantly fishy in smell and taste. Using amaranth in tempeh preparation is a viable alternative for diversifying the uses of this grain, as its sensory profile is neutral and it can be combined with various foods.

ACKNOWLEDGMENTS

The authors thank the Secretaría de Ciencias, Humanidades, Tecnología e Innovación (SECIHTI) for funding the first author's research project. They also thank the Colegio de Postgraduados for their support of this research study. Finally, they thank the UTCV for allowing the sensory study to be conducted on its campus and Professor Sandra Luz Valladolid for her support of the sensory study at that university.

REFERENCES

- Ahnan-Winarno, A. D., Cordeiro, L., Winarno, F. G., Gibbons, J., & Xiao, H. (2021). Tempeh: A semicentennial review on its health benefits, fermentation, safety, processing, sustainability, and affordability. *Comprehensive Reviews in Food Science and Food Safety*, 20(2), 1717-1767. <https://doi.org/10.1111/1541-4337.12710>
- Baraniak, J., & Kania-Dobrowolska, M. (2022). The dual nature of amaranth—functional food and potential medicine. *Foods*, 11(4), 618. <https://doi.org/10.3390/foods11040618>

- Bavia, A.C.F., Silva, C.E. D., Ferreira, M. P., Leite, R. S., Mandarino, J. M. G., & Carrão-Panizzi, M. C. (2012). Chemical composition of tempeh from soybean cultivars specially developed for human consumption. *Food Science and Technology*, 32, 613-620. doi.org/10.1590/S0101-20612012005000085
- Borshchevskaya, L. N., Gordeeva, T. L., Kalinina, A. N., & Sineokii, S. P. (2016). Spectrophotometric determination of lactic acid. *Journal of analytical chemistry*, 71(8), 755-758. <https://doi.org/10.1134/S1061934816080037>
- Chandel, N. S. (2021). Glycolysis. *Cold Spring Harbor Perspectives in Biology*, 13(5), a040535. [10.1101/cshperspect.a040535](https://doi.org/10.1101/cshperspect.a040535)
- Chedea, V. S., & Jisaka, M. (2013). Lipoxygenase and carotenoids: A co-oxidation story. *African Journal of Biotechnology*, 12(20). <https://doi.org/10.5897/AJB12.2944>
- Codex Alimentarius Commission (2013). REGIONAL STANDARD FOR TEMPE (CODEX STAN 313R-2013). Food and Agriculture Organization of the United Nations. Retrieved from https://www.fao.org/input/download/standards/13304/CXS_313Re_2015.pdf. Accessed February 15, 2025.
- Das, D., Mir, N. A., Chandla, N. K., & Singh, S. (2021). Combined effect of pH treatment and the extraction pH on the physicochemical, functional and rheological characteristics of amaranth (*Amaranthus hypochondriacus*) seed protein isolates. *Food Chemistry*, 353, 129466. <https://doi.org/10.1016/j.foodchem.2021.129466>
- Do Prado, F. G., Pagnoncelli, M. G. B., de Melo Pereira, G. V., Karp, S. G., & Soccol, C. R. (2022). Fermented soy products and their potential health benefits: A review. *Microorganisms*, 10(8), 1606. <https://doi.org/10.3390/microorganisms10081606>
- Dufossé, L. (2024). Fungi and Fungal Metabolites for the Improvement of Human and Animal Life, Nutrition and Health. *Journal of Fungi*, 10(12), 863. <https://doi.org/10.3390/jof10120863>
- FAO (2024). Promoviendo la Transformación de los Sistemas Agroalimentarios en México: El Rol del amaranto. Retrieved from <https://www.fao.org/mexico/noticias/detail-events/en/c/1681339/>. Accessed January 20, 2025.
- Ferreira, M. P., Oliveira, M. C. N. D., Mandarino, J. M. G., Silva, J. B. D., Ida, E. I., & Carrão-Panizzi, M. C. (2011). Changes in the isoflavone profile and in the chemical composition of tempeh during processing and refrigeration. *Pesquisa agropecuária brasileira*, 46, 1555-1561. <https://doi.org/10.1590/S0100-204X2011001100018>
- Grand View Research. (2023). The global tempeh market size is expected to reach USD 7.9 billion by 2030: Grand View Research, Inc. Retrieved from <https://www.grandviewresearch.com/press-release/global-tempeh-market>. Accessed February 25, 2025.
- Gunawan-Puteri, M. D. P. T., Hassanein, T. R., Prabawati, E. K., Wijaya, C. H., & Mutukumira, A. N. (2015). Sensory characteristics of seasoning powders from overripe tempeh, a solid state fermented soybean. *Procedia Chemistry*, 14, 263-269. doi.org/10.1016/j.proche.2015.03.037
- Jeleń, H., Majcher, M., Ginja, A., & Kuligowski, M. (2013). Determination of compounds responsible for tempeh aroma. *Food Chemistry*, 141(1), 459-465. doi.org/10.1016/j.foodchem.2013.03.047
- Kim, J. Y., Lee, S. Y., & Choi, H. S. (2013). Molecular and morphological identification of fungal species isolated from rice meju. *Food Science and Biotechnology*, 22, 721-728. <https://doi.org/10.1007/s10068-013-0137-2>
- Kohli, V., & Singha, S. (2024). Protein digestibility of soybean: how processing affects seed structure, protein and non-protein components. *Discover Food*, 4(1), 7. <https://doi.org/10.1007/s44187-024-00076-w>

- Lemes, E. M., & Catão, H. C. R. M. (2024). Soybean seed Coat cracks and Green seeds—predisposing conditions, identification and management. *Seeds*, 3(1), 133-148. <https://doi.org/10.3390/seeds3010011>
- Mahdi, S., Astawan, M., Wulandari, N., & Muhandri, T. (2023). Sensory profiling of Tempe functional drink powder using Rate-All-That-Apply method. *Food Res*, 7, 19-26. [https://doi.org/10.26656/fr.2017.7\(S2\).3](https://doi.org/10.26656/fr.2017.7(S2).3)
- Măties, A., Negrusier, C., Roșca Mare, O., Mintas, O.S., Zanc Săvan, G., Odagiu, A.C.M., Andronie, L., & Păcurar, I (2024). Characterization of nutritional potential of *Amaranthus* sp. grain production. *Agronomy*, 14(3), 630. <https://doi.org/10.3390/agronomy14030630>
- Meyners, M., Jaeger, S. R., & Ares, G. (2016). On the analysis of rate-all-that-apply (RATA) data. *Food quality and preference*, 49, 1-10. <https://doi.org/10.1016/j.foodqual.2015.11.003>
- Mintel (2025). Emerging Trends in the Plant-Based Industry. Retrieved from <https://www.mintel.com/insights/food-and-drink/emerging-trends-in-the-plant-based-industry/>. Accessed May 15,2025.
- Ninfali, P., Panato, A., Bortolotti, F., Valentini, L., & Gobbi, P. (2020). Morphological analysis of the seeds of three pseudocereals by using light microscopy and ESEM-EDS. *European Journal of Histochemistry: EJH*, 64(1), 3075. <https://doi.org/10.4081/ejh.2020.3075>
- Paul, V., Singh, A., & Pandey, R. (2010). Determination of titrable acidity (TA). *Post-harvest physiology of fruits and flowers*, 44.
- Prativi, M. B. N., Astuti, D. I., Putri, S. P., Laviña, W. A., Fukusaki, E., & Aditiawati, P. (2023). Metabolite changes in Indonesian Tempe production from raw soybeans to over-fermented Tempe. *Metabolites*, 13(2), 300. <https://doi.org/10.3390/metabo13020300>
- Raji, A. O., & Famurewa, J. A. V. (2008). Effect of Hull on the Physico-Chemical Properties of Soyflour. *Agricultural Engineering International: CIGR Journal*.
- Sandoval, J. F., Gallagher, J., Rodriguez-Garcia, J., Whiteside, K., & Bryant, D. N. (2024). Improved nutritional value of surplus bread and perennial ryegrass via solid-state fermentation with *Rhizopus oligosporus*. *npj Science of Food*, 8(1), 95. <https://doi.org/10.1038/s41538-024-00338-y>
- Tan, Z. J., Abu Bakar, M. F., Lim, S. Y., & Sutimin, H. (2024). Nutritional composition and sensory evaluation of tempeh from different combinations of beans. *Food Research*, 8(2), 138-146. [https://doi.org/10.26656/fr.2017.8\(2\).088](https://doi.org/10.26656/fr.2017.8(2).088)
- Toor, B. S., Kaur, A., & Kaur, J. (2022). Fermentation of legumes with *Rhizopus oligosporus*: effect on physicochemical, functional and microstructural properties. *International Journal of Food Science and Technology*, 57(3), 1763-1772. <https://doi.org/10.1111/ijfs.15552>
- Wikandari, R., Kinanti, D. A., Permatasari, R. D., Rahmaningtyas, N. L., Chairunisa, N. R., Sardjono, Hellwing, C., & Taherzadeh, M. J. (2021). Correlations between the chemical, microbiological characteristics and sensory profile of fungal fermented food. *Fermentation*, 7(4), 261. <https://doi.org/10.3390/fermentation7040261>

PRESSURE-STATE-RESPONSE MODEL FOR THE DIAGNOSIS OF ENVIRONMENTAL IMPACTS ON A PROTECTED FOREST ECOSYSTEM

Dafne Fernanda Juárez-Zavala¹, Elizabeth Hernández-Acosta^{2*}

¹Universidad Autónoma Chapingo. División de Ciencias Forestales. Carretera México-Texcoco km 38.5, Texcoco, State of Mexico, Mexico. C. P. 56227.

²Universidad Autónoma Chapingo. Departamento de Enseñanza Investigación y Servicio en Suelos. Posgrado en Ciencias Forestales y del Ambiente. Carretera México-Texcoco km 38.5, Texcoco, State of Mexico, Mexico. C. P. 56227.

* Author for correspondence: ehernandez@chapingo.mx

ABSTRACT

The Molino de Flores Nezahualcóyotl National Park has a high ecological and cultural relevance in the periurban area of Texcoco, Mexico. The aim of this study was to evaluate the environmental pressures, the state of the ecosystem, and the effects of management activities through the use of the Pressure-State-Response (PSR) model. The proposed hypothesis suggests that anthropogenic pressures negatively affect the health of the forest, while restoration efforts are designed to alleviate these impacts. The information was obtained by interviewing authorities, making field observations, and conducting perception surveys on visitors. The results identified intensive tourism, invasive exotic species, and forest fires as the main sources of pressure. The state of the ecosystem reflects a high resilience and a biological wealth of 540 registered species, with evidence of the recovery of native fauna and flora after management interventions. Institutional responses emphasize the implementation of mycorrhizal reforestation, fire management strategies, and environmental education initiatives. In conclusion, the PSR model is an effective tool for an integrated diagnosis. Although the system is resilient, it is imperative to strengthen funding and public awareness to ensure the sustainability of the area against urban pressure.

Keywords: environmental management, intensive tourism, biological wealth, protected natural areas.

INTRODUCTION

Forest ecosystems face diverse, increasing environmental pressures derived from human activities, climate change, and degradation processes that jeopardize their balance, ecological functionality, and the provision of vital ecosystem services (Albanbaeva *et al.*, 2025). In Mexico, nearly 70 % of the territory is covered by forest ecosystems, indicating the need for solid methodological tools to evaluate the impacts on the environment in an integral manner and thus provide elements that guide decision-making processes towards sustainable management (CONAFOR, 2021).

Citation: Juárez-Zavala DF, Hernández-Acosta E. 2026. Pressure-State-Response model for the diagnosis of environmental impact on a protected forest ecosystem. *Agrociencia* 60(3): 372-388. <https://doi.org/10.47163/agrociencia.v60i3.3596>

Editor in Chief:
Dr. Fernando C. Gómez Merino

Received: November 24, 2025.

Approved: April 07, 2026.

Published in Agrociencia:
April 16, 2026.

This work is licensed under a Creative Commons Attribution-Non- Commercial 4.0 International license.



The Pressure-State-Response (PSR) model developed by the Organization for Economic Cooperation and Development (OECD) helps diagnose the causality between human activities and the health of ecosystems. It is arranged into three components: Pressure, associated with human and natural factors that affect the resilience of ecosystems; State, which describes the current conditions of the forests; and Response, which refers to the sustainable management actions and policies (Solís-Mendoza *et al.*, 2025). This model is relevant in forest ecosystems in Mexico. The National Forestry Commission (CONAFOR) incorporates it as a conceptual framework for forest assessment and management, integrating it into the National Forest Information System (SNIF) to promote systematic monitoring and decision-making based on scientific evidence (CONAFOR, 2021). The PSR model has been successfully applied in national forest contexts to identify weaknesses in waste management and environmental policies (Vázquez-Valencia and García-Almada *et al.*, 2018).

The Molino de Flores Nezahualcóyotl National Park (PNMFN), located in a peri-urban transition area between natural and urban areas, is a site of interest for the use of the PSR model, as it undergoes diverse environmental pressures due to tourism, urbanization, and the invasion of exotic species, among others, which jeopardize its ecological functionality and its biological wealth. The Protected Natural Area (PNA) is maintained with environmental education programs and the permanent effort of authorities to maintain the balance between its ecological and cultural conservation. Due to the above, the aim of this study was to evaluate the environmental pressures, the state of the ecosystem, and the effects of the management activities implemented in the PNMFN, with the help of the PSR model. The hypothesis proposed is that the anthropogenic pressures found in the park exert a negative influence on the state of the forest, whereas the management and restoration actions implemented are responses aimed at mitigating these impacts and to promote their recovery.

MATERIALS AND METHODS

Area of study

The investigation was carried out in the PNMFN, located in the municipality of Texcoco, State of Mexico, which was designated as a PNA in 1937 and stands out for its ecological, socioeconomic, and cultural relevance for the region. It covers a surface of 50.22 ha, with approximate geographic coordinates of 19° 31' N and 98° 53' W and an altitude between 2250 and 2450 m. It is located in a transition area between the Mexican Central Highlands and the mountain systems of San Miguel Tlaixpan, La Purificación, the San Nicolás Tlaminca range, and Nativitas, within the Valley of Mexico basin (SEMARNAT, 2016).

Its soils are predominantly of volcanic origin (Regosols and Andosols), with textures varying from clay loam to sandy, which show low water retention, as well as signs of compaction and erosion in degraded areas (INEGI, 2020a). The climate is classified

as subhumid temperate (C(w0)(w)) with rains in the summer. Its mean annual temperature fluctuates between 14 and 18 °C, and annual rainfall varies between 600 and 800 mm. It has a notable seasonal stability, which has a direct influence on the dynamics of the vegetation (INEGI, 2020b).

The PNMFN provides ecosystem regulation, provision, and recreation services supported by tree species such as pines (*Pinus* spp.), the ahuehuete or Montezuma cypress (*Taxodium mucronatum* Ten.), and ash (*Fraxinus udhei* (Wenz.) Lingelsh.). These plant communities harbor fauna such as the hummingbird (*Archilochus colubris* Linnaeus, 1758), vireo (*Vireo* spp.), thrush, oriole, snakes (*Thamnophis* spp.), lizards (*Sceloporus* spp.), and frogs (Ranidae) (CONANP, 2023; iNaturalist, 2025).

The map of the polygon corresponding to the PNMFN, provided by the Park Directorate, with modifications made by the author for this study, shows the internal zoning of the PNA, which comprises the areas of El Jardín, the CONAFOR nursery, Cuchilla, Upper Nursery, Casco, Ahuehuetes-Eucaliptos, Capilla, Aguacatera, La Loma, Loma Alta, and Loma Baja (Figure 1).

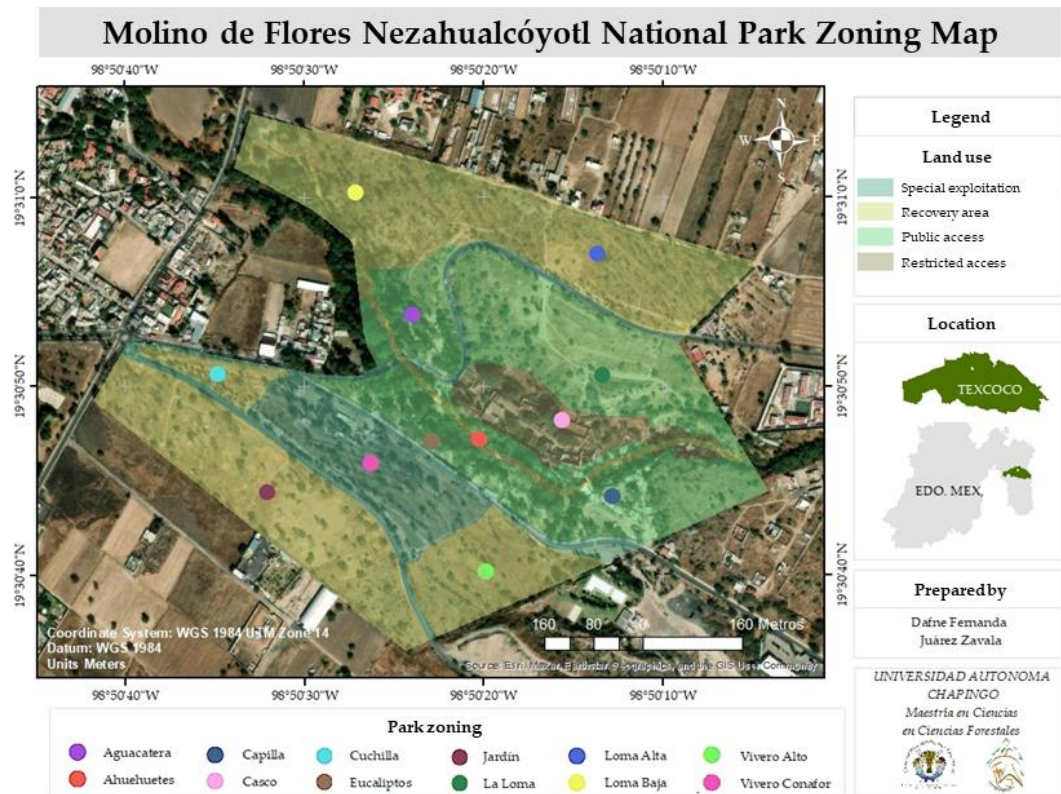


Figure 1. Location and zoning of the Molino de Flores Nezahualcóyotl National Park (PNMFN).

Evaluation of the environmental impacts

To evaluate the environmental impacts on the PNMFN, a mixed quantitative-qualitative approach was adopted based on the PSR model developed by the OECD and adapted by the Secretariat of Environment and Natural Resources for its use in forest ecosystems (Figure 2) (SEMARNAT, 2014). This model enabled the analysis of the causal relationships between human activities, the state of the environment, and the institutional responses through the identification of pressure (P), state (S), and response (R) indicators.

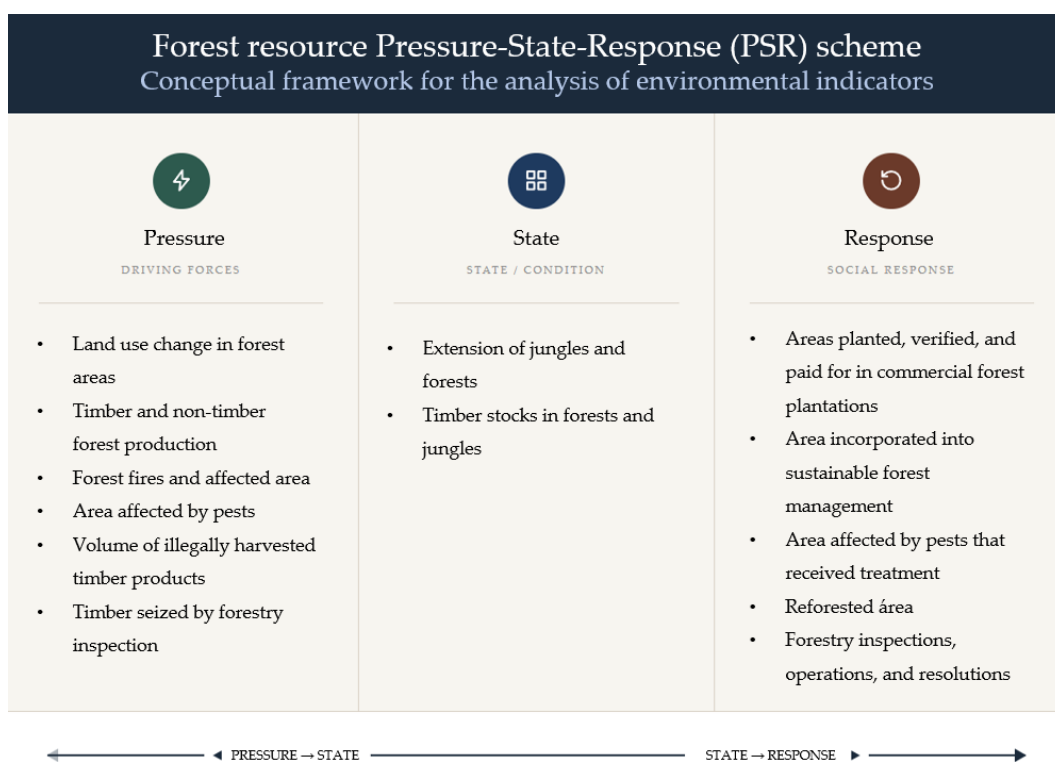


Figure 2. Pressure-State-Response (PSR) conceptual framework applied to the forestry sector. Solid arrows indicate the causal sequence between the dimensions of the model. Model adapted from SEMARNAT (2014).

The administrative structure of the PNMFN is officially composed of one director and two technicians (N = 3). In addition, the area supports an environmentalist brigade composed, on average, by eight elements (N = 8). To obtain operative and management information, a target population of 11 individuals (official staff plus brigade members) was defined. Due to the specialization of the functions and the reduced population sizes, a non-probabilistic purposive (judgmental) sampling method was used. The

sample ($n = 2$) consisted of the park director and an engineer in renewable natural resources, who was a member of the ecological brigade.

Interviews were used to document the environmental pressure-generating actions, the current state of the ecosystem, and the management activities implemented as a response to the pressures. They were carried out using a structured script, which was based on methodological recommendations for environmental perception studies (Díaz-Pérez *et al.*, 2025).

In addition, surveys were conducted on 120 park visitors, chosen by simple randomized sampling during days of tourist visits. An annual population of 120 000 visitors has been estimated, according to the data provided by the PNMFN Directorate. This figure helps gauge the anthropic pressure to which the area is exposed and underscores the importance of the management strategies implemented. This sample size provides an approximate accuracy of $\pm 9\%$ (margin of error, ME) for proportion estimations at a confidence level of 95%. This calculation is based on a conservative proportion ($p = 0.5$, $z = 1.96$). The margin of error was estimated using:

$$ME = z \times \sqrt{\frac{p(1-p)}{n}} \approx 1.96 \times \sqrt{\frac{0.25}{120}} \approx 0.09$$

The instrument helped explore the perception of visitors on the state of the ecosystem, the recreational activities carried out in the park, and their knowledge on conservation measures (Díaz-Pérez *et al.*, 2025).

Visits were made to different areas of the park to document anthropic pressure indicators (solid waste, traces of fires, and soil compaction) and validate the information from interviews and surveys, as well as identify indicators of the state of the ecosystem. Fieldwork took place from January 2024 to August 2025, during which the necessary information was collected.

Model application

To apply the PSR model of the PNMFN, a systematization matrix was developed based on the methodological structure proposed by SEMARNAT (2014) on forest resources. In this matrix, the main pressure factors, the current state of the ecosystem, and the institutional responses implemented were categorized. The selection and classification of indicators were carried out using information obtained with interviews, surveys, and field observations. This process prioritized the most recurring or relevant factors in the environmental dynamics of the park. Subsequently, every indicator was classified depending on its function within the socioenvironmental system: pressure, when it represented activities or actions that lead to alterations in the ecosystem; state, when it described the current conditions of the environment; and response, when it corresponded to institutional measures or management strategies aimed at mitigating or controlling the identified impacts.

The combination of interviews, surveys, and observations helped integrate and contrast the different sources of information, which strengthened the validity in the identification of indicators and the interpretation of the causal relations between activities. From this process onwards, the information was structured systematically, helping identify the main environmental pressures, the state of the ecosystem and the management responses in the PNMFN.

RESULTS AND DISCUSSION

Social perception of the site

The social characterization of the study area ($n = 120$) shows that the park is a well-established recreation area for middle-aged adults (53.3 %). Visitors express a mostly stable perception of the ecosystem and consider its quality to be “moderate” (Table 1). Although anthropic pressures derived from tourist and commercial influx are identified, users acknowledge conservation efforts, though they suggest strengthening the visibility of the reforestation actions and interpretative infrastructure to improve the experience of connecting with nature.

Visitors indicated reforestation, the establishment of local nurseries, and the restoration of degraded areas as their main proposals. They also mentioned the need to strengthen cleaning efforts, improve waste management, prevent forest fires, and broaden environmental education activities through interpretative signage and workshops for the public.

The Pressure-State-Response Model in the forest ecosystem

The indicators of the PSR model summarize the causal relations between pressures, states, and responses in the forest ecosystem of the PNMFN (Figure 3). Implementing the model in the PNMFN helped evaluate the socioecological dynamics that influence the integrity of the ecosystem, following the methodological structure proposed by the SEMARNAT (2014) for PNAs. The results indicate a complex interaction between human and natural pressures, the current state of biodiversity, and institutional responses.

In Mexico, the application of the PSR model in the forestry sector was documented in the years 2006 and 2013. The most recent study was made by Vázquez-Valencia and García-Almada *et al.* (2018), in Cihuatlán, Jalisco. The authors report pressure indicators related to inadequate waste management, vulnerability to climate change, atmospheric pollution, and deterioration of biodiversity. Regarding the state indicators, the authors specify that the ecosystem is deteriorating, with evident loss of biodiversity that negatively affects the quality of life in the municipality. In addition, they underscore that the institutional responses are insufficient, which highlights the inefficiency in the application of the existing legislation.

Table 1. Descriptive analysis of the social perception and environmental management of the Molino de Flores Netzahualcoyotl National Park (PNMFN).

	Variable/category	%	<i>n</i> = 120
	1. Reasons for visiting		
Main reason	Tourism/recreation	71.7	86
	Connecting with nature	20.0	24
	Other (research, conservation, gathering, etc.)	8.3	10
	2. Quality of the forest ecosystems		
Perceived quality of the forest	Regular	45.0	54
	Good	30.0	36
	Bad	20.0	24
	Very bad	3.3	4
	Very good	1.7	2
	3. Perception of reforestation		
Reforestations observed	Found reforestation	56.7	68
	Did not find reforestation	43.3	52
	4. Perception of biodiversity (fauna and flora)		
Diversity perceived	Little diversity	45.0	54
	Broad diversity	43.3	52
	Very diverse	8.3	10
	No perceptible diversity	3.3	4
	5. Human impact (visibility)		
Visibility of the negative impact	Very visible	58.3	70
	Moderately visible	25.0	30
	Slightly visible	15.0	18
	Not visible	1.7	2
	6. Evaluation of conservation actions		
Grading actions	Regular	55.0	66
	Bad	20.0	24
	Good	15.0	18
	Very bad	5.0	6
	Very good	5.0	6

Solís-Mendoza *et al.* (2025) indicate that this model facilitates the understanding of the cause-effect processes and the identification of adaptive strategies, such as polycentric governance, the maintenance of biodiversity, and diversified forest management, in order to face pressures such as climate change, market globalization, and outdated forest policies that interfere with the biological wealth, resilience, and local livelihoods.

Pressure indicators

The analysis of anthropic and natural pressures identified in the PNMFN helped acknowledge the main factors that influence the integrity of the ecosystem. Intensive tourism represents a significant pressure, with an annual influx of 100 000 to 120 000

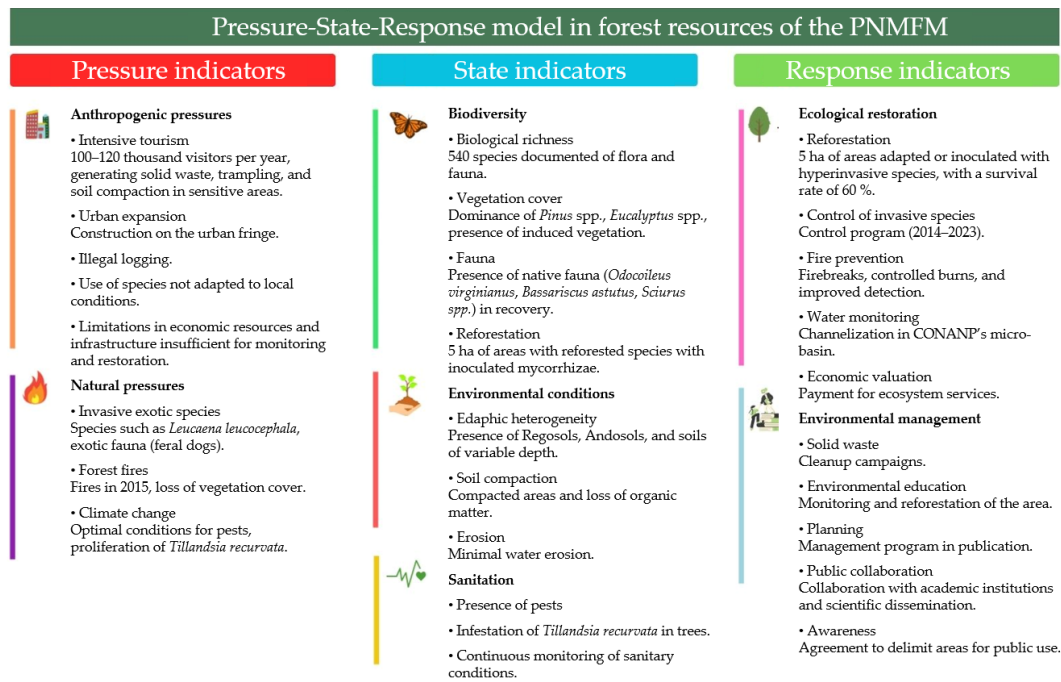


Figure 3. Pressure-State-Response Model applied to the Molino de Flores Netzahualcóyotl National Park (PNMFN) focused on its forest ecosystem. Based on the modified scheme by SEMARNAT (2014).

visitors, concentrated mainly in the commercial and ahuehuetes areas, according to the information provided by the park director during the interviews conducted for this study.

The descriptive analysis of the surveys conducted indicates that 71.7 % of visitors indicated recreation as the main reason for their visit (Table 1). This concentration of tourists in the PNA generates a visible accumulation of urban solid wastes, both organic and inorganic. This problem was pointed out by the park director and the engineer of the environmental brigade, and 58.3 % of the people surveyed identified it as the most highly visible environmental impact. Thus, the recreational and commercial activities appear to be one of the main triggers of environmental deterioration. Out of all the users, 31.7 % claim to visit the park on a regular basis, which implies a recurring anthropogenic burden on the ecosystem.

Although intensive tourism is an important economic activity, it can also become a direct source of environmental impact, mainly due to the accumulation of solid waste, soil compaction and erosion, the loss of native vegetation, and the alteration of habitats. These results coincide with reports from diverse studies. For example, Pereira *et al.* (2022) documented that trampling on tourist paths increased soil compaction, with apparent densities near 1.6 g cm⁻³ and reduced porosity, which promotes surface runoff and losses of up to 10 Mg ha⁻¹ of silt and 6 Mg ha⁻¹ of clay. In the PNMFN, the

perception of the quality of the ecosystem in the most visited areas was graded by 45 % of tourists as moderate (Table 1).

The findings coincide with studies that document the impacts of unregulated tourism in natural ecosystems. Mendoza-González *et al.* (2012) point out that this activity leads to contamination by solid waste and to soil compaction. Pérez-Ramírez and Flores-Montes (2019) reported, in Piedra Herrada, State of Mexico, that visitor overload exceeds the carrying capacity, leading to soil compaction and a reduction in biodiversity. Lara-Pulido *et al.* (2021) documented that unplanned tourism in Baja California Sur reduced the natural geomorphology by more than 40 %, and in the Iztaccíhuatl-Popocatepetl National Park, the accumulation of waste, soil compaction, and land use changes affecting the ecological balance have been recorded (Baloch *et al.*, 2022). In field tours and interviews in the PNMFN, areas with limited access to tourism, designed to preserve the ecosystem, were observed to have healthier vegetation and a lower soil compaction.

Another important pressure factor is the presence of exotic invasive species, such as *Ricinus communis* L. (castor bean) and *Leonotis nepetifolia* (L.) R. Br. (lion's ear), which were identified in field tours within the area. According to the perceptions of visitors, there is no difference in the percentage (45 and 43 %) when evaluating the biodiversity (Table 1). The invasion of exotic species affects the natural regeneration processes, particularly in herbaceous and shrub communities, reducing biodiversity (CONABIO, 2023). The local fauna, such as cats and dogs, constitutes a direct pressure on the native fauna in the PNMFN. The control of invasive species in the PNAs helps native communities to regenerate. However, its success depends on adequate management of the ecological factors, removal of invasive species, active restoration, and constant monitoring (Petri and Ibáñez, 2025).

Forest fires are a recurring pressure that originates from the combustion of light materials such as grasses and bushes, which spread across the soil cover. The documented evidence proves that forest fires are a relevant threat since they not only degrade vegetation but also release large amounts of greenhouse gases, feeding into climate change (Gajendiran *et al.*, 2024). In the case of the PNMFN, according to information provided by the director during the interviews, in 2024 alone, eight fires were recorded in different points of the PNA, mainly in the area of "El jardín" during the dry season, which displays the recurrence of this type of disturbance in the area.

In the PNMFN, climate change is also manifested with the proliferation of *Tillandsia recurvata* L. (ball moss). This phenomenon compromises forest health by modifying the structure of the tree canopy and promoting the presence of pathogens. Under water stress conditions, the incidence of pests increases, which can cause massive tree mortality, particularly with water stress in the soil and altitudinal shifts of species, thereby altering the energy dynamics of forest communities. For example, in *Bursera copallifera* (Sessé and Moc. ex DC.) Bullock, branches with *T. recurvata* present a lower rate of survival and sprout production, as well as a reduction of up to 43 % in the aptitude of the host tree. When the epiphyte is removed, the vigor of the tree increases (Vergara-Torres *et al.*, 2024).

Urban expansion is one of the greatest threats, associated with the municipal demographic growth in the periphery of the park. A concrete example is the recent construction of a housing development adjacent to the area "El Jardín," which increases the pressure on the natural resources and fragmentation of the ecosystem. Real estate development reduces ecological connectivity, which affects biodiversity and limits the ability of the PNAs to fulfill their conservation function, especially in the outskirts and metropolitan areas (Aguilar *et al.*, 2022).

This impact is also evident in other PNAs. In the Nevado de Toluca National Park, urbanization has generated acid rains and soil degradation (García-Solorio *et al.*, 2022), whereas Aguilar *et al.* (2022) documented rates of plant coverage loss of up to 30 % in accelerated expansion periods. Caro-Borrero *et al.* (2021) indicate that this process can reduce ecological connectivity by over 40 %, limiting the mobility of fauna and natural regeneration.

The director in charge of the PNA mentioned that the location of the park in an altitude transition causes imbalances in the soil and climate conditions, which influences the selection of species for reforestation programs. The quality of the ecosystem is perceived mostly as regular (45 %), which reflects the technical challenges mentioned by the administration. This situation, along with the historical agricultural use of the land, explains the problems resulting from the reforestations with improperly adapted species, as shown in earlier restoration attempts due to nutrient and water restrictions, which represents a potential risk in the context of the PNMFN, particularly during the dry seasons (Juan-Ovejero *et al.*, 2022).

The lack of economic resources is an identified pressure that limits the implementation of restoration, monitoring, and conservation projects, including the lack of specialized laboratories for the detailed characterization of the park (Baker and Gittman, 2024). This institutional deficiency translates into a negative perception among users, who rate the current conservation measures as deficient.

State indicators

The evaluation of the state of the forest ecosystem of the PNMFN revealed a considerable biological wealth. There is a record of 540 fauna and flora species, a figure that comes from the technical inventories performed for the creation of the park management program. This document is in the integration phase before its publication, which sustains the validity and relevance of the biological information presented. The area stands out for its relevance as a conservation core, since it maintains an important species diversity. Despite its lower extension in comparison with other Mexican PNAs such as the Lago de Texcoco National Park, which houses 370 fauna species and 250 flora species in its 14 000 ha, the PNMFN displays a considerable density of species per surface unit (CONAGUA, 2025).

The plant structure presented a dominance of species introduced in reforestations, mainly *Pinus* sp., *Eucalyptus* sp., and *Quercus* sp. These species present a noticeable dominance of the higher canopy in all areas of the park, which displaces the natural

succession of native species. This situation is reflected as a documented pattern, where this dominance generates a structural and functional homogenization, which compromises long-term ecological resilience (Arnesi *et al.*, 2024). This degradation coincides with the perceptions of the visitors: 45 % graded the ecosystem quality as “regular” and 20 % as “bad,” mainly due to concerns over the integrity of the vegetation and cleanliness (Table 1).

The actions to remove exotic invasive species carried out in 2024 and 2025 consisted of the manual and selective elimination of infestation hotspots in priority regeneration areas. Although these preventive actions do not involve a measurable volumetric extraction, the release of space favors an increase in the density of native species, particularly in shrub and herbaceous communities. This improvement was pointed out by the park director and the brigade technician, who recorded the increase in population density during field surveys and flower inventories. These measures enable the recovery of native flora.

According to Maynard-Bean and Kaye (2019), these interventions are efficient for the stability and restructuring of native communities, which coincides with the observations in the area under study. Jiménez-Hernández *et al.* (2023) evaluated the removal of *Hedera helix* L. (English ivy) in temperate forests in Mexico City, which resulted in the recovery of native species and a floral composition similar to that of non-invaded sites within a year, highlighting the quick response of native vegetation after the elimination of invasive species and the resilience of altered ecosystems.

The wild fauna presented a positive response after the park access restrictions implemented during the COVID-19 pandemic in 2020. According to reports by the park director and the brigade technician, an increase was recorded in the abundance and distribution of species such as opossums (*Didelphis virginiana* Kerr, 1792), ringtails (*Bassariscus astutus* Lichtenstein, 1830), and squirrels (*Sciurus* sp.), which currently cover areas from which they are absent or restricted to specific areas such as the CONAFOR nursery. These results coincide with those reported by Ewart *et al.* (2024), who pointed out that the abundance of native fauna is lower in non-protected areas or in those with a greater presence of humans or domestic fauna. This situation is evident in the park, with the increase in the population density of species due to the restriction of access to specific parts of the PNA. The perception of the biodiversity among the visitors is split: 45 % consider its diversity to be scarce, whereas 43.3 % consider it to be broad, suggesting the need to strengthen interpretative resources to make the recovery of the biota of the ecosystem visible (Table 1).

The qualitative observations in the soils displayed degradation in frequently transited areas, with visible compaction and a loss of organic matter as a result of forest fires. Agbeshie *et al.* (2022) indicate that severe fires consume surface organic matter, reduce organic carbon, and affect the stability of soil aggregates; they also note that frequent transit increases compaction, which limits water infiltration and promotes erosion. However, the erosive processes in the PNMFN remain at minimum levels due to the presence of a natural accumulation zone in the river and the stability provided by the

remaining vegetation. The director in charge mentioned that in the 1990s, the area of “El Jardín” received the addition of exogenous soils originating from activities related to the construction of a nearby shopping mall. The origin and quality of these soils are unknown, which causes variability in their characteristics and in the terrain of the area.

Response indicators

The implemented institutional responses integrate ecological restoration and environmental management components. The forest rehabilitation programs have covered 5 ha since 2020, and they incorporate native species adapted to the local climate conditions, such as *Vachellia farnesiana* (L.) Wight and Arn., *Quercus* sp., *Acacia farnesiana* (L.) Willd., and *Pinus* sp. inoculated with edible ectomycorrhizal fungi (*Suillus kaibabensis* (Thiers) Kretzer and Bruns, *Hebeloma mesophaeum* (Pers.) Quél., and *Laccaria laccata* (Scop.) Cooke). This strategy enables a survival rate of over 60 %. A nursery was established for the production of plants inoculated with these mycorrhizae, and 56.7 % of the visitors identified the results of the reforestations carried out in the park (Table 1).

Inoculation with edible ectomycorrhizal fungi is an adequate strategy, since this symbiosis promotes the absorption of nutrients and water, with an increase in the survival of trees under adverse conditions (Rodríguez-Gómez Tagle *et al.*, 2024). Its effectiveness depends on the compatibility between the fungus and the host species, as well as on its adaptation to local conditions (Policelli *et al.*, 2020). These actions, along with the removal of harmful species, lead to favorable results, particularly in areas near the gallery forest and parking lots.

Indicators were established in the PNMFN to evaluate the state of conservation, which includes the follow-up of plant survival, the evaluation of forest health, and systematic inventories to identify and characterize the species of the different ecosystems of the park. This integral approach has been applied in diverse regions. Ortiz-Fernández *et al.* (2024) used indicators such as species inventories, the monitoring of coverage, vegetative composition, and the proportion of native vs. introduced species. Pío-León *et al.* (2024) include counts of species richness and endemism, inventories of flora and fauna, and georeferenced records to identify priority areas and information gaps.

Cleanup and environmental education programs in 2023 had up to 200 participants, according to the brigade technician. These programs display advances in the sensibilization of visitors, although their impact is limited in relation to the high number of visitors. Mahbubi *et al.* (2025) indicate that the integration of digital media and participatory workshops can improve their effectiveness.

Forest fire prevention management includes the implementation of firebreaks in critical urban-forest interface zones, controlled burns, and preventive cleaning, complemented by training for technical staff and coordination with firefighters and municipal civil protection. The design of the firebreaks, adjusted annually based on fuel load and priority areas, effectively prevents the spread of fire. Gómez-Mendoza and Rodríguez-

Trejo (2021) point out that prescribed burns and mechanical treatments are efficient in pine forests in Mexico, whereas Gao *et al.* (2024) document reductions of over 50 % in fires with preventive measures. Nevertheless, the recurrence of these events in the park underscores the need to enhance monitoring with advanced technologies and continuous training in the face of budgetary limitations.

In the last decade, a collaboration system was established with academic institutions to implement conservation actions, which strengthens the identification of priority areas and the creation of projects aimed at ecological restoration. González *et al.* (2023) point out that this collaboration provides methodological rigor, technological access, and adaptive management. Another program was implemented to monitor the composition and structure of the natural resources in forests and scrublands, following protocols by the National Protected Natural Areas Commission (CONANP), enabling the follow-up of changes in biodiversity. The strategy integrates local connectivity with training programs aimed at young people and the local population, with activities such as beekeeping and environmental awareness (Vallejo-Chávez, 2022).

Agreements were made with shopkeepers to regulate public use and restrict access to protected or special use areas, ensuring the continuity of economic activities under criteria compatible with the conservation of the PNA. The exclusion of visitors from critical areas favored the integrity of the ecosystems, the recovery of the wild fauna, and the reestablishment of functional habitats, which intensified after the restrictions due to the COVID-19 pandemic. As a part of this management, an unregulated tourism-monitoring system and control measures were implemented to mitigate environmental impacts derived from anthropogenic activity, given that human pressure reduces ecosystem resilience and increases the risk of loss of biodiversity (Keith *et al.*, 2023).

Likewise, a management program was developed nearing its publication, which includes the zoning of priority sites and a list of species with their relative abundance. This instrument represents an integral response to the understanding of biodiversity and optimizing ecosystem management. Zoning enables the application of specific measures according to the needs of each area, maximizing results and reducing conflicts between development and conservation (Xie *et al.*, 2024). The use of standardized protocols ensures comparability with other PNAs and strengthens integral management based on social, ecological, technical, and economic knowledge (CONANP, 2020). Most visitors perceive conservation actions as regular (55 %), which reflects an intermediate valuation of the park management efforts (Table 1).

CONCLUSIONS

The Pressure-State-Response model in the Molino de Flores Nezahualcóyotl National Park helped evaluate environmental pressures, the state of the ecosystem, and the effects of the implemented management actions in an integrated manner. Additionally, it helped organize and analyze the environmental information of the park, which

displays its use as a support tool for management and to make decisions in protected natural areas.

ACKNOWLEDGEMENTS

The authors wish to acknowledge the Secretariat of Science, Technology, and Innovation (SECIHTI) for the financial support provided for this investigation. We would particularly like to thank the geographer Agustín Tagle, director of the Molino de Flores National Park, for the institutional assistance provided and for his valuable support during the development of the study. We extend our gratitude to brigade member Eng. Magdalena García for her collaboration and specialized knowledge in the area of study that strengthened our results. Finally, we acknowledge the Molino de Flores National Park for allowing our research to be conducted on its premises and for the conservation actions that inspire this work.

REFERENCES

- Agbeshie AA, Abugre S, Atta-Darkwa T, Awuah R. 2022. A review of the effects of forest fire on soil properties. *Journal of Forestry Research* 33 (5): 1419–1441. <https://doi.org/10.1007/s11676-022-01475-4>
- Aguilar G, Flores MA, Lara LF. 2022. Peri-urbanization and land use fragmentation in Mexico City. Informality, Environmental Deterioration, and Ineffective Urban Policy. *Frontiers in Sustainable Cities* 4. <https://doi.org/10.3389/frsc.2022.790474>
- Albanbaeva D, Amerkulova Z, Chaldanbaeva A, Zainiev R, Asanov R. 2025. Monitoring economic risks associated with forest landscape degradation. *Ukrainian Journal of Forest and Wood Science* 16 (1): 82–107. <https://doi.org/10.31548/forest/1.2025.82>
- Arnesi EA, López DR, Barberis IM. 2024. Relationship between degradation and the structural-functional complexity of subtropical xerophytic forests in the Argentine Wet Chaco. *Forest Ecology and Management* 562: 121957. <https://doi.org/10.1016/j.foreco.2024.121957>
- Baker R, Gittman R. 2024. Co-funding robust monitoring with living shoreline construction is critical for maximizing beneficial outcomes. *Estuaries and Coasts* 48 (1). <https://doi.org/10.1007/s12237-024-01433-9>
- Baloch QB, Shah SN, Iqbal N, Sheeraz M, Asadullah M, Mahar S, Khan AU. 2022. Impact of tourism development upon environmental sustainability: A suggested framework for sustainable ecotourism. *Environmental Science and Pollution Research* 30 (3): 5917–5930. <https://doi.org/10.1007/s11356-022-22496-w>
- Caro-Borrero A, Carmona-Jiménez J, Rivera-Ramírez K, Bieber K. 2021. The effects of urbanization on aquatic ecosystems in peri-urban protected areas of Mexico City: The contradictory discourse of conservation amid expansion of informal settlements. *Land Use Policy* 102: 105226. <https://doi.org/10.1016/j.landusepol.2020.105226>
- CONABIO (Comisión Nacional para el Conocimiento y Uso de la Biodiversidad). 2023. Estrategia nacional sobre especies invasoras en México: Prevención, control y erradicación. <https://www.biodiversidad.gob.mx/especies/Invasoras/estrategia> (Retrieved: March 2026).
- CONAFOR (Comisión Nacional Forestal). 2021. Programa Nacional Forestal 2020-2024. México. Secretaría de Medio Ambiente y Recursos Naturales. Comisión Nacional Forestal. Ciudad de México. México. 111 p.

- CONAGUA (Comisión Nacional del Agua). 2025. Parque Ecológico Lago de Texcoco. Gobierno de México. Comisión Nacional del Agua. Ciudad de México, México. <http://www.gob.mx/conagua/acciones-y-programas/proyecto-ecologico-lago-de-texcoco> (Retrieved: March 2026).
- CONANP (Comisión Nacional de Áreas Naturales Protegidas). 2020. Programa Nacional de Áreas Naturales Protegidas 2020-2024. Gobierno de México. Comisión Nacional de Áreas Naturales Protegidas. Ciudad de México, México. <http://www.gob.mx/conanp/documentos/programa-nacional-de-areas-naturales-protegidas-2020-2024> (Retrieved: March 2026).
- CONANP (Comisión Nacional de Áreas Naturales Protegidas). 2023. Molino de Flores Netzahualcóyotl. Gobierno de México. Comisión Nacional de Áreas Naturales Protegidas. Ciudad de México, México. <https://descubreanp.conanp.gob.mx/es/conanp/ANP?suri=113> (Retrieved: March 2026).
- Díaz-Pérez FM, García-González CG, Fyall A, Fu X, Deel G, Fernández-Hernández C. 2025. The altered perceptions of visitors to national parks: A comparison between a pre and post-covid-19 periods. *Social Sciences and Humanities Open* 11: 101219. <https://doi.org/10.1016/j.ssa.2024.101219>
- Ewart H, Pasqualotto N, Paolino RM, Jensen K, Chiarello A. 2024. Effects of anthropogenic disturbance and land cover protection on the behavioural patterns and abundance of Brazilian mammals. *Global Ecology and Conservation* 50: e02839. <https://doi.org/10.1016/j.gecco.2024.e02839>
- Gajendiran K, Kandasamy S, Narayanan M. 2024. Influences of wildfire on the forest ecosystem and climate change: A comprehensive study. *Environmental Research* 240: 117537. <https://doi.org/10.1016/j.envres.2023.117537>
- Gao M, Chen S, Suo A, Chen F, Liu X. 2024. Response of fuel characteristics, potential fire behavior, and understory vegetation diversity to thinning in *Platycladus orientalis* forest in Beijing, China. *Forests* 15 (9): 1667. <https://doi.org/10.3390/f15091667>
- García-Solorio L, Muro C, de La Rosa I, Amador-Muñoz O, Ponce-Vélez G. 2022. Organochlorine pesticides and polychlorinated biphenyls in high mountain lakes, Mexico. *Environmental Science and Pollution Research International* 29 (32): 49291–49308. <https://doi.org/10.1007/s11356-022-19177-z>
- Gómez-Mendoza FF, Rodríguez-Trejo DA. 2021. Fuego, mortalidad y rebrotación en especies forestales de la Sierra Norte de Puebla. *Madera y Bosques* 27 (3). <https://doi.org/10.21829/myb.2021.2732148>
- González A, Chase J, O'Connor M. 2023. A framework for the detection and attribution of biodiversity change. *Philosophical Transactions of the Royal Society of London. Series B, Biological Sciences* 378 (1881): 20220182. <https://doi.org/10.1098/rstb.2022.0182>
- iNaturalist. 2025. Observaciones del proyecto Parque Nacional Molino de Flores Netzahualcóyotl. https://mexico.inaturalist.org/observations?page=2&project_id=parque-nacional-molino-de-flores-netzahualcoyotl&subview=table&verifiable=any&view=species (Retrieved: March 2026).
- INEGI (Instituto Nacional de Estadística y Geografía). 2020a. Geografía y medio ambiente. Edafología. Ciudad de México, México. <https://www.inegi.org.mx/temas/edafologia/> (Retrieved: March 2026).
- INEGI (Instituto Nacional de Estadística y Geografía). 2020b. Geografía y medio ambiente. Climatología. Ciudad de México, México. <https://www.inegi.org.mx/temas/climatologia/> (Retrieved: March 2026).

- Jiménez-Hernández H, Bonilla-Valencia L, Martínez-Orea Y, Zamora-Almazán M, Espinosa-García F, Ccastillo-Argüero S. 2023. Effects of *Hedera helix* L. removal on the understory early regeneration in an oak temperate forest in Mexico City. *Ecological Processes* 12 (1). <https://doi.org/10.1186/s13717-023-00443-y>
- Juan-Ovejero R, Castro J, Querejeta JI. 2022. Low acclimation potential compromises the performance of water-stressed pine saplings under Mediterranean xeric conditions. *Science of the Total Environment* 831: 154797. <https://doi.org/10.1016/j.scitotenv.2022.154797>
- Keith DA, Benson DH, Baird IRC, Watts L, Simpson CC, Krogh M, Gorissen S, Ferrer-Paris JR, Mason TJ. 2023. Effects of interactions between anthropogenic stressors and recurring perturbations on ecosystem resilience and collapse. *Conservation Biology: The Journal of the Society for Conservation Biology* 37 (1): e13995. <https://doi.org/10.1111/cobi.13995>
- Lara-Pulido JA, Guevara-Sanginés A, Pérez-Cirera V, Arias-Martelo C, Jiménez-Quiroga CI. 2021. Economic spillover from natural protected areas to conventional tourist destinations. *Economía, Sociedad y Territorio* 21 (67): 745–774. <https://doi.org/10.22136/est20211690>
- Mahbubi M, Cholili A, Syi'bul Huda AA, Shuhada. 2025. Enhancing educational quality through effective communication in private universities. *Journal of Education and Learning Sciences* 5 (1): 25–38. <https://doi.org/10.56404/jels.v5i1.124>
- Maynard-Bean E, Kaye M. 2019. Invasive shrub removal benefits native plants in an eastern deciduous forest of North America. *Invasive Plant Science and Management* 12 (1): 3–10. <https://doi.org/10.1017/inp.2018.35>
- Mendoza-González G, Martínez M, Lithgow D, Pérez-Maqueo O, Simonin P. 2012. Land use change and its effects on the value of ecosystem services along the coast of the Gulf of Mexico. *Ecological Economics* 82: 23–32. <https://doi.org/10.1016/j.ecolecon.2012.07.018>
- Ortiz-Fernández FR, Carmona-Jiménez J, Temis-García LG, Caro-Borrero AP, González-Hidalgo B. 2024. The hydromorphological quality of the basin of Mexico: A proposal of its indicator value of the ecological state in the riparian ecosystem. *Revista Internacional de Contaminación Ambiental* 40. <https://doi.org/10.20937/rica.54895>
- Pereira LS, Rodrigues AM, Oliveira CJ, Guerra AJ, Booth CA, Fullen MA. 2022. Detrimental effects of tourist trails on soil system dynamics in Ubatuba Municipality, São Paulo state, Brazil. *CATENA* 216: 106431. <https://doi.org/10.1016/j.catena.2022.106431>
- Pérez-Ramírez C, Flores-Montes A. 2019. Turismo rural, impacto ambiental y resiliencia en Piedra Herrada, México. *Agricultura, Sociedad y Desarrollo* 16 (4): 429–450. <https://doi.org/10.22231/asyd.v16i4.1278>
- Petri L, Ibáñez I. 2025. Successful recovery of native plants post-invasive removal in forest understories is driven by native community features. *Ecological Applications* 35 (2). <https://doi.org/10.1002/eap.70012>
- Pío-León JF, Munguía-Lino G, González-Gallegos JG, González-Elizondo M. 2024. Priority areas for conservation based on endemic vascular plant species and their biocultural attributes: A case study in Sinaloa, Mexico. *Revista Mexicana de Biodiversidad* 95: e955446. <https://doi.org/10.22201/ib.20078706e.2024.95.5446>
- Policelli N, Horton T, Hudon A, Patterson T, Bhatnagar J. 2020. Back to roots: The role of ectomycorrhizal fungi in boreal and temperate forest restoration. *Frontiers in Forests and Global Change* 3. <https://doi.org/10.3389/ffgc.2020.00097>
- Rodríguez-Gómez Tagle G, Vargas-Hernández JJ, López-Upton J, Pérez-Moreno J. 2024. Diversidad de morfotipos de hongos ectomicorrizógenos y adaptación al hospedero en

- poblaciones contrastantes de *Pinus greggii* var. *Australis* (Pinaceae). *Acta Botánica Mexicana* 131. <https://doi.org/10.21829/abm131.2024.2151>
- SEMARNAT (Secretaría de Medio Ambiente y Recursos Naturales). 2014. Indicadores básicos del desempeño ambiental. Gobierno de México. Secretaría de Medio Ambiente y Recursos Naturales. Ciudad de México, México. https://apps1.semarnat.gob.mx:8443/dgeia/indicadores14/conjuntob/07_forestales/07_forestales_esquema.html (Retrieved: March 2026).
- SEMARNAT (Secretaría de Medio Ambiente y Recursos Naturales). 2016. 79 aniversario del Molino de Flores Nezahualcóyotl. Gobierno de México. Secretaría de Medio Ambiente y Recursos Naturales. Ciudad de México, México. <https://www.gob.mx/semarnat/articulos/79-aniversario-del-molino-de-flores-netzahualcoyotl> (Retrieved: September 2025).
- Solís-Mendoza LE, Galicia L, Ávila-Foucat SV, Mwampamba TH. 2025. Conceptual model of social-ecological resilience in Mexican forests communities. *Frontiers in Forests and Global Change* 8. <https://doi.org/10.3389/ffgc.2025.1490278>
- Vallejo-Chávez LE. 2022. The invisible impacts of violence and crime on biodiversity and communities in Mexican natural protected areas. *Biodiversity* 23 (3–4): 164–166. <https://doi.org/10.1080/14888386.2022.2149621>
- Vázquez-Valencia RA, García-Almada RM. 2018. Indicadores PER y FPEIR para el análisis de la sustentabilidad en el municipio de Cihuatlán, Jalisco, México. *Nóesis. Revista de Ciencias Sociales y Humanidades* 27 (53): 1–26. <https://doi.org/10.20983/noesis.2018.3.1>
- Vergara-Torres C, Valencia-Díaz S, García-Franco J, Flores-Palacios A. 2024. Do epiphytes affect the fitness of their phorophytes? The case of *Tillandsia recurvata* on *Bursera copallifera*. *Journal of Tropical Ecology* 40. <https://doi.org/10.1017/s0266467424000117>
- Xie Y, Wang S, Xiang S, Wang Z, Li Y, Wang Z, Zhou M, Wang Y, Gao M. 2024. Ecological zoning and dynamic assessment of effectiveness in the Three Gorges Reservoir Area, China. *Ecological Modelling* 487: 110563. <https://doi.org/10.1016/j.ecolmodel.2023.110563>

Agrociencia

YOLOV8-POWERED COMPUTER VISION FOR COFFEE CHERRY RIPENESS, DEFECT, AND MORPHOLOGICAL ASSESSMENT

Kavitha Subramani¹, Senduru Srinivasulu², Saravanan Raju³, Surendran Rajendran^{4*}

¹Panimalar Engineering College. Department of Computer Science and Engineering. Chennai, Tamil Nadu 600123, India.

²Sathyabama Institute of science and Technology. School of Computing, Department of Computer Science and Engineering. Chennai, Tamil Nadu 600119, India.

³Vel Tech HighTech Dr.Rangarajan Dr.Sakunthala Engineering College. Department of Computer Science and Engineering. Avadi, Tamil Nadu 600062, India.

⁴Saveetha School of Engineering. Saveetha Institute of Medical and Technical Sciences, Department of Computer Science and Engineering. Chennai, Tamil Nadu 602117, India.

* Author for correspondence: surendranr.sse@saveetha.com

ABSTRACT

The present investigation describes an advanced multi-task deep learning framework for automated inspection of coffee cherry quality using YOLOv8 with color-based segmentation and Vision Transformer-Convolutional Neural Network (ViT-CNN) feature extraction. The model performs ripeness stage classification, defect detection, and size and shape analysis. For ripeness detection, YOLOv8 was enhanced with a color segmentation module, achieving class-wise accuracies of 90–95 % for unripe, partially ripe, and fully ripe cherries, with moderate performance (85 %) for overripe samples. ViT-CNN feature maps improved segmentation clarity and bounding-box localization, particularly in high-density clusters. Defect detection was carried out across five categories (healthy, blackened, moldy, wrinkled, and insect-damaged), achieving F1-score values between 0.88 and 0.96 and mean average precision at 50 % intersection over union (mAP@50) values above 0.97 for key defect classes after 150 training epochs. Quantitative evaluation of morphological characteristics for size and shape assessment further demonstrated model robustness, with insect-damaged cherries reaching a contour accuracy of 0.98 and an Intersection over Union (IoU) of 0.96. Comparative analysis with YOLOv5 and Faster Region-Based Convolutional Neural Network (Faster R-CNN) showed superior performance of the proposed architecture across all metrics, including precision, recall, F1-score, and mAP. By incorporating contextual embeddings and attention mechanisms, the framework enables accurate, real-time sorting for smart agricultural systems.

Keywords: ViT-CNN feature extraction, smart sorting systems, Sustainable agriculture, computer vision, deep learning.

Citation: Subramani K, Srinivasulu S, Raju S, Rajendran S. 2026. YOLOv8-powered computer vision for coffee cherry ripeness, defect, and morphological assessment. *Agrociencia* 60(3): 389-411. <https://doi.org/10.47163/agrociencia.v60i3.3485>

Editor in Chief:
Dr. Fernando C. Gómez Merino

Received: May 22, 2025.
Approved: March 23, 2026.
Published in Agrociencia:
April 15, 2026.

This work is licensed under a Creative Commons Attribution-Non-Commercial 4.0 International license.



INTRODUCTION

The coffee-growing industry plays a critical role in the global economy, with millions of farmers relying on coffee cultivation as their primary source of income. Coffee (*Coffea* sp.) cherry harvesting is a decisive stage that directly affects product quality, market value, and overall production efficiency. Traditionally, harvesting is performed manually, with workers visually assessing cherry ripeness prior to picking (Napier *et al.*, 2025). However, manual harvesting is labor-intensive, time-consuming, and prone to subjective error, often leading to inconsistencies in ripeness selection and quality assessment. These limitations have driven the demand for more efficient and accurate methods for coffee cherry evaluation.

Recent advances in computer vision and deep learning have enabled the development of automated systems capable of real-time ripeness classification, defect detection, and size and shape assessment of coffee cherries (Ye *et al.*, 2025). Among deep learning-based object detection approaches, You Only Look Once (YOLO) has emerged as one of the most efficient algorithms for real-time applications due to its high detection speed and accuracy. YOLO-based systems can process video streams captured by cameras mounted on harvesting machinery, unmanned aerial vehicles (UAVs), or fixed installations to identify and classify coffee cherries throughout the harvesting process. This automated approach ensures selective harvesting of ripe cherries, improves coffee quality, and reduces dependence on manual labor.

Beyond ripeness classification, defect identification is essential for maintaining coffee quality (Selvanarayanan *et al.*, 2024b). Defects such as mold, insect damage, bruising, and blackening can negatively affect flavor and aroma. Integrating defect detection into a YOLO-based framework allows faulty cherries to be identified and removed before processing, ensuring that only premium-quality beans proceed to production and strengthening overall quality control.

UAVs play a key role in automating coffee harvest monitoring by capturing high-resolution video data. Captured footage is transmitted wirelessly via mobile networks, Wi-Fi, or long-term evolution (LTE) networks to cloud platforms for real-time analysis. Onboard edge computing enables preliminary preprocessing to reduce latency before data upload. Video data, typically stored in formats such as MP4 or AVI, are transferred through cloud services including Amazon S3, Google Cloud, or Microsoft Azure for deep learning-based analysis. High frame rates of 30–60 frames per second (FPS) support accurate segmentation for ripeness classification, defect detection, and size analysis (Arwatchananukul *et al.*, 2024). This workflow enhances harvest efficiency, reduces labor costs, and improves quality control through artificial intelligence (AI)-driven automation. Size and shape analysis further contribute to post-harvest classification and processing decisions. Larger, more uniform cherries are generally preferred for specialty coffee production, whereas smaller or irregularly shaped cherries may require alternative processing pathways. YOLO's ability to detect and quantify morphological characteristics enables automated sorting, reducing waste and optimizing post-harvest handling. Consequently, YOLO-based computer vision

systems offer scalable and efficient solutions for improving coffee quality, lowering labor requirements, and increasing sustainability within the coffee sector (Ji *et al.*, 2024).

Related research in intelligent agriculture further supports the feasibility of such systems. For example, an AI-driven camera system was proposed for tomato yield estimation using YOLO for fruit detection combined with point cloud data for size analysis (Sangamithrai *et al.*, 2024). Ripeness was classified based on color, independent of greenhouse lighting conditions, achieving a prediction error of 6.85 % (Okabe *et al.*, 2025). Multi-vision localization techniques have also been explored to improve robotic harvesting accuracy. Using red-green-blue-depth (RGB-D) cameras and motion capture systems, both analytical and model-based approaches were evaluated. Adaptive Boosting (AdaBoost) regression achieved an accuracy of 88.8 % with a 4.4 mm error, outperforming single-camera methods and improving robotic picking efficiency (Beldek *et al.*, 2025).

Machine vision has been applied to automated grading and sorting of agricultural products based on size and maturity. Unlike manual grading, which is often inconsistent, computer vision systems enable nondestructive classification using image processing and machine learning, improving efficiency and product quality (Lalam *et al.*, 2025). In strawberry sorting, an automated system combining image processing, automation, and aerial sorting classified fruits into five quality categories using a 640 × 320-pixel camera, LabVIEW 2018 for processing, and a programmable logic controller (PLC) for control. The system achieved 93.78 % accuracy and processed 3273 fruits per hour, significantly outperforming manual sorting (Amaroek *et al.*, 2025).

More recently, automated broccoli harvesting has benefited from enhanced YOLO-based segmentation. An improved YOLO version 8 nano (YOLOv8n-seg) model, termed YOLO-Broccoli-Seg, incorporated a triplet attention module to improve feature fusion. The model achieved substantial gains in mean average precision (mAP50 and mAP95) for both bounding box and mask detection. A three-dimensional point cloud-based attitude estimation approach further achieved a coefficient of determination (R^2) of 0.934, allowing accurate assessment of broccoli growth angles (He *et al.*, 2025).

Prior studies report strong performance in isolated tasks or specific crop contexts; however, many exhibit limited generalizability, constrained scalability, or reliance on specialized sensing hardware (Table 1). In contrast, the proposed framework addresses these limitations by unifying ripeness classification, defect detection, and size-shape analysis within a single YOLO-based architecture designed for real-world, scalable coffee harvesting applications.

This study aims to develop an intelligent computer vision framework that integrates classification of coffee cherry ripeness, defect detection, and size-shape analysis to enhance automation in coffee harvesting. The proposed system enables accurate, real-time assessment under field conditions, supporting selective harvesting, early defect identification, and automated sorting. By unifying these tasks within a single multi-task architecture, the framework seeks to improve harvesting efficiency, reduce labor

Table 1. Comparative analysis of existing computer vision-based agricultural harvesting and quality assessment frameworks.

Author	Data sources	Focus	Methodology	Scalability	Disadvantage	Future scope
Zhang <i>et al.</i> (2025)	Field trials, simulation analysis	Dual-arm harvesting	Asynchronous dual-arm coordination; ST-FSH path planning	Effective for multi-arm systems	Damage rate limited to specific crop types	Improved end-effectors; AI path planning
Dong <i>et al.</i> (2025)	Greenhouse environment images, depth information	Tomato peduncle localization	DRCANet with multiscale convolution modules	Greenhouse-scale; limited field transfer	Occlusion and lighting sensitivity	Environmental conditions adaptability; real-time robotic implementation
Yang <i>et al.</i> (2025)	Hyperspectral images (400–1000 nm)	Mushroom browning detection	PCA-FCM segmentation; k-NN, PLS-DA classification	Portable quality monitoring	Requires hyperspectral setup	Broader storage conditions; deep learning
Xie <i>et al.</i> (2025)	Real-field experimental data	Mushroom cut-surface quality improvement	YOLOv8n-seg with enhanced feature modules	High accuracy; real-world conditions adaptability	Limited species generalization	Extended approach to other mushroom species; optimized computational efficiency
Zhao <i>et al.</i> (2025)	Shiitake mushroom cap images	Trait measurement for mushroom breeding	Edge detection and SVM optimization	High-throughput phenotyping	Limited to visual traits	Multi-species extension; IoT integration
Santoso <i>et al.</i> (2025)	Grayscale coffee bean images	Coffee bean classification	ResNet-101-based CNN with feature extraction	Potential scalability to new datasets	Limited real-world bean validation	Incorporation of multi-TL strategies; broader datasets
Alhasson <i>et al.</i> (2025)	Robusta coffee bean images	Automated defect detection	YOLO-based mobile application	Suitable for large-scale processing	Low accuracy for some defects	Dataset expansion; IoT-based sorting

ST-FSH: Shortest-Time-Based First-See-Harvest; RGB-D: Red-Green-Blue-Depth; DRCANet: Deep Residual Convolutional Attention Network; PCA: Principal Component Analysis; FCM: Fuzzy C-Means; k-NN: k-Nearest Neighbors; PLS-DA: Partial Least Squares Discriminant Analysis; YOLO: You Only Look Once; CNN: Convolutional Neural Network; SVM: Support Vector Machine; IoT: Internet of Things; TL: Transfer Learning.

dependence, minimize quality variability, and enhance decision-making in smart and sustainable coffee production systems.

MATERIALS AND METHODS

Ripeness classification was carried out using a Vision Transformer-Convolutional Neural Network (ViT-CNN), and defect detection was performed using YOLOv8. Image processing and model training were implemented using OpenCV and

TensorFlow. The workflow includes data acquisition, preprocessing, ripeness categorization, defect identification, and contour-based size analysis for precision agricultural harvest monitoring.

Data acquisition and preprocessing

Drone-mounted surveillance systems equipped with high-resolution Parrot Anafi AI 4K high-definition (HD) cameras were used to record continuous video of coffee plants. The drones fly over the plantation fields and capture footage at 30–60 FPS, ensuring comprehensive coverage. Video streams were processed by extracting frames at predefined intervals for analysis. The acquired data were transmitted wirelessly to cloud platforms such as Amazon Web Services (AWS), Google Cloud, or Microsoft Azure for advanced AI processing, allowing ripeness classification, defect detection, and size-shape analysis.

To improve model robustness and generalization, image data augmentation was applied to the extracted frames from both drone-based and fixed-position cameras. Augmentation techniques include rotation, flipping, brightness adjustment, Gaussian noise addition, contrast enhancement, and color space conversion from red-green-blue (RGB) to hue-saturation-value (HSV) or CIELAB ($L^*a^*b^*$). In addition, synthetic data generation using Generative Adversarial Networks (GANs) is employed to increase dataset diversity. These strategies enhance the performance of the YOLO-based model in ripeness classification, defect identification, and morphological assessment.

Preprocessing of video-derived image data is performed to improve analytical accuracy. This includes noise reduction using Gaussian blur and median filtering, color space conversion to HSV or CIELAB for improved ripeness discrimination, and contrast enhancement via histogram equalization. Contour-based segmentation was applied to separate coffee cherries from the background. Images were subsequently resized (e.g., 640×640 pixels) and normalized to meet YOLO input requirements, allowing accurate ripeness categorization, defect detection, and size-shape analysis (Gope *et al.*, 2024).

Feature extraction using ViT-CNN

The hybrid feature extraction framework (Figure 1) combines ViT-CNNs to classify coffee cherry images by ripeness stage and defect presence. Input images are first processed through multiple CNN modules (Module 1 to Module 4), each designed to capture localized spatial features such as texture, shape, and edge information at different scales (Table 2). The resulting feature maps from each CNN module are then forwarded to corresponding ViT encoders that operate on embedded image patches. Within each ViT encoder, patch embedding converts image patches into vector representations, followed by normalization and multi-head self-attention to capture global contextual relationships across the image. A feed-forward multilayer perceptron (MLP) refines these representations for enhanced feature encoding. Outputs from all ViT encoders are concatenated and passed through an attention gate to emphasize

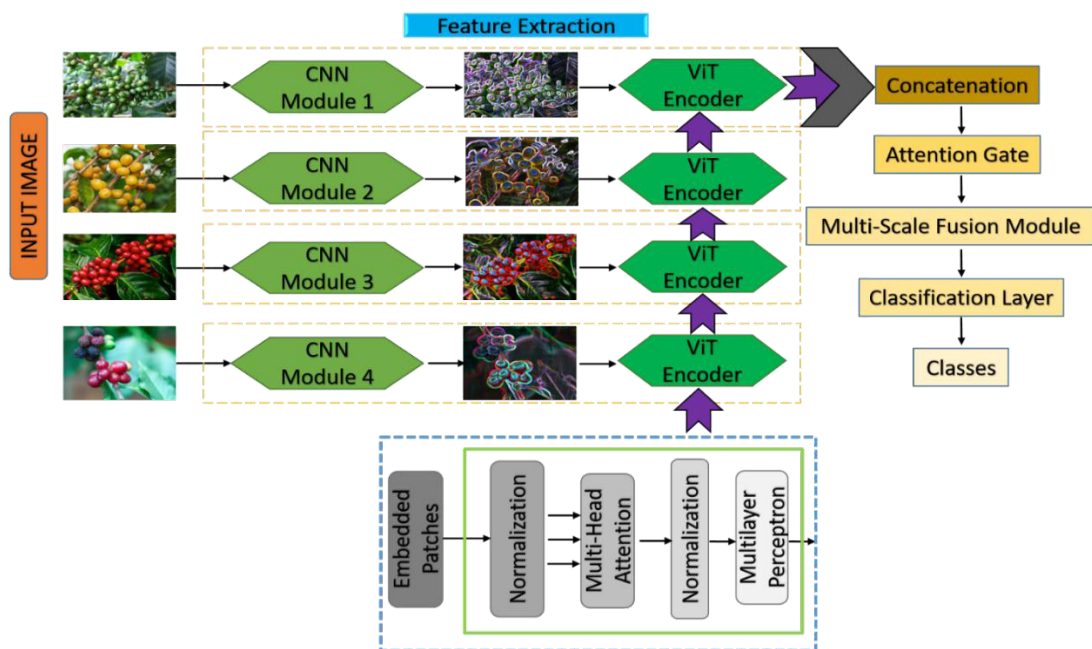


Figure 1. Hybrid vision Transformer-Convolutional Neural Network (ViT-CNN) pipeline to capture both local and global coffee cherry features.

Table 2. Visual results of ripeness stage detection of coffee cherries using YOLOv8 combined with color-based segmentation.

Ripeness stage	Label color	Detection accuracy	Bounding box precision	Segmentation clarity	Observation
Under ripe cherries	Purple	High (~90 %)	Sharp and well localized	High	Most under-ripe cherries are accurately detected and localized.
Partially ripe cherries	Blue	High (~88-92 %)	Precise, minor overlaps	High	Clearly segmented; good distinction even when clustered.
Fully ripe cherries	Orange	Very high (~95 %)	Very accurate	Excellent	Strong performance in identifying ripe cherries even in dense clusters.
Over ripe cherries	Green	Moderate to high (~85 %)	Good with few overlaps	Moderate to high	Slight mislabeling in few areas; could improve with more data or color tuning.

the most salient features. Finally, a multi-scale fusion module integrates the extracted information into a unified representation, which is fed into the classification layer to generate the final output classes (unripe, partially ripe, fully ripe, and overripe).

Ripeness stage detection using YOLOv8 with color-based segmentation

Color-based segmentation is an important preprocessing step to distinguish coffee cherries at different maturity stages (Figure 2). This step enables preliminary classification based on color prior to the application of deep learning models, supporting more accurate downstream categorization. Segmentation is performed in the HSV color space, where hue represents the actual color (0–360°), saturation indicates color purity (0–1), and value corresponds to brightness (0–1). Thresholding is primarily applied to the hue component to categorize cherries according to maturity stage (Selvanarayanan *et al.*, 2024a).

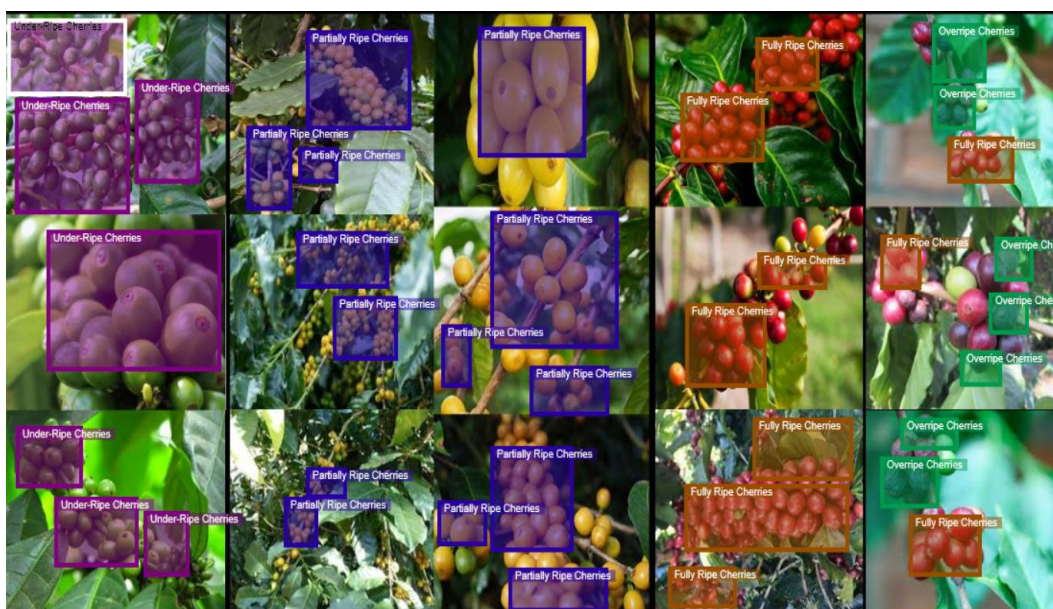


Figure 2. Ripeness stage detection of coffee cherries using YOLOv8, combined with color-based segmentation.

Under-ripe cherries (green shades)

Green cherries correspond to the initial stages of maturity and are characterized by lower hue values, typically ranging from 30 to 80°. Pixels within this interval were classified as under-ripe cherries using the following equation:

$$Mask_{green} = (30^\circ \leq H \leq 80^\circ) \wedge (S > S_{MIN}) \wedge (V > V_{MAX})$$

where H denotes the hue component representing pixel color in the HSV space, S represents saturation to exclude low-color-intensity pixels, and V corresponds to pixel brightness. The threshold condition for under-ripe classification is defined by a hue range between 30 and 80°.

Partially ripe cherries (half green to yellow-red)

Cherry transition from green to yellow and then to red is reflected by progressively higher hue values within the mid-range of the HSV color space (80–150°). Pixels with hue values in this interval were therefore classified as partially ripe:

$$Mask_{partially\ ripe} = (80^\circ \leq H \leq 150^\circ) (S > S_{MIN})^{V > V_{MAX}}$$

Fully ripe cherries (red shades)

When cherries reach full ripeness, they exhibit a bright red coloration, with hue values in the higher range of the HSV spectrum (150–180°). Pixels falling within this interval were classified as ripe cherries:

$$Mask_{ripe} = (150^\circ \leq H \leq 180^\circ) (S > S_{MIN})^{V > V_{MAX}}$$

Overripe cherries (dark brown/black shades)

Overripe cherries darken to deep brown or black, characterized by hue values exceeding 180°. Pixels exhibiting high hue values combined with low brightness were therefore classified as overripe as follows:

$$Mask_{over\ ripe} = (H > 180^\circ) (S > 0.2)^{V > 0.5}$$

where the $H > 180^\circ$ condition ensures capturing hues associated with darker shades like brown and black. Since overripe cherries appear dark, their brightness (V) must be below a certain threshold.

Coffee cherry defect detection

The defect detection process for coffee cherries using YOLOv8 (Figure 3) follows a structured architecture composed of three main components: the backbone, neck, and head. The input layer receives images of size $640 \times 640 \times 3$, which corresponds to the spatial resolution and the RGB color channels. These images typically contain multiple coffee cherries exhibiting various defects, such as blackening, mold growth, wrinkling, or insect damage (Figure 4). Within the backbone layer, the input image is initially processed by a convolutional module in the stem layer to extract basic visual features, including edges, textures, and color patterns.

The input image is processed through a sequence of four stages (Stage 1 to Stage 4) using convolutional modules, C2f blocks, and Darknet bottleneck modules. Each stage progressively reduces spatial resolution while increasing feature abstraction. Stage 1 downsamples the image to 320×320 pixels and extracts mid-level features. Stage 2 further reduces the resolution to 160×160 , emphasizing patterns associated with surface defects. Stage 3 operates at an 80×80 resolution to capture coarse and abstract features, such as shape distortions. Stage 4 processes features at 40×40 and 20×20 resolutions, focusing on high-level semantic characteristics, including pronounced wrinkling or mold development.

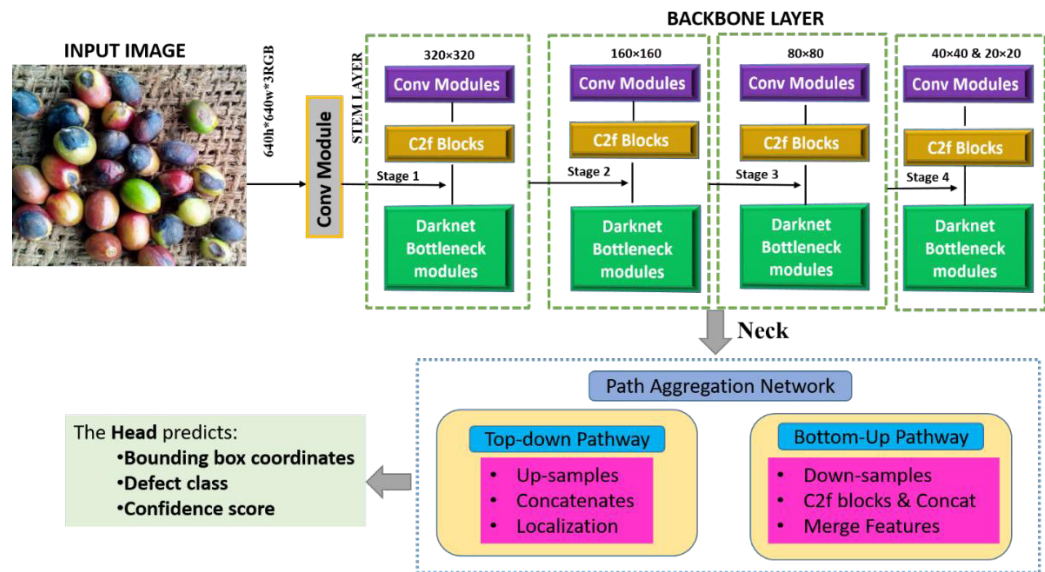


Figure 3. YOLOv8-based architecture for automated coffee cherry defect detection, showcasing multi-stage feature extraction and confidence-driven classification using a backbone, neck, and object prediction head.

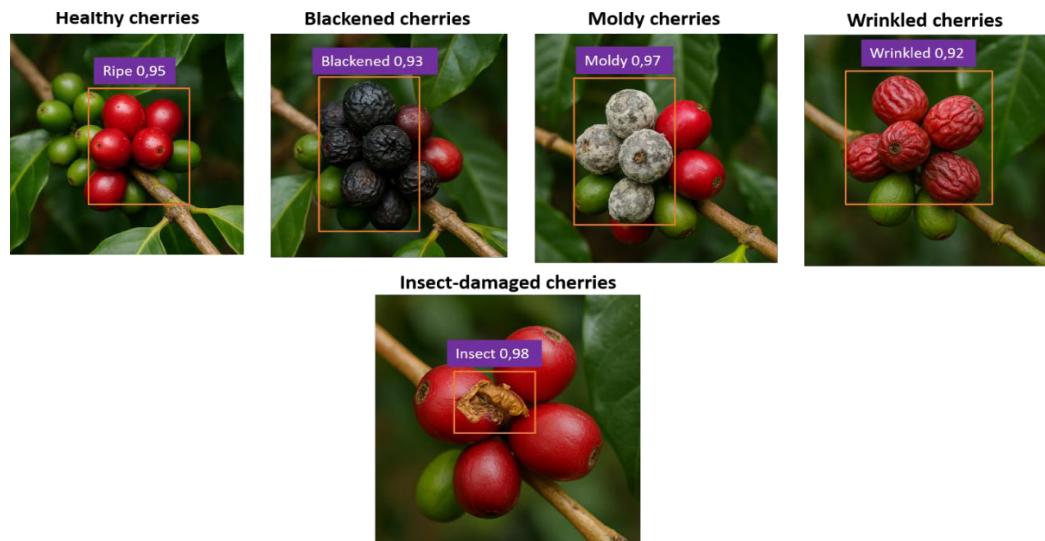


Figure 4. YOLOv8-powered classification of coffee cherries into five categories: healthy, blackened, moldy, wrinkled, and insect-damaged based on defect type and confidence scores for precision in quality assessment.

Convolutional feature extraction at each stage is performed according to the following expression:

$$F_{conv} = \sigma(W * I_{norm} + b)$$

where σ denotes the activation function (e.g., SiLU), W is the convolution kernel, $*$ represents the convolution operation, and b is the bias term.

C2f blocks improve feature reuse and learning efficiency through feature concatenation, as defined by:

$$F_{C2f} = \text{Concat}(F_1, F_2, \dots, F_n)$$

where F_i represents the feature maps generated by the internal convolutional layers within the C2f block.

Darknet bottleneck modules further incorporate residual connections, facilitating the effective learning of deeper and more complex feature representations. The resulting multi-scale features are then forwarded to the Neck, implemented as a Path Aggregation Network (PAN), which enables feature fusion across different spatial scales.

In the top-down pathway, small-scale defects such as minor surface patches or fine creases are emphasized through upsampling, feature concatenation, and localization, according to the expression:

$$F_{td}^i = \text{Concat}(F_{Upsampled}^{i+1}, F_{Backbone}^i)$$

Conversely, the bottom-up pathway applies downsampling and integrates multi-resolution features using C2f blocks, enhancing contextual understanding of defects distributed over larger regions, such as widespread mildew, as follows:

$$F_{bu}^i = \text{Concat}(F_{Downsampled}^{i+1}, F_{Backbone}^i)$$

The YOLOv8 Head receives the fused multi-scale features and generates three outputs in a single forward pass: (i) bounding box coordinates for localizing defective cherries, (ii) defect class labels (blackened, moldy, wrinkled, or insect-damaged), and (iii) confidence scores that quantify the reliability of each prediction.

Size and shape analysis using YOLOv8 for object contour detection

YOLOv8 detection identifies coffee cherries and generates bounding boxes for each detected object. Each bounding box includes a class label, a confidence score, and spatial

coordinates ($x, y, width, height$). For contour-based analysis, the segmentation variant YOLOv8-Seg was used, which produces precise object masks rather than bounding boxes alone. These masks are binary, pixel-level representations of each detected cherry. Contours are extracted from the YOLOv8-Seg output using the *findContours()* function in OpenCV applied to the binary masks. The resulting contours consist of ordered (x,y) coordinate sets that delineate the boundary of each identified cherry. Size estimation was performed using the bounding rectangle computed for each extracted contour. The width and height of the bounding rectangle were measured, and the diameter was derived from the minimum enclosing circle. Pixel measurements were then converted to physical units by applying a pixel-to-centimeter calibration based on a reference object or a known camera scale factor. The conversion of an object's pixel width to its actual physical width (*RealW*), expressed in centimeters or millimeters, was performed using the relationship between pixel measurements and the camera field of view, where *PixelW* denotes the object width in pixels, *ImageWidth* represents the total image width in pixels, and *RealFieldWidth* corresponds to the true physical width of the camera's field of view.

$$RealW = \left(\frac{PixelW}{ImageWidth} \right) * RealFieldWidth$$

The diameter of approximately circular objects, such as coffee cherries, was computed from their projected area to obtain a scale-invariant size estimate as follows:

$$Diameter = \sqrt{4 \times \frac{area}{\pi}}$$

Object elongation and symmetry were characterized using the aspect ratio of the bounding box, which reflects shape irregularities.

$$Aspect\ ratio = \frac{width}{height}$$

Circularity was quantified to assess how closely an object resembles a perfect circle, where an ideal circular shape yields a circularity value of one, while irregular or elongated shapes produce lower values that are indicative of defective or misshapen cherries.

$$Circularity = 4\pi \times \frac{area}{perimeter^2}$$

Solidity, defined as the ratio between the object area and the area of its minimum convex hull, was used to evaluate compactness, with lower values suggesting voids, shrinkage, or surface deformations.

$$\text{Solidity} = \frac{\text{Contour}_{Area}}{\text{ConvexHull}_{Area}}$$

Finally, the extent metric measured the proportion of the bounding box area occupied by the object, where lower values indicate uneven or non-compact shapes, detecting wrinkled, undersized, or defective cherries.

$$\text{Extent} = \frac{\text{Contour}_{Area}}{\text{Bounding}_{RectArea}}$$

Performance evaluation

Precision quantifies the accuracy of classified ripeness stages (e.g., fully ripe, overripe) or defects (e.g., moldy, blackened). High precision reduces false positives in both ripeness assessment and defect identification, and it was calculated according to the following equation (Kumanan, T *et al.*, 2025 and Kumanan, S *et al.*, 2025).

$$\text{Precision} = \frac{\text{True positive}}{\text{True positive} + \text{False positive}}$$

Recall evaluates the model's ability to identify all relevant instances. High recall ensures that ripeness stages or defective cherries are not missed during detection or size assessment.

$$\text{Recall} = \frac{\text{True positive}}{\text{True positive} + \text{False negative}}$$

The F1-score provides a balanced measure of precision and recall, making it particularly suitable for evaluating ripeness detection and defect classification in imbalanced datasets.

$$\text{F1 - Score} = 2 * \frac{\text{Precision} * \text{Recall}}{\text{Precision} + \text{Recall}}$$

Mean Average Precision at an IoU threshold of 0.5 (mAP@50) was used to evaluate ripeness classification and defect detection, requiring at least 50 % overlap between predicted and ground-truth bounding boxes. It was calculated as follows:

$$\text{mAP } 50 = \frac{1}{N} \sum_{i=1}^N Ap_i$$

The COCO-style $mAP@50-95$ provides evaluation across multiple IoU thresholds, making it essential for fine-grained shape-based classification, especially in crowded or overlapping cherry scenarios.

$$mAP@50-95 = \frac{1}{10} \sum_{i=0.50}^{0.95} mAP@t$$

The confidence score reflects the probability that a detected object correctly corresponds to a specific ripeness stage or defect class (e.g., insect-damaged or fully ripe). Detection results typically display this value as an overlay. It was calculated as:

$$\text{Confidence Score} = \text{Objectness} * \text{Class probability}$$

Model size, expressed as the number of parameters in millions (Params, M), indicates computational complexity. Lightweight models are preferred for real-time field applications such as ripeness and defect detection.

$$\text{Params (M)} = \frac{\text{Total trainable weights}}{1\,000\,000}$$

Frames per second (FPS) measures inference speed and is important for real-time size and shape analysis in drones, mobile devices, or on-site quality assessment systems.

$$\text{FPS} = \frac{\text{Total frames processed}}{\text{Total time (seconds)}}$$

Contour accuracy serves as a key metric for size and shape analysis, enabling the differentiation of healthy cherries from wrinkled or misshapen ones through precise edge and contour detection.

$$\text{Contour accuracy} = \frac{\text{Correctly detected contour pixels}}{\text{Total ground true contour pixels}}$$

Intersection over Union (IoU) evaluates how accurately predicted bounding boxes align with the true cherry contours.

$$\text{IoU} = \frac{\text{Area of vverlap}}{\text{Area of union}}$$

Evaluation setup and dataset collection

Python 3.6.5 was used to develop the model on a system equipped with an Intel i5-8600K CPU, a GeForce GTX 1050 Ti GPU (4 GB), 16 GB RAM, a 250 GB SSD, and a 1

TB HDD. Model construction and training were performed using Keras 2.7. Training parameters were set to a batch size of 32, 150 epochs, a dropout rate of 0.5, and a learning rate of 0.01. Input images were resized to $640 \times 640 \times 3$, and the experimental setup focused on detecting four ripeness stages. Evaluation metrics included True Positive (TP), True Negative (TN), False Positive (FP), and False Negative (FN), as well as derived measures such as Precision, Recall, F1-score, and mean Average Precision (mAP).

The coffee cherry dataset was collected from selected Meraca Gold Estate plantations in the Coorg district of Karnataka, India, specifically in the Kushalanagar and Suntikoppa regions. Data acquisition was performed using UAVs, digital single-lens reflex (DSLR) cameras, and fixed-position cameras installed along plantation rows to capture high-resolution images under diverse lighting and environmental conditions. All images were manually annotated using LabelImg, with bounding boxes marking the regions of interest. A total of 4200 labeled images were collected to ensure class balance across the four ripeness levels. The dataset was partitioned into training (70 %), validation (15 %), and testing (15 %) subsets.

RESULTS AND DISCUSSION

Training convergence and optimization behavior

To evaluate the learning stability and convergence characteristics of the proposed framework, training and validation accuracy-loss curves were analyzed over 150 epochs (Figure 5). The model demonstrates stable convergence across ripeness detection, defect detection, and size-shape analysis tasks, with no evidence of overfitting. Validation loss decreases consistently while accuracy improves progressively, indicating effective generalization and balanced learning across tasks.

Performance evaluation for ripeness stage detection

The proposed YOLOv8 model with integrated color-based segmentation was evaluated and compared against YOLOv5 and Faster Region-Based Convolutional Neural Network (Faster R-CNN) with a ResNet50 backbone. Model performance was assessed at training epochs of 50, 100, and 150. The YOLOv8 framework demonstrated improved convergence and generalization (Table 3), as evidenced by an increase in mAP@50 from 0.88 at epoch 50 to 0.93 at epoch 150. This performance gain was further reflected in the mAP@50:95 metric, where the proposed approach achieved 0.78, outperforming the baseline YOLOv5 (0.71) and the more computationally intensive Faster R-CNN (0.69).

YOLOv8 demonstrated improved detection performance for overlapping and visually similar categories such as “Overripe” cherries, due to the synergistic effect of deep semantic features and color-space segmentation enhancement. The model achieved high precision (0.91), recall (0.89), and F1-score (0.9), making it highly reliable for real-

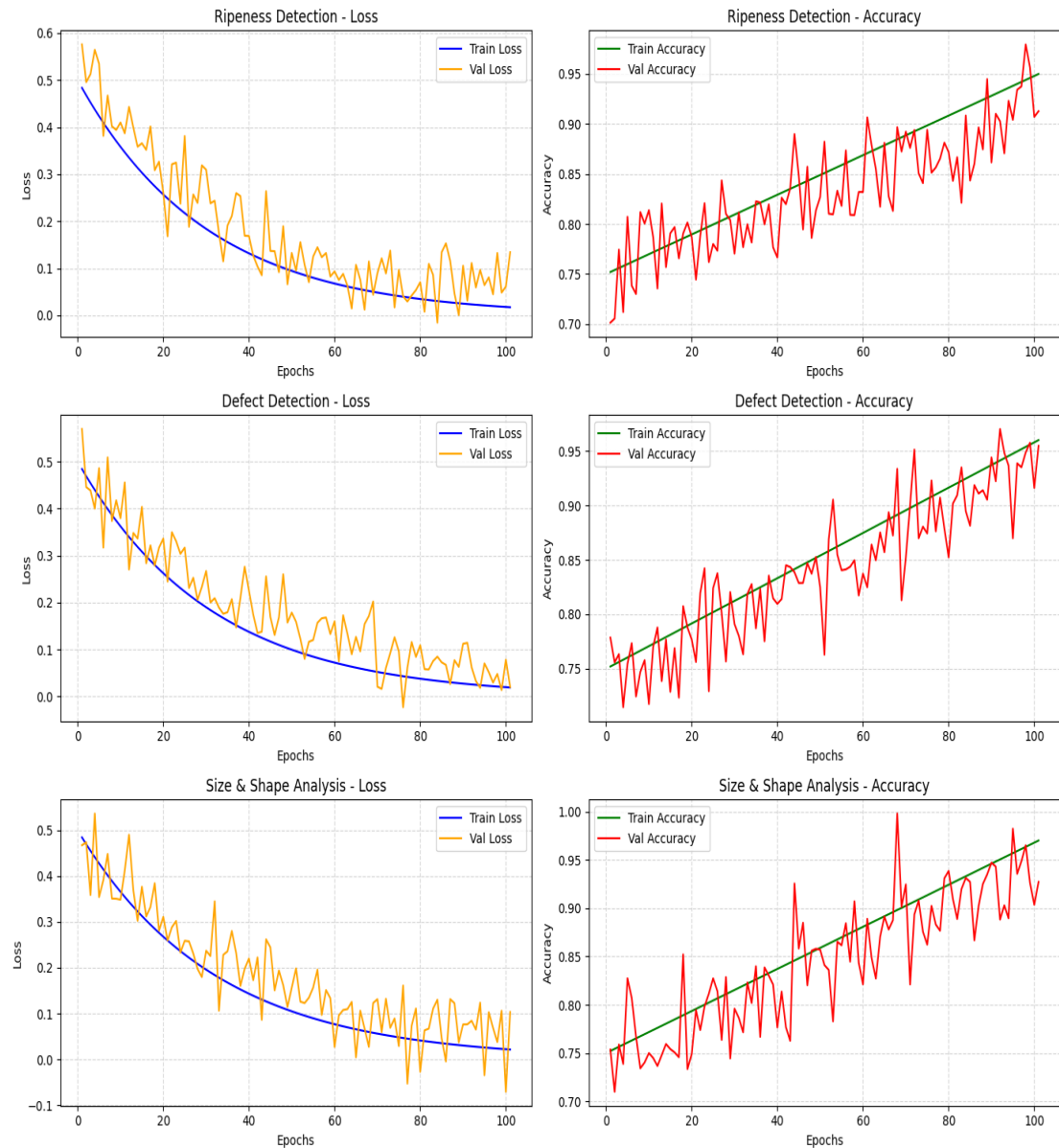


Figure 5. Training and validation accuracy against loss curves for ripeness detection, defect detection, and size and shape analysis tasks using YOLOv8 across 150 epochs.

time deployment, with an inference speed of 57 FPS. YOLOv5 showed a consistent performance trend; however, it did not reach comparable segmentation accuracy in complex background conditions. In contrast, Faster R-CNN, although effective for static image detection tasks, operated at a lower speed (12 FPS), which limits its applicability in dynamic real-time agricultural environments. The proposed model

Table 3. Comparative performance of YOLOv8 with color-based segmentation, YOLOv5, and Faster Region-Based Convolutional Neural Network (Faster R-CNN) for coffee cherry ripeness stage detection across training epochs.

Epochs	Model	Ripe	Partially ripe	Fully ripe	Over ripe	mAP50	mAP 50-95	Precision	Recall	F1-Score
50	YOLOv8 + Color segmentation	0.85	0.87	0.89	0.80	0.88	0.70	0.86	0.84	0.85
	YOLOv5	0.81	0.83	0.86	0.76	0.84	0.65	0.82	0.80	0.81
	Faster R-CNN (ResNet50)	0.77	0.80	0.83	0.72	0.81	0.60	0.78	0.77	0.77
100	YOLOv8 + Color segmentation	0.88	0.90	0.93	0.83	0.91	0.75	0.89	0.87	0.88
	YOLOv5	0.84	0.86	0.89	0.79	0.87	0.69	0.86	0.82	0.84
	Faster R-CNN (ResNet50)	0.80	0.82	0.87	0.75	0.84	0.65	0.83	0.79	0.81
150	YOLOv8 + Color segmentation	0.90	0.92	0.95	0.85	0.93	0.78	0.91	0.89	0.90
	YOLOv5	0.86	0.88	0.91	0.81	0.89	0.71	0.88	0.84	0.86
	Faster R-CNN (ResNet50)	0.83	0.85	0.90	0.78	0.87	0.69	0.85	0.82	0.83

integrates spatial and chromatic features to deliver a robust and scalable framework for high-precision coffee cherry ripeness detection across different maturation stages.

Performance evaluation for defect detection

As the number of training epochs increases from 50 to 150, a clear upward trend in detection and classification accuracy was found across all defect categories: healthy (ripe), blackened, moldy, wrinkled, and insect-damaged cherries (Table 4).

With F1-scores of 0.9 and 0.88 and mAP@50 values of 0.93 and 0.91, respectively, the YOLOv8 model demonstrated strong initial performance at epoch 50, particularly for insect-damaged and moldy cherries. These categories also show high visual confidence scores (above 0.97), indicating robust visual discrimination even during early training phases. However, lower F1-scores for wrinkled (0.82) and blackened cherries (0.84) suggest that additional feature learning is required for these classes due to texture and color overlap with healthy cherries.

At epoch 100, all defect categories exhibited measurable improvement. The model showed consistent gains in both precision and recall, increasing F1-scores to above 0.9 for most classes, especially moldy and insect-damaged cherries. The corresponding rise in mAP@50 values indicates more accurate and confident localization of defective regions. By epoch 150, the YOLOv8 model achieved near-optimal performance. The F1-score reached 0.95 for moldy cherries and 0.96 for insect-damaged cherries, with a mAP@50 of 0.97. Previous lower-performing categories, such as wrinkled and

Table 4. Performance comparison of coffee cherry defect detection across training epochs.

Epoch	Category	Precision	Recall	F1-Score	mAP@50	Confidence score (visual)
50	Healthy (ripe)	0.88	0.85	0.86	0.89	0.95
	Blackened	0.85	0.83	0.84	0.87	0.93
	Moldy	0.90	0.86	0.88	0.91	0.97
	Wrinkled	0.83	0.82	0.82	0.85	0.92
	Insect-damaged	0.92	0.89	0.90	0.93	0.98
100	Healthy (ripe)	0.91	0.89	0.90	0.92	0.95
	Blackened	0.89	0.87	0.88	0.90	0.93
	Moldy	0.94	0.91	0.92	0.94	0.97
	Wrinkled	0.86	0.84	0.85	0.88	0.92
	Insect-damaged	0.95	0.93	0.94	0.96	0.98
150	Healthy (ripe)	0.94	0.92	0.93	0.95	0.95
	Blackened	0.92	0.90	0.91	0.93	0.93
	Moldy	0.96	0.94	0.95	0.96	0.97
	Wrinkled	0.89	0.88	0.88	0.90	0.92
	Insect-damaged	0.97	0.95	0.96	0.97	0.98

blackened cherries, improved to F1-scores of 0.88 and 0.91, respectively. Confidence scores across all categories consistently exceed 0.92, confirming the model’s visual reliability and stability.

Performance evaluation for size and shape

All categories showed progressive improvement in performance metrics as the number of training epochs increased, showing the model’s ability to learn subtle visual defects and complex shape deformations. In particular, contour accuracy and bounding box IoU increased from 0.9 and 0.87 at epoch 50 to 0.96 and 0.94 at epoch 150, reflecting improved boundary detection and localization accuracy (Table 5).

Insect-damaged cherries consistently achieved the highest scores across all epochs, reaching a contour accuracy of 0.98 and a confidence score of 0.98, due to their distinct shape and texture characteristics. Moldy cherries also demonstrated strong performance, with an F1-score of 0.94 at 150 epochs, attributed to their pronounced surface irregularities. Categories such as wrinkled and blackened cherries, characterized by less distinct edges and subtle color variations, showed marked improvements by epoch 150, with contour accuracies of 0.91 and 0.92, respectively.

Precision-recall and F1-recall analysis

The robustness of the detection framework was further evaluated using precision-recall and F1-recall curves (Figure 6). The graphs demonstrate high area under the curve across all tasks, indicating strong class separability and stable threshold behavior.

Table 5. Performance comparison of coffee cherry size and shape analysis across training epochs.

Epoch	Category	Contour accuracy	Bounding box IoU	Precision	Recall	F1-score	Confidence score (visual)
50	Healthy (ripe)	0.90	0.87	0.88	0.85	0.86	0.95
	Blackened	0.88	0.85	0.86	0.83	0.84	0.93
	Moldy	0.93	0.91	0.91	0.89	0.90	0.97
	Wrinkled	0.86	0.83	0.84	0.81	0.82	0.92
	Insect-damaged	0.95	0.93	0.94	0.92	0.93	0.98
100	Healthy (ripe)	0.93	0.90	0.91	0.89	0.90	0.95
	Blackened	0.90	0.88	0.89	0.87	0.88	0.93
	Moldy	0.95	0.93	0.94	0.92	0.93	0.97
	Wrinkled	0.89	0.86	0.87	0.85	0.86	0.92
	Insect-damaged	0.97	0.95	0.96	0.94	0.95	0.98
150	Healthy (ripe)	0.94	0.91	0.93	0.90	0.91	0.95
	Blackened	0.92	0.89	0.90	0.88	0.89	0.93
	Moldy	0.96	0.94	0.95	0.93	0.94	0.97
	Wrinkled	0.91	0.88	0.89	0.87	0.88	0.92
	Insect-damaged	0.98	0.96	0.97	0.95	0.96	0.98

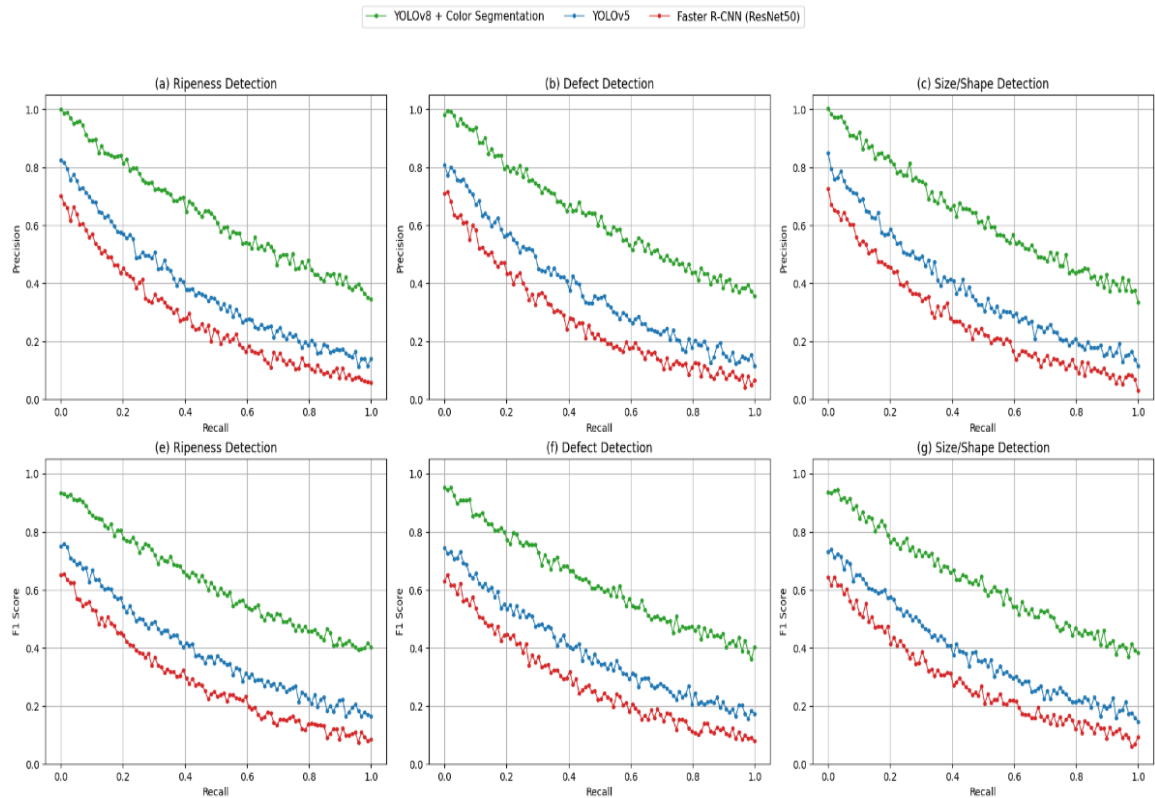


Figure 6. Precision-recall and F1 score-recall curves for ripeness detection, defect detection, and size/shape detection tasks.

Ablation experiment

A preliminary experiment on the coffee cherry dataset used YOLOv8 as the baseline model. To evaluate the effectiveness of the proposed technique within the Visionary Harvest framework, a series of ablation experiments were conducted to assess the individual contributions of each module: ViT-CNN feature extraction, ripeness stage detection, defect detection, and size and shape analysis.

The ablation study began with standard YOLOv8 without architectural modifications, establishing a strong baseline for coffee cherry detection. A ViT-CNN module was integrated to enhance spatial and contextual feature representation, improving the model's ability to distinguish subtle ripeness variations and fine surface textures. Additionally, attention mechanisms were incorporated to refine feature weighting and emphasize discriminative regions (Figure 7), which collectively enhance detection robustness in complex field conditions.

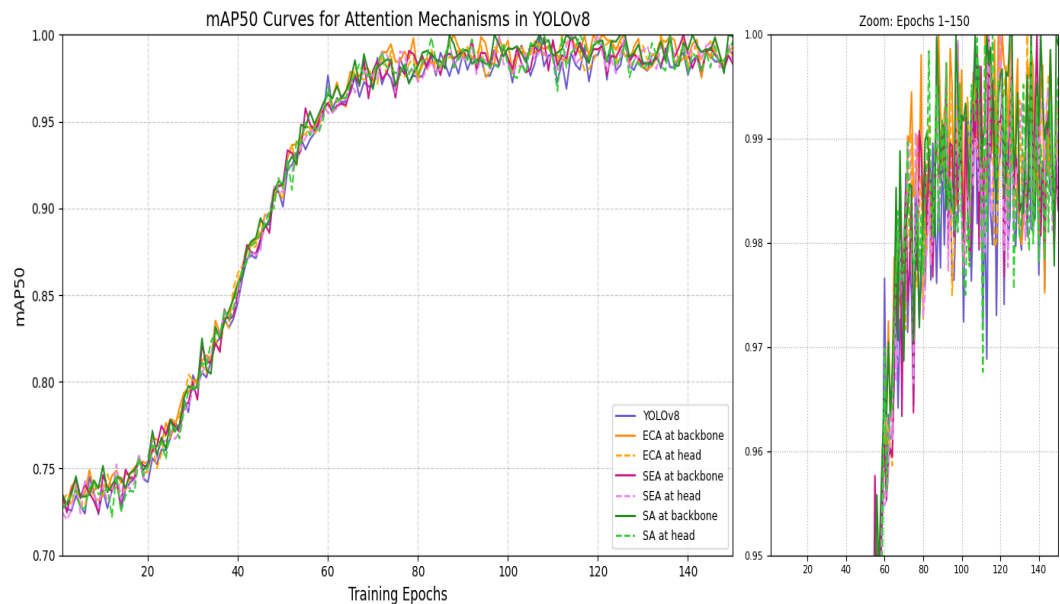


Figure 7. Impact of attention mechanisms (Efficient Channel Attention (ECA), Spatial and Efficient Channel Attention (SEA), and Self-Attention (SA)) on YOLOv8 detection performance through enhanced multi-stage feature refinement.

Subsequently, color-based ripeness segmentation was incorporated into the YOLOv8 detection pipeline to strengthen stage-wise classification (unripe, mid-ripe, ripe, and overripe), particularly under mixed-ripeness conditions commonly observed in field environments. A dedicated defect detection head was introduced to identify cracks, holes, and fungal spots, enabling multi-task learning without significant computational

overhead. Finally, YOLOv8-based contour detection was implemented for analyzing size and shape, enhancing the precision of quality assessments beyond just ripeness and defect detection (Figures 8 and 9).

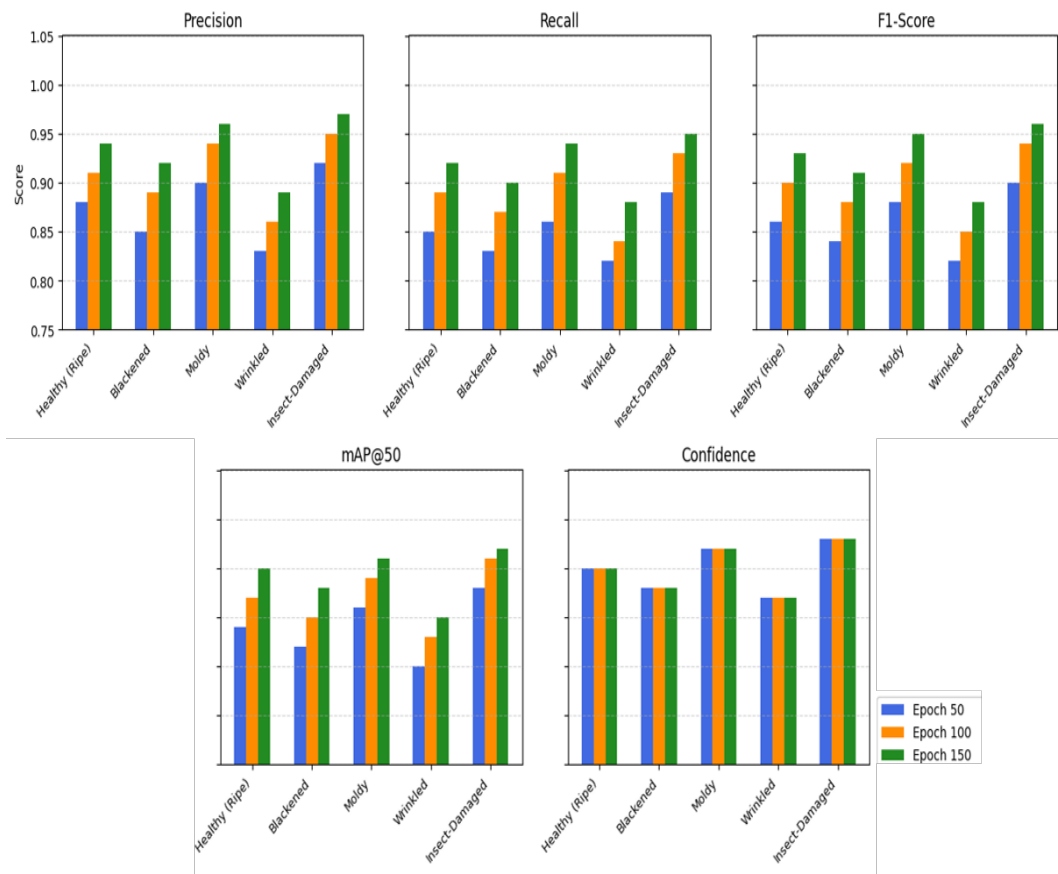


Figure 8. Comparison of model performance metrics (precision, recall, F1-score, mAP@50, and confidence) across three training stages (epochs 50, 100, and 150) for five categories of coffee cherries: healthy (ripe), blackened, moldy, wrinkled, and insect-damaged. The progressive improvement indicates better classification and detection performance as training advances.

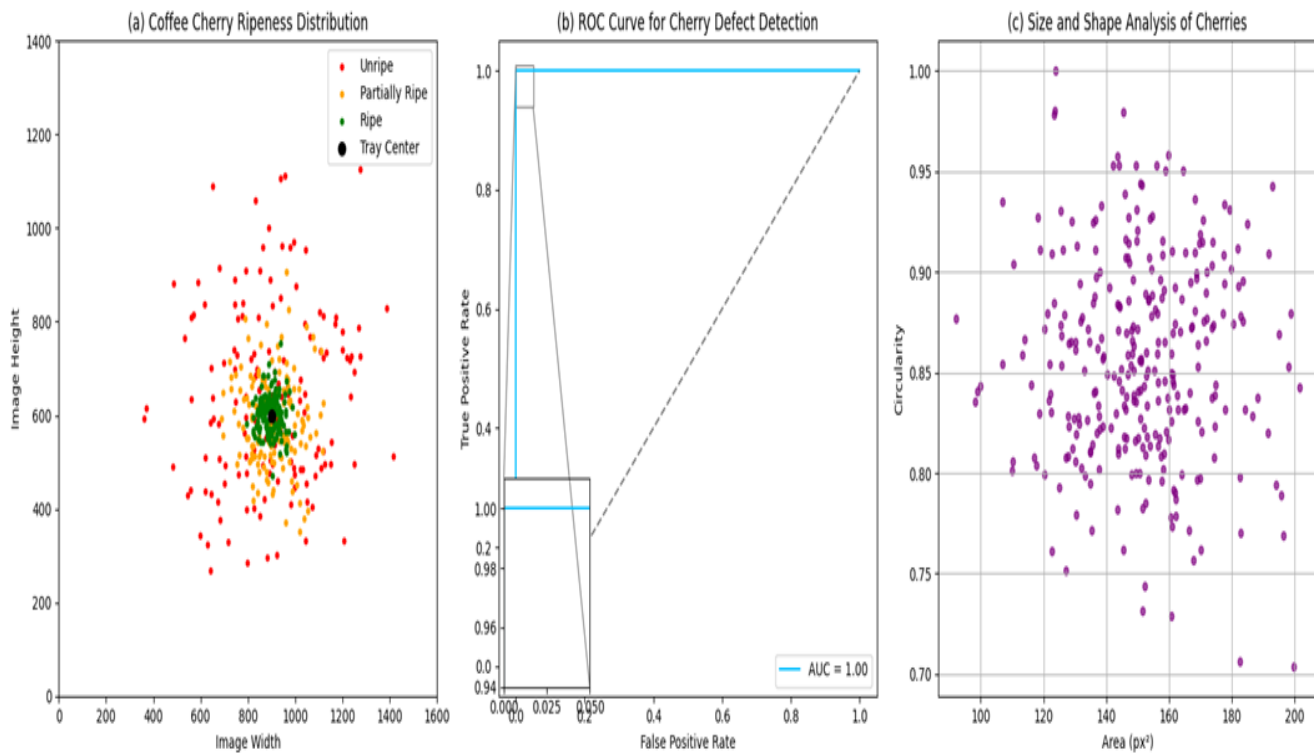


Figure 9. A: Spatial distribution of coffee cherry centers based on ripeness stages, showing unripe (red), partially ripe (orange), and ripe (green) cherries relative to the tray center (black); B: Receiver Operating Characteristic (ROC) curve illustrating the performance of the deep learning model in detecting defective cherries, with an inset zoom showing the high-accuracy region and area under the curve (AUC) performance; C: Scatter plot of cherry size versus circularity representing morphological variation, useful for grading and quality assessment during post-harvest processing.

CONCLUSION

The proposed method classifies coffee cherries into multiple ripeness stages (unripe, partially ripe, and ripe), identifies surface defects, and analyzes morphological features within a unified framework. Using an optimized YOLOv8 model, the system accurately localizes cherry instances and employs performance visualizations to interpret detection behavior. Defect classification is supported by Receiver Operating Characteristic (ROC) analysis, with thresholds derived from an Area Under the Curve (AUC)-optimized framework to ensure robustness and sensitivity.

Spatial distribution patterns were analyzed relative to a reference tray center to simulate real-world sorting conditions. The inclusion of size and shape measurements adds an additional layer of quality assessment, strengthening grading decisions beyond ripeness and defect detection. However, defect categorization is limited to

observable surface irregularities; internal rot or shriveling caused by disease or moisture loss was not evaluated due to sample constraints. Although the architecture was optimized for efficiency, slight accuracy reductions were observed in complex detection scenarios, and environmental factors such as illumination and camera angle may influence prediction reliability. Future work would integrate near-infrared (NIR) or hyperspectral imaging through multimodal sensing to detect internal abnormalities and subtle ripeness signals not visible in RGB images.

DATA AVAILABILITY

Raveena S. 2025. Visionary harvest with YOLOv8-powered coffee cherry ripeness, defect detection, size, and shape assessment. Zenodo. <https://doi.org/10.5281/zenodo.15222509>. The coding method and supplementary data are available upon proper request from the primary and coauthors.

REFERENCES

- Alhasson HF, Alharbi SS. 2025. Classification of Saudi coffee beans using a mobile application leveraging squeeze vision transformer technology. *Neural Computing and Applications* 37 (14) 8629–8649. <https://doi.org/10.1007/s00521-025-11024-9>
- Amaroek S, Manop R, Pongrawee N, Kittisak K, Niti P, Sorawit C, Supattanakij P. 2025. Research and development of strawberry quality sorting machine with image processing. *Agricultural and Biological Engineering* 2 (2): 44–51.
- Arwathananukul S, Dan X, Phasit C, Sai AM, Rattapon S. 2024. Implementing a deep learning model for defect classification in Thai Arabica green coffee beans. *Smart Agricultural Technology* 9: 100680. <https://doi.org/10.1016/j.atech.2024.100680>
- Beldek C, Dunn A, Cunningham J, Sariyildiz E, Phung SL, Alici G. 2025. Multi-vision-based picking point localisation of target fruit for harvesting robots. *In* 2025 IEEE International Conference on Mechatronics. Institute of Electrical and Electronics Engineers: Wollongong, Australia. <https://doi.org/10.1109/icm62621.2025.10934868>
- Dong L, Zhu L, Zhao B, Wang R, Ni J, Liu S, Chen K, Cui X, Zhou L. 2025. Semantic segmentation-based observation pose estimation method for tomato harvesting robots. *Computers and Electronics in Agriculture* 230: 109895. <https://doi.org/10.1016/j.compag.2025.109895>
- Gope HL, Fukai H, Ruhad FM, Barman S. 2024. Comparative analysis of YOLO models for green coffee bean detection and defect classification. *Scientific Reports* 14 (1). <https://doi.org/10.1038/s41598-024-78598-7>
- He Z, Yuan F, Zhou Y, Cui B, He Y, Liu Y. 2025. Stereo vision based broccoli recognition and attitude estimation method for field harvesting. *Artificial Intelligence in Agriculture* 15 (3): 526–536. <https://doi.org/10.1016/j.aiaa.2025.02.002>
- Ji Y, Xu J, Yan B. 2024. Coffee green bean defect detection method based on an improved YOLOv8 model. *Journal of Food Processing and Preservation* 20 (1): 2864052. <https://doi.org/10.1155/2024/2864052>
- Kumanan, T., Nagarathna, K., Vinodha, R., Balasubramani, S., Prasad, S.S.E. and Sujatha, S., 2025, April. Improving Grape Quality in Viticulture with Autonomous Robots Using Deep

- Learning and Sensor Fusion. In 2025 3rd International Conference on Advancement in Computation & Computer Technologies (InCACCT) (pp. 521-525). IEEE.
- Kumaran, S., Rekha, V. and Kavida, A.C., 2025, September. Deep Learning-Based Ripeness Detection and Quality Grading of Mangoes Using Real-Time Image Processing. In 2025 5th International Conference on Emerging Research in Electronics, Computer Science and Technology (ICERECT) (pp. 1-6). IEEE.
- Lalam R, Lavanya K, Nadella V, Kiran BR. 2025. Automatic sorting and grading of fruits based on maturity and size using machine vision and artificial intelligence. *Journal of Scientific Research and Reports* 31 (1): 153–163. <https://doi.org/10.9734/jsrr/2025/v31i12754>
- Napier CC, Cook DM, Armstrong LJ. 2025. Coffee berry pathogen anomaly detection using colour and shape separation via L-systems. *BIO Web of Conferences* 167: 05003. <https://doi.org/10.1051/bioconf/202516705003>
- Okabe Y, Hiraguri T, Endo K, Kimura T, Hayashi D. 2025. Classification of tomato harvest timing using an AI Camera and analysis based on experimental results. *AgriEngineering* 7 (2): 48. <https://doi.org/10.3390/agriengineering7020048>
- Sangamithrai, K. and Richard, T., 2024, April. Design and development of a plant leaf disease identification system using improved deep learning strategy. In 2024 Ninth International Conference on Science Technology Engineering and Mathematics (ICONSTEM) (pp. 1-7). IEEE.
- Santoso BR, Sari CA, Rachmawanto EH. 2025. Coffee beans classification using convolutional neural networks based on extraction value analysis in grayscale color space. *Journal of Applied Informatics and Computing* 9 (1): 31–37. <https://doi.org/10.30871/jaic.v9i1.8916>
- Selvanarayanan R, Surendran R, Gomathi T, Kartheesan L. 2024a. Hybrid vision transformer and CNN for detection of overripe coffee berry disease (OCBD) in coffee plantation. In 2024 International Conference on Emerging Research in Computational Science. Institute of Electrical and Electronics Engineers: Coimbatore, India. <https://doi.org/10.1109/icercs63125.2024.10895612>
- Selvanarayanan R, Surendran R, Youseef A. 2024b. Early detection of *Colletotrichum kahawae* disease in coffee cherry based on computer vision techniques. *Computer Modeling in Engineering and Sciences* 139 (1): 759–782. <https://doi.org/10.32604/cmcs.2023.044084>
- Xie L, Jing J, Wu H, Kang Q, Zhao Y, Ye D. 2025. MPG-YOLO: Enoki mushroom precision grasping with segmentation and pulse mapping. *Agronomy* 15 (2): 432. <https://doi.org/10.3390/agronomy15020432>
- Yang K, Zhao M, Argyropoulos D. 2025. Machine learning based framework for the detection of mushroom browning using a portable hyperspectral imaging system. *Postharvest Biology and Technology* 219: 113247. <https://doi.org/10.1016/j.postharvbio.2024.113247>
- Ye B, Xue R, Xu H. 2025. ASD-YOLO: A lightweight network for coffee fruit ripening detection in complex scenarios. *Frontiers in Plant Science* 16: 1484784. <https://doi.org/10.3389/fpls.2025.1484784>
- Zhang P, Dai N, Wang Z, Yuan J, Xin Z, Liu X, Papadakis G. 2025. A parallel dual-arm robotic control method of white asparagus based on moving-looking-harvesting coordination and asynchronous harvest cooperation. *Computers and Electronics in Agriculture* 232: 110046. <https://doi.org/10.1016/j.compag.2025.110046>
- Zhao J, Zheng W, Wei Y, Zhao Q, Dong J, Zhang X, Wang M. 2025. Machine vision-based detection of key traits in shiitake mushroom caps. *Frontiers in Plant Science* 16: 1495305. <https://doi.org/10.3389/fpls.2025.1495305>

GEOGRAPHIC INFORMATION SYSTEMS AS KEY TOOLS IN THE PHYTOSANITARY MANAGEMENT OF MEZCAL AGAVE (*Agave angustifolia* Haw) IN THE STATE OF MEXICO, MEXICO

Atenas **Tapia-Rodríguez**¹, José Francisco **Ramírez-Dávila**^{2*}, Agustín David **Acosta-Guadarrama**³, Alfredo **Ruiz-Orta**⁴

¹Tecnológico Nacional de México. Tecnológico de Estudios Superiores de Villa Guerrero. Carretera Toluca-Ixtapan de la Sal km 64.5, La Finca, Villa Guerrero, State of Mexico, Mexico. C. P. 51763.

²Universidad Autónoma del Estado de México. Facultad de Ciencias Agrícolas. Carretera Toluca-Ixtlahuaca km 15, El Cerrillo, Piedras Blancas s/n, entronque a El Cerrillo, Toluca, State of Mexico, Mexico. C. P. 50200.

³Universidad Mexiquense del Bicentenario. Unidad de Estudios Superiores Coatepec Harinas. El Reinoso, Coatepec Harinas, State of Mexico, Mexico. C. P. 51700.

⁴Universidad Autónoma del Estado de México. Centro Universitario UAEM Tenancingo. Carretera Tenancingo-Villa Guerrero km 1.5, Tenancingo de Degollado, State of Mexico, Mexico. C. P. 52400.

* Author for correspondence: jframirez@uaemex.mx

ABSTRACT

Mezcal agave (*Agave angustifolia* Haw.) is a key resource for the economy and culture of the State of Mexico. However, it faces a phytosanitary crisis due to pests such as the agave weevil (*Scyphophorus acupunctatus* Gyllenhaal, 1838) and diseases such as *Fusarium oxysporum* wilt, causing losses of up to 50 % in production. The lack of efficient monitoring systems justifies the development of a Geographic Information System (GIS) to optimize phytosanitary management. This study aimed to design a GIS that integrates biophysical and management variables to identify risk zones and facilitate integrated management strategies. Four plots were monitored in the municipalities of Malinalco and Zumpahuacán in 2024, with 100 plants per plot georeferenced. The incidence of *S. acupunctatus* and *F. oxysporum* was assessed monthly, along with environmental and management variables. Data were processed using QGIS 3.24, generating risk maps through interpolation (Inverse Distance Weighted (IDW) and Kriging) and spatial correlation analysis (Moran's I). Statistical analyses included analysis of variance (ANOVA) and multiple regression. The results demonstrated that GIS-generated risk maps allow highly accurate identification of infestation hotspots. In Malinalco Centro, weevil incidence was positively correlated with accumulated precipitation ($r = 0.65$, $p < 0.05$) and clay soils, exhibiting a spatial aggregation pattern (Moran's $I = 0.42$, $p < 0.01$). For *F. oxysporum*, soil moisture (>60 %) was the most influential factor ($\beta = 0.62$; $p = 0.002$), with critical zones expanding radially at 15 m per month. The Random Forest model predicted weevil incidence with 88.2 % accuracy (AUC-ROC = 0.91). This integrated approach, replicable in other agave-growing regions, would contribute to crop sustainability by enabling spatially targeted interventions, optimizing resources, and reducing input use.

Citation: Tapia-Rodríguez A, Ramírez-Dávila JF, Acosta-Guadarrama AD, Ruiz-Orta A. 2026. Geographic information systems as key tools in the phytosanitary management of mezcal agave (*Agave angustifolia* Haw) in the State of Mexico, Mexico.

Agrociencia 60(3): 412-423. <https://doi.org/10.47163/agrociencia.v60i3.3540>

Editor in Chief:
Dr. Fernando C. Gómez Merino

Received: June 24, 2025.
Approved: April 20, 2026.
Published in Agrociencia:
May 11, 2026.

This work is licensed under a Creative Commons Attribution-Non-Commercial 4.0 International license.



Keywords: *Scyphophorus acupunctatus*, *Fusarium oxysporum*, geospatial analysis, integrated pest management, precision agriculture.

INTRODUCTION

The mezcal agave (*Agave angustifolia* Haw.) is a vital phylogenetic resource for the State of Mexico due to its central role in mezcal production, its contribution to the economic livelihoods of thousands of rural families, and its role in maintaining traditional agroecological systems. However, in recent years, the crop has faced an unprecedented phytosanitary crisis. The combination of factors such as climate change, extensive monoculture, and the lack of integrated management techniques has led to an increase in pests and diseases that threaten the sustainability of its production chain (SENASICA, 2026; IPBES, 2019).

Among the main phytosanitary problems affecting mezcal agave in the region, the pineapple rot complex stands out, associated with pathogens such as *Fusarium oxysporum* and the agave weevil (*Scyphophorus acupunctatus* Gyllenhaal, 1838). These causal agents generate losses ranging from 30 to 50 % of production in critical agricultural cycles (SADER, 2023). The situation is further aggravated by the lack of monitoring and early warning systems that would allow producers to implement timely and effective control measures.

In this context, geotechnology emerges as an innovative alternative for phytosanitary management. Geographic Information Systems (GIS) have proven effective in managing strategic crops worldwide. Studies such as that of Birhan (2023) on coffee cultivation and that of Villegas-Monter *et al.* (2024) on citrus in Veracruz demonstrate how integrating spatial variables (climate, soil, and topography) with biological data can accurately predict the occurrence of disease outbreaks. Specifically for agave, Quezada-Chico *et al.* (2026) conducted a geospatial analysis using remote sensing techniques and field visits to identify changes in land use and the replacement of traditional vegetation. This analysis links soil type with the growth of new plantations, exploring how agave has taken over areas that were once used for local crops.

Despite these advances, a technological gap persists in the State of Mexico regarding geospatial management applied to mezcal agave. The few existing systems are limited to agricultural land registries (SIAP, 2023) and do not incorporate key phytosanitary variables. This limitation hinders both the implementation of effective public policies and the optimization of resources by producers.

This work is based on the hypothesis that developing a specialized GIS that integrates biophysical and phytosanitary information layers through predictive models will allow the identification of epidemiological risk zones in mezcal agave cultivation. This, in turn, can facilitate the implementation of integrated management strategies adapted to the specific conditions of the State of Mexico. The overall objective of the study is to design a GIS for the phytosanitary management of mezcal agave that enables visualization of the spatial distribution of key pests and diseases and serves as a basis for implementing spatially differentiated integrated management.

The relevance of this research extends beyond the academic sphere, as it is framed within critical economic, social, and environmental dimensions for the state. This study aligns with the 2017–2023 State Development Plan, specifically its “Sustainable Rural Development” focus, and directly contributes to Sustainable Development Goals (SDGs) two (Zero Hunger), nine (Industry, Innovation and Infrastructure), and 15 (Life on Land).

MATERIALS AND METHODS

Study area

The study was conducted in the municipalities of Malinalco and Zumpahuacán, located in the State of Mexico. These regions are known for their significant activity in agave cultivation (Secretaría del Campo, 2022). The climatic and edaphic conditions are typical for agave cultivation, with altitudes ranging from 1500 to 2000 m and a semi-warm sub-humid climate (INEGI, 2022; Municipio de Malinalco, 2025).

Experimental design and sampling

Four plots belonging to cooperating producers (two per municipality) were selected using targeted, non-random sampling, prioritizing those with a history of phytosanitary problems. In Malinalco, the selected plots were Malinalco Centro (18° 56' 43.5" N, 99° 29' 38.2" W) and El Caporal (18° 57' 15.8" N, 99° 30' 1.5" W), while in Zumpahuacán, San Gaspar (18° 48' 22" N, 99° 33' 45" W) and La Perla (18° 49' 10.5" N, 99° 34' 20.1" W) were included. Monitoring was conducted throughout 2024 via monthly assessments. In each plot, 100 randomly selected plants were georeferenced using a high-precision GPS (Garmin GPSMAP 64s; error ≤ 3 m) (INEGI, 2022).

Variables evaluated

The incidence of the agave weevil (*S. acupunctatus*) was evaluated by counting the number of affected plants and, in a subsample, determining the number of insects per plant. Symptoms associated with *F. oxysporum* wilt, such as yellowing and leaf collapse, were also observed. The severity of the wilt was assessed using the scale developed by Jiménez-González *et al.* (2017), which rates damage on a scale from 0 to 100 % for each plant.

Additionally, environmental variables were analyzed, including climatic data such as precipitation and temperature obtained from local stations. Soil characteristics, including texture, pH, and electrical conductivity, were determined through laboratory analyses conducted at the Faculty of Agricultural Sciences of the Autonomous University of the State of Mexico. Management variables, including irrigation type and plant density, were also considered.

Data processing and thematic map creation

Data were organized in an Excel matrix and processed using QGIS 3.24. For spatial representation, monthly thematic maps were generated using Inverse Distance Weighted (IDW) interpolation for *S. acupunctatus* and ordinary Kriging for *F. oxysporum*, allowing visualization of incidence and severity. Spatial autocorrelation was assessed using Moran's I index.

For predictive analysis of *S. acupunctatus* incidence, the Random Forest algorithm was applied. The model was trained and validated in RStudio using the caret and randomForest packages. Predictor variables included environmental and management factors. The dataset was split into 70 % for training and 30 % for validation, and model performance was evaluated based on accuracy and the area under the receiver operating characteristic curve (AUC-ROC).

Statistical analysis

Analysis of variance (ANOVA) was used to compare incidence across municipalities and months, followed by Tukey's test ($p \leq 0.05$) using Minitab 21.4. Multiple regression analyses were conducted to evaluate the influence of environmental variables on wilt severity.

RESULTS AND DISCUSSION

Spatiotemporal analysis of the agave weevil (*S. acupunctatus*) and *F. oxysporum* wilt across four plots in Malinalco and Zumpahuacán revealed clear spatial structure in their distribution. Thematic maps generated through GIS-based interpolation (IDW and Kriging) (Appendices 1 and 2) showed pronounced heterogeneity in incidence and severity. When integrated with statistical and predictive modeling, these spatial outputs enabled the detection of aggregation patterns, their associated environmental drivers, and the dynamics of their spread. The interpretation of these patterns is fundamental for transitioning from uniform management to integrated, site-specific crop management.

The mapping of weevil incidence using the Inverse Distance Weighted (IDW) method (Appendix 1) revealed marked heterogeneity both between and within the sampled plots. In the Malinalco Centro plot, the map corresponding to June 2024 clearly shows the formation of "hotspots," or areas of high infestation, with values reaching up to 4.5 insects per plant on average during the peak of the rainy season (June–September). This visual pattern was statistically confirmed by a positive and significant Moran index ($I = 0.42$, $p < 0.01$), indicating an aggregated spatial distribution of the pest. The areas of greatest aggregation were located in zones with steep slopes (>15 %) and clay soils, conditions that, combined with accumulated rainfall greater than 800 mm, generate microhabitats with high soil humidity favorable for the insect's biological cycle.

This spatial behavior is not an isolated finding. Recent studies in the same region, such as that of González-Dávila *et al.* (2024), which used the Spatial Analysis of Distances Index (SADIE) in plots in Malinalco, corroborate the aggregated nature of *S. acupunctatus* populations, reporting aggregation indices (Ia) consistently higher than 1. The agreement between different methodologies (SADIE versus Moran indices and IDW interpolation) applied in the same geographic area lends considerable robustness to this conclusion: the agave weevil is not randomly distributed but instead forms stable foci of infestation in space.

Furthermore, González-Dávila *et al.* (2024) documented the short-term temporal stability of these hotspots, a phenomenon that, while not explicitly quantified in this study, aligns with the observed persistence of hotspots in Malinalco Centro throughout the sampling period. The practical implications are significant: if high-risk areas are spatially predictable and remain stable over time, it becomes both feasible and advisable to prioritize and efficiently direct monitoring and control efforts, such as applying biocontrol agents or removing infected plants, toward these areas. This approach would optimize resource use and minimize environmental impact.

In contrast, the El Caporal plot, also in Malinalco, showed a different spatial pattern. The incidence map (not shown) revealed an early infestation in June, but with more isolated outbreaks and less subsequent dispersal, with fewer than one insect per plant in 75 % of the area. This contrast, made evident through GIS, suggests that local factors such as sandy loam soil (which promotes faster drainage and reduces persistent soil moisture) and management practices such as crop rotation acted as barriers to the spread and establishment of large pest aggregations. In Zumpahuacán, the San Gaspar and La Perla plots showed moderate and dispersed incidence, without the formation of defined “hotspots” in the interpolation maps. The lack of clear aggregation may be associated with lower overall environmental and soil humidity, as well as landscape fragmentation, which could hinder insect mobility and colonization.

The correlation analysis (Table 1) quantified the influence of these factors. Accumulated precipitation showed the strongest positive correlation with weevil incidence ($r = 0.65$,

Table 1. Correlation analysis between environmental variables and the incidence of the agave weevil in Malinalco and Zumpahuacán, State of Mexico.

Environmental variable	Range/data	Correlation coefficient (r)	Significance (p-value)
Accumulated precipitation	>800 mm (vs. <500 mm)	0.65	<0.05
Soil type (clay)	pH 6.5–7.0 (vs. sandy-loam)	0.58	<0.05
Slope	>15 % (vs. <5 %)	0.52	<0.05
Mean temperature	20–25 °C (vs. 15–18 °C)	0.32	>0.05
Altitude	1500–2000 m	-0.41	<0.05
Moran index	0.42 (Spatial aggregation)	-	0.01

$p < 0.05$), followed by clay soil type ($r = 0.58$, $p < 0.05$) and slope ($r = 0.52$, $p < 0.05$). These results reinforce the hypothesis that soil moisture, enhanced by topography and soil texture, is the main epidemiological factor explaining the aggregated distribution of *S. acupunctatus* in the study region.

The application of ordinary Kriging to model the severity of *F. oxysporum* allowed the generation of highly accurate risk maps, such as that for a plot in Zumpahuacán in September 2024 (Appendix 2). This map not only locates diseased plants but also interpolates risk across the spatial continuum, clearly identifying three critical zones or “hotspots” with severity greater than 25 %. The underlying geostatistical analysis (with nugget values = 0.12 and sill values = 0.85) indicated a high degree of spatial structuring of the disease.

By incorporating the temporal dimension, these hotspots expanded radially at a rate of 15 m per month ($R^2 = 0.89$), reflecting a centrifugal expansion pattern typical of soilborne pathogens with limited dispersal mechanisms, such as *Fusarium* spp. The ability of GIS to visualize and quantify this spatiotemporal dynamic is crucial, as it allows anticipation of disease trajectories and the establishment of sanitary barriers or containment zones around hotspots before further expansion.

The robustness of this methodological approach is supported by extensive research in geostatistics applied to phytosanitary problems. Pioneering work by the group at the Autonomous University of the State of Mexico has consistently validated the use of these techniques. For example, Rivera-Martínez *et al.* (2017) used Kriging to model Thysanoptera distribution in avocado, demonstrating that even when the pest is present throughout a plot, density maps allow the identification of areas with higher pressure, enabling targeted control measures and more efficient resource use.

Similarly, Rivera-Martínez *et al.* (2022) applied geostatistics to characterize the spatial behavior of the avocado seed weevil *Copturus aguacatae*, concluding that this approach significantly improves understanding of pest dynamics and, consequently, management strategies. Martínez-Martínez *et al.* (2021) determined the aggregated distribution of *Hemiberlesia lataniae* in ‘Hass’ avocado using density maps and fitted semivariograms to theoretical models (spherical and exponential) to describe spatial structure. The present study on agave aligns with this body of knowledge and extends it to a crop of high economic and cultural importance, demonstrating the replicability and analytical strength of geostatistics for site-specific management of phytosanitary problems.

The multiple regression model (Table 2) identified the factors associated with wilt severity. Soil moisture (>60 %) emerged as the most influential variable ($\beta = 0.62$; $p = 0.002$), followed by a temperature range of 18–22 °C ($\beta = 0.41$; $p = 0.016$) and low values of the Normalized Difference Vegetation Index ($\text{NDVI} < 0.35$; $\beta = -0.55$; $p = 0.001$). The model explained 78 % of the observed variability (adjusted $R^2 = 0.78$). The strong negative correlation with NDVI is particularly revealing, suggesting a negative feedback loop in which plant stress and reduced vigor (reflected by low NDVI values) increase susceptibility to infection, or conversely, that infection itself leads to a rapid

Table 2. Multiple regression model for the severity of *Fusarium oxysporum* in mezcal agave plots.

Variable	Coefficient (β)	<i>p</i> -value	Confidence interval (95 %)
Soil moisture	0.62	0.002	0.51, 0.73
Temperature (°C)	0.41	0.016	0.29, 0.53
NDVI	-0.55	0.001	-0.67, -0.43
Plant density	0.19	0.042	0.05, 0.33

NDVI: Normalized difference vegetation index.

decline in plant vitality. This finding highlights NDVI, a variable readily obtained through remote sensing, as a potential early indicator of epidemiological risk.

The predictive model developed using Random Forest for the incidence of *S. acupunctatus* showed excellent predictive capacity, with an overall accuracy of 88.2 % and AUC-ROC of 0.91, indicating strong discrimination between the presence and absence of the pest. A novel and particularly interesting finding was the high relative importance of soil electrical conductivity (EC), which contributed 23 % to the model's accuracy. This factor has been little explored in the ecology of the agave weevil. High EC may be associated with greater concentrations of salts and nutrients, potentially influencing plant physiology and making plants more attractive or susceptible to insect attack. Alternatively, it may act as an indicator of higher soil moisture or compaction. The model-derived hypothesis opens a new and relevant line of research that targeted studies should further explore.

However, the model also revealed an important limitation, as its accuracy decreased markedly in areas with steep slopes (>25 %), with a corresponding increase in root mean square error (RMSE = 4.7). This reduction in performance is attributable to topographic shadowing and geometric distortion affecting satellite imagery in rugged terrain, a problem well documented in the literature (Matese and di Gennaro, 2015). While this limitation does not invalidate the model, it calls for caution when applying it under complex topographic conditions and points to a clear avenue for improvement. The integration of complementary technologies, such as unmanned aerial vehicles (drones) equipped with multispectral sensors, would enable low-altitude data acquisition, minimizing shadow effects and providing higher spatial and spectral resolution, thereby improving predictive accuracy in these areas.

Taken together, the results demonstrate that GIS is not merely a visualization tool but a robust analytical platform capable of quantifying the spatial heterogeneity of phytosanitary problems (Tapia-Rodríguez *et al.*, 2025). The maps serve as central evidence to guide decision-making, supporting a transition from uniform and indiscriminate management to site-specific strategies. Interventions such as the application of biocontrol agents, including *Trichoderma harzianum*, whose effectiveness against *Fusarium* has been reported at up to 83 % in tequila agave by Silva *et al.* (2022), as

well as improved drainage in clay soils or irrigation adjustments, can be concentrated in identified “hotspots” and their surrounding areas. This approach not only increases control effectiveness, as observed in Malinalco Centro with a 60 % reduction in weevil incidence following targeted interventions, but also reduces the use of chemical and biological inputs, contributing to both economic and environmental sustainability. The persistence of low levels of pests and disease even after intervention indicates that management must be continuous, preventive, and genuinely integrated. As noted by Martínez-Martínez *et al.* (2021), understanding spatial distribution is only the first step and must be followed by the development of integrated management programs combining targeted biological control with cultural practices at both plot and landscape scales. These include drainage management, agroecosystem diversification, the use of trap plants, and continuous training for producers. Community participation in monitoring, supported by the interpretation of simplified risk maps, represents a critical step for scaling up this approach and ensuring its long-term adoption, thereby strengthening the sustainability of the mezcal agave production chain under increasing climate and phytosanitary pressures.

CONCLUSIONS

The distribution of weevil (*Scyphophorus acupunctatus*) and the incidence of *Fusarium oxysporum* wilt in mezcal agave in the State of Mexico were determined by a specific combination of soil and climatic factors and management practices, with soil moisture standing out as the main epidemiological driver. The risk maps allowed visualization and quantification of the spatial aggregation of these problems, identifying hotspots with high precision. This capacity for spatial localization is fundamental to designing and implementing spatially differentiated integrated management strategies, optimizing resource use and increasing control effectiveness. Predictive models such as Random Forest offer considerable potential for anticipating risk zones, although their accuracy may be constrained under complex topographic conditions. The identification of soil electrical conductivity as a relevant variable in weevil modeling opens new perspectives for research on the mechanisms underlying infestation. The implementation of artificial drainage practices in clay soils is recommended to reduce soil moisture, along with irrigation adjustments based on the spatial risk of wilt. Future research should incorporate continuous monitoring through sensors and information and communication technologies, as well as metagenomic analyses to improve early pathogen detection. In addition, integrating socioeconomic variables into predictive models will enable the development of adaptive strategies that combine local knowledge with technological innovation, thereby strengthening the sustainability of mezcal agave cultivation.

ACKNOWLEDGEMENTS

We thank the Mexican Council of Science and Technology (COMECYT) for the valuable support and encouragement given through the Programa Investigadoras e Investigadores COMECYT-EDOMEX 2025.

REFERENCES

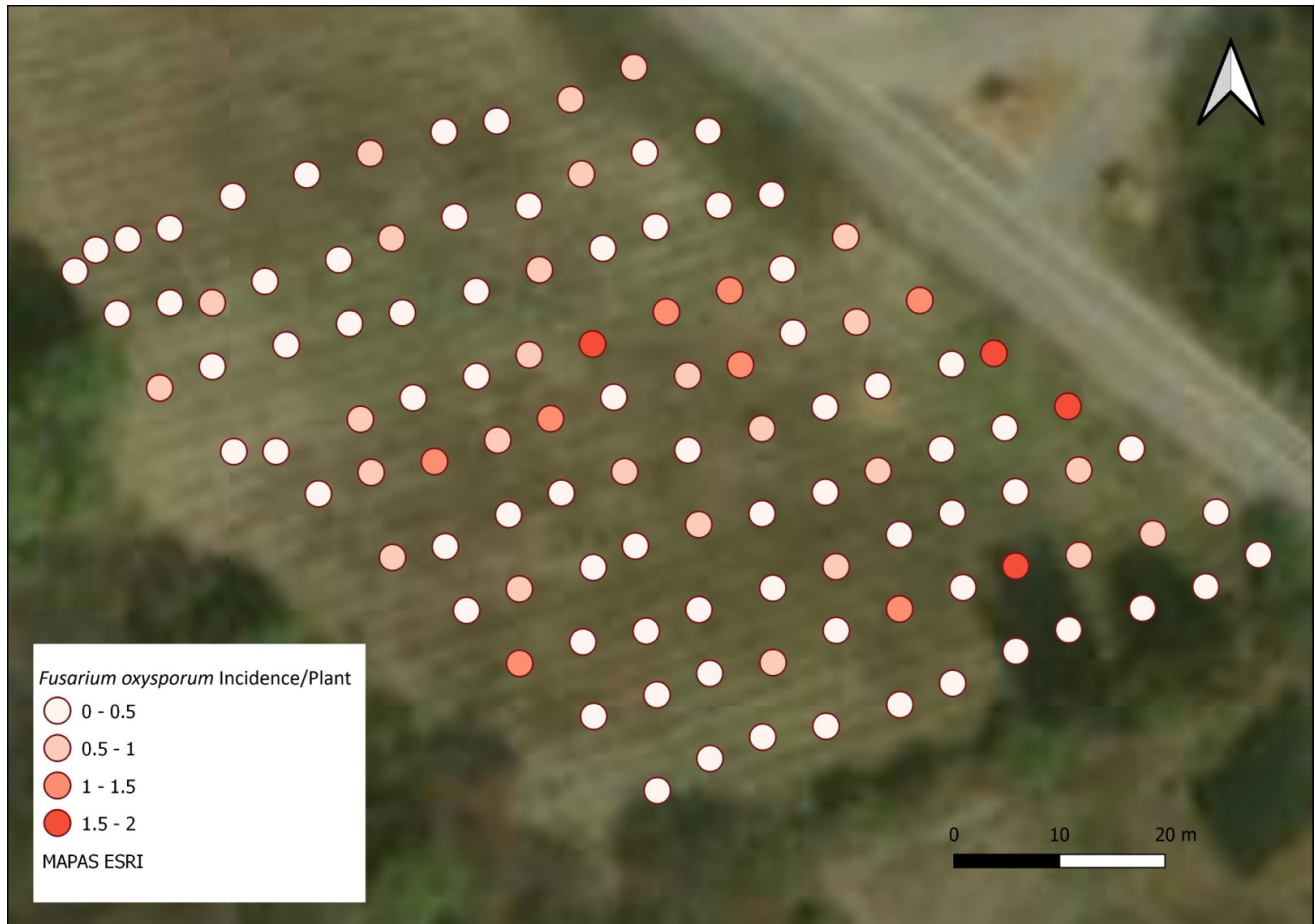
- Birhan M. 2023. A case study of the management information system in the coffee industry in SW Ethiopia. *Qeios*. <https://doi.org/10.32388/TIWVE7>
- González-Dávila A, Ramírez-Dávila JF, Acosta-Guadarrama AD, Figueroa-Figueroa DK. 2024. Study by spatial distance index analysis of the agave weevil *Scyphophorus acupunctatus* Ghynlled in the State of Mexico. *Southwestern Entomologist* 49 (4): 1528–1548. <https://doi.org/10.3958/059.049.0411>
- INEGI (Instituto Nacional de Estadística y Geografía). 2022. Anuario estadístico y geográfico por entidad federativa 2022. Ciudad de México, México. <https://www.inegi.org.mx/app/biblioteca/ficha.html?upc=889463910534> (Retrieved: March 2026).
- IPBES (Intergovernmental Science-Policy Platform on Biodiversity and Ecosystem Services). 2019. Global assessment report on biodiversity and ecosystem services of the Intergovernmental Science-Policy Platform on Biodiversity and Ecosystem Services. Zenodo. <https://doi.org/10.5281/zenodo.3831673>
- Jiménez-González LR, Mendoza-Ramos C, Santana-Peñaloza B, Coria-Contreras JJ, Delgado-Mora F, Acevedo-Sánchez G, Guzmán-Hernandez E, Mora-Aguilera G. 2017. Escala logarítmica diagramática de severidad para medición de pudrición seca del cogollo, marchitez y mancha gris del agave azul. *Revista Mexicana de Fitopatología* 35 (S): 177.
- Martínez-Martínez N, Ramírez-Dávila JF, Mejía-Carranza J, Vera-Noguez S. 2021. Spatial behaviour of *Hemiberlesia lataniae* (Signoret) on 'Hass' avocado in Estado de Mexico. *Ingeniería Agrícola y Biosistemas* 13 (1): 33–52. <https://doi.org/10.5154/r.inagbi.2021.01.005>
- Matese A, di Gennaro SF. 2015. Technology in precision viticulture: A state of the art review. *International Journal of Wine Research* 7: 69–81. <https://doi.org/10.2147/ijwr.s69405>
- Municipio de Malinalco. 2025. Medio físico. Administración 2025-2027. Malinalco, México. <https://www.malinalco.gob.mx/municipio/medio-fisico/> (Retrieved: March 2026).
- Quezada-Chico G, Vargas-Inclán M, Acevedo-Rosas R, Cuevas-Elicerío JM, Izquierdo-Saguilan AP. 2026. Análisis espacial del agave, condiciones edáficas y desplazamiento de cultivos tradicionales en la Región Centro de Jalisco. *Geografía Aplicada* 2 (1): 174–199. <https://doi.org/10.36677/geografiaaplicada.v2i1.27558>
- Rivera-Martínez R, Ramírez-Dávila JF, Rubí-Arriaga M, Domínguez-López A, Acosta-Guadarrama AD, Figueroa-Figueroa DK. 2017. Spatial modeling thrips (Insecta: Thysanoptera) in growing avocado (*Persea americana*). *Revista Colombiana de Entomología* 43 (2): 131–140.
- Rivera-Martínez R, Tapia-Rodríguez A, Figueroa-Figueroa DK, Ruiz-Orta A, Ramírez-Dávila JF. 2022. Spatial distribution of *Copturus aguacatae* in avocado plantations in central Mexico. *Ingeniería Agrícola y Biosistemas* 14 (2): 19–32. <https://doi.org/10.5154/r.inagbi.2022.05.035>
- SADER (Secretaría de Agricultura y Desarrollo Rural). 2023. Informe anual 2023: Manejo fitosanitario en cultivos básicos. Gobierno de México. Secretaría de Agricultura y Desarrollo Rural. Servicio Nacional de Sanidad, Inocuidad y Calidad Agroalimentaria. Ciudad de México, México. 7 p.

- Secretaría del Campo. 2022. En 15 municipios del EdoMéx se cultiva agave mezcalero. Gobierno del Estado de México. Toluca, México. <https://elvalle.com.mx/2022/02/25/en-15-municipios-del-edomex-se-cultiva-agave-mezcalero/> (Retrieved: March 2026).
- SENASICA (Servicio Nacional de Sanidad, Inocuidad y Calidad Agroalimentaria). 2016. Ficha técnica del picudo del agave *Scyphophorus acupunctatus* Gyllenhal. Secretaría de Agricultura, Ganadería, Desarrollo Rural, Pesca y Alimentación. Servicio Nacional de Sanidad, Inocuidad y Calidad Agroalimentaria. Tecámac, México. 16 p.
- SIAP (Sistema de Información Agroalimentaria y Pesquera). 2023. Cierre de la producción agrícola 2023. Gobierno de México. Sistema de Información Agroalimentaria y Pesquera. Ciudad de México, México. https://nube.agricultura.gob.mx/cierre_agricola/ (Retrieved: March 2026).
- Silva LG, Camargo RC, Mascarín GM, Nunes PSO, Dunlap C, Bettiol W. 2022 Dual functionality of *Trichoderma*: Biocontrol of *Sclerotinia sclerotiorum* and biostimulant of cotton plants. *Frontiers in Plant Science* 13: 983127. <https://doi.org/10.3389/fpls.2022.983127>
- Tapia-Rodríguez A, Ramírez-Dávila JF, Acosta-Guadarrama AD. 2025. Plagas y enfermedades del agave mezcalero: una visión geoespacial con el uso de los SIG. *Enfoque Rural* 3 (2).
- Villegas-Monter A, Alarcon-Zuniga B and Contreras-Maya R. 2024. Diagnosis and distribution of Citrus tristeza virus in northern Veracruz, Mexico. *Agro Productividad*. <https://doi.org/10.32854/agrop.v17i5.2706>

Agrociencia



Appendix 1. Thematic map of the incidence of *Scyphophorus acupunctatus* in Malinalco, State of Mexico, in June 2024 (prepared by Inverse Distance Weighted (IDW) interpolation in QGIS 3.24).



Appendix 2. Thematic map of the incidence of *Fusarium oxysporum* in Zumpahuacan, State of Mexico during September 2024 (prepared by ordinary Kriging in QGIS 3.24).

INFLUENCE OF HEALTH ON THE WORK PERFORMANCE OF RASPBERRY PICKERS: A PILOT STUDY

Alejandra **García-Becerra**¹, María Guadalupe **Sánchez-Cervantes**¹,
Nancy María **Aguilar-Hernández**¹, Silvia Rosario **Villa-Ramos**¹, José Abel **Chocoteco-Campos**^{1*}

¹Tecnológico Nacional de México. Instituto Tecnológico de Ciudad Guzmán. Avenida Tecnológico 100, Colonia Centro, Ciudad Guzmán, Jalisco, Mexico. C. P. 49000.

* Author for correspondence: jose.cc1@cdguzman.tecnm.mx

ABSTRACT

Raspberry pickers are a specific group of agricultural workers whose labor conditions have received limited attention in research. Their working conditions, the health problems they face, and the factors affecting their performance remain scarcely explored. The aim of this pilot study was to analyze the relationship between farmworkers' self-perceived health status and their work performance, measured by the number of buckets harvested and the income derived from piece-rate work. Data were collected through a daily self-evaluation survey administered to a group of pickers over 53 harvest days. Workers' perceived health status was recorded at the beginning, during, and at the end of each workday, along with the number of buckets harvested per day. Simple correlation analysis yielded an *r* coefficient of 0.66, corresponding to a determination coefficient (R^2) of 0.44, indicating a moderate relationship between self-perceived health status and work performance. The results showed that poorer self-perceived health status was associated with a 21 % reduction in the number of buckets harvested relative to the group average. This reduction led to income differences of up to 35 % between the most and least productive pickers. These findings highlight the impact of health on both productivity and income among these workers. For future research, studies with larger samples and models incorporating additional factors are recommended to further clarify the relationship between health and productivity in this type of work.

Keywords: health condition, work performance, berry pickers, southern Jalisco.

INTRODUCTION

In 2023, Mexico's economically active population consisted of 60.8 million people (INEGI, 2023a), of which only 22.2 million were enrolled in the Mexican Institute of Social Security (IMSS). Within this group, at least 10 million people suffer from a chronic disease (IMSS, 2022). This situation places Mexico among the 10 countries with the greatest number of working-age people with chronic diseases, such as obesity and diabetes (Lin *et al.*, 2020).

Since the beginning of this century, various studies have shown that workers' health affects their performance, particularly among those with chronic diseases (Grossman,

Citation: García-Becerra A, Sánchez-Cervantes MG, Aguilar-Hernández NM, Villa-Ramos SR, Chocoteco-Campos JA. 2026. Influence of health on the work performance of raspberry pickers: A pilot study. *Agrociencia* 60(3): 424-438. <https://doi.org/10.47163/agrociencia.v60i3.3347>

Editor in Chief:
Dr. Fernando C. Gómez Merino

Received: November 10, 2025.

Approved: April 22, 2026.

Published in Agrociencia:

April 29, 2026.

This work is licensed under a Creative Commons Attribution-Non-Commercial 4.0 International license.



2000; Tompa, 2002; Berger *et al.*, 2003; Mattke *et al.*, 2007; Loeppke *et al.*, 2009). Nevertheless, Munir *et al.* (2005) and Siu *et al.* (2013) suggest that workers with chronic diseases are not always less productive. In some cases, their performance can match or even surpass that of healthy workers due to self-management of the disease through the adaptation of coping routines and strategies.

Despite this evidence, there remains a significant gap in research on the health of agricultural day laborers, particularly in Mexico, where these workers face precarious conditions, low wages, and limited social protection (Barrón-Pérez, 2019; Flores-Mariscal, 2021; Aguilar-Cuevas and Colín-Martínez, 2022; Salgado-Viveros, 2023). Harvesting fruits and vegetables involves long working hours under demanding conditions, increasing health risks due to high temperatures and exposure to agrochemicals, as documented in studies conducted in Mexico (Palacios-Nava, 2003; Ortega-Martínez *et al.*, 2019; Day *et al.*, 2021) and in other countries (Cayir *et al.*, 2019). In addition, little is known about berry pickers working in greenhouses, who perform their activities in enclosed spaces under high temperatures.

The number of agricultural day laborers in Mexico has increased significantly in recent years, especially in states such as Baja California, Sonora, Sinaloa, Jalisco, and Michoacán (Barrón-Pérez and Ortiz-Marín, 2022). Much of this growth has been driven by migrants from Oaxaca, Guerrero, Veracruz, and Chiapas seeking opportunities in the agricultural sector. It is estimated that more than 2 million day laborers work in the country's farmlands, of which 12.7 % of them are women. When their families are included, this population reaches approximately 8.5 million people (UN Women, 2022).

In Jalisco, the increase of day laborers is linked to the establishment of national and transnational agro-industrial companies in the southern region of the state, where climate and soil conditions are favorable for crops such as berries and avocado (Macías-Macías and Sevilla-García, 2022). According to the 2022 Agricultural Census, 189 324 agricultural production units were recorded in Jalisco, along with an agricultural surface of 2 127 242 ha. These figures reflect the importance of the sector in the state, which has shown a tendency toward technification through systems such as protected agriculture (INEGI, 2023b). This trend is particularly evident in Zapotlán El Grande, where the marked increase in enclosed greenhouses between 2007 and 2022 illustrates agricultural expansion and modernization.

Despite economic development in the region (Lagunes-Fortiz *et al.*, 2020; Cruz-López *et al.*, 2022; Macías-Macías and Sevilla-García, 2022), working conditions for agricultural laborers, particularly those harvesting berries in enclosed greenhouses, are characterized by exposure to high temperatures, increasing the risk of heat stroke, dehydration, and other health issues. This is compounded by exposure to agrochemicals, whose effects may be intensified under high-temperature conditions, further increasing health risks.

Previous studies have identified risk factors in the working conditions of Mexican day laborers, including exposure to toxic chemical products (Palacios-Nava,

2003; Haro-Encinas, 2007; Ortega-Martínez *et al.*, 2019; Alvarado-Ibarra *et al.*, 2019; Sánchez-Gervacio *et al.*, 2020) and limited access to medical services (Aranda and Castro-Vázquez, 2016; Escobar-Latapí *et al.*, 2019; Arellano-Gálvez *et al.*, 2023). These conditions increase worker vulnerability, as they often must cover their own medical expenses due to the lack of employment benefits that include specialized care.

The relationship between health and productivity among agricultural workers has received limited attention in the scientific literature. Some studies have examined how high temperatures affect the physical health of day laborers working outdoors and their impact on productivity (Sahu *et al.*, 2013; Amini *et al.*, 2021; Castillo *et al.*, 2021; Pan *et al.*, 2021). However, no specific studies have been identified, either in Mexico or internationally, focusing on berry pickers working in greenhouses.

This study seeks to document the self-perceived health status of a group of raspberry pickers during their workday and to analyze how it influences their performance and income. The hypothesis is that, in raspberry harvesting under protected agriculture in southern Jalisco, workers who report a poorer self-perception of their health status show, on average, lower work performance compared to those with better perceived health conditions.

MATERIALS AND METHODS

The study was conducted in an agro-industrial company dedicated to raspberry (*Rubus idaeus* L.) production under protected agriculture, located in the town of Usmajac, municipality of Sayula, in the southern region of Jalisco, Mexico, during the first harvest season of the year, between March and May 2024. The area is characterized by a growing concentration of greenhouses and a high demand for day-laborer workforce. The work dynamic is based on daily harvesting shifts under a piece-rate payment scheme, in which workers' income depends directly on the harvested volume. Participants were seasonal agricultural laborers with limited access to social security services, a situation commonly observed in this type of production system.

The selected greenhouses consisted of roofed polyethylene macro-tunnels. At the time of the study, the plants were two years old and produced fruit continuously throughout the 53-day harvesting period. A non-probabilistic convenience sampling approach was used, selecting a crew of 10 raspberry pickers (five men and five women), aged 25 to 49 years, with varying levels of experience with the crop. Monitoring initially began with a larger group; however, due to the high turnover typical of temporary agricultural employment, only 10 individuals completed the 53 consecutive days of records. This sample represents 25 % of the total workforce (40 workers) in the greenhouse, which is adequate for a longitudinal exploratory study.

Given the nature of the design, priority was given to the depth of temporal monitoring rather than sample size. Continuous recording over 53 days allowed the generation of a database of 530 observations, constituting a robust time series per individual. This approach minimizes bias from isolated measurements and enables observation of

performance variability in relation to fluctuations in health conditions, providing the statistical rigor required for correlation analysis at a microergonomic level.

Participants worked from Monday to Saturday in shifts from 07:30 to 16:00, with the possibility of overtime depending on demand. The relevance of analyzing this group lies in the regional context of Usmajac and southern Jalisco, which concentrates one of the highest densities of economic units dedicated to greenhouse red fruit production. This sector represents a key source of employment that requires specific studies on worker health and productivity (INEGI, 2024).

A simple correlation model was used to evaluate the relationship between health condition, measured through perceptual self-evaluation, and worker performance. The analysis was based on Pearson’s correlation coefficient (r), with perceived health condition as the independent variable and daily productivity, measured by the number of buckets harvested, as the dependent variable, which may be influenced by factors such as the piece-rate payment scheme and worker experience.

At the beginning of the study, sociodemographic information was collected through individual, face-to-face interviews, recording variables such as sex, age, and years of experience in berry harvesting. Additionally, a section was included to identify chronic diseases or specific physical and mental health conditions (Table 1). Information on diseases was obtained from workers’ self-reports.

It is recognized that some participants may not know the formal diagnosis of their health condition or may be unaware of undiagnosed conditions due to limited access to healthcare services. For this reason, the analysis is based on perceived health status rather than clinical diagnoses. It is important to note that, due to the commitment to anonymity, the high labor mobility in the sector, and the need to avoid any perception of harassment toward workers, only self-perception scales and self-reports were used instead of official clinical or institutional medical records.

A self-evaluation questionnaire was designed to measure perceived health status at the beginning, during, and at the end of each shift, using a numerical scale from 1 to

Table 1. Sociodemographic and self-reported health conditions questionnaire administered during personal interviews.

Worker number: ____ Sex: M F Age: ____ Experience (in years): ____

Please indicate the diseases you have:

Allergies	High cholesterol	Glaucoma	Thyroid problems
Anemia	Colitis	Hypertension	Cysts in ovaries
Anxiety	Convulsions	Incontinence	Migraine
Arthritis	Diabetes	Insomnia	Prostate disorder
Asthma	Depression	Kidney failure	Skin disorder
Bronchitis	Emphysema	Obesity	Mammary disorder
Cancer	Endometriosis	Hearing loss	Psychological disorder
Cataracts	Fibromyalgia	Kidney stones	Ulcers/reflux
Blood clots	Gastritis	Heart problems	Other(s): _____

10 (1 = worst condition, 10 = best condition) (Table 2). Each day, workers recorded the total number of buckets harvested on a form pre-filled with their identification number and the date. A short questionnaire format was selected to minimize disruption to participants' daily activities. The use of a longer instrument, such as those applied in the National Health and Nutrition Survey (ENSANUT), would have been impractical for daily use, as it could have reduced engagement and affected response quality. Physical exhaustion accumulated at the end of the workday may influence perceived health status, making it difficult to distinguish between the effects of pre-existing conditions and fatigue derived from the work shift. This aspect is considered an inherent limitation of the study design.

Table 2. Daily self-assessment form for perceived health status and productivity in raspberry pickers.

Worker: _____ Date: _____

On a scale of 1 to 10, 1 being the worst and 10 being the best, mark your answer with an "x" in each section.

Question	Moment	1	2	3	4	5	6	7	8	9	10
How would you rate your health condition in the three moments of your shift?	At the start During the shift At the end										
How many buckets did you harvest today?											

The study was conducted in accordance with ethical research principles, ensuring that all participants provided informed consent. The confidentiality of the information was protected through the use of anonymous identifiers and secure data handling. In addition, workers received a simple explanation of the study's purpose and of the concept of health status in terms they could easily understand, ensuring clarity in their responses: "When we speak of health status or health condition, we mean how you feel physically and mentally to do your work, whether you have energy, if you feel well, or if something is bothering you, such as a headache, fatigue, or discomfort. We want to know if, when you start, continue, or finish your shift, you notice any difference in how your body feels and how that may affect the number of buckets you are able to harvest."

This approach promoted active and honest participation without requiring technical knowledge of health. The administration and supervision of the questionnaire were carried out by one of the authors during her professional residency in the greenhouse, which made it possible to build trust with participants, address questions immediately, and ensure consistency in data collection. The questionnaire was administered daily over a period of 53 harvest days, exclusively on days when the full crew was present

and reported no symptoms of acute illness, such as flu, diarrhea, or physical injuries. Days with such incidents were recorded and excluded from the statistical analysis. Workers' shifts began at 07:30, when they collected their equipment, consisting of buckets and belts. At 08:00, they entered the assigned tunnels to begin harvesting, maintaining the same assignments throughout the season. At 10:00, they paused for breakfast and then continued working until 16:00, when they finished their shift and returned their equipment to the packing area. The number of buckets harvested each day was recorded and verified at the end of the workday, as workers' income depended directly on the number of buckets delivered. Although regular working hours were from 07:30 to 16:00, shifts often extended depending on production demand, with the option of overtime. This study considered only the buckets harvested during regular hours.

The daily thermal progression in Usmajac emerged as a determining environmental factor in this study. Weather conditions reached levels classified as "very hot" after 14:00 (Figure 1), which, together with the microclimate generated by polyethylene macro-tunnels, represented a physiological challenge for berry pickers. This temperature increase and the accumulation of thermal stress not only reduce the metabolic efficiency required to maintain piece-rate work but may also influence the self-perception of health status.

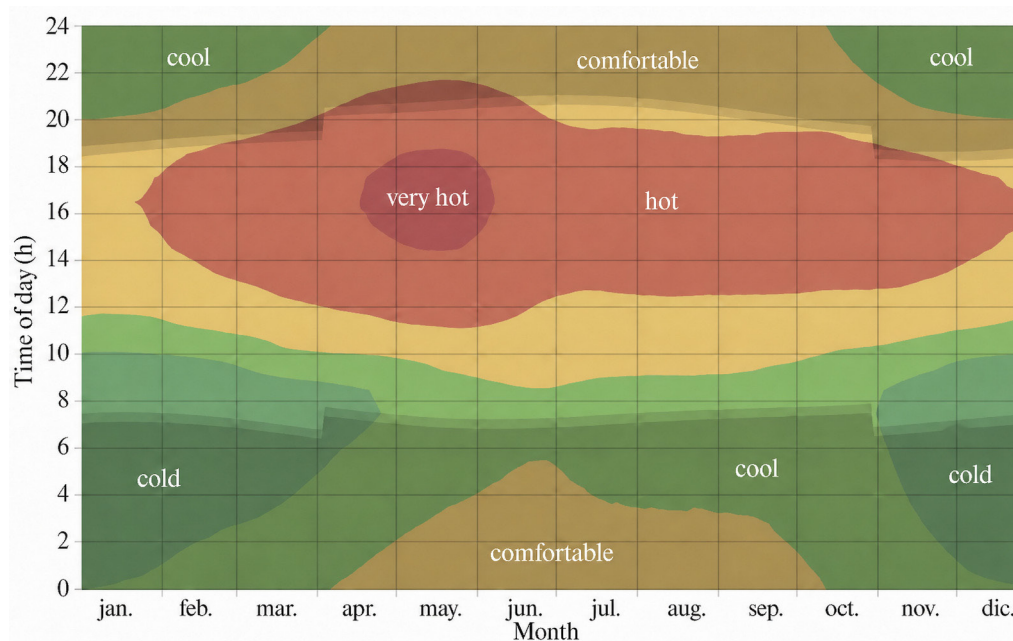


Figure 1. Average annual temperature per hour in Usmajac, in the south of the state of Jalisco, Mexico (Weather Spark, 2026).

In this context, it is likely that symptoms reported by workers, such as migraine and irritable bowel syndrome (IBS), are aggravated by mild dehydration or thermal fatigue resulting from prolonged heat exposure. Work performance in the berry sector is therefore not an isolated variable, but the outcome of a complex interaction between workers' chronic health conditions and the extreme microclimatic conditions of the agricultural environment.

The study design made it possible to capture workers' daily health status without interfering with their activities, which were carried out under continuous workday conditions, with only one break for eating and hydration. This break occurred individually and voluntarily during the course of the work, without structured interruptions, ensuring that evaluations remained consistent throughout the 53-day period.

RESULTS AND DISCUSSION

The personal information of the participating workers (Table 3) reflects that the majority has at least one chronic disease, with an average of 1.7 diseases per person. The most common conditions were migraine, overweight, diabetes, colitis, hypertension, and anxiety. Overweight, diabetes, and hypertension are consistent with the most common conditions confirmed in Mexican workers (IMSS, 2022).

Table 3. Sociodemographic profile, work experience, and self-reported health conditions of participating workers.

Worker	Sex	Age (years)	Experience (years)	Diseases suffered
T1	F	32	12	Anxiety, diabetes, and overweight
T2	M	39	5	Diabetes and hypertension
T3	F	44	12	Depression
T4	F	49	10	Migraine
T5	M	34	8	Irritable bowel syndrome and overweight
T6	M	45	25	Hypertension and migraine
T7	F	26	3	Migraine
T8	M	25	5	Bronchitis
T9	F	27	6	Anxiety, colitis, and overweight
T10	M	27	5	None

The average perceived health status reported by workers was calculated for each moment of the shift over the 53 days of the study (Figure 2). This metric reflects the variability of perceptions recorded at three key moments of the work shift: at the beginning (08:00–10:00), during the shift (10:00–14:00), and at the end (14:00–16:00). This dispersion analysis is crucial for assessing the consistency of individual reports

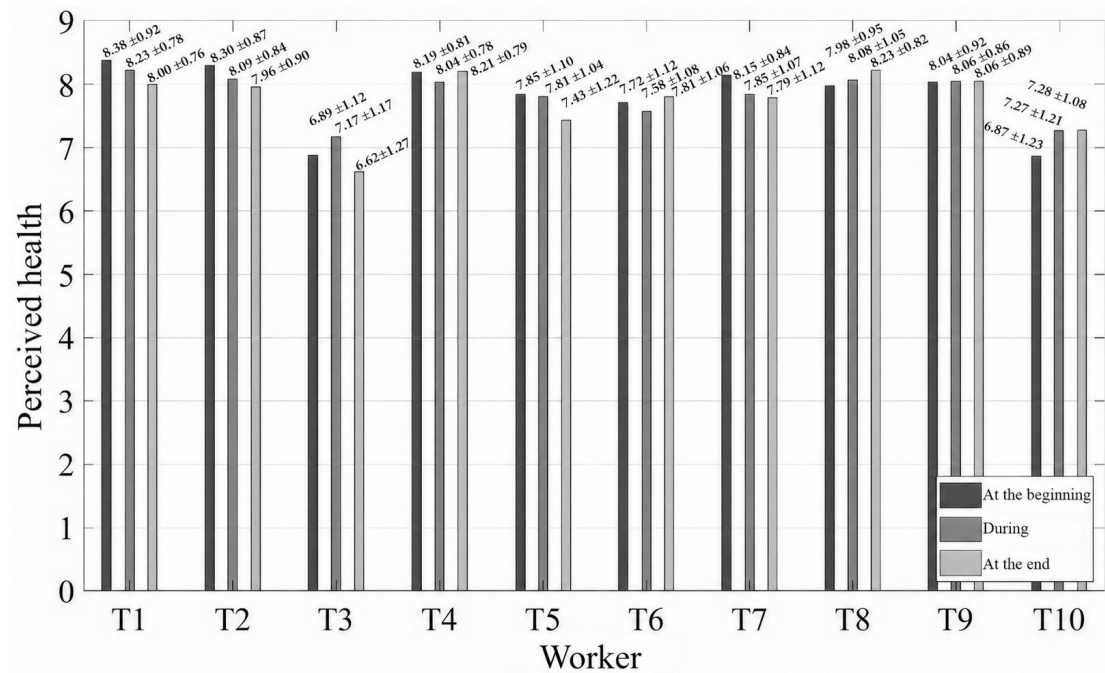


Figure 2. Average perceived health status, reported by workers on a scale of 1 to 10, during three periods of the shift. This data is calculated from the average over the 53 days of the study, which took place during a shift from 08:00 to 16:00.

in relation to environmental conditions and changing thermal stress throughout the sampling period. Half of the workers rated their health status slightly above level 8 (on a 1–10 scale).

Variability between moments of the day was minimal (below 0.5); however, variability between workers was evident, particularly in T3 and T10, who reported averages around 7.0. Worker T3 reported depression. Workers T1, T2, T3, T5, and T7 reported a slight decline in health status as the day progressed. This reduction may be related to fatigue and increasing greenhouse temperatures, effects supported by previous studies under field conditions (Sahu *et al.*, 2013; Amini *et al.*, 2021; Castillo *et al.*, 2021; Pan *et al.*, 2021). The health status of two workers (T4 and T9) remained stable, while in three workers (T6, T8, and T10) it improved during the shift. All workers whose health remained unchanged or declined reported at least one chronic condition, in contrast to T10, whose health improved and who reported no disease.

Regarding productivity (Figure 3), the average number of buckets harvested per worker was calculated over the 53 days of monitoring. A general variability of 40.04 buckets was recorded in daily performance, allowing quantification of fluctuations in individual output and operational consistency under work demands. Despite their health conditions, workers T1, T4, T8, and T9 harvested the highest number

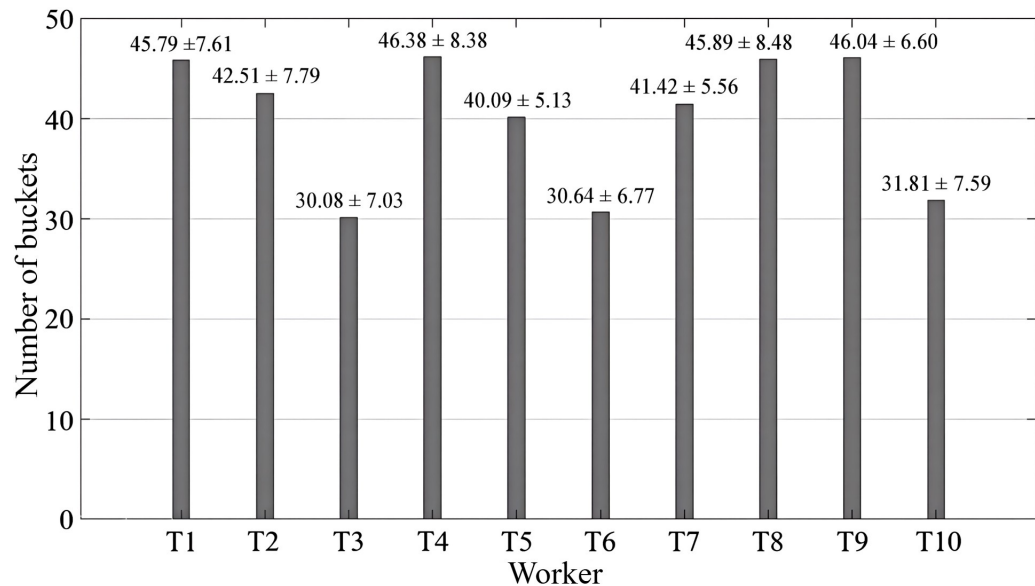


Figure 3. Average daily productivity, measured as the number of buckets harvested per worker during the 53 days of monitoring.

of buckets. T1 and T9, both women, reported three chronic conditions each. This supports observations by Munir *et al.* (2005) and Siu *et al.* (2013), suggesting that workers with health conditions can be as productive as, or more productive than, the average, highlighting the role of self-management. However, the higher performance observed among female workers may also reflect sex-related differences, which were not independently analyzed in this study.

In contrast, workers T3, T6, and T10 harvested fewer buckets than average. T3 and T6 were the oldest and most experienced workers, both reporting at least one chronic condition. T10, one of the youngest (27 years old), had relatively low experience (5 years) and reported no chronic disease. This disparity should not be attributed to attitudinal factors; rather, it suggests the influence of unmeasured variables, such as limited technical dexterity due to experience level or strategies for self-regulation of physical effort under prevailing environmental conditions. This highlights the importance of considering physiological factors and technical expertise before drawing conclusions about individual performance.

The relationship between self-perceived health status and the number of buckets harvested (Figure 4) yielded a correlation coefficient (r) of 0.66, indicating a moderate positive association between the variables. In general, workers reporting better health tended to harvest more buckets. Workers T3 and T4 represented contrasting cases of performance. Both were women of similar age and experience in berry harvesting. Worker T3, with an average of 30.08 buckets, showed lower productivity, whereas

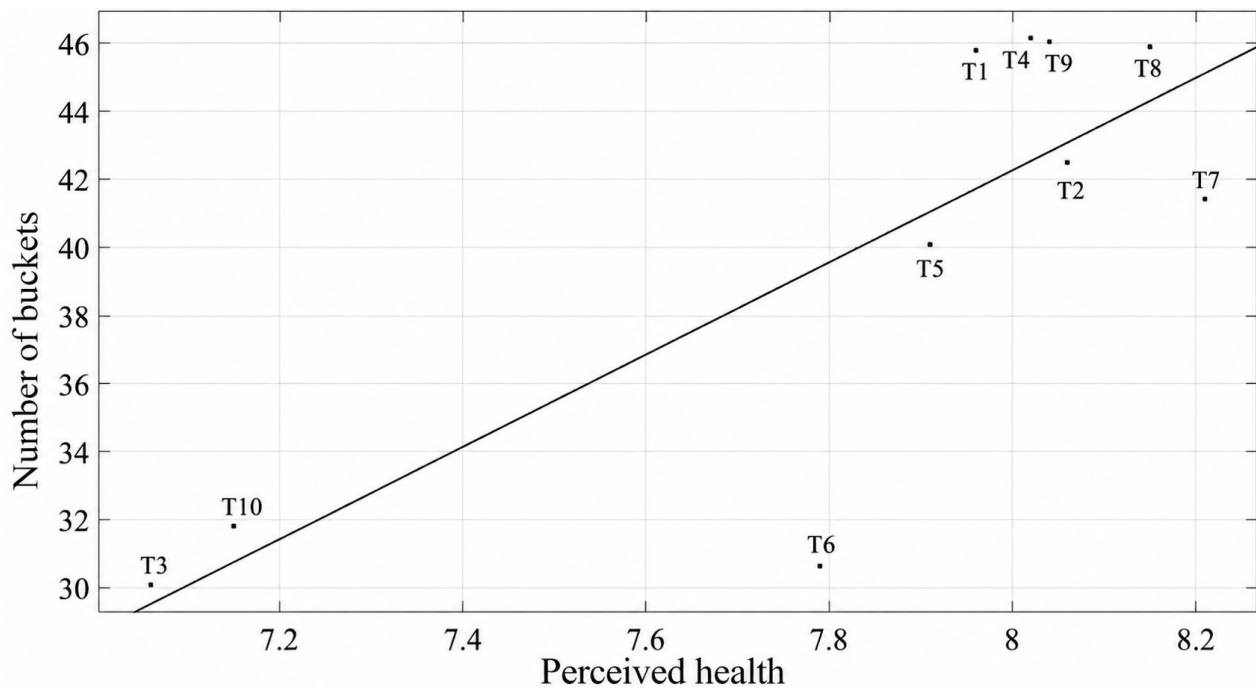


Figure 4. Correlation between the health condition of the workers and the buckets gathered during their workday.

T4 achieved higher performance with an average of 46.15 buckets. This contrast highlights the influence of the type of condition (depression in T3 versus migraine in T4) and health status (7.15 vs. 8.02) on productivity.

The visual comparison of individual harvesting performance during the study period (Figure 5) shows a clear difference between the seven most productive and the three least productive workers. This performance gap reflects the influence of physical well-being on productivity, particularly in physically demanding activities such as raspberry harvesting. The reduction in the number of buckets harvested over time is explained by the nature of the crop, as raspberries are harvested daily (except Sundays), leading to a gradual decrease in available fruit as the season progresses. During the study period, each bucket harvested in a regular shift was paid at MXN 18. Worker T3 earned a total of MXN 28 696.6, while T4 earned MXN 44 027.1, representing a difference of 34.82 %, excluding additional company benefits. Compared to the average, wage reductions for T3, T6, and T10 ranged from 20 % to 22 %, exceeding the 4–6 % reported by Castillo *et al.* (2021) for fruit pickers and the 5–10 % estimated by Levasseur (2019) for workers in other piece-rate sectors.

In terms of age and years of experience in berry harvesting (Figure 6), no significant relationship was found with the number of buckets harvested. The highest correlation value obtained ($r = 0.23$) confirms that age and experience did not have a relevant influence on productivity in this context.

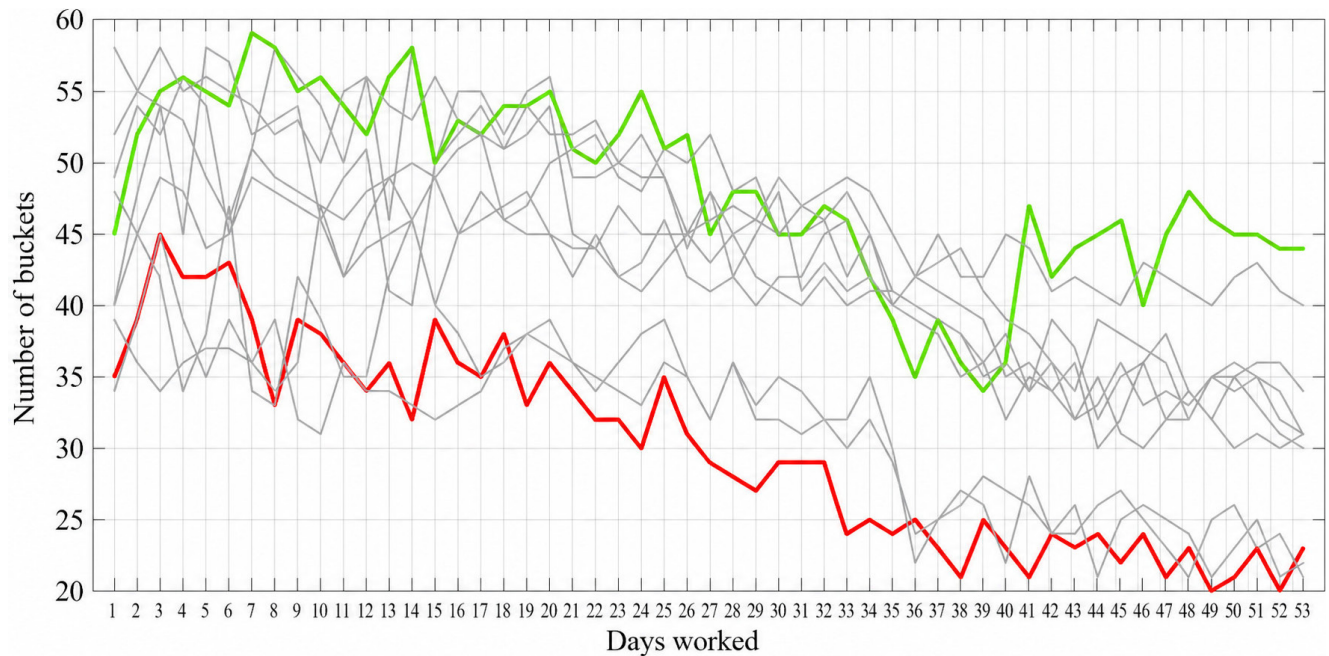


Figure 5. Daily number of buckets picked per worker during the study period. The harvest of worker T3 is highlighted in red (lowest performance) and in green, the harvest of worker T4 (highest performance).

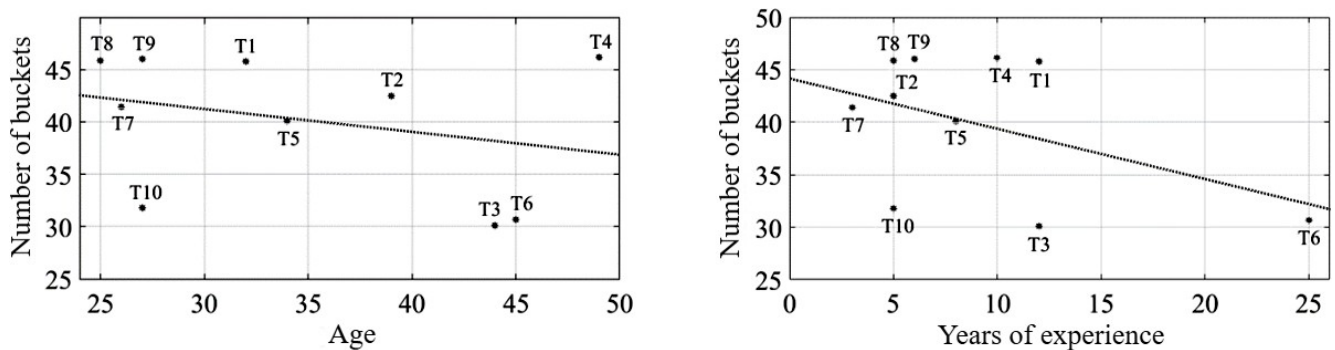


Figure 6. Relationship between worker age, years of experience, and number of buckets harvested.

This study recognizes that the relationship between self-perceived health status and the work performance of agricultural workers does not occur in isolation, but is influenced by a combination of factors. Internal factors include emotional state and coping strategies, while external factors encompass productivity demands and exposure to environmental risks, such as high temperatures inside macrotunnels. The results are consistent with previous studies documenting significant reductions

in productivity under adverse health conditions (Adhvaryu *et al.*, 2020; Cole and Neumayer, 2006), as well as with studies reporting losses of similar magnitude (18 to 30 %) associated with thermal stress (Ferro *et al.*, 2025; Sheng *et al.*, 2025).

Under this premise, and considering the multicausal nature of the phenomenon, the current design is recognized as capable of incorporating a greater number of intervening variables. Factors such as fruit biological density, accumulated worker experience, and precise microclimatic variation mediate the observed relationship. Nevertheless, as an exploratory phase, the results establish the relevance of these dimensions in a high-demand context such as Usmajac and southern Jalisco, where one of the highest densities of economic units dedicated to greenhouse berry production is concentrated (INEGI, 2024). This aligns with Parsons *et al.* (2022), who suggest that thermal impact is a multivariate challenge linking activity intensity with individual responses. In this sense, the findings from Usmajac contribute to refining Exposure-Response Functions (ERF), establishing a basis for disaggregating the economic impact in agricultural sectors of middle latitudes.

CONCLUSIONS

This preliminary study shows that agricultural workers engaged in greenhouse berry harvesting present a high prevalence of chronic diseases, with 9 out of 10 participants reporting at least one condition. The relationship between self-perceived health status and job performance indicates that poorer health reduces work output and, consequently, workers' wages by 21 % compared to the crew average. Some workers maintained high productivity levels despite having chronic conditions, suggesting that self-management of health may mitigate certain negative effects on performance. Although the results show a significant correlation between self-perceived health status and work performance ($r = 0.66$), it is essential to recognize that agricultural productivity is a multicausal phenomenon. In this initial sample, a spectrum of conditions was identified, ranging from chronic metabolic diseases (diabetes, hypertension, and overweight) to socio-emotional and psychosomatic disorders (anxiety, depression, and irritable bowel syndrome). This diversity indicates that health affects not only physical capacity but also cognitive and emotional well-being, both of which are critical in piece-rate work systems.

This study provides a basis for a subsequent multivariate design integrating mental health dimensions, agronomic factors, and extreme weather conditions. Future research with larger samples ($N > 50$) will aim to quantify the contribution of each health dimension and incorporate the Wet Bulb Globe Temperature Index (WBGT) to adjust results according to actual heat load. This approach will enable a more comprehensive and precise understanding of the relationship between health and productivity in technified agricultural environments.

ACKNOWLEDGEMENTS

This work is part of research project M00-PR-03-256 R01 No. 21052, funded by the National Technological Institute of Mexico. We acknowledge the institutional support and the resources provided, which made the development of this study possible. We also thank the participating agricultural workers, whose willingness and trust were essential for the successful completion of this research.

REFERENCES

- Adhvaryu A, Kala N, Nyshadham A. 2020. The light and the heat: Productivity co-benefits of energy-saving technology. *The Review of Economics and Statistics* 102 (4): 779–792. https://doi.org/10.1162/rest_a_00886
- Aguilar-Cuevas PE, Colín-Martínez R. 2022. Precariedad laboral de los jornaleros agrícolas del cultivo de la fresa en el municipio de Purépero, Michoacán. *HorizonTes Territoriales* 2 (3): 1–19.
- Alvarado-Ibarra J, Valencia-López CA, Castillo-Moreno MR, Luna-Reyes PD, Borboa-Servin JA, Mexia-Apodaca ME, Ruiz-Sandoval NC. 2019. Agroquímicos organofosforados y su potencial daño en la salud de trabajadores agrícolas del campo sonoreño. *Ciencia Ergo Sum* 26 (1): 1–11. <https://doi.org/10.30878/ces.v26n1a8>
- Amini M, Ibrahim GL, Rangkooy H, Fouladi DB. 2021. Climate change and its effects on farm workers. *Environmental Health Engineering and Management Journal* 8 (3): 179–185.
- Aranda P, Castro-Vázquez MC. 2016. El campo de la agroindustria en el noroeste de México y la salud de sus jornaleras: una propuesta de estudio. *Salud Colectiva* 12 (1): 55–70. <https://doi.org/10.18294/sc.2016.878>
- Arellano-Gálvez MC, Castro-Vásquez MC, Aranda-Gallegos P. 2023. ¿Apoyos o derechos?: acceso a servicios de salud entre población jornalera del noroeste de México. *Revista de Ciencias Sociales y Humanidades* 44 (94): 221–249.
- Barrón-Pérez MA, Ortiz-Marín C. 2022. La población jornalera agrícola migrante en tiempos de pandemia en México. *Revista Latinoamericana de Antropología del Trabajo* 6 (14): 1–25.
- Barrón-Pérez MA. 2019. Migración y salarios, efectos contradictorios entre los jornaleros agrícolas de San Quintín, Baja California. *Textual* 74: 353–390. <https://doi.org/10.5154/r.textual.2019.74.11>
- Berger ML, Howell R, Nicholson S, Sharda C. 2003. Investing in healthy human capital. *Journal of Occupational and Environmental Medicine* 45 (12): 1213–1225. <https://doi.org/10.1097/01.jom.0000102503.33729.88>
- Castillo F, Sánchez-Vargas A, Gilles J, Wehner M. 2021. The impact of heat waves on agricultural labor productivity and output. *In Extreme Events and Climate Change: A Multidisciplinary Approach*. Wiley: Hoboken, NJ, USA. <https://doi.org/10.1002/9781119413738.ch2>
- Cayir A, Coskun M, Coskun M, Cobanoglu H. 2019. Comet assay for assessment of DNA damage in greenhouse workers exposed to pesticides. *Biomarkers* 24 (6): 592–599. <https://doi.org/10.1080/1354750x.2019.1610498>
- Cole MA, Neumayer E. 2006. The impact of poor health on total factor productivity. *The Journal of Development Studies* 42 (6): 918–938. <https://doi.org/10.1080/00220380600774681>
- Cruz-López DF, Caamal-Cauich I, Pat-Fernández VG, Reza-Salgado J. 2022. Competitividad de las exportaciones de aguacate Hass de México en el mercado mundial. *Revista Mexicana de Ciencias Agrícolas* 13 (2): 355–362. <https://doi.org/10.29312/remexca.v13i2.2885>

- Day A, Magaña-González CR, Wilson K. 2021. Examining Indigenous perspectives on the health implications of large-scale agriculture in Jalisco, Mexico. *The Canadian Geographer* 65 (1): 36–49. <https://doi.org/10.1111/cag.12642>
- Escobar-Latapí A, Martín P, Stabridis O. 2019. Farm labor and Mexico's export produce industry. Wilson Center: Washington, DC, USA. 231 p.
- Ferro AM, Raggi M, Viaggi D, Targetti S. 2025. Impacts of heat waves on agricultural workers: An analysis of adaptation measures. *Bio-Based and Applied Economics* 14 (3): 97–107. <https://doi.org/10.36253/bae-16905>
- Flores-Mariscal J. 2021. Determinantes de la precariedad del trabajo jornalero agrícola en México: un análisis histórico-institucional. *Región y Sociedad* 33: e1487. <https://doi.org/10.22198/rys2021/33/1487>
- Grossman M. 2000. The human capital model. In Culyer AJ, Newhouse JP. (eds.), *Handbook of Health Economics*. North-Holland: Amsterdam, Netherlands. <https://doi.org/10.3386/w7078>
- Haro-Encinas JA. 2007. Globalización y salud de los trabajadores: Jornaleros agrícolas y producción de uva en Pesqueira, Sonora. *Región y Sociedad* 19 (40): 73–105.
- IMSS (Instituto Mexicano del Seguro Social). 2022. IMSS y sector empresarial preparan estrategia para prevenir accidentes de trabajo y mejorar la salud de las personas trabajadoras. Portal de Prensa IMSS. Ciudad de México, México. <https://www.imss.gob.mx/prensa/archivo/202204/197> (Retrieved: January 2026).
- INEGI (Instituto Nacional de Estadística y Geografía). 2023a. Indicadores de ocupación y empleo. Sala de prensa. Ciudad de México, México. <https://www.inegi.org.mx/app/saladeprensa/noticia.html?id=8508> (Retrieved: January 2026).
- INEGI (Instituto Nacional de Estadística y Geografía). 2023b. Resultados oportunos del Censo Agropecuario 2022 Jalisco. Comunicado de prensa núm. 325/23. Ciudad de México, México. 8 p.
- INEGI (Instituto Nacional de Estadística y Geografía). 2024. Directorio estadístico nacional de unidades económicas. Sector 11: Agricultura, cría y explotación de animales. Ciudad de México, México. <https://www.inegi.org.mx/app/mapa/denue/> (Retrieved: January 2026).
- Lagunes-Fortiz ER, Lagunes-Fortiz E, Gómez-Gómez AA, Leos-Rodríguez JA, Omaña-Silvestre JM. 2020. Competitividad y rentabilidad de la producción de frutillas en Jalisco. *Revista Mexicana de Ciencias Agrícolas* 11 (8): 1815–1826. <https://doi.org/10.29312/remexca.v11i8.2595>
- Levasseur P. 2019. Implementing a regression discontinuity design to explore the heterogeneous effects of obesity on labour income: The case of Mexico. *Journal of Public Health* 27 (1): 89–101. <https://doi.org/10.1007/s10389-018-0925-5>
- Lin X, Xu Y, Pan X, Xu J, Ding Y, Sun X, Song X, Ren Y, Shan PF. 2020. Global, regional, and national burden and trend of diabetes in 195 countries and territories: An analysis from 1990 to 2025. *Scientific Reports* 10 (1). <https://doi.org/10.1038/s41598-020-71908-9>
- Loeppke R, Taitel M, Haufler V, Parry T, Kessler RC, Jinnett K. 2009. Health and productivity as a business strategy: A multiemployer study. *Journal of Occupational and Environmental Medicine* 51 (4): 411–428. <https://doi.org/10.1097/jom.0b013e3181a39180>
- Macías-Macías A, Sevilla-García YL. 2022. El fracaso del desarrollo y la opción por el buen vivir. *Comunicación Científica*: Ciudad de México, México. 687 p. <https://doi.org/10.52501/cc.034>
- Mattke S, Balakrishnan A, Bergamo G, Newberry SJ. 2007. A review of methods to measure health-related productivity loss. *American Journal of Managed Care* 13 (4): 211–217.

- Munir F, Jones D, Leka S, Griffiths A. 2005. Work limitations and employer adjustments for employees with chronic illness. *International Journal of Rehabilitation Research* 28 (2): 111–117. <https://doi.org/10.1097/00004356-200506000-00003>
- Ortega-Martínez LD, Pérez-Armendáriz B, Waliszewski S, Gómez-Arroyo S, Baños-Lara MR, Terán-Cervantes M, Castro-Carranza G, Martínez-Valenzuela MC. 2019. Daño genético y citotóxico provocado por plaguicidas en jornaleros que laboran en invernaderos en Atlixco, Puebla, México. *Revista Internacional de Contaminación Ambiental* 35 (2): 271–279. <https://doi.org/10.20937/rica.2019.35.02.01>
- Palacios-Nava ME. 2003. Aplicación de un instrumento para evaluar exposición a plaguicidas organofosforados, efectos agudos y subagudos en la salud de trabajadores agrícolas. *Revista de la Facultad de Medicina de la UNAM* 46 (1): 22–27.
- Pan Q, Sumner DA, Mitchell DC, Schenker M. 2021. Compensation incentives and heat exposure affect farm worker effort. *PLoS ONE* 16 (11): e0259459. <https://doi.org/10.1371/journal.pone.0259459>
- Parsons LA, Masuda YJ, Kroeger T, Shindell D, Wolff NH, Spector JT. 2022. Global labor loss due to humid heat exposure underestimated for outdoor workers. *Environmental Research Letters* 17 (1): 014050. <https://doi.org/10.1088/1748-9326/ac3dae>
- Sahu S, Sett M, Kjellstrom T. 2013. Heat exposure, cardiovascular stress and work productivity in rice harvesters in India: Implications for a climate change future. *Industrial Health* 51 (4): 424–431. <https://doi.org/10.2486/indhealth.2013-0006>
- Salgado-Viveros C. 2023. El ocaso laboral: trabajo y vejez en los cultivos de berries del sur de Jalisco. *Región y Sociedad* 35: e1765. <https://doi.org/10.22198/rys2023/35/1765>
- Sánchez-Gervacio BM, Bedolla-Solano R, Rosas-Acevedo JL, Legorreta-Soberanis J, Valencia-Quintana R, Juárez-López AL. 2020. Pesticide management by subsistence farmers in Mexico: Baseline of a pilot study to design an intervention program. *Human and Ecological Risk Assessment: An International Journal* 27 (4): 1112–1125. <https://doi.org/10.1080/10807039.2020.1807903>
- Sheng D, Zhao X, Edmonds JA, Morris ST, Patel P, O'Neill BC, Tebaldi C, Wise MA. 2025. Omitting labor responses underestimates the effects of future heat stress on agriculture. *Communications Earth and Environment* 6 (1). <https://doi.org/10.1038/s43247-025-02318-w>
- Siu AM, Hung A, Lam AY, Cheng A. 2013. Work limitations, workplace concerns, and job satisfaction of persons with chronic disease. *WORK: A Journal of Prevention, Assessment and Rehabilitation* 45 (1): 107–115. <https://doi.org/10.3233/wor-121550>
- Tompa E. 2002. The impact of health on productivity: Empirical evidence and policy implications. *The Review of Economic Performance and Social Progress*. McGill-Queen's University Press: Montreal, Canada. 300 p.
- UN Women. 2022. Jornaleras agrícolas mexicanas luchan por sus derechos y la protección del medio ambiente. *UN Women Americas and the Caribbean*. New York, NY, USA. <https://lac.unwomen.org/es/stories/noticia/2022/03/jornaleras-agricolas-mexicanas-luchan-por-sus-derechos-y-la-proteccion-del-medio-ambiente> (Retrieved: January 2026).
- Weather Spark. 2026. El clima y el tiempo promedio en todo el mundo. <https://es.weatherspark.com> (Retrieved: January 2026).

CONSUMER PREFERENCES AND WILLINGNESS TO PAY FOR TRADITIONAL TORTILLA USING CONTINGENT VALUATION

Judith de la Cruz-Marcial¹, Miguel A. Martínez-Damian^{1*}, Enrique Melo-Guerrero², Juan Hernández-Ortiz³, Gustavo Ramírez-Valverde¹

¹Colegio de Postgraduados Campus Montecillo. Carretera México-Texcoco km 36.5, Montecillo, Texcoco, State of Mexico, Mexico. C. P. 56264.

²Universidad Autónoma del Estado de Hidalgo. Instituto de Ciencias Agropecuarias. Avenida Universidad km 1, Exhacienda Aquetzalpa, Tulancingo, Hidalgo, Mexico. C. P. 43600.

³Universidad Autónoma Chapingo. División de Ciencias Económico Administrativas. Carretera México-Texcoco km 38.5, Chapingo, Texcoco, State of Mexico, Mexico. C. P. 56227.

* Author for correspondence: angel01@colpos.mx

ABSTRACT

The tortilla is a staple food in the Mexican diet. However, in recent years, it has been declining in quality and nutritional value due to the use of flour and the industrialization of production processes. Fresh traditional tortillas are known to possess superior nutritional and nutraceutical properties compared to commercially produced tortillas, along with unmatched flavor and texture. Consumers have increased their preferences for local, more natural products produced in an eco-friendly agricultural manner. Thus, soil degradation, water pollution, and the loss of biodiversity are avoided. However, the price consumers are willing to pay for a tortilla with these attributes is unknown. Using the contingent valuation method (CVM) in its referendum and double-bounded formats, the aim of this investigation was to estimate consumers' willingness to pay (WTP) for the tortilla they consume with the following attributes: native maize content, organic production, and traditional nixtamalization. Moreover, the variables that explained the behavior of the WTP were determined. A total of 216 surveys were conducted between January and March 2024 in 15 municipalities of the State of Mexico belonging to the metropolitan area of the Valley of Mexico. The double-bounded CVM displayed the highest theoretical consistency. The variables of price, monetary income, gender, education level, economic dependents, and age of the respondent helped estimate the WTP. The estimated value was MXN 36.12 per kg of tortilla.

Keywords: food, nutrition, local product, natural, *Zea mays* L.

INTRODUCTION

The tortilla is part of the identity of Mexicans. It has a cultural and mythical origin and has accompanied the Mexican culinary culture, both in rural and urban spheres. It is a key ingredient in the majority of everyday and festive dishes (Calleja-Pinedo and Valenzuela, 2016; Torres-Sombra, 2018). However, not all maize tortillas are the same,

Citation: de la Cruz-Marcial J, Martínez-Damian MA, Melo-Guerrero E, Hernández-Ortiz J, Ramírez-Valverde G, Mora-Flores S. 2026. Consumer preferences and willingness to pay for traditional tortilla using contingent valuation.

Agrociencia 60(3): 439-452.
<https://doi.org/10.47163/agrociencia.v60i3.3343>

Editor in Chief:

Dr. Fernando C. Gómez Merino

Received: September 03, 2025.

Approved: April 20, 2026.

Published in *Agrociencia*:

April 24, 2026.

This work is licensed under a Creative Commons Attribution-Non-Commercial 4.0 International license.



as their quality and nutritional content depend on decisions taken in the field and the food transformation processes.

According to Sainz-Trapaga *et al.* (2022), out of the total of pre-packaged maize tortillas, 93 % are made with nixtamalized flour, and only 7 % claim they are made with nixtamalized maize. These authors identified 145 additives in pre-packaged tortillas and tostadas, out of which 119 were sold without a clear and detailed declaration of the ingredients or substances they are made of. The most common ones are preservatives (21 %), softeners (13 %), anti-stick agents (12 %), bleaching agents (12 %), and texturizers (8.4 %). These tortillas made with nixtamalized maize flour show significant differences in their nutritional contributions compared to traditional tortillas, particularly in terms of reduced calcium content (Colín-Chávez *et al.*, 2020). Out of all the tortillas consumed in Mexico, 90.4 % contain sequences of transgenic maize. This is also the case for 82 % of the tostadas, flours, cereals, and snacks produced with this grain. The presence of glyphosate has also been found in industrial tortillas. In contrast, traditional tortillas made with native maize present a much lower frequency of transgenes and do not contain glyphosate (González-Ortega *et al.*, 2017). Fresh traditional tortillas have nutritional and nutraceutical properties far superior to the industrial tortilla, such as a higher content of free phenols, dietary fiber, calcium, and antioxidant capacity. Handmade tortillas made from blue maize have a ferulic acid content 4.5 times higher than the commercially produced white maize tortillas and thus may be a good source of phenolic antioxidants, particularly ferulic acid (Colín-Chávez *et al.*, 2020).

In recent years, consumers tend to prefer healthier and more eco-friendly products. Environmental awareness has increased and become more popular worldwide. Most countries apply laws to protect it and develop a sustainable economy (Kipāne and Vilks, 2022), such as the United States, Colombia, Peru, South Korea, and Mexico (OECD, 2024). Aprile *et al.* (2016) mention that a recent consumer preference expression includes locally produced foods, driven by their demand for sensory perception, nostalgia for local processes, healthy attributes, environmental care, and dietary habit changes.

Recent studies on consumer preferences in common tortillas (produced with nixtamalized flour, nixtamal dough, or a mixture of dough and flour) show that the consumers prefer nixtamalized maize dough tortillas (Espejel-García *et al.*, 2016; Escobedo-Garrido and Jaramillo-Villanueva, 2019). However, there are not many studies on the preferences for differentiated tortillas, such as the traditional tortilla. Jaramillo-Villanueva (2016) conducted a study on preferences and willingness to pay (WTP) for organic maize tortilla consumption in Puebla and reported that consumers are willing to pay MXN 1.6 kg⁻¹, equivalent to 16 % above-the floor price per kilogram of tortillas. Blare *et al.* (2020) report that, in Texcoco, State of Mexico, consumers were willing to pay 42 % more for blue maize tortillas when they ate out, but not for everyday home consumption.

Based on the above information, a niche market is found for eco-friendly, traditional tortillas made from native maize. However, the price that consumers are willing to pay and the attributes they value the most are unknown. One of the most widely used methods to obtain this information is the contingent valuation method (CVM), which used a flexible stated-preference approach applied to the valuation of non-market goods across a range of contexts and policies (Haab *et al.*, 2020). To apply it, a market is simulated using surveys to potential customers, with the purpose of measuring the changes in the well-being of people and societies against variations in goods and services, with these goods and services being monetized in order to determine WTP. Within the CVM, there are two formats to estimate the WTP: referendum and double-bound. According to Brugnaro (2010), Gelo and Koch (2015), and Tudela-Mamani *et al.* (2018), the double-bound format helps obtain more efficient and accurate estimations. The aim of this investigation is to estimate, using the CVM in its referendum and double bound formats, the WTP of consumers for hand-produced tortillas made with native organic maize and traditional nixtamalization, as well as to determine the variables that explain the behavior of the WTP. The hypothesis is that consumers are willing to pay an upcharge price for the traditional, native, organic, and nixtamalization attributes, and that the magnitude of this overprice is explained by the price, income, consumer tastes, and preferences, as well as their sociodemographic characteristics.

MATERIALS AND METHODS

The study was held between January and March 2024 in 15 municipalities of the State of Mexico, belonging to the metropolitan area of the Valley of Mexico: Chalco, Chicoloapan, Chimalhuacán, Coacalco de Berriozábal, Ecatepec de Morelos, Ixtapaluca, Cuautitlán Izcalli, Naucalpan de Juárez, Nezahualcóyotl, La Paz, Tecámac, Texcoco, Tlalnepantla, Tultitlán, and Valle de Chalco Solidaridad.

To estimate the sample, the population of interest (individuals over the age of 18) was identified from the total population of the State of Mexico, which stands at 16 992 418 inhabitants according to the Population and Household Survey (INEGI, 2020). Following recommendations by Ahmed (2024), the sample size was determined using an equation for large or infinite populations:

$$n = \frac{Z^2 pq}{d^2}$$

where n is the sample size, Z is the value z associated with the desired confidence level (1.96 for 95 % confidence), p is the proportion of the population willing to pay for the improvement (equal to 0.5), q is the proportion of the population not willing to pay (equal to 0.5), and d is the allowable estimation error or precision (7 %).

The questionnaires used were based on focus group discussions between housewives, consumers, and experts on the topic. Subsequently, preliminary studies were held

on 100 consumers to find erroneous interpretations of the questions. Based on the equation for calculating sample size, an estimated 196 questionnaires were conducted. However, since four prices were evaluated, 216 surveys were administered, distributed as 54 for each proposed price.

Referendum model of willingness to pay

The model is a popular method in the dichotomous choice design; its popularity stems from the recommendations of the United States National Oceanic and Atmospheric Administration (NOAA) (Arrow *et al.*, 1993), and it uses a “take it or leave it” format. According to Tudela-Mamani *et al.* (2018), the modelling process considers the random utility approach through the following expression:

$$U_{ih} = v_{ih}(p_h, M_i, s_i) + \varepsilon_{ih}$$

where the utility (U) of the alternative (h) for the individual (i) is based on s , which represents the individual characteristics; p_h is the price of alternative h , and M is the individual's income. The utility is composed of a deterministic component (v_{ih}) and a non-observable random error component (ε_{ih}), independent and identically distributed, with a mean of zero and a constant variance. Individual i chooses the alternative that provides the greatest utility. Therefore, the behavior establishes that the alternative h is chosen if and only if: $U_{ih} > U_{ij} \forall h \neq j$. The probability (Pr) of the individual choosing alternative h is given by the following equations:

$$\Pr(h) = \Pr\{U_{ih} > U_{ij}\}$$

$$\Pr(h) = \Pr\{\varepsilon_{ij} - \varepsilon_{ih} < v_{ih}(p_h, Z_{ih}, M_i, s_i) - v_{ij}(p_j, Z_{ij}, M_i, s_i)\}$$

In order to estimate the impacts on well-being, that is, the WTP for a change from the status quo (alternative j) to the chosen state (alternative h), the following equation is used:

$$\Delta v = v_{ih}(p_h, M_i - VC, s_i) - v_{ij}(p_j, M_i, s_i)$$

where VC is the compensatory variation, which is interpreted as the highest amount of money that an individual would be willing to pay to access a favorable change. In this case, for individual i , alternative h improves their well-being in comparison to alternative j .

The willingness to pay (WTP) for each respondent was estimated using the following equation:

$$WTP_i = \frac{\alpha + \beta_2(INC) + \beta_3(GEN) + \beta_4(EDL) + \beta_5(DEP) + \beta_6(PRICEKG)}{-\beta_1}$$

$$i = 1, 2, \dots, 216$$

where INC is the respondent's income level, GEN corresponds to the gender, EDL is the education level, DEP is the number of economic dependents of the household, and PRICEKG is the price per kilogram of tortilla (MXN). The referendum model consists in giving the respondent two answer alternatives: yes or no. The dependent variable is discrete; therefore, the regression is carried out using a logit or probit model. This investigation uses the logit model.

The estimation is solved with the maximum likelihood method with the log-likelihood (LL) function:

$$LL = \prod_{i=1}^n [(1 - y_i) \ln(1 - F(\beta'x_i)) + y_i \ln(F(\beta'x_i))]$$

where y_i is the dependent binary variable that takes the value of one if the response to the WTP is "yes" and, otherwise, zero. The maximum likelihood estimator is obtained by maximizing this function.

Double-bounded willingness-to-pay model

When assuming that an individual faces two "take it or leave it" offers related to their WTP, an initial offer is first presented, and they respond yes or no. Based on this response, a second offer is made: if they reject the first, a lower one is made; if they accept it, a higher offer is made (Gelo and Koch, 2015). The initial question is asked again in this second step as PMA or PME, where PMA corresponds to the price proposed after a positive response and PME, to the price proposed after a negative response (Tudela-Mamani, 2017).

According to Hanemann *et al.* (1991) and Aikoh *et al.* (2018), responses in terms of probability can be expressed as shown in the following equations:

$$\begin{aligned} \Pr(YES, YES) &= 1 - F(\beta'x_i^u) \\ \Pr(YES, NO) &= F(\beta'x_i^u) - F(\beta'x_i) \\ \Pr(NO, YES) &= F(\beta'x_i) - F(\beta'x_i^d) \\ \Pr(NO, NO) &= F(\beta'x_i^d) \end{aligned}$$

For the double-bounded case, the log-likelihood function is stated as follows:

$$LL = \sum_{i=1}^n \left\{ \begin{array}{l} d_i^{ss} \ln \left(1 - \frac{1}{1 + \exp^{-(\beta'x_i^u)}} \right) + d_i^{sn} \ln \left(\frac{1}{1 + \exp^{-(\beta'x_i^u)}} - \frac{1}{1 + \exp^{-(\beta'x_i)}} \right) + \\ d_i^{ns} \ln \left(\frac{1}{1 + \exp^{-(\beta'x_i)}} - \frac{1}{1 + \exp^{-(\beta'x_i^d)}} \right) + d_i^{nn} \ln \left(\frac{1}{1 + \exp^{-(\beta'x_i^d)}} \right) \end{array} \right\}$$

where d_i^{ss} , d_i^{sn} , d_i^{ns} , d_i^{nn} , are binary variables that take the value of one when the respondent's answer corresponds to that category and zero otherwise. The maximum likelihood estimator is obtained by maximizing this function. Once the estimations of the parameters are obtained, the monetary measure of welfare is calculated. The formulas to calculate the WTP, both in the referendum and double-bounded formats, are derived from the functional form of Δv (Vásquez-Lavín *et al.*, 2007).

The questionnaire was split into three sections. The first one included the sociodemographic aspects and the consumption patterns of the respondents (age, gender, civil status, education, monthly household income, and number of members). The second one addresses the consumption frequency and preferences related to the attributes of the maize tortilla considered important by consumers: organic, native, color, nixtamalization, and traditional production. In the third section, the valuation scenario was presented, and the respondents were informed about the proposed improvements for the tortillas as well as the social benefits associated with their consumption. The central question was, "Suppose a new presentation is about to be released with the following characteristics: native maize-based, produced organically, nixtamalized, and produced traditionally (by hand and on a hot plate). For one kilogram of this tortilla, would you be willing to pay X?"

In the first round, the poll taker applied the initial bid price (PPI) with four values: 20, 30, 40, and 50, conducting 54 surveys for each one. Based on the response of each individual ("yes" or "no"), the second question was asked. If the initial response was "yes," the high bid vector (PMA) was used: 22, 32, 42, and 52. If the initial response was "no," the low bid vector (PME) was applied: 18, 28, 38, and 48. In both the double-bounded and the referendum formats, the variables were used to calculate the econometric logit model (Table 1).

RESULTS AND DISCUSSION

In the referendum contingent valuation, out of 216 participants, 58 % claimed to be willing to pay an overprice to consume a tortilla produced with native maize, produced organically, nixtamalized with the traditional process, and prepared traditionally (by hand and on a hotplate). In particular, 70 % of all respondents were willing to pay a price of MXN 30 kg⁻¹, whereas only 20 % answered affirmatively to a cost of MXN 50 kg⁻¹. As the price increased, the proportion of positive answers decreased (Table 2).

Table 1. Description of variables used in the analysis.

Variable	Description	Response
PSI	Probability of answering YES to the willingness to pay	1 = if the response in first round is YES, 0 = Negative response
PPI	Initial proposed price (MXN)	20, 30, 40, and 50
PME	Lower price (MXN)	18, 28, 38, and 48
PMA	Higher price (MXN)	22, 32, 42, and 52
DYY	Dummy variable for YES-YES	If the response in the first round is YES, 1 = if the response in second round is YES; 0 = otherwise
DYN	Dummy variable for YES-NO	If response in the first round is YES, 1 = if the response in the second round is NO; 0 = otherwise
DNY	Dummy variable for NO-YES	If the response in the first round is NO, 1 = if the response in the second round is YES; 0 = otherwise
DNN	Dummy variable for NO-NO	If the response in first round is NO, 1 = if the response in second round is NO; 0 = otherwise
INC	Income level (MXN)	1 = less than 5000, 2 = between 5000 and 7000, 3 = between 7001 and 9000, 4 = between 9001 and 11000, 5 = between 11001 and 13000, 6 = between 13001 and 15000, 7 = between 15001 and 17000, 8 = between 17001 and 20000, 9 = between 20001 and 25000, 10 = between 25001 and 30000, 11 = over 30000
INCR	Monetary income (MXN)	Whole number (arithmetic average of each category of the ING variable)
MUNICIP	Municipality in which respondent lives	1 = Ecatepec de Morelos, 2 = Nezahualcóyotl, 3 = Naucalpan de Juárez, 4 = Chimalhuacán, 5 = Tlalnepantla, 6 = Cuautitlán Izcalli, 7 = Tecámac, 8 = Ixtapaluca, 10 = Tultitlán 12 = Chalco, 13 = Valle de Chalco Solidaridad, 14 = La Paz, 15 = Coacalco de Berriozábal, 18 = Texcoco, 19 = Chicoloapan
GEN	Gender	Woman = 1, Man = 0
CIVSTAT	Civil status	1 = Single, 2 = Married, 3 = Widowed, 4 = Divorced, 5 = Free union
AGE	Age	Whole number (years)
EDL	Education level	1 = Elementary, 2 = Middle high, 3 = Highschool, 4 = Technical degree, 5 = Bachelors, 6 = Graduate school, 7 = No studies
INTEGRAN	Number of individuals in the respondent's household	Whole number
DEP	Number of economic dependents of the head of household	Whole number
PRICEKG	Price of a kilogram of tortillas (MXN) at the place where the respondent buys them.	Whole number
FREQ	Frequency with which respondent buys tortillas	1 = Every day, 2 = Every third day, 3 = Once a week, 4 = Occasionally, 5 = Does not buy tortillas
CONORG	Knowledge on organic products	1 = yes, 0 = no

Table 1. Continued

Variable	Description	Response
CONCONVE	Knowledge on conventional agriculture	1 = yes, 0 = no
CONHIB	Knowledge on hybrid maize	1 = yes, 0 = no
CONCRI	Knowledge on native maize	1 = yes, 0 = no
CONNIX	Knowledge on the nixtamalization process	1 = yes, 0 = no
ELAB	Knowledge on the raw materials used to make the tortilla	1 = Maize flour, 2 = Hybrid maize dough, 3 = Native maize dough, 4 = Mixture of maize flour/hybrid maize dough

Table 2. Frequency of affirmative responses to the initial prices proposed.

Initial price (PPI)	Number of surveys	Affirmative responses	
		Number	%
20	54	52	96
30	54	38	70
40	54	24	44
50	54	11	20
Total	216	125	58

In the second round (double-bound), 48 % responded affirmatively to the valuation question (YES/YES, NO/YES) (Table 3). Diverse econometric models were estimated, and the selection of the optimum model was based on the following criteria: 1) the coefficients must present the expected signs, reflecting a logical relation with the dependent variable; 2) the coefficients must be significant at an acceptable reliability level; and 3) the maximum log-likelihood must reach a high value.

In the referendum and double-bounded format, the results of the regressions of the logit binomial models (Table 4) indicated a selection of a linear model. In the referendum format, the model displayed a percentage of prediction of 74.53 % and

Table 3. Frequency of responses in the contingent valuation survey (referendum and double-bounded).

Format	Price	18	20	22	28	30	32	38	40	42	48	50	52	Total
Referendum	YES		52			38			24			11		125
	NO		2			16			30			43		91
Double-bounded	YES/YES			45			26			11			7	89
	YES/NO			7			12			13			4	36
	NO/YES	1			6			3			4			14
	NO/NO	1			10			27			39			77

Table 4. Econometric estimations referendum model and double-bounded.

Variables	Referendum	Double-bounded
Constant	5.457 (3.007)***	3.935 (2.807)***
PPI	-0.139 (-7.229)***	-0.168 (-9.408)***
INCR	0.00005 (1.590)	0.00004 (1.330)
GEN	0.593 (1.497)	0.306 (0.851)
EDL	0.126 (0.943)	0.196 (1.463)
DEP	-0.092 (-0.758)	-0.191 (-1.621)
PRICEKG	-0.065 (-0.811)	0.055 (0.914)
Logarithm of likelihood	-102.982	229.515
Reason for likelihood	88.100	459.030
Pseudo R	0.299	
Correct prediction (%)	74.537	

*** Significance at 1 %. The Z statistic is found in parentheses. PPI: hypothetical initial price; INCR: monetary income; GEN: gender of respondent; EDL: education level; DEP: number of economic dependents of the head of the household; PRICEKG: price per kilogram of tortilla in the establishment where the respondent makes the purchase.

a McFadden's R^2 of 0.299, a value within the expected range for this type of studies (0.2–0.4), equivalent to an R^2 of 0.7–0.9 in an ordinary squared minimum regression (Tudela-Mamani *et al.*, 2011, 2018; Melo-Guerrero *et al.*, 2020).

In the models estimated with the double-bounded format, the linear model was selected, as it registered the highest value of the log-likelihood and, consequently, the highest likelihood ratio. In most cases, the absolute value of the "Z" statistic was higher than that of the referendum models, which indicates lower variances in the coefficients and greater statistical significance. This suggests a better approximation to the respondents' true WTP. These results are consistent with those reported by Tudela-Mamani *et al.* (2018), Cahui-Cahui *et al.* (2019), and Torres-Ramírez *et al.* (2023). The results of the double-bounded model showed the expected signs of the coefficients. The PPI coefficient was negative, indicating that the higher the price of tortillas, the lower the probability of getting a positive response. The price was the variable with the least significance in comparison with the rest. The income variable (INCR) presented a positive sign; therefore, a higher income increases the probability of an affirmative response. The coefficient associated with gender was also positive, which implies a higher probability of a positive response when the respondent is female. This result

is consistent with the one by Brugnaro (2010), Hernández-Valdivia *et al.* (2019), and Torres-Ramírez *et al.* (2023).

The EDL coefficient displayed a positive sign, in such a way that a higher education level increases the probability of an affirmative answer, as reported by Hernández-Valdivia *et al.* (2019) and Lugo-Sandoval *et al.* (2020). By contrast, the variable DEP presented a negative sign, as expected. The greater the number of economic dependents, the lower the WTP, since tortillas are a staple food. A larger household typically results in higher overall spending. The variable PRICEKG presented a positive sign, indicating that the higher the tortilla price in the habitual venue of purchase, the higher the WTP for the valued product.

The WTP obtained using the double-bounded format was MXN 36.11 (Table 5), equivalent to an overprice of 77 % relative to the average price of MXN 20.37 in the surveyed areas and of 56 % in regard to the national average of MXN 23.15 (SNIIM, 2024). Jaramillo-Villanueva (2016) found that consumers in Puebla would pay an overprice of MXN 1.6 kg⁻¹ for organic maize tortillas, equivalent to 16 % of the base price.

Table 5. Estimation of the mean willingness to pay (WTP) in the referendum and double-bounded models.

Format	Mean	Standard deviation	Minimum	Maximum
Linear referendum	38.548	3.711	28.237	54.125
Double-bounded	36.110	3.452	24.466	46.919

In general, consumers were found to be willing to pay a higher premium when their consumption was occasional; however, their WTP decreased with daily consumption. This coincides with Blare *et al.* (2020), who found a WTP 42 % higher for blue maize tortillas eaten outside the household but lower for everyday consumption at home. Altogether, consumers are willing to pay an overprice for organic (Jaramillo-Villanueva, 2016; Marozzo *et al.*, 2023), eco-friendly (Tokuoka *et al.*, 2024), or traditional products (Aprile *et al.*, 2016; Ortez *et al.*, 2024).

The data adjusted to a normal distribution. In the referendum model (Figure 1A), the highest frequency of WTP was concentrated between MXN 34.709 and 41.181. In contrast, the double-bounded model (Figure 1B) showed a concentration between MXN 30.882 and 40.504. Most values were clustered around the mean. According to Czajkowski *et al.* (2024), the selection of the adequate parametric distribution depends fundamentally on the behavior of the data.

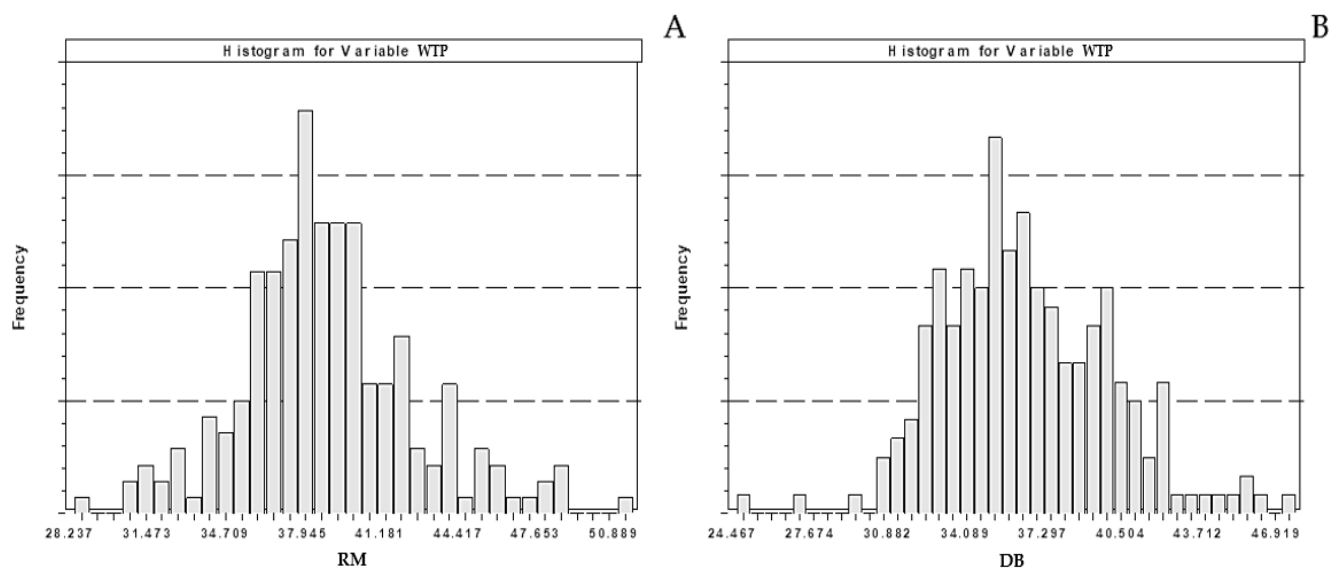


Figure 1. Distribution of the estimated willingness to pay (WTP). A: Referendum model (RM); B: Double-bounded (DB) model.

CONCLUSIONS

The double-bounded contingent valuation model displayed a higher individual and joint significance of the parameters than the referendum model. Consumers are willing to pay an overprice for a tortilla produced with native maize, produced organically, and nixtamalized and prepared in the traditional way. On average, consumers expressed a willingness to pay MXN 36.12 kg⁻¹, which represents a 77 % premium over the average price of MXN 20.37 in the surveyed areas and a 56 % premium compared to the national average of MXN 23.15. The variables of price, income, gender, education level, economic dependents, and age had an influence when determining the WTP.

ACKNOWLEDGEMENTS

The authors wish to express their full gratitude to the Secretariat of Science, Humanities, Technology and Innovation (SECIHTI) for funding the project, and to the Postgraduate College for the facilities and the support provided during the development of the study.

REFERENCES

- Ahmed SK. 2024. How to choose a sampling technique and determine sample size for research: A simplified guide for researchers. *Oral Oncology Reports* 12: 100662. <https://doi.org/10.1016/j.oor.2024.100662>
- Aikoh T, Shoji Y, Tsuge T, Shibasaki S, Yamamoto K. 2018. Application of the double-bounded dichotomous choice model to the estimation of crowding acceptability in natural recreation areas. *Journal of Outdoor Recreation and Tourism* 32: 100195. <https://doi.org/10.1016/j.jort.2018.10.006>

- Aprile MC, Caputo V, Nayga JRM. 2016. Consumers' preferences and attitudes toward local food products. *Journal of Food Products Marketing* 22 (1): 19–42. <https://doi.org/10.1080/10454446.2014.949990>
- Arrow K, Solow R, Leamer EP, Portney P, Randner R, Schuman H. 1993. Report on NOAA panel on contingent valuation. National Oceanic and Atmospheric Administration. Washington, DC, USA. 38 p.
- Blare T, Donovan J, García-Medina M. 2020. The right tortilla for the right occasion: Variation in consumers' willingness to pay for blue maize tortillas based on utilization. *Journal of Food Products Marketing* 26 (8): 564–579. <https://doi.org/10.1080/10454446.2020.1832637>
- Brugnaró C. 2010. Valuing riparian forests restoration: A CVM application in Corumbatai river basin. *Revista de Economía e Sociología Rural* 48 (3): 507–520. <https://doi.org/10.1590/S0103-20032010000300001>
- Cahui-Cahui E, Tudela-Mamani JW, Huamani-Peralta A. 2019. Determinantes socioeconómicos en la estimación de la disponibilidad a pagar del proyecto de agua potable y saneamiento en el centro poblado de Paxa, distrito de Tiquillaca – Puno 2017. *Comuni@cción: Revista de Investigación en Comunicación y Desarrollo* 10 (1): 81–91.
- Calleja-Pinedo M, Valenzuela MB. 2016. La tortilla como identidad culinaria y producto de consumo global. *Región y Sociedad* 28 (66): 161–194.
- Colín-Chávez C, Virgen-Ortiz JJ, Serrano-Rubio LE, Martínez-Télez MA, Astier M. 2020. Comparison of nutritional properties and bioactive compounds between industrial and artisan fresh tortillas from maize landraces. *Current Research in Food Science* 3: 189–194. <https://doi.org/10.1016/j.crfs.2020.05.004>
- Czajkowski M, Zawojka E, Meade N, da Motta RS, Welsh M, Ortiz RA. 2024. On the inference about a willingness-to-pay distribution using contingent valuation data. *Ecological Economics* 222: 108207. <https://doi.org/10.1016/j.ecolecon.2024.108207>
- Escobedo-Garrido JS, Jaramillo-Villanueva JL. 2019. Las preferencias de los consumidores por tortillas de maíz. El caso de Puebla, México. *Estudios Sociales. Revista de Alimentación Contemporánea y Desarrollo Regional* 29 (53): e19627. <https://doi.org/10.24836/es.v29i53.627>
- Espejel-García MV, Mora-Flores JS, García-Salazar JA, Pérez-Elizalde S, García-Mata R. 2016. Caracterización del consumidor de tortilla en el Estado de México. *Agricultura, Sociedad y Desarrollo* 13 (3): 371–384.
- Gelo D, Koch SF. 2015. Contingent valuation of community forestry programs in Ethiopia: Controlling for preference anomalies in double-bounded CVM. *Ecological Economics* 114: 79–89. <https://doi.org/10.1016/j.ecolecon.2015.03.014>
- González-Ortega E, Piñeyro-Nelson A, Gómez-Hernández E, Monterrubio-Vázquez E, Arleo M, Dávila-Velderrain J, Martínez-Debat C, Álvarez-Buylla ER. 2017. Pervasive presence of transgenes and glyphosate in maize-derived food in Mexico. *Agroecology and Sustainable Food Systems* 41 (9–10): 1146–1161. <https://doi.org/10.1080/21683565.2017.1372841>
- Haab T, Lewis LY, Whitehead J. 2020. State of the art of contingent valuation. In *Oxford Research Encyclopedia of Environmental Science*. Oxford University Press: Oxford, UK. <https://doi.org/10.1093/acrefore/9780199389414.013.450>
- Hanemann M, Loomis J, Kanninen B. 1991. Statistical efficiency of double-bounded dichotomous choice contingent valuation. *American Journal of Agricultural Economics* 73 (4): 1255–1263. <https://doi.org/10.2307/1242453>

- Hernández-Valdivia MS, Valdivia-Alcalá R, Hernández-Ortíz J. 2019. Valoración de servicios ambientales y recreativos del Bosque San Juan de Aragón, Ciudad de México. *Revista Mexicana de Ciencias Forestales* 10 (54). <https://doi.org/10.29298/rmcf.v10i54.557>
- INEGI (Instituto Nacional de Estadística, y Geografía). 2020. Información demográfica y social. Censo de población y vivienda (CPV) 2020. Ciudad de México, México. <https://www.inegi.org.mx/programas/ccpv/2020/> (Retrieved: November 2025).
- Jaramillo-Villanueva JL. 2016. Preferencias del consumidor y disposición a pagar por el consumo de tortilla de maíz orgánico. *Estudios Sociales. Revista de Alimentación Contemporánea y Desarrollo Regional* 25 (47): 144–160
- Kipāne A, Vilks A. 2022. Legal framework for environmental protection in the context of sustainable development. *European Journal of Sustainable Development* 11 (4): 169. <https://doi.org/10.14207/ejsd.2022.v11n4p169>
- Lugo-Sandoval M, Valdivia-Alcalá R, Monroy-Hernández R, Hernández-Ortíz J, Sandoval-Romero F, Contreras-Castillo JM. 2020. Valoración económica de los servicios ambientales del Monte Tláloc, Texcoco, Estado de México. *Revista Mexicana de Ciencias Forestales* 11 (61). <https://doi.org/10.29298/rmcf.v11i61.672>
- Marozzo V, Costa A, Crupi A, Abbate T. 2023. Decoding Asian consumers' willingness to pay for organic food product: A configurational-based approach. *European Journal of Innovation Management* 26 (7): 353–384. <https://doi.org/10.1108/ejim-10-2022-0591>
- Melo-Guerrero E, Hernández-Ortiz J, Aguilar-López A, Rodríguez-Laguna R, Martínez-Damián MÁ, Valdivia-Alcalá R, Razo-Zárate R. 2020. Experimentos de elección para el manejo del Parque Nacional Los Mármoles, México. *Revista Chapingo Serie Ciencias Forestales y del Ambiente* 26 (2). <https://doi.org/10.5154/r.rchscfa.2019.06.043>
- OECD (Organisation for Economic Co-operation and Development). 2024. Environmental justice: Context, challenges and national approaches. OECD Publishing: Paris, France. <https://doi.org/10.1787/0e810fce-es>
- Ortez M, Thompson T, Kilders V, Widmar NO. 2023. Quantifying demand and willingness to pay for local food production. *Q Open* 4 (1). <https://doi.org/10.1093/qopen/qoae006>
- Sainz-Trapaga RM, Ortega-Leal S, Álvarez-Ramírez MM, Rosas-Nexticapa M. 2022. Aditivos químicos añadidos a la tortilla y tostada de maíz y su regulación en la legislación mexicana. *Estudios Sociales. Revista de Alimentación Contemporánea y Desarrollo Regional* 32 (60) <https://doi.org/10.24836/es.v32i60.1215>
- SNIIM (Servicio de Información e Integración de Mercados). 2024. Información mensual de precios diarios de tortilla en tortillerías y autoservicios de México. Gobierno de México. Secretaría de Economía. Ciudad de México, México. <http://www.economia-sniim.gob.mx/TortillaMesPorDia.asp> (Retrieved: November 2025).
- Tokuoka Y, Katayama N, Okubo S. 2024. Japanese consumer's visual marketing preferences and willingness to pay for rice produced by biodiversity-friendly farming. *Conservation Science and Practice* 6 (3). <https://doi.org/10.1111/csp2.13091>
- Torres-Ramírez R, Martínez-Damián MÁ, Valdivia-Alcalá R. 2023. Cerro de Amalucan: disponibilidad a pagar (DAP) de una tarifa por el método de valoración contingente-doble límite. *Ad-Gnosis* 12 (12): 1–12. <https://doi.org/10.21803/adgnosis.12.12.615>
- Torres-Sombra J. 2018. La tortilla de maíz mexicana. Un símbolo milenario. *In* Hoyos-Gómez GM. (ed.), *Algunos Componentes Generales, Particulares y Singulares del Maíz en Colombia y México*. Medellín, Colombia.

- Tudela-Mamani JW, Leos-Rodríguez JA, Zavala-Pineda MJ. 2018. Estimación de beneficios económicos por mejoras en los servicios de saneamiento básico mediante valoración contingente. *Agrociencia* 52 (3): 467–481.
- Tudela-Mamani JW, Martínez-Damián MA, Valdivia-Alcalá R, Romo-Lozano JL, Portillo-Vázquez M, Rangel-González RV. 2011. Valoración económica de los beneficios de un programa de recuperación y conservación en el Parque Nacional Molino de Flores, México. *Revista Chapingo Serie Ciencias Forestales y del Ambiente* 17 (2): 231–244
- Tudela-Mamani JW. 2017. Estimación de beneficios económicos por el mejoramiento del sistema de tratamiento de aguas residuales en la ciudad de Puno (Perú). *Desarrollo y Sociedad* 79: 189–237.
- Vásquez-Lavín F, Cerda-Urrutia A, Orrego-Suaza S. 2007. *Valoración económica del ambiente, fundamentos económicos, econométricos y aplicaciones*. Thomson Learning. Buenos Aires, Argentina. 368 p.

Agrociencia

ORGANIC SHADE-GROWN COFFEE: A PRODUCTION SYSTEM WITH A LOW CARBON FOOTPRINT AND HIGH SUSTAINABILITY POTENTIAL

Adán Villa-Herrera¹, Martín Alejandro Bolaños-González^{1*},
José Manuel Salvador-Castillo¹, Luz María Ramírez-Armas¹

¹Colegio de Postgraduados Campus Montecillo. Posgrado en Hidrociencias. Carretera México- Texcoco km 36.5, Montecillo, Texcoco, State of Mexico, Mexico. C. P. 56264.

* Author for correspondence: martinb72@gmail.com

ABSTRACT

The production of organic coffee (*Coffea arabica* L.) under shade contributes to mitigating climate change, as it generates lower greenhouse gas (GHG) emissions than conventional cultivation, thereby reducing its carbon footprint (CF). This study estimated the CF of coffee produced by the Comon Yaj Noptic SPR de RL cooperative in the municipality of La Concordia, Chiapas, Mexico, with the aim of identifying critical emission points and opportunities for environmental improvement. Information was collected from 161 plots through visits and interviews with producers, and wet milling data was integrated using emission factors from the Intergovernmental Panel on Climate Change (IPCC). The CF was estimated per kilogram of green coffee produced, considering emissions from plot management to the packaging of the final product. In the primary stage (plot management to parchment coffee), CF was 0.401 ± 0.079 kg CO₂e, with variability associated with altitude, plantation age, and planting density. The main sources were pulp decomposition (0.262 kg) and wastewater (0.078 kg) due to methane and nitrous oxide emissions. During processing (roasting, grinding, and packaging), CF was 0.415 kg CO₂e, with roasting being the main source (0.304 kg), followed by packaging (0.086 kg) and grinding (0.009 kg). The average CF for the entire production chain was 0.816 kg CO₂e, with a range of 0.758–1.271 kg CO₂e, showing consistency and low impact compared to conventional systems. The results confirm that shade-grown organic coffee has low CF and show high sustainability potential. However, opportunities for improvement were identified, such as the use of clean energy, efficient wastewater management, and the use of pulp as a by-product.

Keywords: *Coffea arabica* L., cooperative, greenhouse gases, agroforestry systems.

INTRODUCTION

The global agri-food system is one of the main sources of greenhouse gas (GHG) emissions. In 2015, it generated approximately 18 billion Mg of carbon dioxide equivalent (CO₂e), corresponding to 34 % of total anthropogenic emissions, with an estimated range between 25 and 42 % (Crippa *et al.*, 2021). This sector is a determining factor in climate change due to its intensive use of energy and land, as well as the

Citation: Villa-Herrera A, Bolaños-González MA, Salvador-Castillo JM, Ramírez-Armas LM. 2026. Organic shade-grown coffee: A production system with a low carbon footprint and high sustainability potential. *Agrociencia* 60(3): 453-466. <https://doi.org/10.47163/agrociencia.v60i3.3300>

Editor in Chief:
Dr. Fernando C. Gómez Merino

Received: November 14, 2025.
Approved: April 14, 2026.
Published in Agrociencia:
April 24, 2026.

This work is licensed under a Creative Commons Attribution-Non-Commercial 4.0 International license.



processes associated with food production, processing, transport, and consumption. In this context, the carbon footprint (CF) has established itself as a fundamental tool for quantifying and comparing the climate impact of products, processes, or organizations throughout their life cycle. CF is defined as the total amount of GHGs emitted, directly or indirectly, into the atmosphere by an individual, organization, or activity during a given period (Pandey *et al.*, 2011). This metric provides a comprehensive estimate of a production system's contribution to global warming, ranging from direct CO₂ emissions to broader assessments based on life cycle analysis (Samaniego and Schneider, 2010).

CF is expressed in units of carbon dioxide equivalent (CO₂e) and is calculated based on the inputs used at each stage of the value chain (kilograms of fertilizers, kWh of electricity, and liters of fuel), multiplied by their respective emission factors (EF) (Nojonen *et al.*, 2012; Bockel and Schiettecatte, 2018). However, most of the available EFs have been developed under production, energy, and technological conditions typical of industrialized countries, which limits their applicability in traditional agroecosystems in coffee-producing regions.

Contextual differences can introduce uncertainty into CF estimates by not accurately reflecting management practices, energy efficiency, or local soil and climate conditions, which could lead to overestimates or underestimates of actual emissions (Nojonen *et al.*, 2012). Nevertheless, CF remains a fundamental tool for quantifying GHG emissions throughout the life cycle of products and assessing their global warming potential (Samaniego and Schneider, 2010).

The functional unit used for estimating the CF is one kilogram of green coffee or coffee cherry production. This unit allows emissions to be linked to a specific measure of the product, enabling comparisons of results across different stages of its life cycle or between various studies (Bockel and Schiettecatte, 2018). In this regard, Segura and Andrade (2012) evaluated CF according to different certification standards, considering emissions during the production of *Coffea arabica*. On the other hand, Nojonen *et al.* (2012) estimated the CF in conventionally managed coffee systems (0.26–0.67 kg CO₂e kg⁻¹ of coffee cherry) and organic systems (0.12–0.52 kg CO₂e kg⁻¹ of coffee cherry). These results reflect a wide variability in the reported values and emphasize the necessity of local studies that integrate all stages of the production process.

In 2024, *C. arabica* was grown in 79 countries, harvested from a total area of 12 362 994 ha, with a production of 11 248 094.3 Mg of green coffee. Mexico ranked eighth in harvested area (659 699 ha) and 12th in production (194 470 Mg of green coffee), although its average yield (294.8 kg ha⁻¹) remained among the lowest worldwide (FAO, 2025). At the national level, coffee is grown in 14 states, of which Chiapas accounts for around 35.7 % of production, consolidating its position as the main coffee-growing state (SIAP, 2022).

Coffee farming in Chiapas not only provides economic sustenance to thousands of producers but also constitutes a model of sustainable agricultural practices (Folch and Planas 2019). Although conventional farming is the most common and is associated with negative effects such as biodiversity loss and chemical fertilizer pollution, interest in organic shade-grown systems as an environmentally responsible alternative has

grown. However, scientific information quantifying the CF of these systems remains limited, especially in local cooperatives and with a comprehensive life cycle analysis approach.

This study aimed to estimate the carbon footprint of organic shade-grown coffee produced by the Comon Yaj Noptic cooperative in La Concordia, Chiapas, considering emissions from plot management to ground coffee packaging. The results provide quantitative evidence on the climate impact and sustainability potential of this system, contributing to the strengthening of replicable low-carbon production strategies in Mexican coffee farming. Understanding emissions throughout the production cycle is essential for optimizing agricultural practices, improving environmental management, and promoting low-carbon production models.

MATERIALS AND METHODS

Study area

The study was conducted at the Comon Yaj Noptic SPR de RL organic coffee cooperative, based in the community of Nuevo Paraíso, in the municipality of La Concordia, Chiapas. Founded on May 19, 1995, this cooperative comprises 141 producers who manage 161 plots across 12 communities (Figure 1). According to data from weather

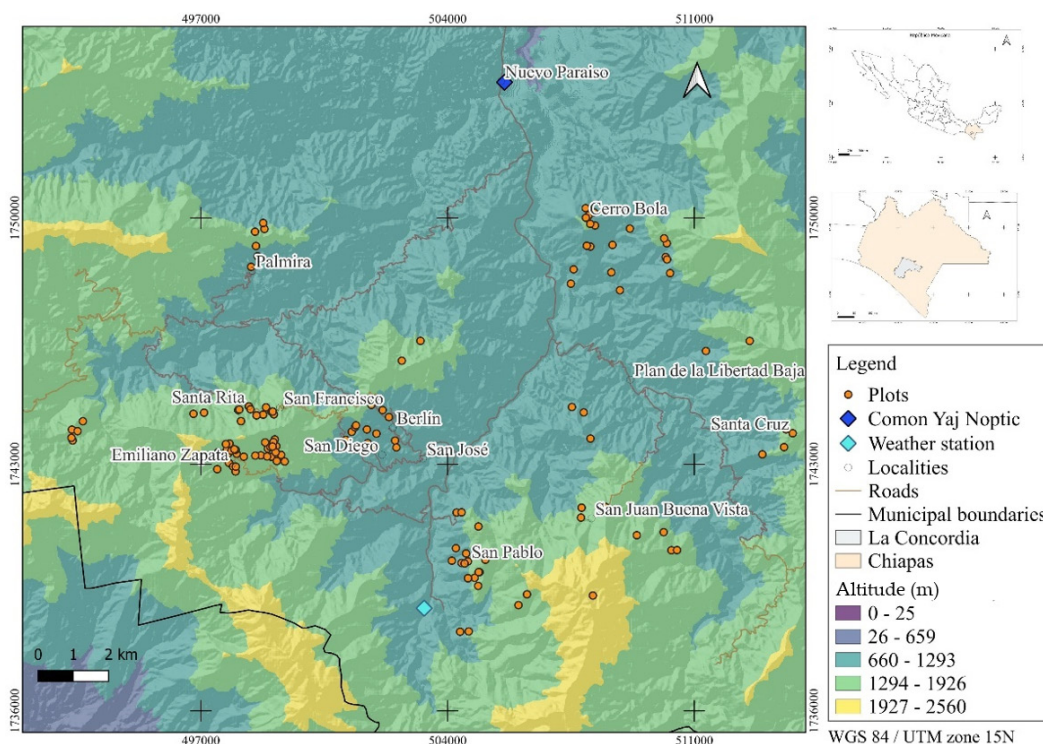


Figure 1. Location of the plots and main communities in the study area in the municipality of La Concordia, Chiapas, Mexico.

station 00007037 Finca Cuxtepeques (SMN, 2025), located at 15° 43' 43" N, 92° 58' 08" W, and an altitude of 1550 m, the average temperature in the area is 22.3 °C, with an average annual precipitation of 2110.2 mm.

The sampling period corresponded to the 2022–2023 production cycle. The survey of production units and the first stage of crop data collection took place between July and October 2022. Subsequently, in February 2023, during the harvest and post-harvest phase, a second stage of data collection was carried out, focusing on practices associated with harvesting, wet processing, and parchment coffee processing.

In both stages, structured interviews were conducted with producers, supplemented by an analysis of technical data sheets for each production unit. This made it possible to identify the specific management practices used on the coffee plots, including planting densities, age of plantations, shade species, yields, doses, and frequencies of input application, as well as the routes and types of transport used. The survey was designed based on the methodological recommendations of the IPCC (2006) and Noponen *et al.* (2012) for the collection of primary data in studies on GHG and CF emissions and was adapted to the cooperative's production context.

Stages considered in the CF estimate

Similar to the procedure followed by Noponen *et al.* (2012), GHG emissions associated with land use change were not considered, given that more than 20 years had elapsed since the land was converted for the establishment of coffee plantations. Carbon storage in vegetation and soil was also not considered, as the objective of the study was to estimate emissions associated with production operations. The analysis was structured into two main stages: 1) the primary stage, covering activities from plot management to the production of dry parchment coffee, including wet processing and transport to the cooperative; and 2) the processing stage, covering operations from threshing to packaging the final product.

In the primary stage, emissions were considered from several sources: plantation renewal, transportation, application of inputs (such as compost and PSD dihydro solubilizing enhancer), pulping, pulp decomposition, and the wastewater generated during the wet processing stage. These emissions are associated with the agronomic management phase and the immediate post-harvest phase. The processing stage included the industrial operations carried out at the cooperative, comprising the threshing of parchment coffee to obtain green coffee, roasting, grinding, weighing, and packaging of the final product (Figure 2).

The activities considered included the renewal of plantations by transporting plants from the cooperative's nursery to the plots to maintain productivity, as well as the transport of inputs, specifically compost and PSD, from the cooperative to the communities. PSD was applied at a dose of 50–100 g per plant to improve the health and productivity of the coffee trees. Pulping consisted of separating the beans from the pulp using pulpers, mainly electric (109 units) and, to a lesser extent, gasoline-powered (11 units).

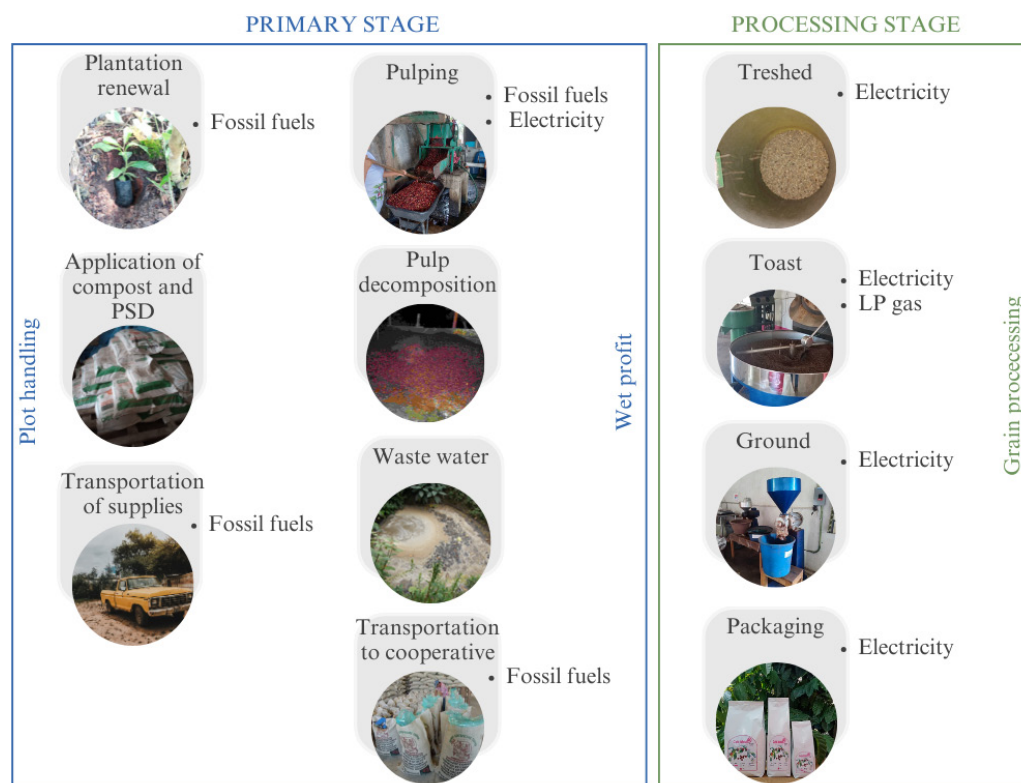


Figure 2. Stages and inputs in the coffee production process.

Emissions from the fermentation and decomposition of pulp and wastewater from washing were also considered, as these processes generate methane (CH_4) and nitrous oxide (N_2O). Threshing involved removing the parchment coffee husk to obtain green coffee, using a five-horsepower (HP) electric machine. Roasting was carried out at controlled temperatures, using LP gas and electricity to power a two-HP motor that ensures the homogeneity of the process. Subsequently, the roasted beans were ground with a three-HP electric grinder to produce ground coffee. Finally, packaging was carried out using an electric packaging machine and an electronic weighing scale (model BAR-8) for distribution and sale.

All GHG emissions were normalized to the defined functional unit, following the methodology proposed by Nojonen *et al.* (2012). Specific conversions for the production system were calculated in the field through direct measurements taken during the second sampling phase in the wet and dry mills. It was established that 4.7 kg of coffee cherry is required to obtain 1 kg of parchment coffee and 1.28 kg of parchment coffee are required to obtain 1 kg of green coffee. These values reflect the actual processing conditions of the Comon Yaj Noptic cooperative and were used to normalize emissions throughout the production chain. This relationship was fundamental for distributing emissions among the different stages of the process and

calculating the CF of each emission source, in accordance with the approach of Segura and Andrade (2012).

The CF results for each activity were expressed in kilograms of CO₂e per kilogram of green coffee produced. To improve understanding of the text, the reported values are presented only in kg of CO₂e. The classification of activities by stage made it possible to identify the processes with the highest emissions and provided a solid basis for proposing GHG mitigation strategies in the coffee production chain.

Procedure for calculating CF

GHG emissions were calculated by multiplying specific EFs by the amount corresponding to the activity data (liters of gasoline, kWh of electricity, or kilograms of PSD). The EFs used were obtained from scientific literature and reports from the Intergovernmental Panel on Climate Change (IPCC, 2006). To calculate emissions from fertilization and liming, an EF of 0.01 kg N₂O kg⁻¹ N was applied for nitrogen. In the case of calcium carbonate and magnesium carbonate, 0.12 kg C kg⁻¹ CaCO₃ and 0.122 kg C kg⁻¹ MgCO₃ were used, respectively (IPCC, 2006).

Furthermore, CH₄ and N₂O emissions from pulp decomposition were estimated in terms of CO₂e using a global warming potential of 28 g CO₂e g⁻¹ for CH₄ and 298 g CO₂e g⁻¹ for N₂O (IPCC, 2006). To quantify the amount of pulp generated, a conversion factor of 0.4 was applied, representing the percentage of pulp relative to the weight of the cherry (Rodríguez-Durán *et al.*, 2019). In addition, an EF of 0.12 was used for the combined emissions of CO₂, CH₄, and N₂O associated with the process, in accordance with the value reported by Villa-Herrera *et al.* (2025), who adopt it as a technical reference.

Regarding CH₄ emissions from wastewater, water consumption during pulping was considered to be 7 L kg⁻¹ of coffee cherry, determined from measurements at wet mills. In addition, the biochemical oxygen demand of the effluent (0.00025 kg L⁻¹) was considered, together with a CH₄ EF of 0.3 kg CO₂e kg⁻¹ of green coffee, in accordance with the IPCC Good Practice Guidance (IPCC, 2006).

Water samples were collected at five wet mills (out of a total of 120) at representative points in the process (the supply source, pulping, washing, and wastewater reception pits). The number of mills sampled was limited due to access restrictions resulting from high insecurity in the area. However, the selected subset is representative of the local processing system, since in all cases wet processing is used, the same basic operations are performed, and waste management follows a consistent pattern. Most of the pulp is deposited in nearby sites without treatment, and wastewater is discharged into pits. This similarity in management practices allowed validly inferring the results for the cooperative's processing facilities as a whole.

Biochemical oxygen demand analyses were performed at the Environmental Sciences Laboratory of the Postgraduate College, using the modified Winkler method with the addition of sodium acid (APHA, 2005). CO₂e emissions from transport were estimated based on gasoline consumption for the transport of inputs and parchment coffee. The

distance traveled from the producer communities to the cooperative was determined using the QGIS software, version 3.16.9, with the EPSG:6370 reference system, Mexico ITRF2008/UTM, zone 15N, and an average vehicle fuel efficiency of 8 km L⁻¹. The calculation considered the route usually used by producers, which in most cases is the only one available due to the geographical isolation of the study area. An EF of 2.33 kg CO₂e L⁻¹ of gasoline was used (IPCC, 2006).

During the threshing, roasting, grinding, and packaging stages, energy consumption was estimated based on the capacity and power of the machines. An EF of 1.595 kg CO₂e L⁻¹ was considered for LP gas and 0.3 kg CO₂e kWh⁻¹ for electricity, the latter corresponding to the national value reported for Mexico in the 2022 Climate Transparency Report (Climate Transparency, 2022). Additionally, for the packaging process, an EF of 1.99 kg CO₂e kg⁻¹ of plastic bags used was considered (Castaño-Peláez and Botero-Agudelo, 2017).

Data analysis

A database was constructed with information from 161 plots, and yields were standardized in kilograms of green coffee per hectare. Data management was performed using Microsoft Excel worksheets. Statistical analysis was performed using the R program (version 4.3.1) and its RStudio interface (version 2023.6.0.421) (R Core Team, 2023). Descriptive statistics were calculated using the *pastecs* library and the *stat.desc* function. Graphs were created using the *ggplot2* library and the *ggplot* function.

RESULTS AND DISCUSSION

Production system

Descriptive statistics for the variables associated with the plots provided a detailed overview of the coffee production conditions (Table 1). Plot size ranged from 0.5 to 6 ha, while altitude ranged from 769 to 1846 m. Similarly, planting density showed a wide range (1050–9800 plants ha⁻¹) and a coefficient of variation of 0.372 (Table 1),

Table 1. Descriptive statistics of the variables analyzed in the coffee plots studied in La Concordia, Chiapas, Mexico.

Variables	Units	Mínimum	Maximum	Median	Mean	Standard deviation	Coefficient of variation
Surface	ha	0.5	6	1.5	1.95	1.276	0.656
Altitude	m	769	1846	1429	1369.2	225.93	0.165
Planting density	Plants ha ⁻¹	1050	9800	4090	4316.7	1606	0.372
Age	Years	1.7	26	9.3	10.1	5.465	0.542
Shade species	Quantity	1	50	12	13.2	5.754	0.436
Performance (cherry)	kg ha ⁻¹	216.2	8648	2162	2767.4	1829.05	0.663
Distance	km	12.43	32.5	22.04	21.96	5.915	0.269

confirming a high relative dispersion and reflecting the adoption of different agronomic practices among producers. The coffee plantations were between 1.7 and 26 years old, which could have direct implications for yield. The coefficient of variation for yield was 0.663, reflecting high variability attributable to differences in management practices implemented by producers. The distance between the communities where wet processing was carried out and the cooperative's facilities ranged from 12.43 to 32.5 km.

The number of shade trees per plot ranged from 1 to 50, with a median of 12. Species of the genus *Inga* (*I. oerstediana* Benth., *I. vera* Willd.), *Alchornea latifolia* Sw., *Tabebuia rosea* (Bertol.) DC., *Cecropia obtusifolia* Bertol., and *Liquidambar styraciflua* L. predominated, as did fruit species of economic value such as *Mangifera indica* L. and *Persea americana* Mill. According to the classification of agroforestry systems used by Chéron-Bessou *et al.* (2024), most of the systems were classified as complex. The high number of shade species not only benefits biodiversity but also influences CO₂ capture (van Rikxoort *et al.*, 2014; Casanova-Lugo *et al.*, 2016) and the provision of other regulatory ecosystem services, such as climate adjustment, erosion, humidity, soil fertility, and biological control of pests and diseases (Altieri and Nicholls, 2020).

CF during the primary phase

The CF of transporting inputs averaged 0.0133 kg CO₂e and had a median of 0 kg CO₂e, indicating that more than half of the plots did not record emissions associated with this activity (Table 2). Of the 161 plots analyzed, only 73 carried out individual transport of inputs; of these, PSD was applied in 58, while the rest did not report any travel because they did not apply inputs during the period evaluated. Zero values were assigned in cases with no evidence of travel or with collective distribution, which explains the asymmetry observed in the data. The standard deviation of 0.0248 kg CO₂e reflects moderate variability, mainly attributable to differences in distances traveled and frequency of trips.

The transportation of inputs contributed, on average, to 1.6 % of total CF. However, its wide variability and high emissions in some plots indicate room for improvement. Strategies such as optimizing transportation or reducing the frequency of trips could reduce emissions in this phase of the process (Pramulya *et al.*, 2022). GHG emissions associated with PSD application ranged from 0 to 0.272 kg CO₂e, with an average of 0.027 kg CO₂e and a median of 0 kg CO₂e, representing 3.3 % of total CF. This low contribution is due to the fact that PSD is applied in small doses and in a localized manner.

With regard to activities related to plot management, GHG emissions were recorded in 74 of the 161 plots evaluated. The values ranged from 0 to 0.465 kg CO₂e, with an average of 0.04 kg CO₂e and a standard deviation of 0.072 kg CO₂e, reflecting high variability among production units. This suggests that there are opportunities to optimize management practices to reduce emissions on certain plots.

Table 2. Carbon footprint (CF) of activities in the primary and processing stages of shade-grown organic coffee on the coffee plots studied in La Concordia, Chiapas, Mexico.

Activity	Number of plots	Minimum	kg CO ₂ e kg ⁻¹ of green coffee				Standard deviation	% Total CF %
			Average	Maximum	Median			
Transportation of supplies	161	0	0.013	0.193	0	0.022	1.6	
Application of PSD	161	0	0.027	0.272	0	0.052	3.3	
Pulping	161	0.001	0.002	0.012	0.001	0.002	0.2	
Pulp decomposition	161	ND	0.262	ND	ND	ND	32.1	
Wastewater	161	ND	0.078	ND	ND	ND	9.5	
Transportation of parchment	161	0.003	0.017	0.113	0.013	0.016	2.5	
Threshing	NA	NA	0.013	NA	NA	NA	1.6	
Roasting	NA	NA	0.304	NA	NA	NA	37.2	
Grinding	NA	NA	0.009	NA	NA	NA	1.1	
Packaging (bags)	NA	NA	0.086	NA	NA	NA	10.5	
Weighing	NA	NA	0.001	NA	NA	NA	0.1	
Sealing	NA	NA	0.002	NA	NA	NA	0.2	
CF of the primary phase	161	0.343	0.401	0.856	0.372	0.079	49.2	
CF of the processing stage	ND	ND	0.415	ND	ND	ND	50.8	

NA corresponds to activities that do not apply at the plot level, as they were carried out centrally at the cooperative's facilities (threshing, roasting, grinding, packaging, weighing, and sealing). ND indicates that it was not possible to obtain disaggregated information by plot, as no individual measurements were taken; in these cases, emissions were estimated from representative averages derived from measurements taken at the wet mills sampled.

The average estimated emissions per plot (0.04 kg CO₂e kg⁻¹ of green coffee) were lower than those reported in Brazil and Vietnam (0.05 and 0.08 kg CO₂e kg⁻¹ of green coffee in sustainable systems) (Nab and Maslin, 2020); Veracruz, Mexico (1.41 kg CO₂e kg⁻¹ of green coffee in a conventional production system) (Giraldi-Díaz *et al.*, 2018), and Costa Rica (1.02 kg CO₂e kg⁻¹ of green coffee in traditional production systems) (Killian *et al.*, 2013). However, the highest value found in this study (0.465 kg CO₂e) was higher than the averages for some of these systems. This highlights the importance of taking into account the variability of agricultural practices and the specific conditions of each plot. The highest emissions were mainly associated with the use of nitrogen fertilizers, in line with the findings of Arellano and Hernández (2023) and Trinh *et al.* (2020).

GHG emissions from wet processing

The CF associated with the use of gasoline-powered pulpers was 0.012 kg CO₂e, while for electric pulpers it was 0.001 kg CO₂e, with an overall average of 0.002 kg CO₂e. The predominance of electric equipment (90.83 %) explains the low average emissions at this stage, given that these are more energy efficient and reduce dependence on fossil fuels, which is an environmentally friendly alternative.

Emissions from pulp decomposition and methane (CH₄) from wastewater were the main sources of wet processing, with 0.262 and 0.078 kg CO₂e, equivalent to 32.1 and

9.5 % of total CF, respectively. According to van Rikxoort *et al.* (2014), the variability in CF in this process reflects differences in water management during fermentation and washing, as well as in the efficiency of the inputs applied. Likewise, Chéron-Bessou *et al.* (2024) highlight that the initial DBO conditions of the wastewater directly influence the magnitude of GHG emissions.

In the present study, the largest contribution came from pulp decomposition, while Pramulya *et al.* (2019) reported the opposite pattern: 0.125 kg CO₂e kg⁻¹ for wastewater and 0.015 kg CO₂e kg⁻¹ for pulp. This difference is attributed to the fact that, in the study region, pulping is carried out dry, leaving the pulp exposed to the environment for decomposition, while water is mainly used for washing, which concentrates organic matter in the pulp and increases CH₄ and N₂O emissions. Together, these processes contributed about 85 % of wet mill emissions, compared to 65 % reported by Pramulya *et al.* (2019).

Similarly, van Rikxoort *et al.* (2014) recorded much higher emissions (4.7 ± 2.8 kg CO₂e kg⁻¹ of parchment coffee), attributable to intensive water use (80 L kg⁻¹) compared to the 7 L kg⁻¹ used in this study. These differences confirm that water management is a determining factor in the magnitude of emissions during wet processing. The average CF of wet processing was 0.359 ± 0.016 kg CO₂e, indicating consistency and low dispersion among producers, as homogeneous water volumes, DBO values, and emission factors were used. This value was lower than that reported by Killian *et al.* (2013) (0.48 kg CO₂e kg⁻¹) and much lower than that of van Rikxoort *et al.* (2014) (3.0 ± 2.1 kg CO₂e kg⁻¹ of parchment coffee), but higher than the values reported by Nab and Maslin (2020) (0.08–0.1 kg CO₂e kg⁻¹), who did not consider emissions from pulp decomposition or wastewater.

The transport of parchment coffee contributed 0.017 kg CO₂e, equivalent to 2.5 % of total CF. This result is lower than that reported by Maina *et al.* (2016) (0.036 kg CO₂e kg⁻¹ of parchment coffee), which is attributed to the lower conversion factor applied (1.28). Overall, the primary stage, from plantation management to the production of parchment coffee, recorded values between 0.343 and 0.856 kg CO₂e, with an average of 0.401 kg CO₂e and a coefficient of variation of 19.6 %, reflecting moderate variability in production practices. This value was higher than that estimated by Pramulya *et al.* (2019) (0.341 kg CO₂e kg⁻¹ of green coffee) but lower than the range reported by Arias-Hernández *et al.* (2018) (1.05–3.56 kg CO₂e kg⁻¹ of parchment coffee), confirming the low climate impact of the organic shade-grown system analyzed in this study (Table 2).

CF grain processing

The total CF of the processing stage was 0.415 kg CO₂e (Figure 3). Threshing contributed 0.013 kg CO₂e, roasting 0.304 kg CO₂e, grinding 0.009 kg CO₂e, plastic bags 0.086 kg CO₂e, weighing 0.001 kg CO₂e, and sealing 0.002 kg CO₂e. Roasting had a higher CF than the 0.19 kg CO₂e kg⁻¹ of green coffee reported by Killian *et al.* (2013). However, post-roasting emissions were lower (0.098 kg CO₂e) than the 0.13 kg CO₂e kg⁻¹ of green coffee reported by Killian *et al.* (2013). In contrast, these results were lower than those

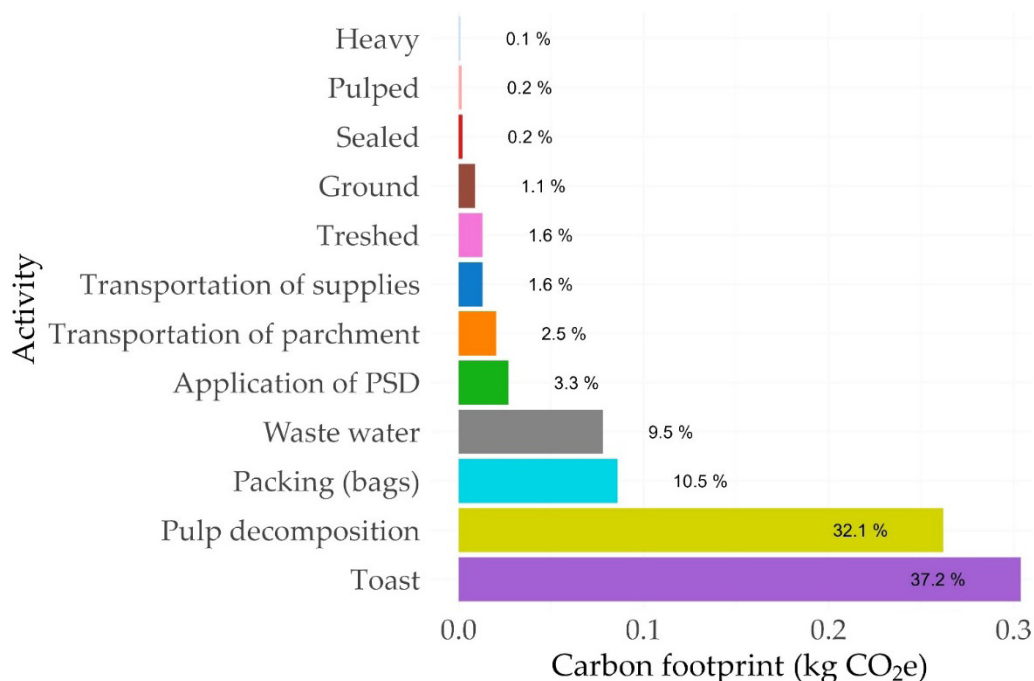


Figure 3. Relative contribution of production chain activities to the carbon footprint (CF) of shade-grown organic coffee on the coffee plots studied in La Concordia, Chiapas, Mexico.

of Giraldi-Díaz *et al.* (2018), who obtained CF values of 1.5 and 2.82 g CO₂e kg⁻¹ of ground coffee.

CF of the entire production chain

The average CF for the entire production chain was 0.816 kg CO₂e, ranging from 0.758 to 1.271 kg CO₂e. The activities with the highest contribution were roasting, pulp decomposition, packaging bags, and wastewater (Figure 3). These results are within the range reported for organic coffee systems, although they are slightly higher than the values of 0.64–0.647 kg CO₂e kg⁻¹ of green coffee obtained by Trinh *et al.* (2020), who did not consider emissions from pulp decomposition or wastewater management. In contrast, Maina *et al.* (2016) documented a considerably higher CF (4 kg CO₂e kg⁻¹ of parchment coffee) in conventional systems. Similarly, Pramulya *et al.* (2022) reported intermediate values, from 1.48 to 1.93 kg CO₂e kg⁻¹ of green coffee, considering the stages from harvest to packaging.

According to Maina *et al.* (2016), the differences observed in CF values between studies can be attributed mainly to variations in production methods, especially in the type and management of fertilization. Similarly, Pramulya *et al.* (2019) highlight that discrepancies in CF estimates may also be due to differences in calculation methods, DBO values used, or EFs considered.

The main sources of GHG emissions identified in this study corresponded to wet processing, in particular pulp decomposition and wastewater management, which together accounted for 41.6 % of total CF. Similarly, Killian *et al.* (2013) identified wastewater as a significant source of emissions and demonstrated that the use of biodigesters can reduce CH₄ emissions from 0.374 to 0.340 kg CO₂e kg⁻¹ of green coffee. For their part, van Rikxoort *et al.* (2014) proposed that mitigation strategies in Latin American coffee production should focus on: 1) conserving carbon stocks in biomass and preventing deforestation; 2) reducing emissions from fertilizer use through efficient management practices; and 3) reducing wastewater emissions through dry processing or the implementation of improved wet processing methods.

CONCLUSIONS

The analysis of organic shade-grown coffee production at the Comon Yaj Noptic cooperative revealed high variability in management conditions and production characteristics across plots, which is reflected in differences in the estimated carbon footprint for each production unit. Overall, the results confirm the low climate impact and environmental efficiency of this system compared to conventional models, showing the potential of organic agroforestry systems to contribute to mitigating greenhouse gas emissions in Mexican coffee farming.

Areas for improvement were also identified with a view to increasing the sustainability of the process, particularly through the incorporation of clean energy in the processing and packaging stages, the optimization of water use and treatment during wet processing, and the recovery of coffee pulp as an agricultural by-product. The case study indicates that shade-grown organic coffee is a viable alternative for moving toward low-emission coffee farming with greater environmental resilience. Although the results correspond to a specific context, they offer a useful reference for promoting sustainable practices that can be replicated in other producing regions of the country.

ACKNOWLEDGEMENTS

To the Comon Yaj Noptic SPR de RL cooperative, for its invaluable collaboration in this study and the work it does, demonstrating that it is possible to produce responsibly and sustainably. To the College of Postgraduates and the Ministry of Science, Humanities, Technology, and Innovation (SECIHTI) for their institutional support and funding to carry out this research.

REFERENCES

- Altieri MA, Nicholls CI. 2020. Agroecology: Challenges and opportunities for farming in the Anthropocene. *International Journal of Agriculture and Natural Resources* 47 (3): 204–215. <https://doi.org/10.7764/ijanr.v47i3.2281>
- APHA (American Public Health Association). 2005. *Standard methods for the examination of water and wastewater* (21st edition). Washington, DC, USA. 1368 p.

- Arellano C, Hernández C. 2023. Carbon footprint and carbon storing capacity of Arabica coffee plantations of Central America: A review. *Coffee Science* 18: e182072. <https://doi.org/10.25186/v18i.2072>
- Arias-Hernández JJ, Riaño-Herrera NM, Riaño-Becerra AM, Ariza-Camacho W, Posada-Suarez HJ, Valenzuela-Andrade J, Vega-Cano MA, Murgueitio-Cortes YP, Castro-Chavez JF. 2018. Determinación de la huella de carbono en el sistema de producción de café pergamino seco de cuatro municipios del sur del departamento del Huila (Colombia). *Revista de Investigación Agraria y Ambiental* 9 (2): 109–120.
- Bockel L, Schiettecatte LS. 2018. Life cycle analysis and the carbon footprint of coffee value chains. In Lashermes P. (ed.), *Achieving Sustainable Cultivation of Coffee*. Burleigh Dodds Science Publishing: Sawston, UK, pp: 359–382. <https://doi.org/10.19103/as.2017.0022.20>
- Casanova-Lugo F, Ramírez-Avilés L, Parsons D, Caamal-Maldonado A, Piñeiro-Vázquez AT, Díaz-Echeverría V. 2016. Environmental services from tropical agroforestry systems. *Revista Chapingo Serie Ciencias Forestales y del Ambiente* 22 (3): 269–284. <https://doi.org/10.5154/r.rchscfa.2015.06.029>
- Castaña-Peláez HI, Botero-Agudelo JL. 2017. Evaluación ambiental del proceso de elaboración de bolsas plásticas en Colombia utilizando la metodología de análisis de ciclo de vida. *Revista Politécnica* 13 (24): 9–18.
- Chéron-Bessou C, Acosta-Alba I, Boissy J, Payen S, Rigal C, Setiawan AAR, Sevenster M, Tran T, Azapagic A. 2024. Unravelling life cycle impacts of coffee: Why do results differ so much among studies? *Sustainable Production and Consumption* 47: 251–266. <https://doi.org/10.1016/j.spc.2024.04.005>
- Climate Transparency. 2022. Climate transparency report. G20 response to the energy crisis: critical for 1.5 °C. Bali Nusa Dua, Indonesia. 59 p.
- Crippa M, Solazzo E, Guizzardi D, Monforti-Ferrario F, Tubiello FN, Leip A. 2021. Food systems are responsible for a third of global anthropogenic GHG emissions. *Nature Food* 2 (3): 198–209. <https://doi.org/10.1038/s43016-021-00225-9>
- FAO (Food and Agriculture Organization of the United Nations). 2025. FAOSTAT. Crops and livestock products. Rome, Italy. <https://www.fao.org/faostat/en/#data/QCL> (Retrieved: December 2025).
- Folch A, Planas J. 2019. Cooperation, fair trade, and the development of organic coffee growing in Chiapas (1980–2015). *Sustainability* 11 (2): 357. <https://doi.org/10.3390/su11020357>
- Giraldi-Díaz MR, de Medina-Salas L, Castillo-González E, León-Lira R. 2018. Environmental impact associated with the supply chain and production of grinding and roasting coffee through life cycle analysis. *Sustainability* 10 (12): 4598. <https://doi.org/10.3390/su10124598>
- IPCC (Intergovernmental Panel on Climate Change). 2006. 2006 IPCC guidelines for national greenhouse gas inventories, Volumen 4. Agriculture, forestry and other land use. Kanagawa, Japan. <https://www.ipcc-nggip.iges.or.jp/public/2006gl/vol4.html> (Retrieved: November 2025).
- Killian B, Rivera L, Soto M, Navichoc D. 2013. Carbon footprint across the coffee supply chain: the case of Costa Rican coffee. *Journal of Agricultural Science and Technology* B3: 151–170.
- Maina J, Mutwiwa UN, Kituu GM, Githiru M. 2016. Evaluation of greenhouse gas emissions along the small-holder coffee supply chain in Kenya. *Journal of Sustainable Research in Engineering* 2 (4): 111–120.
- Nab C, Maslin M. 2020. Life cycle assessment synthesis of the carbon footprint of Arabica coffee: Case study of Brazil and Vietnam conventional and sustainable coffee production and export to the United Kingdom. *Geography and Environment* 7 (2). <https://doi.org/10.1002/geo2.96>

- Noponen MRA, Edwards-Jones G, Haggard JP, Soto G, Attarzadeh N, Healey JR. 2012. Greenhouse gas emissions in coffee grown with differing input levels under conventional and organic management. *Agriculture, Ecosystems and Environment*, 151: 6–15. <https://doi.org/10.1016/j.agee.2012.01.019>
- Pandey D, Agrawal M, Pandey JS. 2011. Carbon footprint: Current methods of estimation. *Environmental Monitoring and Assessment* 178 (1–4): 135–160. <https://doi.org/10.1007/s10661-010-1678-y>
- Pramulya R, Bantacut T, Noor E, Yani M, Romli M. 2022. Life cycle assessment of Gayo Arabica coffee green bean at Aceh Province. *Habitat* 33 (3): 308–319. <https://doi.org/10.21776/ub.habitat.2022.033.3.29>
- Pramulya R, Bantacut T, Noor E, Yani M. 2019. Carbon footprint calculation for Gayo Arabica coffee primer processing. *International Journal of Scientific and Technology Research* 8 (12): 2934–2938.
- R Core Team. 2023. R: A language and environment for statistical computing. R Foundation for Statistical Computing. Vienna, Austria. <https://www.R-project.org/> (Retrieved: November 2024).
- Rodríguez-Durán L, Favela-Torres E, Aguilar C, Saucedo-Castañeda G. 2019. Coffee pulp as potential source of phenolic bioactive compounds. In Chavez-Gonzalez M, Buenrostro-Figueroa JJ, Aguilar CN. (eds.), *Handbook of Research on Food Science and Technology: Volume 1: Food Technology and Chemistry*. Apple Academic Press: New York, NY, USA, pp: 107–132. <https://doi.org/10.1201/9780429487859-5>
- Samaniego J, Schneider H. 2010. La huella del carbono en la producción, distribución y consumo de bienes y servicios. Comisión Económica para América Latina y el Caribe. Comisión Económica para América Latina y el Caribe: Santiago de Chile, Chile. 46 p.
- Segura MA, Andrade HJ. 2012. Huella de carbono en cadenas productivas de café (*Coffea arabica* L.) con diferentes estándares de certificación en Costa Rica. *Luna Azul* 35: 60–77.
- SIAP (Sistema de Información Agroalimentaria y Pesca). 2022. Anuario estadístico de la producción agrícola. Cierre de la producción agrícola por estado. Gobierno de México. Secretaría de Agricultura y Desarrollo Rural. Sistema de Información Agroalimentaria y Pesca. Ciudad de México, México. <https://nube.siap.gob.mx/cierreagricola/> (Retrieved: December 2025).
- SMN (Servicio Meteorológico Nacional). 2025. Normales climatológicas. Gobierno de México. Comisión Nacional del Agua. Ciudad de México, México. https://smn.conagua.gob.mx/tools/RECURSOS/Normales_Climatologicas/Normales9120/chis/nor9120_07037.txt (Retrieved: October 2025).
- Trinh LTK, Hu AH, Lan YC, Chen ZH. 2020. Comparative life cycle assessment for conventional and organic coffee cultivation in Vietnam. *International Journal of Environmental Science and Technology* 17 (3): 1307–1324. <https://doi.org/10.1007/s13762-019-02539-5>
- van Rikxoort H, Schroth G, Läderach P, Rodríguez-Sánchez B. 2014. Carbon footprints and carbon stocks reveal climate-friendly coffee production. *Agronomy for Sustainable Development* 34 (4): 887–897. <https://doi.org/10.1007/s13593-014-0223-8>
- Villa-Herrera A, Bolaños-González MA, Paz-Pellat F, Salvador-Castillo JM, Ramírez-Armas LM, Villagómez-Jiménez C. 2025. Evaluation of the carbon footprint of the coffee production chain: Case study of the Finca Triunfo Verde, Chiapas, México. *Tropical and Subtropical Agroecosystems* 28 (1): 1–14. <https://doi.org/10.56369/tsaes.6043>

